

# **SORLA in Renal and Adrenal Function**

## **Dissertation**

zur Erlangung des akademischen Grades  
doctor rerum naturalium  
(Dr. rer. nat.)

eingereicht am Institut für Biologie  
der Mathematisch-Naturwissenschaftliche Fakultät I,  
Humboldt-Universität zu Berlin

von  
Dipl.-Ing. (FH) Daniel Miltz  
(geb. 02.06.1980 in Berlin)

Präsident der Humboldt-Universität zu Berlin:  
Prof. Dr. Dr. h.c. Christoph Marksches

Dekan der Mathematisch-Naturwissenschaftlichen Fakultät I:  
Prof. Dr. Lutz-Helmut Schön

Gutachter/in:

1. Prof. Dr. Thomas Willnow
2. Prof. Dr. Wolfgang Uckert
3. Prof. Dr. Michael Bader

Datum der Einreichung:

Tag der mündlichen Prüfung:

17. 03. 2010

## Abstract

The type I transmembrane receptor SORLA (also known as LR11) is a member of the mammalian VPS10p-receptor family. The receptor, which is mainly expressed in the central nervous system (CNS), is characterized by high structural homology to endocytosis- and sorting-receptors. Outside the CNS, expression of SORLA can be found in a variety of tissues, including kidney.

This study analyzes the localization and function of the receptor in the murine kidney. While expression of SORLA in the collecting duct has been described before, this work shows that the receptor can also be found in epithelia of the thick ascending limb of Henle's loop (TAL), the distal convoluted tubule and the connecting tubule.

This distinct renal expression pattern suggests a role for SORLA in transepithelial transport processes. To determine which processes the receptor might be involved in, the kidney function of mice, which carry a complete deficiency of the *Sorla* gene, was analyzed. These animals show defects in electrolyte handling: they are wasting  $\text{Na}^+$ ,  $\text{Cl}^-$ ,  $\text{K}^+$ , and  $\text{Ca}^{2+}$  (under normal conditions and/or after water deprivation). The salt loss phenotype is accompanied by decreased mean arterial pressure and heart rate as well as mis-regulated secretion of aldosterone.

In line with this observation, SORLA is also expressed in the adrenal gland, particularly in the zona glomerulosa, the place of aldosterone synthesis. Additionally, microarray-based gene expression analysis in the adrenal gland revealed significant down-regulation of several genes of the epinephrine synthesis pathway in mice lacking SORLA. This defect results in lower adrenal levels of the hormone. Epinephrine influences kidney function by triggering renin release via the  $\beta$ -adrenergic pathway. A decreased release of epinephrine could therefore explain the abnormal arterial pressure in mice with disruption of the *Sorla* gene.

However, this mouse model's renal defects cannot only be explained by adrenal malfunction: In the kidney, the lack of SORLA results in differential expression of the electrolyte transporter NHE3 and, to a lesser extent, ROMK. Even more striking is the altered phosphorylation of the two cation-chloride cotransporters NCC and NKCC2, as their activity is regulated by phosphorylation.

The signaling kinase SPAK has been reported to regulate the activity of NKCC2 and NCC. The transporters' abnormal phosphorylation coincides with the atypical distribution of the kinase in TAL of *Sorla*<sup>(-/-)</sup> mice, suggesting a role of the receptor in establishing the localization of SPAK. This hypothesis was further substantiated by the identification of putative SORLA-interacting proteins involved in trafficking.

**Keywords:** SORLA, LR11, kidney, adrenal gland, NKCC2, SPAK

## Kurzfassung

Der Typ I Transmembran-Rezeptor SORLA (auch LR11) gehört zur VPS10p-Rezeptor Familie in Säugern. Der Rezeptor mit starker Homologie zu Endozytose- und Sorting-Rezeptoren ist am stärksten im zentralen Nervensystem (CNS) exprimiert. Außerhalb des CNS ist SORLA in einer Vielzahl von Geweben zu finden, unter anderem in der Niere.

Diese Arbeit widmet sich der Lokalisation und der Funktion des Rezeptors in der murinen Niere. Zusätzlich zur bereits bekannten Expression SORLAs im Sammelrohr zeigt diese Arbeit eine auf den dicken aufsteigenden Ast der Henleschen Schleife (TAL), den distalen Konvolut und den Verbindungstubulus ausgedehnte Expression.

Das klare distale Expressionsmuster lässt eine Rolle des Rezeptors in transepithelialen Transportprozessen vermuten. Um genau festzustellen, welche Prozesse von SORLA beeinflusst werden, wurde die Nierenfunktion von Mäusen mit einer vollständigen Defizienz des *Sorla*-Gens (*Sorla*<sup>(-/-)</sup>) untersucht. Diese Tiere zeigen Defekte in der renalen Elektrolythomöostase: sie verlieren Na<sup>+</sup>, Cl<sup>-</sup>, K<sup>+</sup>, und Ca<sup>2+</sup> (im Normalzustand und/oder nach Trinkwasserentzug). Eine Erniedrigung von Blutdruck und Herzfrequenz sowie eine fehlregulierte Sekretion von Aldosteron gehen mit dem Salzverlust-Phänotyp einher.

Passend zu dieser Beobachtung konnte eine Expression von SORLA in der Nebenniere – speziell in der Zona glomerulosa, dem Ort der Aldosteron-Synthese – gezeigt werden. Microarray-basierte Genexpressions-Analyse in der Nebenniere offenbarte eine signifikant verminderte Expression mehrerer Gene des Adrenalin-Synthesewegs in *Sorla*<sup>(-/-)</sup>-Mäusen. Dieser Defekt resultiert in einer verringerten Menge des Hormons in den Nebennieren der Tiere. Adrenalin aktiviert die Freisetzung von Renin in der Niere über  $\beta$ -Adrenorezeptoren. Eine reduzierte Freisetzung von Adrenalin könnte daher den gesenkten Blutdruck in Mäusen mit *Sorla* Gen-Defizienz erklären.

Dennoch lassen sich die Nierendefekte des Mausmodells nicht ausschließlich durch gestörte Nebennierenfunktion erklären. In der Niere bewirkt das Fehlen von SORLA eine veränderte Expression der Elektrolyttransporter NHE3 und, in geringerem Maße, ROMK. Noch stärker sticht die veränderte Phosphorylierung der beiden Kation-Chlorid-Cotransporter NCC und NKCC2 hervor, deren Aktivität durch Phosphorylierung reguliert wird.

Es ist bekannt, dass die Signalkinase SPAK die Aktivität von NKCC2 und NCC reguliert. Die anormale Phosphorylierung fällt mit einer untypischen Verteilung der Kinase im TAL der SORLA-defizienten Mäuse zusammen. Dies deutet auf

eine Funktion des Rezeptors beim Trafficking von SPAK hin. Durch die Identifizierung von Transportproteinen als putative Interaktionspartner SORLAs konnte diese Hypothese bekräftigt werden.

**Stichworte:** SORLA, LR11, Niere, Nebenniere, NKCC2, SPAK

# Table of Contents

<b>Abstract.....</b>	<b>2</b>
<b>Kurzfassung.....</b>	<b>4</b>
<b>Table of Contents .....</b>	<b>6</b>
<b>List of Figures.....</b>	<b>10</b>
<b>List of Tables .....</b>	<b>12</b>
<b>List of Abbreviations .....</b>	<b>13</b>
<b>1 Introduction .....</b>	<b>20</b>
1.1 The VPS10p-receptor gene-family.....	20
1.1.1 Non-mammalian VPS10p domain receptors .....	21
1.1.2 The mammalian VPS10p domain receptors .....	22
1.1.3 The VPS10p domain.....	22
1.1.4 Sortilin .....	23
1.1.4.1 Structure of Sortilin .....	24
1.1.4.2 Function of Sortilin.....	24
1.1.4.2.1 Sortilin and Regulation of Neurotrophin Activity .....	24
1.1.4.2.2 Sortilin in GLUT4-containing Vesicles .....	26
1.1.5 SORCS .....	27
1.1.5.1 Structure of the SORCSs .....	27
1.1.5.2 Function of the SORCSs.....	28
1.1.6 SORLA .....	29
1.1.6.1 Structure of SORLA .....	29
1.1.6.2 Function of SORLA.....	31
1.1.6.3 SORLA in Alzheimer's disease.....	31
1.2 SORLA in the kidney .....	33
1.2.1 The kidney .....	33
1.2.2 The renal nephron.....	34
1.3 Aim of this study .....	37
<b>2 Material and Methods.....</b>	<b>38</b>
2.1 Animal Experiments.....	38
2.1.1 Mouse Husbandry.....	38

2.1.2	Mouse Strains.....	38
2.1.3	Timed Matings .....	39
2.1.4	Physiological Parameters .....	39
2.1.4.1	Collection of Urine and Blood .....	39
2.1.4.2	Blood Pressure Telemetry .....	39
2.1.4.3	Endocrine Parameters.....	39
2.1.4.3.1	HPLC-Detection of Catecholamines and Serotonin .....	40
2.1.5	Pharmacological Experiments .....	41
2.1.5.1	Thiazide Treatment .....	41
2.1.5.2	Eplerenone Treatment .....	41
2.1.5.3	Bumetanide Treatment .....	41
2.1.5.3.1	Isolation of the Inner Stripe of the Outer Renal Medulla.....	41
2.1.5.3.2	Enrichment of TAL Tubules .....	42
2.1.5.3.3	Detection of Bumetanide-sensitive Uptake of $^{86}\text{Rb}^+$ .....	42
2.2	Microbiology .....	44
2.2.1	Culture Media and Bacteria .....	44
2.2.2	Generation of Electrocompetent Cells .....	45
2.2.3	Transformation of Bacteria .....	45
2.2.4	Yeast Two-hybrid Assay.....	46
2.3	Nucleic Acid Experiments .....	47
2.3.1	Polymerase Chain Reaction .....	47
2.3.2	Plasmid DNA Extraction .....	48
2.3.2.1	From Bacteria.....	48
2.3.2.2	From Agarose Gels .....	48
2.3.3	Total RNA Extraction .....	49
2.3.4	Enzymatic DNA Restriction .....	49
2.3.5	Agarose Gel Electrophoresis.....	50
2.3.6	DNA Ligation .....	50
2.3.7	DNA Sequencing .....	50
2.3.8	Northern Blot .....	51
2.3.9	<i>In situ</i> Probe Synthesis.....	51
2.3.10	cDNA Synthesis.....	52
2.3.11	Quantitative Real-time PCR .....	53
2.3.12	DNA Microarray-based Gene Expression Analysis .....	55

2.4	Histology .....	57
2.4.1	Cryosections .....	57
2.4.2	Paraffin Sections.....	57
2.4.3	<i>In situ</i> Staining of Sections.....	58
2.4.4	Staining of LacZ Reporter Gene Activity .....	59
2.4.5	Immunohistochemistry .....	59
2.4.5.1	Staining of SORLA in Adrenal Glands .....	59
2.4.5.2	Immuno-staining in Kidney Sections .....	60
2.5	Protein Biochemistry .....	61
2.5.1	Enrichment of Membrane Proteins.....	61
2.5.2	Total Protein Preparation.....	61
2.5.3	Protein Concentration Estimation.....	62
2.5.4	SDS Polyacrylamide Gel Electrophoresis .....	62
2.5.5	Western Blotting.....	63
2.5.6	Peptide Pulldown.....	64
2.6	Special Reagents, Kits and Consumables .....	66
<b>3</b>	<b>Results.....</b>	<b>68</b>
3.1	Renal expression profile of <i>Sorla</i> .....	68
3.2	Electrolyte homeostasis.....	72
3.3	Investigating a renal versus an adrenal phenotype in SORLA-deficient mice .....	77
3.3.1	Adrenal glands.....	79
3.3.2	Kidney .....	91
3.3.3	Confirmation of Affymetrix results via TaqMan analysis .....	97
3.4	Pharmacological Experiments.....	99
3.4.1	Blockage of NCC activity with thiazide.....	99
3.4.2	Blockage of aldosterone-induced action with eplerenone.....	101
3.4.3	Bumetanide-sensitive NKCC2-mediated K <sup>+</sup> -transport in isolated TAL .....	102
3.5	Electrolyte transporters in the distal nephron.....	105
3.6	Signaling in distal renal ion-homeostasis.....	107
3.7	Identification of interaction partners .....	109
3.7.1	Yeast Two-Hybrid .....	110
3.7.2	Peptide pull-down.....	111



<b>4 Discussion .....</b>	<b>115</b>
4.1 SORLA in the murine kidney .....	115
4.1.1 <i>Sorla</i> <sup>(-/-)</sup> animals are wasting Na <sup>+</sup> and K <sup>+</sup> respectively .....	117
4.2 SORLA and aldosterone .....	119
4.2.1 SORLA is expressed in the adrenal gland .....	119
4.2.2 SORLA-deficiency influences adrenal gland function .....	120
4.3 Effect of <i>Sorla</i> -deficiency on the renal transcriptome .....	121
4.4 Electrolyte transporters in the kidney .....	122
4.4.1 Pharmacological intervention .....	122
4.4.2 Evidence for a misregulation of NCC: <i>Sorla</i> <sup>(-/-)</sup> mice suffer from calciuria.....	124
4.4.3 Evidence for a misregulation of NKCC2: The renal <i>Sorla</i> <sup>(-/-)</sup> phenotype shares elements with the Bartter syndrome.....	124
4.4.4 <i>Sorla</i> <sup>(-/-)</sup> mice are hypotonic .....	126
4.4.5 SORLA influences SPAK activity .....	127
4.5 Conclusion: <i>Sorla</i> -deficiency has an impact on regulated salt homeostasis 128	
<b>Bibliography.....</b>	<b>131</b>
<b>Appendix .....</b>	<b>153</b>
<b>Selbständigkeitserklärung .....</b>	<b>153</b>
<b>Danksagung.....</b>	<b>154</b>
<b>Lebenslauf .....</b>	<b>155</b>
<b>Publikationen .....</b>	<b>156</b>

## List of Figures

### List of Figures

Figure 1: VPS10p-receptor family .....	20
Figure 2: Trafficking pathways of SORLA.....	30
Figure 3: The nephron.....	35
Figure 4: Workflow of target labeling for Affymetrix analysis.....	56
Figure 5: Northern blot for <i>SORLA</i> , <i>SORTILIN</i> and <i>ACTB</i> (beta-actin).....	68
Figure 6: Partial sequence of the <i>Sorla</i> cDNA covering the template region for realtime PCR .....	69
Figure 7: Transcriptional expression of all members of the VPS10p receptor family in the developing kidney and brain relative to <i>Gapdh</i> .....	70
Figure 8: In-situ hybridization of <i>Sorla</i> transcripts and <i>Sortilin</i> transcripts in the murine embryonic kidney .....	71
Figure 9: <i>Sorla</i> expression in the adult nephron .....	73
Figure 10: Excretion of Na <sup>+</sup> Cl <sup>-</sup> and K <sup>+</sup> in wild type and SORLA-deficient mice	75
Figure 11: <i>Sorla</i> expression in the adrenal gland.....	78
Figure 12: Correlation plot and unsupervised hierarchical clustering of the adrenal data sets .....	80
Figure 13: Principal component plot for adrenal gland Affymetrix data .....	81
Figure 14: Volcano plots representing the adrenal Affymetrix data.....	82
Figure 15: GO-term categories found for significantly changed probe sets in adrenal gland and kidney .....	86
Figure 16: Amounts of norepinephrine, epinephrine and dopamine in the adrenal glands of wild type and <i>Sorla</i> <sup>(-/-)</sup> mice .....	89

Figure 17: Amount of serotonin in adrenal gland, brain, intestine kidney and lung of wild type and SORLA-deficient mice under normal conditions and after thirsting.....	90
Figure 18: Correlation plot and unsupervised hierarchical clustering of the adrenal data sets .....	92
Figure 19: Principal component plot for kidney Affymetrix data .....	93
Figure 20: Volcano plots representing the renal Affymetrix data.....	94
Figure 21: Secreted hourly amount of $\text{Na}^+$ , $\text{Cl}^-$ and $\text{K}^+$ (in $\mu\text{mol}$ per hour) before and after administration sodium-hydrochlorothiazide.....	100
Figure 22: Ratio of urinary $\text{Na}^+$ and $\text{K}^+$ concentrations before and after administration of eplerenone .....	102
Figure 23: Isolation of TAL fragments and major $\text{K}^+$ transport mechanisms in TAL .....	103
Figure 24: Isolated thick ascending limb tubules .....	103
Figure 25. Bumetanide-sensitive $^{86}\text{Rb}^+$ uptake in isolated thick ascending limb tubules.....	104
Figure 26: NKCC2 in the thick ascending limb .....	105
Figure 27: Western blots of barttin, the $\alpha$ -subunit of ENaC, KCC4, $\text{Na}^+/\text{K}^+$ -ATPase, NHE3 and ROMK in wild types and mice lacking SORLA.....	106
Figure 28: Western blots of NCC in wild types and in mice lacking SORLA ....	107
Figure 29: Western blots of immunoprecipitated SPAK in wild types and in mice lacking SORLA .....	108
Figure 30: Localization of SPAK and NKCC2 in the thick ascending limb .....	109
Figure 31: Auto-activation test of the bait constructs for SORLA and SORCS3	111
Figure 32: SORLA peptide pull-down optimization whole kidney lysate .....	112
Figure 33: Pull-down of interaction partners from whole kidney lysate.....	113
Figure 34: Induction of aldosterone and its effects .....	118

Figure 35: Adrenal catecholamine synthesis pathway .....	120
Figure 36: Nephron segments targeted by pharmacological intervention .....	122
Figure 37: Na <sup>+</sup> -transporting components in TAL.....	125
Figure 38: Mechanisms responsible for the activation of NKCC2 and NCC ...	128

## List of Tables

### List of Tables

Table 1: Mouse strains with targeted disruption of the <i>Sorla</i> gene.....	38
Table 2: Bacterial culture media .....	44
Table 3: <i>Escherichia coli</i> strains .....	45
Table 4: Primers used for cloning of the carboxy-terminus of human SORLA into pBTM117c. ....	46
Table 5: Vectors used in the yeast two-hybrid screen .....	47
Table 6: PCR programs for Taq polymerase and Phusion polymerase. ....	48
Table 7: Primers used for cloning of the carboxy-terminus of human SORLA into pBTM117c .....	52
Table 8: Primers and probes used for TaqMan quantitative real-time PCRs. ....	54
Table 9: List of primary antibodies .....	63
Table 10: List of peptides covering the cytosolic tail sequence of human SORLA .....	64
Table 11: List of special chemicals, kits and consumables used.....	66
Table 12: Urine volume and urinary electrolyte concentrations .....	74
Table 13: Serum electrolyte concentrations .....	76
Table 14: Physiological parameters .....	77

Table 15: Highly differential probe sets in the adrenal gland.....	83
Table 16: Number of probe sets being significantly changed in adrenal glands ...	85
Table 17: Probe sets for genes involved in the catecholamine pathway with fold change and p-value in adrenal glands.....	87
Table 18: Highly differential probe sets in the kidney .....	95
Table 19: Number of probe sets being significantly changed in kidneys.....	96
Table 20: Fold-changes and p-values of selected transcript in adrenal gland and kidney, determined by Affymetrix and TaqMan analyses .....	98

## List of Abbreviations

%	percent
~	aproximately
×	-times / -fold
μ	Micro
10CC domain	ten conserved cystein domain
<sup>2</sup>	square
<sup>3</sup>	cubic
3'-end	three prime end
3T3-L1	"3-day transfer, inoculum 3 x 10 <sup>5</sup> " mouse embryo fibroblast tissue cell line
5'-end	five prime end
A	average logarithmic intensities
a.m.	<i>ante meridiem</i>
Ab	amyloid b
ABC	avidin-biotinylated horseradish peroxidase-complex
ACE	angiotensin-converting enzyme
<i>ACTB</i>	b-actin gene
AD	Alzheimer's Disease
AEC	3-amino-9-ethylcarbazole
AG	<i>Arbeitsgruppe</i> (German; English: work group)
Ang	angiotensin
AP	alkaline phosphatase
AP-1	adaptor-related protein complex 1
AP-2	adaptor-related protein complex 2

ApoE	apolipoprotein E
APP	amyloid precursor protein
approx.	aproximately
AQP2	aquaporin 2
Arf	ADP-ribosylation factor
ASDN	aldosterone-sensitive distal nephron
Atm	ataxia telangiectasia mutated
ATP	adenosine triphosphate
AVP	arginine vasopressin
Ba	barium
BCA	bicinchoninic acid
BCIP	5-Bromo-4-chloro-3-indolyl phosphate
BDNF	brain-derived growth factor
BHQ	black hole quencher
bp	base pairs
BSA	bovine serum albumin
BTBR mice	Jackson Laboratory BTBR T+ tf/J mouse strain
C	capacitance
°C	degrees Celsius
ca.	circa
Ca	calcium
CA1	<i>Cornu Ammonis</i> area 1
CA2	<i>Cornu Ammonis</i> area 2
Cap1	CAP, adenylate cyclase-associated protein 1
cat.	catalog
CCD	charge-coupled device
CCD	cortical collecting duct
CD	collecting duct
cDNA	complementary DNA
cf.	<i>confer</i>
Ci	Curie
CI-MPR	cation-independent mannose 6-phosphate receptor
Cl	chloride
ClC-Ka	chloride channel Ka
ClC-Kb	chloride channel Kb
ClCNKa	chloride channel Ka
ClCNKb	chloride channel Kb
CNS	central nervous system
COOH-	carboxy-
Cpeb4	cytoplasmic polyadenylation element binding protein 4
cpm	counts per minute

CPY	carboxypeptidase Y
CR domain	complement-type cluster
cRNA	complementary RNA
CNT	connecting tubule
c <sub>T</sub>	cycle threshold
c-terminal	carboxyl-terminal
CTP	cytidine triphosphate
D	difference
Da	Dalton
DAB	diaminobenzidine
Dbh	dopamine beta-hydroxylase
DCT	distal convoluted tubule
ddAVP	desmopressin
Dde	DOPA decarboxylase
DIG	digoxigenin
DMSO	dimethyl sulfoxide
DNA	deoxyribonucleic acid
DOC buffer	deoxycholate buffer
Doc.	document
dpc	days post coitum
dT	deoxythymidylic acid
<i>E. coli</i>	<i>Escherichia coli</i>
e.g.	<i>exempli gratia</i>
E12.5	embryonal day 12.5
EDTA	ethylenediaminetetraacetic acid
EGF	epidermal growth factor
EGTA	ethylene glycol tetraacetic acid
ENaCa	epithelial Na <sup>+</sup> -channel, α-subunit
ER	endoplasmic reticulum
ERK	extracellular signal-related kinase
F	farad
FAM	carboxyfluorescein
FC	fold change
FCS	fetal calf serum
FMP	Leibniz-Institut für Pharmakologie
G	glomerulus
g	gram
× g	times acceleration of gravity
GAPDH	glyceraldehyde 3-phosphate dehydrogenase
<i>Gapdh</i>	glyceraldehyde 3-phosphate dehydrogenase gene
gcRMA	guanine cytosine robust multichip analysis

GGA	Golgi-localized g-adaptin ear-containing Arf-binding protein
GLUT4	insulin-responsive glutamine transporter type 4
GO	Gene Ontology
GTP	guanosine triphosphate
h	hour
H2afb3	H2A histone family, member B3
HAB	head activator binding protein
Habp2	hyaluronan binding protein 2
HPLC	high-pressure liquid chromatography
HRP	horseradish peroxidase
I.D.	inside diameter
i.e.	<i>id est</i>
Ifi202b	interferon activated gene 202B
IPTG	isopropyl $\beta$ -D-1-thiogalactopyranoside
IRC	insulin-responsive compartment
Isg15	Isg15 ubiquitin-like modifier
ISH	<i>in situ</i> hybridization
ISOM	inner stripe of the outer medulla
IVT	<i>in vitro</i> transcription
JNK	c-Jun N-terminal kinase
K	Kelvin
k	kilo-
K	potassium
kb	kilobases
KCC4	K <sup>+</sup> /Cl <sup>-</sup> -cotransporter 4
Kcne3	potassium voltage-gated channel, Isk-related family, member 3
l	liter
LDL	low-density lipoprotein
LDLR	low-density lipoprotein receptor
log <sub>2</sub>	logarithm to the base of 2
LR11	low-density lipoprotein receptor relative with 11 ligand-binding repeats
LRP2	low density lipoprotein receptor-related protein 2
M	logarithmic intensity ratios
m	meter
m	milli-
M	mol/l
MAP	mean arterial pressure
Mcm6	minichromosome maintenance complex component 6
MD	macula densa
MDC	Max-Delbrück-Centrum für Molekulare Medizin



Mfap1	microfibrillar-associated protein 1
MGB	minor groove binder
min	minute
mmHg	millimeters of mercury
mol	mole
mRNA	messenger RNA
MS	mass spectrometry
n	nano-
n	number/quantity
Na	sodium
NBT	nitro blue tetrazolium
NCC	Na <sup>+</sup> /Cl <sup>-</sup> -cotransporter
NGF	nerve growth factor
NH <sub>2</sub> -	amino-
NHE3	Na <sup>+</sup> /H <sup>+</sup> -Exchanger 3
NKCC1	Na <sup>+</sup> /K <sup>+</sup> /Cl <sup>-</sup> -cotransporter 1
NKCC2	Na <sup>+</sup> /K <sup>+</sup> /Cl <sup>-</sup> -cotransporter 2
No.	number
NP-40	Nonidet P-40
NT3	neurotrophin 3
NT4	neurotrophin 4
n-terminal	amino-terminal
OD <sub>600</sub>	optical density at 600 nm wavelength
P	phosphor
p	pico-
p	p-value
P/N	part number
PACS1	phosphofurin acidic cluster sorting protein
PAGE	polyacrylamide gel electrophoresis
PBS	phosphate-buffered saline
PBST	PBS cotaining 0.05% Tween-20
PDGF-BB	platelet-derived growth factor (B-chain homodimer)
PEP1	carboxypeptidase Y-deficient gene
PEP1p	carboxypeptidase Y-deficient gene protein
PFA	para-formaldehyde
pH	<i>pondus Hydrogenii</i> / <i>potentia Hydrogenii</i> (negative decimal logarithm of the hydrogen ion activity)
Pnmt	phenylethanolamine N-methyltransferase
Pnpt1	polyribonucleotide nucleotidyltransferase 1
PP	protein phosphatase

proBDNF	brain-derived growth factor precursor
proNGF	nerve growth factor precursor
Pttg1	pituitary tumor-transforming 1
R	electrical resistance
RAAS	renin-angiotensin-aldosterone system
RAP	receptor associated protein
RAS	renin-angiotensin system
Rb	rubidium
rcf	relative centrifugal force
Rev.	revision
RIPA buffer	radio immunoprecipitation assay buffer
RMA	robust multichip analysis
RNA	ribonucleic acid
Rnase4	ribonuclease, RNase A family, 4
ROMK	renal outer medullary potassium channel
Rpgrip1	retinitis pigmentosa GTPase regulator interacting protein 1
rpm	revolutions per minute
RT-PCR	reverse transcriptase PCR
Sart3	squamous cell carcinoma antigen recognized by T cells 3
Scd2	stearoyl-CoA desaturase 2
SDS	sodium dodecyl sulfate
sec	seconds
Ser	serine
Sf9	immortalized Spodoptera frugiperda ovary cell line
SH2	src homology 2
SH3	src homology 3
Slc	solute carrier
Slc18a1	vesicular monoamine transporter 1
SNX	sorting nexin
SORCS1	sortilin-related VPS10p-domain containing receptor 1 protein
<i>Sorcs1</i>	gene/mRNA encoding the SORCS1 protein
SORCS2	sortilin-related VPS10p-domain containing receptor 2 protein
<i>Sorcs2</i>	gene/mRNA encoding the SORCS2 protein
SORCS3	sortilin-related VPS10p-domain containing receptor 3 protein
<i>Sorcs3</i>	gene/mRNA encoding the SORCS3 protein
Sord	sorbitol dehydrogenase
SORLA	sortilin-related receptor, LDLR class A repeats-containing protein
<i>Sorla</i>	gene/mRNA encoding the SORLA protein
<i>SORLA</i>	human gene/mRNA encoding the SORLA protein
sortilin	sortilin protein

<i>Sortilin</i>	gene/mRNA encoding the sortilin protein
<i>SORTILIN</i>	human gene/mRNA encoding the sortilin protein
SPAK	serine threonine kinase 39 (STE20/SPS1 homolog)
SSC	saline sodium citrate buffer
T4	bacteriophage T4
TAL	thick ascending limb of the loop of Henle
Taq	<i>Thermus quaticus</i>
TE	Tris EDTA buffer
TGN	trans Golgi network
Th	tyrosine hydroxylase
Thr	threonine
T <sub>m</sub>	melting temperature
Tmem87a	transmembrane protein 87A
Tris	tris(hydroxymethyl)-aminomethan
Trk receptor	tyrosine kinase receptor
tRNA	transfer RNA
TTP	thymidine triphosphate
Txn14a	thioredoxin-like 4A
U	unit
UK	United Kingdom
USA	United States of America
UTR	untranslated region
UV	ultraviolet
V	electromotive force / volt
(v/v)	volume per volume
VHS domain	Vps-27 Hrs STAM domain
viz.	<i>videlicet</i>
Vps	vacuolar protein sorting
VPS10p	vacuolar protein sorting gene 10 protein
(w/v)	weight per volume
(w/w)	weight per weight
WNK	WNK lysine deficient protein kinase
x	-times / -fold
X-gal	bromo-chloro-indolyl-galactopyranoside
Ω	ohm

# 1 Introduction

## 1.1 The VPS10p-receptor gene-family

Recently, a group of type 1 transmembrane proteins with single transmembrane domains and short carboxyl-terminal (c-terminal) cytosolic domains was identified. Its members are characterized by the presence of a homologous amino-terminally (n-terminally) located region of about 700 amino acids. This common feature – the so-called VPS10p domain, being named after the yeast protein VPS10p – endows the gene family with its name: the vacuolar protein sorting 10 protein-receptor (VPS10p-receptors) family (figure 1).

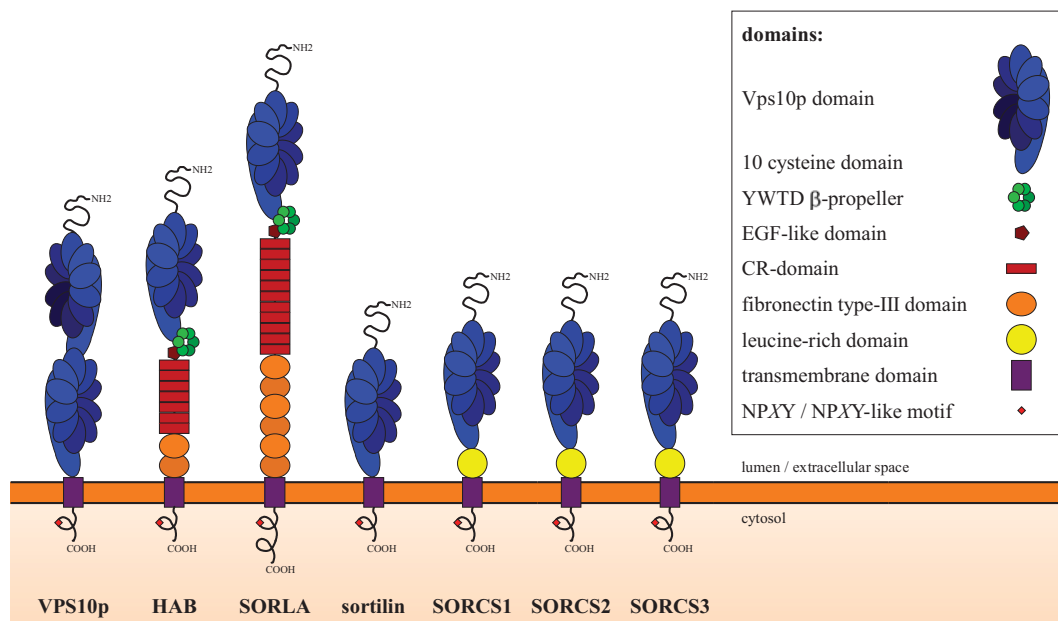


**Figure 1: VPS10p-receptor family.** Cartoon depicting the domain structure of yeast VPS10p, hydra HAB and mammalian members of the VPS10p-receptor family (SORLA, sortilin, SORCS1, SORCS2, and SORCS3). In contrast to other members of the family, SORLA and HAB share structural elements with members of the LDL-receptor family (YWTD  $\beta$ -propeller, EGF-like domain, CR-domain repeats and fibronectin type-III domains).

### 1.1.1 Non-mammalian VPS10p domain receptors

To maintain organelle function in eukaryotic cells, it is important that proteins performing those tasks reach their destination organelle. A system playing a major function in organelle-targeted protein-distribution is the trans-Golgi network (TGN). It directs newly synthesized proteins towards secretory pathways or routes them to endosomal, lysosomal or vacuolar compartments (Alberts, et al., 1995).

By mutational analysis, a number of genes were identified as being essential for proper vacuolar function in baker's yeast (*Saccharomyces cerevisiae*). Assuming a role in protein transport to the vacuole, these genes were designated vacuolar protein sorting (*VPS*)-genes. Gene number ten of this group (*VPS10*; official name: *PEP1*) codes for the protein VPS10p (VPS10 protein, also PEP1p, figure 1) (Marcusson, et al., 1994).

The 210 kDa type 1 transmembrane receptor VPS10p, which mainly localizes to a late Golgi compartment, is the sorting receptor for multiple vacuolar hydrolases. This protein has been shown to be involved in sorting of the soluble yeast vacuolar carboxypeptidase Y (CPY) from the late Golgi compartment to the vacuole via a prevacuolar endosome-like compartment. To achieve this function, the receptor cycles between the late Golgi and prevacuolar endosome-like compartments (Cereghino, et al., 1995; Cooper and Stevens, 1996; Marcusson, et al., 1994; Vida, et al., 1993).

This process is similar to the function carried out by cation-independent mannose 6-phosphate receptors (CI-MPRs) in mammalian cell types. CI-MPRs bind their soluble target enzymes in the TGN and shuttle them to endosomal or lysosomal compartments using small transport vesicles. To achieve this function, the CI-MPRs directly or indirectly bind to adaptor proteins, which initiate vesicular budding by recruiting clathrin and coupling the transport vesicles to the cytoskeleton (Bonifacino and Rojas, 2006; Kornfeld, 1992).

That the VPS10p domain developed early in eukaryotic evolution and also fulfills versatile functions on other branches of the evolutionary tree, is reflected in the metazoan *Chlorohydra viridissima* (hydra) by the head activator binding protein (HAB), a homologue of the mammalian SORLA (figure 1). In contrast to the yeast sorting protein VPS10p, HAB is involved in signaling processes. The 200 kDa protein was isolated by affinity chromatography for factors that bind the head activator peptide of hydra. This neurotrophic peptide stimulates cells to divide. It is responsible for the determination and the final differentiation of nerve cells and head-specific epithelial cells (Schaller, et al., 1996). As a head activator binding receptor, HAB is involved in the head-specific proliferation and determination of stem cells in the freshwater polyp (Hampe, et al., 1999).

### **1.1.2 The mammalian VPS10p domain receptors**

Previously, five receptors sharing the VPS10p domain have been identified and characterized in humans and mice (figure 1): SORLA (Hermans-Borgmeyer, et al., 1998; Jacobsen, et al., 1996), sortilin (Navarro, et al., 2001; Petersen, et al., 1997), SORCS1 (Hermey, et al., 2003; Hermey, et al., 1999) SORCS2 (Nagase, et al., 2000; Rezgaoui, et al., 2001) and SORCS3 (Hampe, et al., 2001; Hermey, et al., 2004; Kikuno, et al., 1999).

All five receptors possess signals for rapid internalization and intracellular sorting in their short carboxyl-terminal cytoplasmic domains (Hermey, et al., 2004). Because of this fact and because of their homology to the yeast VPS10p, a function for the mammalian VPS10p-receptors in trafficking at the TGN has been anticipated.

The most important functions of these receptors are believed to lie in the nervous system, since all of them are expressed in the adult nerve cells and are highly regulated during embryogenesis (Ben-Ari, 2001; Hermans-Borgmeyer, et al., 1998; Hermans-Borgmeyer, et al., 1999; Hermey, et al., 2004; Hermey, et al., 2001; Rezgaoui, et al., 2001). This distinct expression pattern suggests participation of the different VPS10p-receptors in specific neuronal processes. But further expression of VPS10p-receptors in non-neuronal tissue also hints at additional functions of these proteins in other organs.

### **1.1.3 The VPS10p domain**

Before outlining the individual mammalian members of the VPS10p-receptor family and their distinctive features, this section deals with the most significant feature they have in common: the VPS10p domain. There is only a modest sequence similarity between the different VPS10p domains, but they all share common structural features.

Sortilin's VPS10p domain is the best-characterized so far. Its structure was previously predicted by computational methods (Paiardini and Caputo, 2008). Recently, Quistgaard et al. determined the crystal structure of sortilin in complex with its ligand neurotensin (Quistgaard, et al., 2009).

The mature VPS10p domain can be subdivided into two structurally confined sections. At the c-terminal side of sortilin's VPS10p domain, two small (56 and 82 amino acid residues, respectively) domains constitute the so-called 10CC module (depicted as part of the VPS10p domain in figure 1), a motif containing ten conserved cysteines present in all members of the VPS10p family known so far. In

contrast to the rest of the VPS10p domain, the 10CC domain is very similar in all the receptors in terms of primary structure and spacing of the ten cysteines. The large (531 amino acid residues in sortilin) n-terminal portion of the domain forms a ten-bladed  $\beta$ -sheet-propeller. To date, the VPS10p domain receptors form the only known protein family comprising this structural feature. The tunnel formed by the  $\beta$ -propeller is on one side partially blocked by interactions with the 10CC module. The binding of ligands occurs at the inner rim. Different binding partners most probably not only have to compete for their actual binding site, but could also be subject to mutual sterical hindrance within the limited tunnel (Quistgaard, et al., 2009).

The complex structural features of the VPS10p domain is further modified by several posttranslational processing steps. VPS10p-receptors are translated as so-called pre-pro-proteins. Being integral transmembrane proteins, they carry an n-terminal signal peptide (prepeptide) for co-translational translocation into the endoplasmic reticulum (ER). A second peptide (44-100 amino acid residues), the propeptide, is cleaved off by a furin-like protease activity while the receptors transit the TGN (Hermey, et al., 2003; Jacobsen, et al., 2001; Munck Petersen, et al., 1999). The propeptide can have an intrinsic chaperone-like function, facilitating correct folding of the VPS10p domain and changing or blocking the receptors affinity for premature binding of ligands (Jacobsen, et al., 2001; Munck Petersen, et al., 1999; Westergaard, et al., 2004). However, it has been shown for SORCS1 and SORCS3, that they do not require cleavage of the propeptide for ligand binding (Hermey, et al., 2003; Westergaard, et al., 2005).

#### **1.1.4 Sortilin**

The structurally simplest mammalian VPS10p-receptor (cf. figure 1) is sortilin. It was first characterized after purification by affinity-chromatography against the receptor-associated protein RAP, a chaperone binding to receptors of the LDL receptor gene family in the endoplasmic reticulum and thereby preventing premature ligand-binding (Petersen, et al., 1997). In parallel, it was identified as neurotrophin receptor (Mazella, et al., 1998; Petersen, et al., 1999) and as a protein abundant in the low density microsomal vesicles containing the insulin-responsive glucose transporter type 4 (GLUT4) in adipocytes (Morris, et al., 1998).

Sortilin is expressed in a variety of tissues, notably in brain, spinal cord, muscle, testis and kidney. In neuronal tissue, the receptor is found in pyramidal neurons of the cerebral cortex and the hippocampus, in cortical glia, in granule cells of the dentate gyrus and cerebellar Purkinje cells, in postmitotic retinal ganglion cells and in the superior cervical ganglion and dorsal root ganglia (Arnett, et al., 2007; Jansen, et al., 2007; Nykjaer, et al., 2004; Sarret, et al., 2003).

At a subcellular level, approximately 90% of the receptor molecules can be found in the Golgi. Only a minor fraction can be detected at the cell surface at any given time (Morris, et al., 1998; Petersen, et al., 1997). Together with the ability to internalize surface-bound ligands, this finding supports the assumption of sortilin being a trafficking receptor. Retrograde transport of sortilin from the late endosome to the TGN is depending on the cytosolic adaptor sortin nexin 1 (Mari, et al., 2008).

#### **1.1.4.1 Structure of Sortilin**

Even though its extracellular domain consists of only one domain (Petersen, et al., 1997; Quistgaard, et al., 2009), it has been reported, that this domain in sortilin can bind multiple ligands including lipoprotein lipase (Nielsen, et al., 1999), precursor of sphingolipid activator proteins (PSAP) (Hassan, et al., 2004; Lefrancois, et al., 2003), sphingomyelinase (Ni and Morales, 2006), neurotensin (Mazella, et al., 1998; Petersen, et al., 1999) and precursors of the nerve growth factor (proNGF) (Nykjaer, et al., 2004) and the brain-derived growth factor (proBDNF) (Chen, et al., 2005; Teng, et al., 2005).

The carboxyl-terminal region carries a lysosomal sorting motif, the so-called acidic-cluster dileucine motif (DxxLL), shared by the mannose-6-phosphate receptors. This element mediates Golgi-localized  $\gamma$ -ear-containing Arf-binding protein (GGA) -dependent intracellular trafficking from the Golgi apparatus to late endosomes (Bonifacino and Traub, 2003). In addition, sortilin carries a YSVL-motif for rapid internalization (Morinville, et al., 2004; Nielsen, et al., 2001; Tooze, 2001).

The functionality of the receptor's carboxyl-terminal domain as mediator for trafficking has been demonstrated by Nielsen et al. by fusing the cytoplasmic tail of sortilin to the luminal domain of the cation-independent mannose 6-phosphate receptor (CI-MPR). Expression of this chimeric receptor led to a full rescue of the misrouting of lysosomal hydrolases in otherwise CI-MPR-deficient cells (Nielsen, et al., 2001).

#### **1.1.4.2 Function of Sortilin**

##### **1.1.4.2.1 Sortilin and Regulation of Neurotrophin Activity**

Even though the percentage of receptor molecules on the cell surface may be small, it plays an important role in neurotrophin action.

Neurotrophins are growth factors regulating neuronal survival, axon and dendrite specification, target innervations and synaptogenesis (Chao, 2003). They evolved early in the vertebrate lineage from gene duplication events (Hallböök, 1999).



Four neurotrophins, all sharing sequential and structural homologies, are expressed in mammals: nerve growth factor (NGF), brain-derived neurotrophic factor (BDNF), neurotrophin 3 (NT3) and neurotrophin 4 (NT4) (Reichardt, 2006). Various functions of neurotrophins are mediated by binding to neurotrophic tyrosine kinase (Trk) receptors and subsequent downstream signaling. There are three main types of Trk receptors: TrkA is a receptor for NGF, TrkB a receptor for BDNF and NT4, and TrkC is a receptor for NT3 (Lewin and Barde, 1996). Neurotrophic signaling is altered by binding to the low-affinity NGF receptor  $p75^{\text{NTR}}$ , which is a member of the tumor necrosis receptor superfamily (Carter and Lewin, 1997).  $p75^{\text{NTR}}$  can form heteromeric receptor complexes with Trk receptors, but it can also act independently to modulate synaptic activity or switch between antipodal cell programs such as survival or cell death (Chao, 2003; Reichardt, 2006).

The survival actions of  $p75^{\text{NTR}}$  are mediated by mature neurotrophins whereas apoptotic effects are triggered by precursors of NGF (proNGF) or BDNF (proBDNF) (Lee, et al., 2001). Binding of the pro-convertase-cleaved mature form of NGF to a receptor-complex of  $p75^{\text{NTR}}$  and TrkA triggers signaling cascades for cell survival. In contrast, a heteromeric complex of  $p75^{\text{NTR}}$  with sortilin, initiated by the binding the pro-domain of proNGF to sortilin, selectively induces apoptosis (Nykjaer, et al., 2004). Specific sortilin-expression can selectively trigger the cell-death of particular subsets of neuronal cells upon  $p75^{\text{NTR}}$ -mediated pro-apoptotic signal induced by premature neurotrophins. A similar mechanism was shown for proBDNF, whose regulated secretion is also depending on sortilin (Chen, et al., 2005; Teng, et al., 2005).

Different  $p75^{\text{NTR}}$ -mediated signaling mechanisms occur at different subcellular localizations. While activation of the JNK-pathway takes place at the cell-surface (Reichardt, 2006), other signals caused by  $p75^{\text{NTR}}$  require trafficking of the receptor to recycling endosomes to be triggered (Bronfman, et al., 2003). The transport of  $p75^{\text{NTR}}$  is not clearly understood, but it could be facilitated by sortilin. This assumption is strengthened by the facts that Sf9 cells – which do not express sortilin – are unable to internalize  $p75^{\text{NTR}}$  (Gargano, et al., 1997), and that proNGF is not endocytosed by cells expressing  $p75^{\text{NTR}}$  but lacking sortilin (Nykjaer, et al., 2004). Additionally, internalized proNGF can be processed in endosomes and subsequently released in the form of mature NGF, which again activates signaling via extracellular signal-related kinase (ERK) (Boutillier, et al., 2008).

To which extend this mode of action plays a role under physiological conditions remains unclear. However in pathophysiological conditions, such as Alzheimer's disease, retrovirus-induced spongiform encephalomyelopathies, seizures or injuries of the central nervous system, increased proneurotrophin-levels and increased co-expression of  $p75^{\text{NTR}}$  and sortilin suggest a role for sortilin/ $p75^{\text{NTR}}$ -mediated cell-death (Fahnestock, et al., 2001; Harrington, et al., 2004; Jansen, et al., 2007; Stoica, et al., 2008; Volosin, et al., 2008). In addition, transection of the sciatic nerve is accompanied by a selective elimination of neurons expressing both recep-

tors (Arnett, et al., 2007), and during naturally occurring cell-death in the early phase of retinal development, proNGF forms a complex with sortilin and p75<sup>NTR</sup> (Nakamura, et al., 2007).

#### **1.1.4.2.2 Sortilin in GLUT4-containing Vesicles**

With the parallel discovery of sortilin by different groups, the receptor appeared in functionally different backgrounds right from the start. Morris et al. identified sortilin as being present in glucose transporter 4-containing vesicles of adipocytes (Morris, et al., 1998).

Glucose transporter 4 (GLUT4), the major insulin-responsive glucose transporter, belongs to a large family of 12 membrane-spanning domain proteins called the facilitative glucose transporter proteins. Being highly expressed in striated muscle and adipose tissue, GLUT4 is responsible for the post-prandial removal of glucose from the circulation. In the basal state, the transporter undergoes a slow but continuous recycling between the plasma membrane and several intracellular compartments, with only a small fraction of the total GLUT4 protein pool localized to the plasma membrane. Upon acute insulin-treatment, however, the amount of the transporter expressed on the cell surface is increased up to ten times (Holman and Sandoval, 2001; Pessin, et al., 1999).

Several lines of evidence show the importance of proper function of the Golgi-localized  $\gamma$ -ear-containing Arf-binding proteins (GGA proteins) for the biosynthetic sorting of Glut4 from the TGN into so-called insulin-responsive compartments (IRCs) (Hou, et al., 2006; Li and Kandror, 2005). The cargo-binding domain of GGA (VHS domain) cannot associate with GLUT4 directly. Containing a VHS consensus-binding motif (DxxLL) in its cytosolic tail, sortilin has been shown to directly interact with GGA adaptor proteins (Nielsen, et al., 2001) and to play an important role in the formation of the specialized GLUT4 IRC in adipocytes (Shi and Kandror, 2005). It was also demonstrated by surface-biotinylation, that the surface-expression of sortilin is upregulated in 3T3-L1 cells (Morris, et al., 1998).

In 3T3L1 cells, IRCs are formed during the differentiation from the fibroblast to adipocyte state. IRCs form in concert with the induction of sortilin expression before the expression of GLUT4. Moreover, too early overexpression of GLUT4 leads to rapid degradation of the transporter, whereas overexpression of sortilin stabilizes the GLUT4 protein, increases the formation of the IRC and promotes insulin-stimulated glucose uptake (Shi and Kandror, 2005). Supporting the role of sortilin as a cargo adaptor linking GLUT4 to GGA-coated transport vesicles, a direct interaction between the luminal domains of GLUT4 and sortilin was shown by chemical cross-linking and yeast two-hybrid studies (Shi and Kandror, 2007).

### 1.1.5 SORCS

To this day, little is known about a subgroup within the mammalian VPS10p-receptor group, that is formed by the sortilin-related VPS10p domain containing receptors SORCS1 (Hermey, et al., 2003; Hermey, et al., 1999), SORCS2 (Nagase, et al., 2000; Rezgaoui, et al., 2001) and SORCS3 (Hampe, et al., 2001; Hermey, et al., 2004; Kikuno, et al., 1999), depicted on the right side of figure 1.

The neuronal expression of the mammalian SORCS proteins is well characterized. SORCS1 is expressed in neurons of the third and fifth layer of the cerebral cortex, in pyramidal neurons of the CA1 region of the hippocampus and in Purkinje cells of the cerebellum and in the olfactory tubercle (Hermey, et al., 2003; Hermey, et al., 2004; Hermey, et al., 2001). SORCS2 is expressed in neurons in layer 5 of the cerebral cortex, in pyramidal neurons in the CA2 region of the hippocampus, in the dentate gyrus and in Purkinje cells in lobules seven to nine of the cerebellum (Hermey, et al., 2004). SORCS3 can be found in layer five and six of the cerebral cortex, in the hippocampal CA1 region, in basket and stellate cells of the cerebellum and in the mitral cell layer of the olfactory bulbs (Hermey, et al., 2004; Westergaard, et al., 2004). The differential neuronal expression of *Sorcs1* and *Sorcs3* in the hippocampus and dentate gyrus is regulated by synaptic activity, as studies based on kainic acid-induced seizures revealed (Hermey, et al., 2004).

Extraneuronal expression of SORCS receptors has not been studied extensively yet. Northern blot analysis of different tissues suggests *Sorcs1* expression in heart, liver, small intestine and kidney (Hermey, et al., 2003; Hermey, et al., 1999). *Sorcs2* transcripts are found in lung, testis, heart, kidney and epithelial cells of the esophagus (Goldstein, et al., 2007; Rezgaoui, et al., 2001).

In contrast to the other two mammalian VPS10p-receptors sortilin and SORLA, SORCS3 and probably SORCS2 are primarily expressed on the cell surface (Westergaard, et al., 2005). A more complex situation is true for SORCS1: The receptor is seen in different isoforms, which are localizing to different extents either towards the cell surface, to intracellular membranes, or both (Hermey, et al., 2003; Nielsen, et al., 2008).

#### 1.1.5.1 Structure of the SORCSs

The three SORCS receptors each contain an approximately 300 residues long leucine-rich domain between the VPS10p domain and the transmembrane domain (cf. figure 1). This region harbors successive segments of imperfect leucine/isoleucine/valine repeats (Hermey, et al., 1999). Similar repeats found in other receptors and soluble proteins (Dufau, 1998; Hauser, et al., 1997; Selfors, et al., 1998) have been implicated in protein-protein interactions (Jiang, et al., 1995; Kajava, et al., 1995; Kobe and Deisenhofer, 1995).

The cytosolic portion of SORCS1 is subject to alternative splicing (Hermey, et al., 2003; Hermey and Schaller, 2000). Four variants of human SORCS1 are listed in the UniProt database. Three of these isoforms (2, 3 and 4) contain src homology 2 (SH2) domain binding motifs (YxxØ), and di-leucine motifs, described as sorting/internalization signals as well as binding sites of adaptor proteins in signal transduction pathways (Hermey, et al., 1999; Pawson and Scott, 1997; Takatsu, et al., 2001; Zhu, et al., 2001). Polyproline-motifs (PxxP) binding to src homology 3 (SH3) domains can be found in all isoforms (Cohen, et al., 1995; Hermey, et al., 1999; Pawson, 1995). The difference in composition of signalling motifs in the different receptor isoforms explains their abovementioned distinct subcellular distribution (Hermey, et al., 2003; Nielsen, et al., 2008).

#### 1.1.5.2 Function of the SORCSs

Currently, little is known about the function of SORCS receptors. The platelet-derived growth factor-BB (PDGF-BB) has been identified as ligand for SORCS1 and SORCS3 (Hermey, et al., 2006), suggesting a role for these receptors in neurogenesis (Mohapel, et al., 2005). SORCS3 additionally binds NGF and proNGF (Westergaard, et al., 2005).

Concerning *Sorcs1*, two publications reported the mapping of the receptor gene to a type-2 diabetes locus affecting fasting insulin levels in humans and mice (Clee, et al., 2006; Goodarzi, et al., 2007). Obese BTBR mice, a mouse model for obesity-induced diabetes type-2, carry a mutation within the *Sorcs1* gene. Realtime-PCR revealed that control animals express ten times as much *Sorcs1* compared to BTBR mice (Clee, et al., 2006).

Another genetic screen linked *Sorcs1* with a locus associated with late-onset Alzheimer's disease (Grupe, et al., 2006). However, the identified marker was not significant in all samples used in this study. So a potential involvement of SORCS1 in Alzheimer's disease remains to be confirmed by other studies.

### 1.1.6 SORLA

One of the best characterized members of the VPS10p-receptor family is SORLA (**sortilin**-related receptor, **L**[DLR class] **A** repeats-containing). This receptor, also known as LR11 (**low**-density lipoprotein receptor **relative** with **11** ligand-binding repeats), is an orthologue of the hydra HAB (head activator binding protein) (Hampe, et al., 2000; Jacobsen, et al., 1996).

Similar to sortilin, the cytoplasmic tail of SORLA, if fused to the luminal domain of the cation-independent mannose 6-phosphate receptor (CI-MPR), can fully rescue a misrouting of lysosomal hydrolases in otherwise CI-MPR-deficient cells (Nielsen, et al., 2007). This goes along with the observation that in transfected cells, only 10% of the receptor molecules are located on the cell surface. A surplus of the receptor is located on intracellular membranes, mainly in the TGN and in early endosomes (Jacobsen, et al., 2001).

SORLA is expressed in a variety of tissues, with highest expression the central nervous system. In the brain, SORLA expression has been shown in pyramidal neurons and glia of the frontal cortex, pyramidal neurons in the hippocampus, cerebral Purkinje cells and granule cells of the dentate gyrus (Nixon and Cataldo, 2006). Outside the brain, expression of the receptor is found in liver, kidney, lung, testes, lymph nodes, uterus, adrenal and thyroid glands (Jacobsen, et al., 2001; Jacobsen, et al., 1996; Yamazaki, et al., 1996).

#### 1.1.6.1 Structure of SORLA

SORLA shows all characteristics of the VPS10p family: an n-terminal VPS10p domain with the highly conserved 10-cystein domain and a cytosolic c-terminus with internalization signals. Additionally, this receptor shares elements typical for members of the low-density lipoprotein receptor (LDL-receptor) family such as complement type clusters (CR-domains), endothelial growth factor-like (EGF-like) domain, and YWTD  $\beta$ -propeller (Nykjaer and Willnow, 2002). Thus, it is sometimes also annotated as member of the latter gene family.

SORLA is an endocytotic receptor capable of binding and internalizing surface-bound ligands such as neuropeptides, apolipoprotein E, lipoprotein lipase and the receptor-associated protein RAP (Jacobsen, et al., 2001; Jacobsen, et al., 2002; Schmidt, et al., 2007). Like most VPS10p domain receptors, the VPS10p domain of SORLA binds its own propeptide and therewith abolishes binding of ligands to this domain. But in contrast to neuropeptides, the binding of RAP, apolipoprotein E and lipoprotein lipase is not inhibited by the propeptide, demonstrating that different binding sites exist in the extracellular receptor domain (Jacobsen, et al., 2001).

Within the 56 amino acid sequence of the cytoplasmic domain of SORLA, three sequence motifs are worth being mentioned (Jacobsen, et al., 2001; Jacobsen, et al., 1996; Schmidt, et al., 2007; Yamazaki, et al., 1996). Firstly, it harbors a FANSHY-motif – a motif similar to FDNPxY. FDNPxY or NPxY motifs found in many endocytotic receptors and essential for clathrin-mediated endocytosis (Chen, et al., 1990). The second interesting sequence is an acidic cluster motif (DDLGEDDED), identified as interaction site for PACS-1 (phosphofurin acidic cluster sorting protein-1), an adaptor protein responsible for trans-Golgi network (TGN) retrieval (Wan, et al., 1998). The third motif with the sequence DDVPM has been reported to be involved in GGA-binding (Jacobsen, et al., 2002).

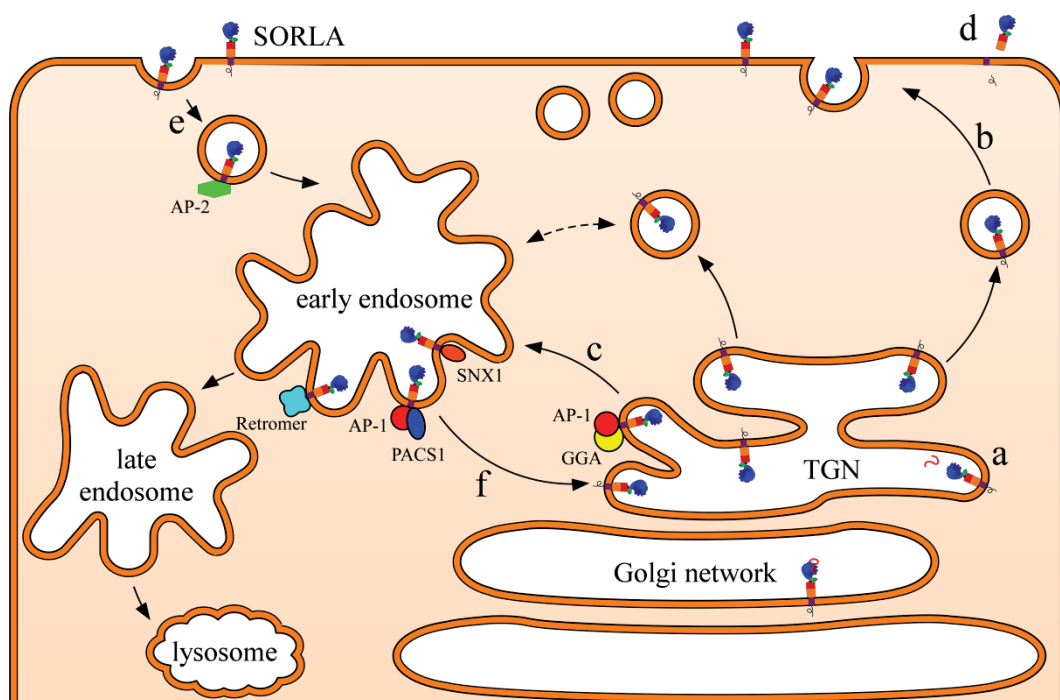


**Figure 2: Trafficking pathways of SORLA.** After translation, SORLA passes the trans-Golgi network (TGN), where the propeptide is cleaved off (a). The mature receptor takes the constitutive secretory route to the cell surface (b) or leaves the TGN via anterograde transport towards early endosomes (c), which is mediated by interaction with adaptors of the GGA family. On the cell surface, SORLA molecules can be cleaved at juxtamembrane extracellular sites (Hermey, et al., 2006) followed by  $\gamma$ -secretase cleavage, upon which the intracellular domain is released into the cytosol (d). Normally, however, re-internalization through clathrin-coated pits occurs upon interaction with the AP-2 complex, routing the receptor to the early endosome compartment (e). From there it is trafficked retrogradely back to the TGN (f) probably by interaction with the retromer complex, SNX1 or PACS1 (in conjunction with AP-1). The graphic was adopted from Willnow et. al (Willnow, et al., 2008).



Besides facilitating rapid internalization via the acidic cluster dileucine-like motif (DDLGEDDED) (Jacobsen, et al., 2001; Jacobsen, et al., 2002) and interacting with members of the GGA family (Jacobsen, et al., 2001; Jacobsen, et al., 2002; Schmidt, et al., 2007), the cytosolic tail of SORLA is also capable of binding the ubiquitous adaptor complexes AP-2. The interaction with AP-2 is obligatory for the receptor to undergo internalization towards the early endosome compartment (Nielsen, et al., 2007). From there, SORLA is retrogradely transported back to the TGN (Nielsen, et al., 2007; Seaman, 2004; Seaman, 2007).

#### **1.1.6.2 Function of SORLA**

SORLA binds ApoE and lipoprotein lipase as ligands with its complement type repeat domains (CR-domains) (Jacobsen, et al., 2001), therewith showing a high functional similarity to members of the LDL receptor family. Accordingly, it may play a role in cholesterol metabolism, as this is one key function of members of the LDL-receptor family (Nykjaer and Willnow, 2002). But SORLA clearly acts in more versatile ways: soluble SORLA has been identified as a marker for atherosclerosis (Bujo and Saito, 2000; Matsuo, et al., 2009) and the receptor plays a role in smooth muscle migration (Jiang, et al., 2008; Zhu, et al., 2004).

#### **1.1.6.3 SORLA in Alzheimer's disease**

To appreciate the contribution of SORLA to Alzheimer's Disease (AD) pathogenesis, it is important to review some molecular key elements of this disease.

The amyloid precursor protein (APP), a type-1 membrane protein expressed in neuronal and non-neuronal cell types, is a key player in AD pathology. APP is subject to proteolysis by two pathways: the amyloidogenic and the non-amyloidogenic pathway. The first one involves  $\beta$ - and  $\gamma$ -secretase activity, finally leading to the production of A $\beta$ , the main component of amyloid plaques (also called senile plaques), a pathological hallmark of AD. The non-amyloidogenic pathway, defined by  $\alpha$ - and  $\gamma$ -secretase cleavage, does not generate the AD-typical A $\beta$  (King and Scott Turner, 2004; Reinhard, et al., 2005).

The involvement of SORLA in the progression of Alzheimer's disease (AD) was first suggested by the finding, that the receptor is transcriptionally downregulated in patients with the sporadic form of AD (Scherzer, et al., 2004), but not in familial forms of this disease (Dodson, et al., 2006). Subsequently it was shown that SORLA colocalizes with APP to Golgi and to endosomal compartments and that overexpression of *Sorla* leads to reduced processing of APP into A $\beta$  (Andersen, et al., 2005; Offe, et al., 2006). SORLA binds the carbohydrate-linked domain of APP with an epitope in its cluster of complement-type repeats (Andersen, et al.,

2006). Similar to the situation in patients with sporadic AD, lack of *Sorla* expression in gene-targeted mouse models leads to increased A $\beta$  production and senile plaque formation (Rohe, et al., 2008).

In neurons, SORLA expression negatively correlates with A $\beta$  production (Andersen, et al., 2005; Nixon and Cataldo, 2006; Rogaeva, et al., 2007; Rohe, et al., 2008; Schmidt, et al., 2007). Which molecular mechanisms are underlying these observations? Studies by several groups provided the relevant working hypothesis. According to these models, SORLA controls the release of APP from the TGN to the cell-surface. This step is crucial for the processing of APP along both, the amyloidogenic and the non-amyloidogenic pathway (Andersen, et al., 2005; Rogaeva, et al., 2007; Schmidt, et al., 2007). Confining APP to the TGN happens most likely by two mechanisms. The first is blockade of APP's transit along the secretory pathway by retentive binding to SORLA within the TGN. The second mechanism involves re-routing of APP from early endosomes to the TGN in line with the ability of SORLA to shuttle between these two compartments (Schmidt, et al., 2007), which is depicted in figure 2 (c and f). Taken together, both mechanisms confine APP to the TGN and the protein avoids  $\beta$ -secretase activity residing in late endosomes, the starting point of the amyloidogenic APP processing pathway.

Shuttling SORLA between the TGN and early endosomes depends on GGAs and PACS1 (cf. figure 2 c and f). Disruption of the binding-motifs for these adaptors in the SORLA tail leads to missorting of the receptor (and APP) and subsequent acceleration of APP processing (Schmidt, et al., 2007).

The mammalian retromer-complex, composed of Vps35, Vps29, Vps26 and sortin nexins 1 (SNX1) and 2 (SNX2), is another adaptor-complex that was reported to contribute to AD pathogenesis (Muhammad, et al., 2008; Seaman, 2005; Small, 2008; Small, et al., 2005). It has been shown in baker's yeast that the retromer can bind VPS10p (Nothwehr, et al., 2000), but a direct interaction of SORLA and the adaptor complex has not yet been reported. However, with such an interaction (figure 2 f), the neurodegenerative effects of retromer defects could be explained by missorted SORLA (Motoi, et al., 1999).



## 1.2 SORLA in the kidney

Given the important function of SORLA in the central nervous system, the question for extraneuronal functions of the receptor remains. One possible focus is represented by the kidney.

Even though initial publications did not suggest a renal expression for the receptor (Jacobsen, et al., 1996; Yamazaki, et al., 1996), refined analyses in later publications showed a clear transcriptional expression in the kidney (Hermans-Borgmeyer, et al., 1998; Mörwald, et al., 1997).

A further characterization of the renal SORLA expression was carried out by Irmgard Hermans-Borgmeyer and colleagues. The work of Riedel et al. was the first using immunological approaches to show not only receptor transcripts, but also localization of the protein itself to specific segments of the kidney (Riedel, et al., 2002).

Using in-situ hybridization on embryonal and adult tissue sections, *Sorla* transcripts were localized to tubular epithelial cells. Based on immunohistochemical colocalization studies with aquaporin 2 (AQP2) and vacuolar proton-ATPase, this former publication confined SORLA expression to one specific tubular region in the kidney: the cortical and medullary collecting duct (see 1.2.2) (Riedel, et al., 2002). Similar to the situation in rat neurons, SORLA expression in renal cell types was predominately found in vesicular structures in the cytosol.

### 1.2.1 The kidney

The kidney carries out different functions, most of them being essential for life (Brenner, 2007): These encompass the excretion of metabolic waste products, the excretion of bioactive substances that affect body function (a number of hormones are at least partially removed by renal processes), the regulation of red blood cell production (the kidney is a major source for erythropoietin, a peptide hormone involved in the control of erythrocyte production), regulation of vitamin D production (the active form of vitamin D, 1,25-dihydroxyvitamin D<sub>3</sub>, is synthesized in the kidney), gluconeogenesis (besides most gluconeogenesis taking place in the liver, a substantial fraction occurs in the kidney, especially during prolonged fasting periods).

Another important function of the organ is the regulation of water and electrolyte homeostasis and therewith the regulation of arterial blood pressure. Maintaining this balance is a very crucial task, since the body's input of water and electrolytes is variable. The kidney is able to regulate water and each of the essential minerals

independently, thereby adjusting fluctuating nutrition intake exactly to body needs. Because of the importance of this function, most renal ATP is used to accomplish the task of reabsorbing sodium ( $\text{Na}^+$ ), chloride ( $\text{Cl}^-$ ) and water. Usually less than one percent of the amount filtered at the renal corpuscle is excreted. These three substances undergo considerable tubular reabsorption, but normally no secretion.

Renal maintenance of  $\text{Na}^+$  and water balance achieves regulation of blood volume which blood pressure ultimately depends on. Thus through volume control, the kidney participates in blood pressure regulation. Furthermore the kidney stimulates the renin-angiotensin system (RAS) by generating renin and also possessing angiotensin converting enzyme (ACE) activity.

In several renal segments, the reabsorption of electrolytes and water is under physiological control by neural, hormonal and paracrine inputs to maintain homeostasis.

### **1.2.2 The renal nephron**

The basic functional unit of the kidney is the nephron, depicted in figure 3. It consists of the renal corpuscle (Bowman's capsule and glomerulus) followed by various tubular segments, each described by different physiological properties: the proximal tubule (proximal convoluted tubule and proximal straight tubule), the loop of Henle (descending thin limb, ascending thin limb and thick ascending limb containing macula densa), the distal convoluted tubule (sometimes divided in early and late distal convoluted tubule, DCT1 and DCT2) and the collecting duct system (connecting tubule and collecting duct which can be divided into a cortical, an outer medullary, an inner medullary and a papillary portion).

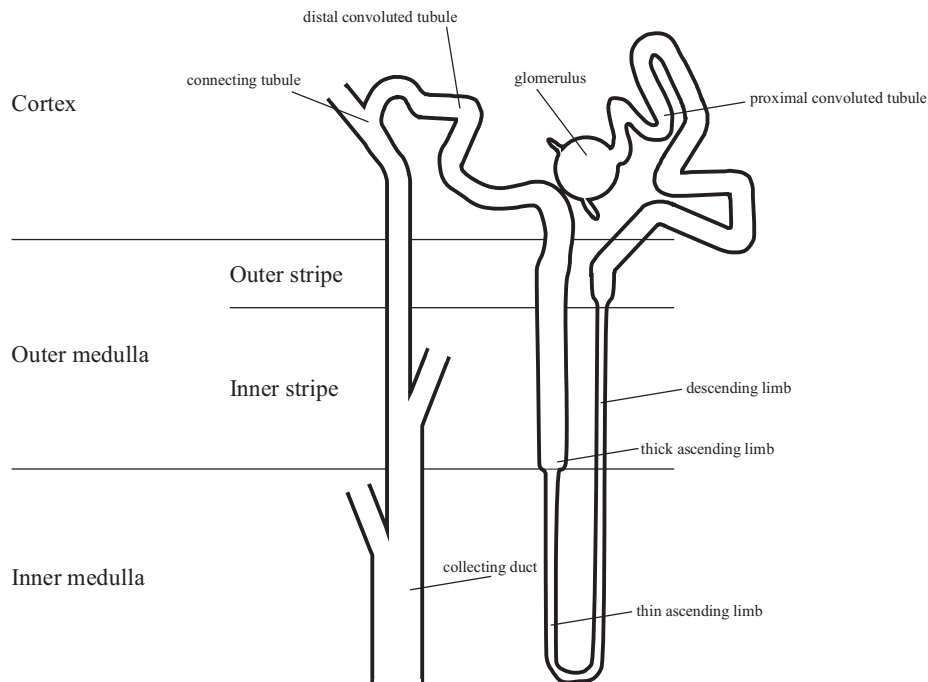


**Figure 3: The nephron.** Blood is filtered at the glomerulus. While urine flows through proximal convoluted tubule, the loop of Henle (consisting of descending limb, thin ascending limb and thick ascending limb), distal convoluted tubule, connecting tubule and collecting duct, controlled transport processes adjust urinary secretion of solutes to maintain homeostasis. Because of its non-mesenchymal origin, the collecting duct system is often not considered as part of the nephron. On the contrary, some sources classify the connecting tubule (of mesenchymal origin) as part of the collecting duct system. Due to the fact that all segments from the glomerulus through the loop of Henle to the collecting duct form one single functional tubular intrarenal unit (even though with continuously changing functional and structural properties), and to clarify the abovementioned divergence in literature, this work refers to this structure – including the collecting duct system – as nephron. The figure is based on Brenner and Rector's *The Kidney* (Brenner, 2007).

All nephrons are completely separate from each other from Bowman's capsule through Henle's loop to the initial collecting tubules. At this point, connecting tubules from several nephrons merge to form the cortical collecting tubules, which on their part form larger collecting ducts.

The tubular epithelium of each segment of the nephron consists of a one-cell layer of one segment-specific cell type. Additionally, the segment-specific cells of the distal convoluted tubule, the connecting tubule as well as the collecting duct, are interspersed with different subtypes of another cell-type, the so-called intercalated cells.

Each tubular segment of the nephron does possess distinctive physiological properties for its own specialized function.

The proximal tubule for example performs most electrolyte reabsorption in the kidney (around 65 percent of the  $\text{Na}^+$ ,  $\text{Cl}^-$  and water filtered at the renal corpuscle and between 55 and 80 percent of the filtered  $\text{K}^+$  are reabsorbed in the entire proximal tubule) in a mainly non-modulated iso-osmotic fashion.

In more distal segments, ion and water is being transported in an uncoupled manner, allowing individual reabsorption of solutes. These processes, which are subject to strict hormonal regulation, are important for fine-tuning homeostasis of individual electrolytes.

### 1.3 Aim of this study

The aim of this study was to understand the role of SORLA in the kidney.

This goal should be achieved by determining the precise localization of the receptor to specific nephron segments. Due to specialized functions of individual tubular segments, this knowledge should allow a detailed analysis of transport pathways possibly influenced by SORLA.

A function of the receptor in these processes should be elucidated by investigating renal defects in mice lacking the *Sorla* gene.

As SORLA is not exclusively expressed in the kidney, this thesis was furthermore concerned whether extra-renal factors controlling kidney function may be influenced in mice lacking the receptor.

In addition, I wanted to identify molecular mechanisms underlying the observed phenotypes.

## 2 Material and Methods

### 2.1 Animal Experiments

#### 2.1.1 Mouse Husbandry

All experiments involving animals were performed according to institutional and National Institutes of Health guidelines and had been approved by the local authorities. Mice were kept at standard conditions at a 12/12 hour light/dark cycle and had access to food and tap water ad libitum (unless stated otherwise).

#### 2.1.2 Mouse Strains

Several wild type strains were used for this study: 129Bl/6 (mixed genetic background, 129SvEmcTer and C57BL/6N), 129Balb/c (mixed genetic background, 129SvEmcTer and Balb/cJ), 129SvJ and Balb/cJ. All lines were bred in-house.

**Table 1: Mouse strains with targeted disruption of the *Sorla* gene.**

Strain designation	Source	Genetic background
SorLA18	generated in our lab as described (Andersen, et al., 2005)	129SvEmcTer and Balb/cJ
SorLA27	generated in our lab as described (Andersen, et al., 2005)	129SvEmcTer and C57BL/6N
SorLA39	generated in our lab as described (Andersen, et al., 2005)	129SvEmcTer and Balb/cJ
SorLA × Balb/c	generated in our lab	Balb/cJ, backcrossed for >10 generations
SorLA Ex255	provided by William C. Skarnes (Wellcome Trust Sanger Center, UK)	insertional mutagenesis of <i>Sor11</i> locus by <i>lacZ</i> reporter gene

Animals lacking *Sorla* gene expression (except SorLA Ex255) were obtained from the sources listed in table 1. All animals gave identical results when compared with age- and sex-matched control mice of corresponding genetic background, unless otherwise stated.

### **2.1.3 Timed Matings**

Timed matings were set up in the evening to obtain embryos at different stages of development. The presence of a vaginal plug in the morning was considered as day 0.5 post coitum (dpc). The embryos were harvested by sacrificing pregnant mice.

### **2.1.4 Physiological Parameters**

#### **2.1.4.1 Collection of Urine and Blood**

Urine was collected by housing mice in individual metabolic cages. The animals had free access to tap water (except stated otherwise). The supply of chow was stopped during collection to prevent chow debris contaminating the urine. Urine was collected for 16 hours overnight and centrifuged at 8,500 rpm in a standard tabletop centrifuge. After discarding any pellet, volume or weight was measured and the urine was frozen at  $-20^{\circ}\text{C}$  until analyzed further.

To collect blood, mice were anesthetized by ether and bled retro-orbitally by using a sterile glass Pasteur pipette. Immediately after withdrawal, the blood was chilled on ice and subsequently centrifuged at  $>10,000 \times g$  for 10 min at  $4^{\circ}\text{C}$ . Blood serum supernatants were stored at  $-20^{\circ}\text{C}$  for further analysis.

The analysis of urine and blood was carried out either by the 'Institut für Labormedizin' (Helios-Klinikum Berlin-Buch) or by 'Labor 28' (Berlin).

#### **2.1.4.2 Blood Pressure Telemetry**

Blood pressure telemetry was performed by the group of Dr. med. habil. Volkmar Groß (MDC / Charité Berlin) using a pressure-sensing catheter in the abdominal aorta as described (Gross, et al., 2005). After surgery, mice were allowed 10 days recovery before baseline blood pressure, heart rate and activity were recorded for 3 consecutive days.

#### **2.1.4.3 Endocrine Parameters**

Levels of renin, aldosterone and vasopressin in serum were measured by Irene Strauß (AG Michael Bader, MDC) or in the 'Klinik für Nuklearmedizin' (Helios

Klinikum Berlin-Buch), both using competitive radio immunosorbent assays (RIA).

#### **2.1.4.3.1 HPLC-Detection of Catecholamines and Serotonin**

Levels of serotonin (5-hydroxytryptophan) and catecholamines (dopamine, norepinephrine and epinephrine) in tissues were measured using high-pressure liquid chromatography (HPLC). Mice were sacrificed by decapitation and the according organs were quickly removed, briefly rinsed in cold PBS and kept on ice during all following steps. 0.2 mol/l perchloric acid (1 ml per 100 mg tissue weight) was added and the organs were homogenized with an Ultra-Turrax (IKA, St. Augustin, Germany) and centrifuged for 20 min at  $20,000 \times g$ . The pellets containing precipitated protein was discarded, the supernatants were stored at  $-80\text{ }^{\circ}\text{C}$  until analyzed by HPLC.

Catecholamines were separated using a 125 mm  $\times$  3 mm I.D. column, packed with Nucleosil 100 C 18, particle size 3  $\mu\text{m}$  at a temperature of  $42\text{ }^{\circ}\text{C}$ . The liquid phase consisted of 10 g/l citric acid, 4 g/l  $\text{KH}_2\text{PO}_4$ , 100 mg/l EDTA, 2%<sub>(v/v)</sub> acetonitril at pH 2.8 and had a flow rate of 0.7 ml/min. Electrochemical detection was carried out with an INTRO detector (ANTEC Leyden, The Netherlands) using a cell potential of 800 mV. Retention times were around 2.2 min for norepinephrine, 2.9 min for epinephrine and 4.9 min for dopamine, allowing a clear separation of these peaks. Concentrations were calculated from peak heights of the recordings by comparison standard curves created from peak heights of catecholamine solutions with defined concentrations of the according catecholamine. The HPLC was carried out in the group of Dr. Wolf-Eberhard Siems (Leibniz-Institute for molecular Pharmacology, FMP Berlin) with the assistance of Dr. Winfried Krause.

Serotonin was also separated using using a 125 mm  $\times$  3 mm I.D. column, packed with Nucleosil 100 C 18, particle size 3  $\mu\text{m}$  at a temperature of  $20\text{ }^{\circ}\text{C}$ . The liquid phase consisted of 1.36 g/l  $\text{KH}_2\text{PO}_4$  and 5%<sub>(v/v)</sub> methanol and had a flow rate of 2 ml/min. Detection was carried out with a RF-10AXL fluorescence detector (Shimadzu, Japan) with excitation at a wavelength of 295 nm, measuring the emission at 345 nm. Concentrations were calculated from peak areas of the recordings by comparison with standard curves created from peak areas of standard serotonin solutions. The HPLC was carried out in the group of Dr. Michael Bader (MDC).

HPLC peaks heights and areas were calculated using the software of the corresponding HPLC system (ANTEC Leyden, The Netherlands; Shimadzu, Japan) and the data was analyzed with Excel 2003 (Microsoft, USA).



## **2.1.5 Pharmacological Experiments**

### **2.1.5.1 Thiazide Treatment**

Mice were kept in metabolic cages for 10 hours. Hydrochlorothiazide was injected intraperitoneally (30 mg/kg body weight) at timepoints 0 and 5 hours. Urine was collected for 5 hours following each injection (from hour 0 to 5 and from hour 5 to 10). Accordingly, control urine was collected from animals injected with 0.9% saline solution (B. Braun Melsungen, Germany).

### **2.1.5.2 Eplerenone Treatment**

The mice received a daily dose of 200 mg eplerenone per kg body weight. The drug was either administered for two consecutive weeks via the chow (by replacing the standard pellets with a dietary mash containing the drug), the drinking water (by replacing the normal water bottles) or via gavage twice a day. Control animals received dietary mash or water without eplerenone.

### **2.1.5.3 Bumetanide Treatment**

Bumetanide treatment was carried out in thick ascending limb (TAL) tubules isolated from the inner stripe of the outer renal medulla (ISOM). The isolation process, modified from Kikeri et al. (Kikeri, et al., 1990), utilizes the high resistance of the TAL against collagenase. While this enzyme cocktail decomposes most the ISOM to individual cells, TAL tubules stay intact. Bumetanide-sensitive flux was determined by measuring uptake of radioactive rubidium ( $^{86}\text{Rb}^+$ ), which was used as a substitute for  $\text{K}^+$ .

#### **2.1.5.3.1 Isolation of the Inner Stripe of the Outer Renal Medulla**

Before use, all reagents (except anaesthetics) were oxygenized by bubbling with carbogen (5%<sub>(v/v)</sub>  $\text{CO}_2$ , 95%<sub>(v/v)</sub>  $\text{O}_2$ ), unless stated otherwise.

Mice were anaesthetized by intraperitoneal injections of 5  $\mu\text{l/g}$  bodyweight Ketavet-Rompun-solution (400  $\mu\text{l}$  2% Rompun, 3.6 ml 10% Ketavet, ad 10 ml 0.9% NaCl-solution; Bayer HealthCare, Leverkusen, Germany, Pfizer, USA, and B. Braun Melsungen, Germany respectively). When the animals were fully anaesthetized, kidneys were taken out of the abdominal cavity and the mice were sacrificed by decapitation. Kidneys were placed in oxygenized ice-cold PBS and the kidney capsules were removed immediately.

All following steps were carried out in ice-cold PBS: Kidney poles, containing only cortical tissue, were cut off and discarded. The remaining organs were sliced

into four equally thick transverse sections. Using a fine spring scissor, the ISOM was excised out of each section by cutting off the outer stripe of the medulla (together with the cortex) and the inner medulla/papillae. The u-shaped isolated ISOM was cut into small chunks (circa 1 mm<sup>3</sup>) and stored in oxygenized ice-cold PBS with continuous oxygen-supply until processed further.

#### **2.1.5.3.2 Enrichment of TAL Tubules**

The minced ISOM was transferred into pre-chilled 14 ml centrifuge tubes and kept on ice. Once all tissues were prepared, the tubes were moved to room-temperature and 4 ml of oxygenized, 37 °C warm collagenase solution (0.8 mg/ml collagenase, crude type Ia in Dulbeccos's Modified Eagle Medium; Sigma Aldrich and Promega, both USA) was added to each tube. Tissues were incubated on a rocking shaker (140 rpm) at room-temperature.

After 10 minutes, the tissue fragments were suspended by pipetting several times up and down with a 10 ml tissue culture pipette. The suspension was allowed to settle for a few seconds to divide large, fast sedimenting chunks of undigested tissue from separated tubules and cells. While the supernatants, containing the digested portion, were transferred into fresh, ice-cold round-bottom centrifuge tube, fresh collagenase solution was added to the remaining undigested ISOM pellets. This procedure was repeated four to six times until no tissue sedimented within a few seconds after resuspension anymore.

Immediately after skimming, the supernatant containing isolated isolated TAL tubules was centrifuged for 4 min at 100 × g at 4 °C to separate contaminating cells of different origin. The supernatant containing non-TAL cells was discarded, and the pellet containing the larger TAL fragments was resuspended in 1 ml of recovery solution (0.1%<sub>(w/v)</sub> BSA, Cohn Fraction V in Dulbeccos's Modified Eagle Medium; Sigma Aldrich and Promega, both USA) and kept on ice.

Fractions containing digested tubules of the same animal were pooled after resuspension in recovery solution. Subsequently, the cells were washed with ice-cold oxygenized basic flux solution (140 mM NaCl, 4.5 mM KCl, 0.5 mM RbCl, 1 mM MgCl<sub>2</sub>, 1 mM CaCl<sub>2</sub>, 10 mM BaCl<sub>2</sub>, 10 mM NaH<sub>2</sub>PO<sub>4</sub>, 10 mM Na<sub>2</sub>SO<sub>4</sub>, 5 mM HEPES, 5 mM Glucose in ultra-pure H<sub>2</sub>O, pH 7.0) twice by centrifugation (600 rpm, 4 °C, 4 min) and resuspension.

#### **2.1.5.3.3 Detection of Bumetanide-sensitive Uptake of <sup>86</sup>Rb<sup>+</sup>**

After centrifugation (600 rpm, 4 °C, 4 min) and resuspension in 37 °C warm oxygenized basic flux solution containing 1 μmol/l desmopressin (ddAVP) and 1 mmol/l ouabain, tubules were allowed to recover for 5 min. ddAVP, acting similar to physiological vasopressin, has been reported to increase NKCC2 activity

(Gimenez and Forbush, 2003). Ouabain is a potent inhibitor of the basolateral  $\text{Na}^+/\text{K}^+$ -ATPase (Gimenez, et al., 2002).  $\text{Ba}^{2+}$ -ions, abound in the basic flux solution, are blocking  $\text{K}^+$ -channels (Taglialatela, et al., 1993). The TAL tubules of each animal were resuspended and immediately split into four parts with equal volume.

The first part was spun down with a tabletop centrifuge for 10 min at max. speed. The pellet was weighted to measure the tubule mass (tubulocrit).

Two portions were treated with 200  $\mu\text{l}$  of 37 °C warm oxygenized basic flux solution containing 1  $\mu\text{M}$  ddAVP, 1 mmol/l ouabain and 0.2  $\mu\text{Ci}/\mu\text{l}$   $^{86}\text{Rb}^+$ , either with or without 250  $\mu\text{mol/l}$  bumetanide. As a passive control, the fourth part of the tubules was incubated with the same volume of ice-cold oxygenized basic flux solution containing 1  $\mu\text{M}$  ddAVP, 1 mmol/l ouabain and 0.2  $\mu\text{Ci}/\mu\text{l}$   $^{86}\text{Rb}^+$  and incubated on ice. After 5 min of incubation with the  $^{86}\text{Rb}^+$ , all three reactions were stopped by addition of 800  $\mu\text{l}$  of ice-cold SWG solution (140 mM potassium-gluconate, 5 mM HEPES and 250  $\mu\text{M}$  Bumetanide in ultra-pure water, pH 7.0). Four subsequent centrifugation (600 rpm, 4 °C, 4 min) and resuspension (in ice-cold SWG solution) steps were carried out to remove extracellular  $^{86}\text{Rb}^+$ . The SWG solution does only contain potassium-gluconate, therefore diluting all other ions. Together with the immediate chilling, addition of the buffer reduces all transport processes mediated by cotransporters (which require simultaneous availability of different electrolyte species for activity) and active transports (which are inhibited at low temperatures). The low temperature, the buffered pH and the physiological osmotic also pressure reduce passive transport by channels.

After the final resuspension step, each portion of TAL tubules was either transferred onto a scintillator plate or suspended in 5 ml of scintillation liquid. The uptake of  $^{86}\text{Rb}^+$ , an isotope emitting beta and gamma radiation, was measured as cpm (average counts per minute, measured over 10 min) on a LS-6000 liquid scintillation counter (Beckman-Coulter, USA) in a completely open window (0 to 1,000) with 100% efficiency according to manufacturer's manual and Beckman-Coulter Isotope Booklet for Liquid Scintillation Counters (November 12, 2002).

The bumetanide-sensitive flux of each tubule preparation was calculated as cpm difference between treatment with and without bumetanide. For comparison between different experiments and animals, bumetanide-sensitive uptake was described as percentage of uptake without addition of bumetanide.

## 2.2 Microbiology

### 2.2.1 Culture Media and Bacteria

**Table 2: Bacterial culture media.**

<b>Name</b>	<b>Broth Recipe</b>	<b>Agar Recipe</b>
LB (Luria-Bertoni medium)	Tryptone 10% <sub>(w/v)</sub> Yeast extract 5% <sub>(w/v)</sub> NaCl 10% <sub>(w/v)</sub> in distilled water. pH 7.5	See broth recipe, additional Agar 15% <sub>(w/v)</sub>  if necessary: ampicillin sodium salt 100 µg/ml
SOC	Tryptone 20% <sub>(w/v)</sub> Yeast extract 5% <sub>(w/v)</sub> NaCl 0.5% <sub>(w/v)</sub> KCl 0.17% <sub>(w/v)</sub> MgCl 0.95% <sub>(w/v)</sub> Glucose 3.6% <sub>(w/v)</sub> in distilled water. pH 7.0	

**Table 3: *Escherichia coli* strains.**

<b>Name</b>	<b>Genotype</b>
<i>E. coli</i> DH5 $\alpha$	F <sup>-</sup> , $\phi$ 80dlacZ $\Delta$ M15, $\Delta$ (lacZYA-argF)U169, deoR, recA1, endA1, hsdR17(rk <sup>-</sup> , mk <sup>+</sup> ), phoA, supE44, $\lambda$ <sup>-</sup> , thi-1, gyrA96, relA1
<i>E. coli</i> HB101	F <sup>-</sup> mcrB mrr hsdS20(r <sub>B</sub> <sup>-</sup> m <sub>B</sub> <sup>-</sup> ) recA13 leuB6 ara-14 proA2 lacY1 galK2 xyl-5 mtl-1 rpsL20(Sm <sup>R</sup> ) glnV44 $\lambda$ <sup>-</sup>
<i>E. coli</i> XL1-blue	endA1 gyrA96(nal <sup>R</sup> ) thi-1 recA1 relA1 lac glnV44 F'[::Tn10 proAB <sup>+</sup> lacI <sup>q</sup> $\Delta$ (lacZ)M15] hsdR17(r <sub>K</sub> <sup>-</sup> m <sub>K</sub> <sup>+</sup> )
<i>E. coli</i> NEB Turbo Competent	F' proA <sup>+</sup> B <sup>+</sup> lacI <sup>q</sup> $\Delta$ lacZM15/fhuA2 $\Delta$ (lac-proAB) glnV gal R(zgb-210::Tn10) Tet <sup>S</sup> endA1 thi-1 $\Delta$ (hsdS-mcrB)5

### 2.2.2 Generation of Electrocompetent Cells

To generate electrocompetent *E. coli*, cells of a fresh overnight culture were used to inoculate 1 l of LB medium at an OD<sub>600</sub> of less than 0.1. The culture was incubated under vigorous shaking at 37 °C until the OD<sub>600</sub> reached 0.5. The cell suspension was chilled on ice for 20 min and cell harvested by 15 min centrifugation at 4,000  $\times$  g and 4 °C. The pellet was resuspended in 1 l of ice-cold sterile 10% glycerol and centrifuged again (see above). This step was repeated again with 500 ml and 20 ml. After the final centrifugation step, the pellet was resuspended in 2 ml of ice-cold 10% glycerol, aliquoted and stored at -80 °C.

### 2.2.3 Transformation of Bacteria

The cells and all materials/reagents needed (except SOC medium) were precooled on ice. 40  $\mu$ l of electrocompetent *E. coli* were gently mixed with 2  $\mu$ l of DNA. After 5 min incubation on ice, the cells were electroporated (R=200  $\Omega$ , C=25  $\mu$ F, V=1.8 kV), immediately cooled down on ice, washed out of the cuvette with SOC medium, transferred into a new reaction tube and incubated for 30 min at 37 °C. Cells were harvested by centrifugation for 5 min at 2,500  $\times$  g, plated on a LB agar plate and incubated at 37 °C overnight. For blue-white screening (e.g. after ligation of DNA into a vector backbone, vide infra), LB agar plates were supplemented with 80  $\mu$ g/ml X-gal and 0.5 mmol/l IPTG.

### 2.2.4 Yeast Two-hybrid Assay

The yeast two-hybrid screen was carried out by Heike Göhler in the lab of Erich Wanker (MDC), as described (Wanker, et al., 1997). For that purpose, the cDNA sequence coding for the cytosolic domain of human SORLA (including the native stop codon) was amplified by PCR using the Phusion enzyme (Finnzymes, Finland) as described below. Primers SorlaF and SorlaR (table 4, Eurogentec, Belgium) were used in a PCR program with an annealing temperature of 62 °C to amplify the 178 bp long product.

**Table 4: Primers used for cloning of the carboxy-terminus of human SORLA into pBTM117c.**

<b>Name</b>	<b>Sequence</b>
SorlaF (amplification primer)	5'-ACGTCGACGCGGAGGCTGCAGAG-3'
SorlaR (amplification primer)	5'-GAGCGGCCGCTCAGGCTATCACCAT-3'
BTMs (sequencing primer)	5'-TCGTAGATCTTCGTCAGCAG-3'
BTMas (sequencing primer)	5'-GGAATTAGCTTGGCTGCAGC-3'

PCR product and bait vector pBTM117c (table 5) were digested with the restriction enzymes *SalI* and *NotI* (New England Biolabs, USA), and ligated as described later. The miniprep DNA of an overnight culture inoculated with a single colony was sequenced with the primers BTMs and BTMas (table 4, Heike Göhler, MDC) to assure proper PCR amplification and ligation results. The sequencing method is described below. Cloning of the insert into the prey vector pACT4-1b was carried out accordingly.

**Table 5: Vectors used in the yeast two-hybrid screen.**

<b>Name</b>	<b>Size</b>	<b>Characteristics</b>
pBTM117c	9.5 kb	promoter ADH1; fusion protein LexA; auxotrophy marker TRP1; ampicillin resistance (Wanker, et al., 1997)
pACT4.1b	7.8 kb	promoter ADH1; fusion protein GAL4-AD; auxotrophy marker LEU2; ampicillin resistance (Erich Wanker, MDC, unpublished)

## 2.3 Nucleic Acid Experiments

### 2.3.1 Polymerase Chain Reaction

Polymerase chain reaction (PCR) was used to selectively amplify a specific DNA sequence from nucleic acid templates. Two enzymes were used for this work: *Thermus aquaticus* (Taq) Polymerase (Invitrogen, USA) and Phusion high-fidelity polymerase (Finnzymes, Finland). Reverse transcription PCR is described later.

Taq polymerase reactions were set up in a 25 µl scale, consisting of 0.5 µl template DNA, 0.2 mmol/l dATP, 0.2 mmol/l dTTP, 0.2 mmol/l dCTP, 0.2 mmol/l dGTP, 0.025 U/µl Taq Polymerase (Invitrogen, USA), 5 mmol/l MgCl<sub>2</sub>, and 0.3 µmol/l of each forward and reverse primer in PCR Buffer (Invitrogen, USA). The PCR program was set up at a PTC-200 thermal cycler (MJ Research, USA) as follows: full denaturing of DNA template 5 min at 95 °C, 40 cycles with 30 sec denaturing at 95 °C, 1 min annealing at a temperature 2 K below the calculated melting-temperature of the PCR-primers (unless otherwise stated) and 1 min/kb elongation at 68 °C. A 10 min elongation step at 68 °C followed the cycling (table 6).

Phusion polymerase reactions were set up in a 25 µl scale, consisting of 0.25 µl template DNA, 0.2 mmol/l dATP, 0.2 mmol/l dTTP, 0.2 mmol/l dCTP, 0.2 mmol/l dGTP, 0.02 U/µl Phusion Polymerase (Finnzymes, Finland), 3% DMSO, and 0.5 µmol/l of each forward and reverse primer in Phusion HF buffer (Finnzymes, Finland). The PCR program was set up at a PTC-200 thermal cycler (MJ Research, USA) as follows: full denaturing of DNA template 1 min at 98 °C, 40 cycles with 5 sec denaturing at 98 °C, 20 sec annealing at a temperature 2 K below the calculated melting-temperature of the PCR-primers (unless stated otherwise) and 20 sec/kb elongation at 72 °C. A 10 min elongation step at 72 °C followed the cycling (table 6).

**Table 6: PCR programs for Taq polymerase and Phusion polymerase.**  $T_m$ : melting temperature of PCR primers.

Taq polymerase			Phusion polymerase		
95 °C	5 min		98 °C	1 min	
95 °C	30 sec		98 °C	5 sec	
$(T_m-2)$ °C *	1 min	40 ×	$(T_m-2)$ °C *	20 sec	40 ×
68 °C	1 min/kb		72 °C	20 sec/kb	
68 °C	10 min		72 °C	10 min	

\* (depending on the primer pair used)

### 2.3.2 Plasmid DNA Extraction

#### 2.3.2.1 From Bacteria

A single *E. coli* colony was picked from a LB agar plate used to inoculate a 5 ml LB culture, which was grown overnight at 37 °C with vigorous shaking.

If small amounts of DNA were sufficient, sells were collected by centrifugation (5 min at  $14,000 \times g$ ) and the pellet was processed using a Plasmid Mini Kit (Qiagen, The Netherlands). For larger amounts, the overnight culture was used to inoculate a 250–500 ml culture. The cells of that culture were centrifuged (as above) and subjected to a Plasmid Midi Kit (Qiagen, The Netherlands). Both kits use an alkaline lysis step and a subsequent anion exchange chromatography to purify plasmid DNA. They were used according to the Qiagen Plasmid Purification Handbook (August 2003).

Concentration and purity of the purified DNA was measured photometrically by using a NanoDrop ND-1000 (NanoDrop Technologies, USA) as described by Gallagher et al. (Gallagher and Desjardins, 2006). DNA was stored at  $-20$  °C.

#### 2.3.2.2 From Agarose Gels

Bands of interest were narrowly cut out under a UV lamp. DNA was purified from the gel slices by using the High Pure PCR Product Purification Kit (Roche Diagnostics, Mannheim, Germany) according to product manual.



### **2.3.3 Total RNA Extraction**

RNase-free solutions were used for all subsequent steps unless stated otherwise. Mice were sacrificed, corresponding tissues removed, briefly rinsed in ice-cold PBS, and either processed on ice immediately or snap-frozen in liquid nitrogen.

Per 100 mg of tissue, 1 ml of ice-cold Trizol (Invitrogen, USA) was added. Organs were homogenized with an Ultra-Turrax (IKA, St. Augustin, Germany). 1 ml of the homogenate was added to 0.2 ml trichloromethane (room-temperature) and mixed vigorously, followed by 5 min incubation at room-temperature. The suspension was mixed for 10 min at  $12,000 \times g$  at 4 °C. The upper phase was collected and gently mixed with 500  $\mu$ l isopropanol for 10 min at room-temperature to precipitate the RNA. It was pelleted by centrifugation ( $12,000 \times g$ , 4 °C, 10 min) and washed by vortexing in 75% ethanol. After a final centrifugation ( $7,500 \times g$ , 4 °C, 10 min), the pellet was briefly air dried at room-temperature and dissolved in RNase-free water.

To remove contaminating DNA, 100  $\mu$ g of RNA were digested with 20 U RNase-free DNase I (Roche Diagnostics, Mannheim, Germany) for 20 min at 37 °C. Enzyme and contaminants resulting from this process were removed using the RNeasy Mini Kit (Qiagen, The Netherlands) following the RNA cleanup method described in the Qiagen RNeasy Mini Handbook (June 2001).

RNA concentration and purity was determined photometrically by using a NanoDrop ND-1000 (NanoDrop Technologies, USA) as described by Gallagher et al. (Gallagher and Desjardins, 2006). RNA quality and degradation was determined by electrophoresis on a Agilent 2100 Bioanalyzer with electrophoresis setup using a RNA 6000 Nano Kit (Agilent Technologies, USA), RNAs with RNA integrity number values of 8 or higher were considered as intact.

### **2.3.4 Enzymatic DNA Restriction**

DNA was incubated with 0.5 U restriction enzyme per  $\mu$ g DNA for 2 h or overnight. All restriction enzymes were obtained from New England Biolabs, USA. Digestions were carried out using buffers and reaction temperatures as recommended in the company's catalog (New England Biolabs, USA). Digested DNA was purified either directly by ion exchange columns (High Pure PCR Product Purification Kit; Roche-Diagnostics, Mannheim, Germany), or by agarose gel electrophoresis and subsequent column purification.

### 2.3.5 Agarose Gel Electrophoresis

To separate DNA molecules according to their molecular weight, the samples were loaded onto agarose gels and stained with ethidium bromide as described in 'Molecular cloning: a laboratory manual' (Sambrook, et al., 1989). For small RT-PCR DNA fragments with an approx. size of 100 bp, 4% gels were prepared using Phor Agarose (Biozym Scientific, Hessisch Oldendorf, Germany, cat. No. 850180).

### 2.3.6 DNA Ligation

Ligation of DNA fragments into a linearized vector backbone was performed solely with molecules having complementary overlaps at the 5'-/3'-ends ('sticky' ends) by using T4 DNA ligase (Invitrogen, USA). Prior to ligation, 5'-phosphoester were hydrolyzed, to prevent religation of linearized vectors. To do so, alkaline phosphatase from calf intestine (Roche Diagnostics, Mannheim, Germany) was used according to manufacturer's instructions. After dephosphorylation, samples were cleaned with PCR Product Purification Kit (Roche Diagnostics, Mannheim, Germany). Vector and insert were mixed in a molar ratio of 1:3 to 1:9, the reaction was set up as described in Invitrogen's package insert and the ligation was incubated at 16 °C overnight.

Ligation into readily linearized pGEM-T Easy vector (pGEM-T Easy Vector System; Promega, USA) was carried out as recommended in the manufacturer's manual. Prior to ligation, PCR products amplified with Phusion high fidelity DNA polymerase (Finnzymes, Finland), were treated with 0.5 U/μl Taq polymerase and 0.2 mmol/l dATP in PCR buffer for 30 min at 68 °C to create 3'-adenosine-overhangs.

Ligated DNA was used for the transformation of electrocompetent *E. coli*.

### 2.3.7 DNA Sequencing

DNA was sequenced using a modified chain-termination method (Sanger, et al., 1977). The presence of fluorescence-labeled dideoxy-nucleotides in the reaction leads to termination of the strand extension, labeling the terminating nucleotide.

The reaction was carried out using the BigDye Terminator v3.1 Cycle Sequencing Kit (Applied Biosystems, USA) according to the kit's manual. The reaction was performed in a PTC-200 thermal cycler (MJ Research, USA) as follows: 1 min initial template denaturation at 96 °C and 25 cycles with 10 sec denaturation (96°C), 5 sec primer annealing (55 °C) and 4 min elongation (60 °C). Surplus primer and (dideoxy-) nucleotides were removed by size-exclusion chromatography on a Sephadex G-50 column (GE Healthcare, USA).

The purified sample was sequenced on a ABI PRISM 377 DNA Sequencer (Applied Biosystems, USA) in the group of Norbert Hübner (MDC). Sequences were analyzed using Lasergene 7.0 Suite (DNASTAR, USA) and ClustalX (<http://www.clustal.org/>).

### 2.3.8 Northern Blot

Northern blot probes were labeled by incorporation of  $^{32}\text{P}$ -labeled ATP (Perkin Elmer, USA). pcDNA3.1 Vectors (Invitrogen, USA) containing full-length cDNAs of the *Sorla* and *Sortilin* were already available in our group.

Inserts of both vectors were cut out with *PmeI* (New England Biolabs, USA) according to manufacturers recommendations and isolated by agarose gel electrophoresis and subsequent purification as described above. Resulting DNA fragments were used as template for the Prime-It II Random Labeling Kit (Stratagene, USA). The labeling with random nonamers was carried out as described in the kit's manual. The generated  $^{32}\text{P}$ -labeled DNA probe fragments were purified using NucAway Spin Columns (Applied Biosystems, USA) as described in the column's instructions.

A premade human adult 12-lane Multiple Tissue Northern Blot membrane (Clontech, USA) was blocked, hybridized and washed according to manufacturer's instructions. The membrane was wrapped in saran wrap (SC Johnson, USA) and transferred together with an isotope detection imaging plate (Fujifilm, Japan) into a cassette. After exposure, the imaging plate was scanned with a Fluorescent Image Analyzer FLA-3000 (Fujifilm, Japan).

### 2.3.9 *In situ* Probe Synthesis

For the *in situ* probes for the detection of transcripts of *Sorla* and *Sortilin*, templates of 976 and 991 bp length respectively were amplified from murine cDNA of both genes. A sequence spanning from *Sorla* exon 42 to the last exon 48 was amplified using primers *Sorla\_probe\_F* and *Sorla\_probe\_R* listed in table 7. PCR amplification with Taq polymerase (Invitrogen, USA) was performed with an annealing temperature of 50 °C as described above. Primers *Sortilin\_probe\_F* and *Sortilin\_probe\_R* were used with an annealing temperature of 53 °C to amplify an untranslated region near the 5'-end of the *Sortilin* cDNA.

**Table 7: Primers used for cloning of the carboxy-terminus of human SORLA into pBTM117c.** Primers were ordered from Eurogentec, Belgium.

Name	Sequence
Sorla_probe_F	5'-TGCCACATCCTTCCTTGAC-3'
Sorla_probe_R	5'-AGCATCTTCATCGTCCTCT-3'
Sortilin_probe_F	5'-GGCATCGCTCATTAT-3'
Sortilin_probe_R	5'-TGCCTTTGCTGTATGGT-3'
SP6 (sequencing primer)	5'-TATTTAGGTGACACTATAG-3'
T7 (sequencing primer)	5'-TAATACGACTCACTATAGGG-3'

Both amplicons were purified and cloned into the pGEM-T Easy vector (Promega, USA). After picking a colony, plasmid DNA from a 5 ml overnight culture was isolated (*vide supra*) and sequenced using the SP6 and T7 primers (table 7). Confirmed clones were grown up in a 250 ml culture and subjected to midiprep plasmid isolation (see above).

Digoxigenin (DIG)-labeled probes for *in situ* hybridization (ISH) were generated by *in vitro* transcription (IVT) with T7 or SP6 polymerase using the DIG labeling kit (Roche Diagnostics, Mannheim, Germany). Template DNA plasmids were linearized either between insert and T7 promoter or between insert and SP6 promoter using suitable restriction enzymes (New England Biolabs, USA). After heat-inactivating restriction enzymes, 1 µg of each linearized plasmid was used for the IVT reaction, which was performed as described in the manufacturer's instructions. Enzyme and residual contaminants resulting from this process were removed using the RNeasy Mini Kit (Qiagen, The Netherlands) following the RNA cleanup method described in the Qiagen RNeasy Mini Handbook (June 2001). RNA quality and degradation was determined by electrophoresis on a Agilent 2100 Bioanalyzer with electrophoresis setup using a RNA 6000 Nano Kit (Agilent Technologies, USA).

### 2.3.10 cDNA Synthesis

First-strand synthesis of mRNA (reverse transcription polymerase chain reaction or RT-PCR) was carried out using SuperScript II reverse transcriptase (Invitrogen, USA) and oligo(dT)<sub>12-18</sub> primers with 1 µg of total RNA as template according to manufacturer's instructions (Rev. Date: November 11, 2003). Two control reactions were set up for each batch: a control with water instead of RNA to check for contamination of the reagents, and a reaction with water instead of reverse-transcriptase to check for DNA contamination in the RNA preparation.

### 2.3.11 Quantitative Real-time PCR

Due to the exponential nature of polymerase chain reaction (PCR) amplifications, the quantification of the amplicon after each cycle can be used to calculate the initial amount of template. To do so, quantitative real-time PCR (here also referred to as TaqMan) was carried out using gene of interest-specific DNA probes 5'-linked to a fluorescent dye –6-FAM (carboxyfluorescein) – and 3'-linked to a quencher – either BHQ-1 (black hole quencher 1) or MGB (minor groove binder). Excitation of the dye does not lead to fluorescence, as all emitted light is reabsorbed by the quencher in the dye's close vicinity.

The probe hybridizes specifically to an exon-exon-boundary of the template cDNA. A *Thermus aquaticus* (Taq)-polymerase based PCR-reaction using specific PCR primers, situated up and downstream of the probe, initiates amplification. During this process, the 5' to 3' exonuclease activity of the polymerase digests the probe, separating fluorophor and quencher. As the quencher molecules are not able to absorb light emitted by distant fluorescein groups, the amount of PCR product can be indirectly determined by fluorescence measurements after each cycle. The combination of a primer pair and a probe specific for the cDNA of a single gene of interest is called assay.

Relative gene expression was determined using the  $\Delta c_T$  method. The used detection system plotted the fluorescence intensity over the PCR cycles. The number of cycles, after which the signal erupts exponentially above a set threshold is called  $c_T$ . The  $c_T$  represents a logarithmic measure for the amount of template of the cDNA of interest. To normalize the  $c_T$  of the gene of interest, the difference to the  $c_T$  of the cDNA of the housekeeper gene *glyceraldehyde-3-phosphate dehydrogenase* () – the  $\Delta c_T$  – is calculated. The antilogarithmic value of the  $\Delta c_T$  is a value for the expression of the gene of interest relative to the expression of *Gapdh*. Standard deviation of  $\Delta c_T$  was calculated by taking the square root of the sum of the squared standard deviations of both individual  $c_T$  values.

**Table 8: Primers and probes used for TaqMan quantitative real-time PCRs.**

<b>Gene of interest</b>	<b>Sequence / Assay ID</b>		<b>Supplier</b>
<i>Gapdh</i>	Forward primer Reverse primer Probe*	5'-GGCAAATTCAACGGCACAGT-3' 5'-AGATGGTGATGGGCTTCCC-3' 5'-AAGGCCGAGAATGGGAAGCTTGTTCATC-3'	Eurogentec, Belgium
<i>Sorla</i>	Forward primer Reverse primer Probe*	5'-TGAACGCAACTGCTTGTATTGG-3' 5'-CCAGGCCGGAATTGATGAT-3' 5'-CCAGCGTCTCTGCTTGAACGGGAG-3'	Eurogentec, Belgium
<i>Sortilin</i>	Forward primer Reverse primer Probe*	5'-GAGTTCTGTCTGTACGGCAAGGA-3' 5'-ACTTCTCTGGCGGGATTCATC-3' 5'-AGCACCTGACAACAAATGGGTACCGG-3'	Eurogentec, Belgium
<i>Sorcs1</i>		Gene Expression Assay (185558947) Mm00491259_m1	Applied Biosystems, USA
<i>Sorcs2</i>		Gene Expression Assay (185558947) Mm00473050_m1	Applied Biosystems, USA
<i>Sorcs3</i>		Gene Expression Assay (185558947) Mm00458702_m1	Applied Biosystems, USA
<i>Atm</i>		Gene Expression Assay (185558947) Mm00431867_m1	Applied Biosystems, USA
<i>Ifi202b</i>		Gene Expression Assay (185558947) Mm00839397_m1	Applied Biosystems, USA
<i>Mfap1A</i>		Gene Expression Assay (185558947) Mm01625090_s1	Applied Biosystems, USA
<i>Mfap1A/B</i>		Gene Expression Assay (185558947) Mm00849648_gH	Applied Biosystems, USA
<i>Pttg1</i>		Gene Expression Assay (185558947) Mm00479224_m1	Applied Biosystems, USA
<i>Sord</i>		Gene Expression Assay (185558947) Mm01730221_mH	Applied Biosystems, USA
<i>Ddc</i>		Gene Expression Assay (185558947) Mm00516688_m1	Applied Biosystems, USA
<i>Dbh</i>		Gene Expression Assay (185558947) Mm00460472_m1	Applied Biosystems, USA
<i>Pnmt</i>		Gene Expression Assay (185558947) Mm00476993_m1	Applied Biosystems, USA
<i>Th</i>		Gene Expression Assay (185558947) Mm00447557_m1	Applied Biosystems, USA
<i>Slc18a1</i>		Gene Expression Assay (185558947) Mm00461868_m1	Applied Biosystems, USA

\* Probes were labelled with 6-FAM at the 5' and with BHQ-1 at the 3'-end.

All TaqMan runs were performed in single-plex reactions – using only one assay per reaction – and were carried out in triplicates using the standard TaqMan-PCR program (denaturing of hot-start Taq polymerase for 15 min at 95 °C, 40 cycles with 15 sec denaturing at 95 °C and 1 min annealing and elongation at 60 °C) at an ABI Prism 7000 Sequence Detection System (Applied Biosystems, USA). Each reaction was set up in a 20 µl scale, consisting of 5 µl cDNA, 10 µl qPCR MasterMix Plus (Eurogentec, Belgium), 0.4 µg/µl BSA (Sigma-Aldrich, USA), 0.25 µmol/l probe and 0.9 µmol/l of each forward and reverse primer. The sources primers and probes were obtained from, are listed in table 8. The data was analyzed using SDS 7000 Software 1.2.3 (Applied Biosystems, USA) and Excel 2003 (Microsoft, USA).

### 2.3.12 DNA Microarray-based Gene Expression Analysis

Microarray technology allows high-throughput analysis of nucleic acid hybridization events. In this work, DNA microarrays from Affymetrix (USA) – solid chips carrying an array of more than 14,000 sets of covalently bound oligomeric cDNA probes – were used to collect semi-quantitative, expression data of more than 39,000 transcripts per sample. The used nucleotides are labeled, positive hybridization can be detected by a scanner.

The Affymetrix platform uses biotin-labeled cRNA synthesized from the sample RNA for hybridization. For that purpose, cDNA is synthesized from sample RNA – using oligo(dT)-primers carrying a T7-promoter sequence for first strand synthesis to only use mRNA as template. In a subsequent T7 RNA polymerase *in-vitro* transcription (IVT) step, cRNA is synthesized from the cDNA template – applying biotinylated ribonucleotide analogues for labeling of the product. The IVT provides signal amplification, as several labeled product molecules are synthesized per template cDNA molecule. Due to this amplification cycle, the labeling method is called one-cycle target labeling.

If the starting amount of RNA is very low, an additional IVT step can be included. The first IVT is carried out without biotin-labeling, the emerging cRNA is employed in a second cDNA synthesis – using random primers as mRNA enrichment is not necessary and T7 promoter already exists – and a second IVT cycle with biotinylated nucleotides produces the labeled cRNA for hybridization. This method is called two-cycle target labeling.

The labeled cRNA is fragmented and hybridized onto the microarray. After hybridization, a streptavidin-conjugated fluorescing dye (phycoerythrin) is added and the chips are scanned. The workflow of both labeling methods is depicted in figure 4.



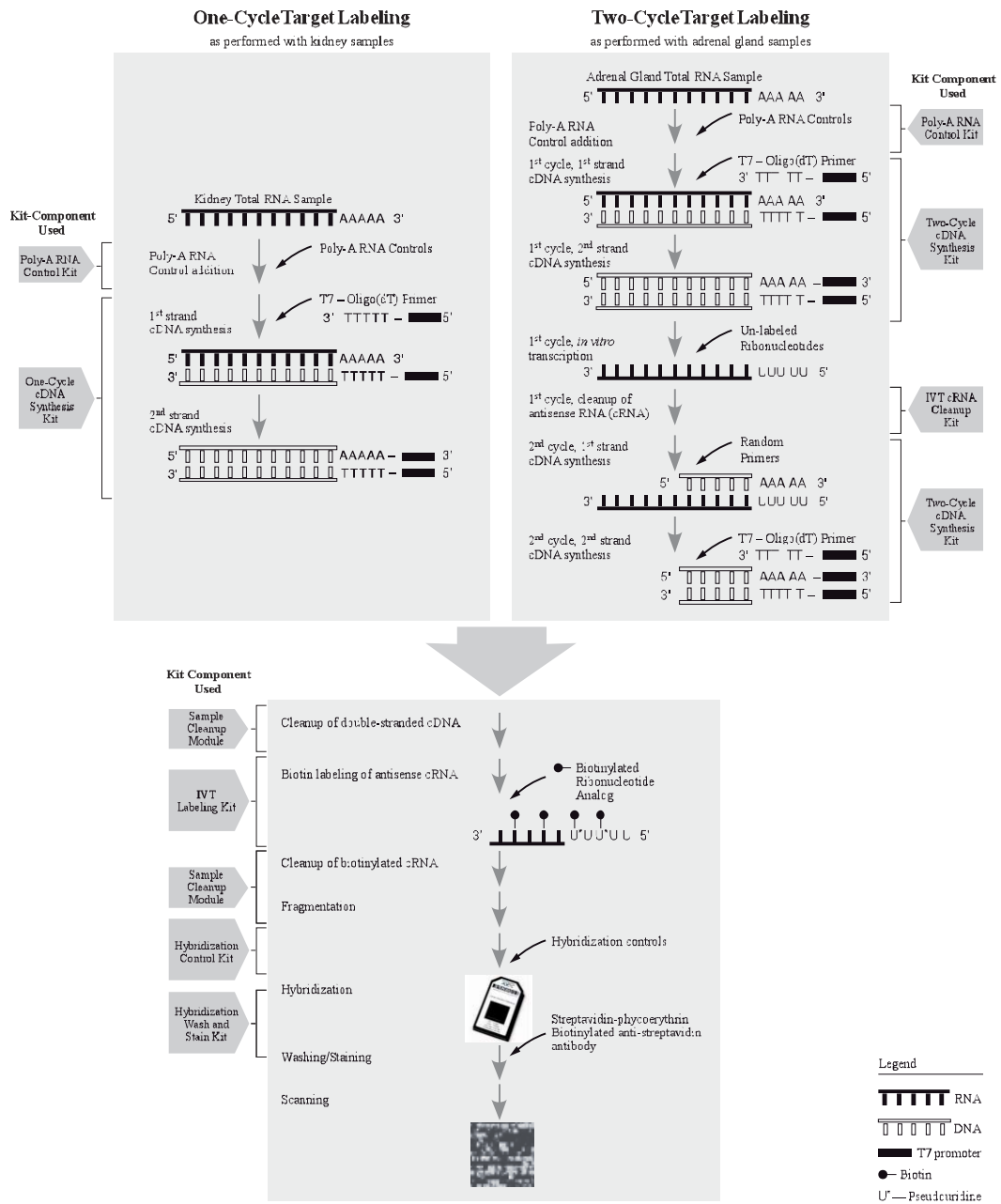


**Figure 4: Workflow of target labeling for Affymetrix analysis as performed for expression analysis in kidney and adrenal gland.** Hybridization and scanning was carried out at the Affymetrix core facility (MDC). Picture adopted from Affymetrix GeneChip Expression Analysis Technical Manual P/N 702232 Rev. 3.

RNA was purified as described above. All further processing steps were carried out according to Affymetrix's manual (GeneChip Expression Analysis Technical Manual P/N 702232 Rev. 2). For kidney samples, 2 µg of total RNA were labeled



with a GeneChip One-Cycle Target Labeling Kit (Affymetrix, USA, part number 900493). For adrenal gland samples, the labeling of 100 ng RNA was carried out using a GeneChip Two-Cycle Target Labeling Kit (Affymetrix, USA, part number 900494) and MEGAscript T7 Kit (Ambion/Applied Biosystems, USA, part number AM1333). Labeled cRNA was hybridized to GeneChip Mouse Genome 430 2.0 Arrays (Affymetrix, USA, part number 900496) and the chips were scanned using a GeneChip Scanner 3000 (Affymetrix, USA). Hybridization and scanning was performed at the Affymetrix core facility (MDC).

The array data was normalized using either the RMA or gcRMA algorithm (Bolstad, et al., 2003; Irizarry, et al., 2003; Wu and Irizarry, 2004). gcRMA-normalized data was analyzed using GeneSpring GX (Agilent, USA); RMA-normalized data was analyzed using Excel 2003 (Microsoft, USA) and PASW Statistics 17 (SPSS, USA). p-values were calculated using either Student's or Welch's t-test (Welch, 1947). False-positive correction (multiple testing) was done by applying the Benjamini-Hochberg false discovery rate algorithm (Benjamini and Hochberg, 1995).

## 2.4 Histology

### 2.4.1 Cryosections

Organs were removed, briefly rinsed in ice-cold PBS and snap-frozen in liquid nitrogen until dissection. Prior to sectioning, frozen tissues were transferred to Tissue-Tek O.C.T. Compound (Sakura, Japan) and cooled down on dry ice.

Solid blocks of Tissue-Tek containing the tissues were dissected at 10  $\mu$ m with a HM 355 S rotary cryotome (Micom/Thermo Fisher Scientific, Walldorf, Germany). The sections were mounted on SuperFrost Plus, air-dried for 30 min at room-temperature and stored at  $-80^{\circ}\text{C}$ .

### 2.4.2 Paraffin Sections

Embryos were sacrificed at embryonal day 14.5 (E14.5) and briefly rinsed in ice-cold PBS. After cutting off the limbs, embryos were punctured at forehead and frontal abdominal cavity. Specimens were fixed for 2 h at room-temperature in 4%<sub>(w/v)</sub> PFA.

Kidneys of adult animals were fixed *in situ* by perfusion with 4% formaldehyde, removed and additionally fixed for in 4% formaldehyde at  $4^{\circ}\text{C}$  overnight. The samples were dehydrated by transfer through a series of graded ethanol/PBS solutions (70%, 80%, 90%, 96%, 100% ethanol in PBS, respectively) for 2 h per step.

The tissues were incubated twice for 2 h each in Roti-Histol (Carl Roth, Karlsruhe, Germany). Preinfiltration with paraffin was carried out for 2 h at 67 °C and a final infiltration step in fresh 67 °C paraffin followed overnight. Specimens were embedded in metal molds and stored at 4 °C until processed.

The solid paraffin blocks containing the samples were sectioned at 5 µm on a rotary microtome (Leica Geosystems, Switzerland). Slides were stored at 4 °C until further use.

### 2.4.3 *In situ* Staining of Sections

*In situ* hybridization was carried out on paraffin sections. All reagents used were RNase-free, all incubation steps were performed at room-temperature unless stated otherwise. Paraffin was dissolved by dipping the object slides with the sections two times for 5 min into Roti-Histol (Carl Roth, Karlsruhe, Germany). The sections were hydrated by transfer through an ethanol series (100%, 96%, 90%, 80%, 70%, 40%, 0% ethanol in PBS, 2 min each). Sections were postfixed for 10 min in 4%<sub>(w/v)</sub> PFA (paraformaldehyde in PBS) at 4 °C, followed by two PBS washing-steps, 5 min each. Endogenous peroxidase activity was inactivated by bathing in 1% hydrogen peroxide in methanol for 20 min. After another two rounds of PBS-washing, endogenous phosphatase activity was quenched by incubating the sections in 0.2 mol/l HCl for 8 min and washing as before. Permeabilization was achieved by treatment with 10 µg/ml proteinase K in 10 mmol/l Tris-HCl (pH 7.5) for 10 min.

After one washing step in PBS for 5 min, the sections were bathed in 0.1 mol/l triethanolamine for 2 min and subsequently acetylated by incubation for 10 min in 0.25% acetic anhydride in 0.1 mol/l triethanolamine.

The sections were washed twice in 2x SSC buffer (20x SSC buffer is 3 mol/l NaCl and 300 mmol/l sodium citrate, pH 7.0) for 10 min each and air-dried. Hybridization buffer (50%<sub>(v/v)</sub> formamide, 2x SSC, 0.02%<sub>(w/v)</sub> BSA, 0.02%<sub>(w/v)</sub> polyvinylpyrrolidone, 0.02%<sub>(w/v)</sub> ficoll, 10%<sub>(w/v)</sub> dextrane sulfate, 0.5 mg/ml yeast tRNA and 0.5 mg/ml hydrolyzed salmon sperm DNA) was mixed with digoxigenin-labeled probes (20 ng/ml final concentration) and 200 µl of this mix were dispensed on the sections. The sections were covered with cover slips and stored inside a humid box. The probes were allowed to hybridize in a hybridization oven overnight at 60 °C. The hybridization temperature was chosen due to the calculated melting temperatures of ca. 62 °C for both *Sorla* and *Sortilin* probes in a buffer containing 50% formamide and 2x SSC (calculated using the Lasergene Suite, DNASTAR, USA) and the requirement for stringent binding. The following day, the sections were washed in 2x SSC for 10 min at 45 °C. Two subsequent stringency washes in 50% formamide 1x SSC at 60 °C for 20 min each were followed by one bath in 60 °C warm 0.2x SSC for 20 min.

Sections were briefly washed in wash buffer (100 mmol/l maleic acid, 150 mmol/l NaCl, 0.3%<sub>(v/v)</sub> Tween-20, pH 7.5) and incubated for 30 min at 37 °C in blocking buffer 1 containing 1%<sub>(w/v)</sub> blocking reagent (Roche Diagnostics, Mannheim, Germany, cat. No. 1096176) and 0.05%<sub>(w/v)</sub> avidin in wash buffer.

After a brief rinse with wash buffer, the sections were incubated for 1 h in anti-DIG-HRP (Abcam, USA) diluted 1:100 in blocking buffer 1 containing 0.005%<sub>(w/v)</sub> biotin. The antibody-solution was removed by washing three times in wash buffer for 5 min each. Sections were blocked with blocking buffer 2 (0.5%<sub>(w/v)</sub> renaissance blocking reagent, NEN Life Science, USA, in 150 mmol/l NaCl and 100 mmol/l Tris-HCl, pH 7.5) for 30 min at 37 °C. Biotinyl-Tyramide was diluted 1:70 in amplification diluents (both NEN Life Science, USA), added to the sections and incubated for 10 min in the dark. Slides were washed three times in wash buffer, 5 min each. The samples were incubated with streptavidin-AP (Perkin Elmer, USA), diluted 1:750 in blocking buffer 1, for 1 h in a dark box. After three 5 min washes with wash buffer and a 10 min wash with detection buffer (10 mmol/l NaCl, 100 mmol/l Tris-HCl, 50 mmol/l MgCl<sub>2</sub>, pH 9.5), the staining was developed in substrate solution (337 µg/ml NBT, 175 µg/ml BCIP, 5 mmol/l levamisole in detection buffer) 5 min to 4 h and stopped in TE buffer (10 mmol/l Tris-HCl, 1 mmol/l EDTA, pH 7.5). The slides were rinsed in water and dehydrated through an Ethanol/PBS series and mounted with Roti-Histokitt (Carl Roth, Karlsruhe, Germany).

#### **2.4.4 Staining of LacZ Reporter Gene Activity**

Cryosections of kidneys from adult Sorla Ex255 mice were thawed and briefly rinsed in PBS. The sections were incubated in X-gal staining solution (100 µg/ml X-gal in 5 mmol/l potassium ferrocyanide, 5 mmol/l potassium ferricyanide, 0.1%<sub>(w/v)</sub> Triton X-100, 0.1 mol/l sodium phosphate, pH 7.5), until the staining became visible. Reactions were stopped by brief rinsing in PBS and pictures were taken immediately.

#### **2.4.5 Immunohistochemistry**

##### **2.4.5.1 Staining of SORLA in Adrenal Glands**

Frozen sections were fixed in -20 °C cold acetone for 5 min. After washing in PBS (3x 5 min), endogenous peroxidase activity was quenched by treatment with 0.3% hydrogen peroxide in PBS for 5 min, followed by another PBS wash (3x 5 min). The sections were blocked using the Biotin Blocking System (Dako, Denmark) according to manufacturer's manual. The tissues were permeabilized for 5 min in 0.2%<sub>(w/v)</sub> Triton X-100, washed in PBS as before and blocked with 3% FCS in PBS for 1 h. After a brief PBS wash (1x 5 min), anti-SORLA antibody (from goat, diluted 1:500 in PBS containing 3% FCS) was applied for 1 h fol-

lowed by PBS wash (3x 5 min). The sections were incubated with a biotinylated secondary antibody (anti-goat), diluted 1:500 in PBS, for 30 min. After briefly washing with PBS (1x 5 min), an avidin-biotinylated horseradish peroxidase-complex (ABC; Vectastain Elite ABC Kit, Vector Laboratories, USA; used according to manual) was added for 30 min. After eliminating non-bound complex by washing with PBS (3x 5 min), the antibody-ABC complex was stained by applying development solution containing AEC (3-amino-9-ethylcarbazole) for 5 to 10 min. Development of the staining was stopped by rinsing the sections in distilled water. Nuclei were counterstained using Mayer's hematoxylin staining for 1 min, followed by washing with tap water. Sections were mounted using aqueous fluorescence mounting medium (Dako, Denmark). Pictures were taken using a brightfield microscope (BX51; Olympus, Japan) with an attached CCD-camera (SPOT RT Slider; Diagnostic Instruments, USA).

#### **2.4.5.2 Immuno-staining in Kidney Sections**

Murine adult kidney sections were deparaffinized by transferring the object slides with the sections two times for 5 min each into Roti-Histol (Carl Roth, Karlsruhe, Germany). The sections were hydrated by transfer through an ethanol series (100%, 96%, 90%, 80%, 70%, 40%, 0% ethanol in PBS, 2 min each). Sections were postfixed for 10 min in 4%<sub>(w/v)</sub> PFA (paraformaldehyde in PBS) at 4 °C, followed by two PBS washing-steps, 5 min each. The tissues were permeabilized for 5 min in 0.2%<sub>(w/v)</sub> Triton X-100, washed in PBS as before and blocked with 3% FCS (donkey serum for fluorescence stainings) in PBS for 1 h, followed by a brief PBS wash (1x 5 min).

For detection of SORLA, anti-SORLA antibody (from goat, diluted 1:500 in PBS containing 3% FCS) was applied for 2 h followed by PBS wash (3x 5 min). The sections were incubated with an HRP-conjugated secondary antibody (anti-goat), diluted 1:500 in PBS. After washing with PBS (3x 5 min), the staining was developed by adding diaminobenzidine (DAB Substrate Kit; Vectorlabs, USA, used according to manufacturer's instructions) until the staining was sufficient. Development of the staining was stopped by rinsing the sections in distilled water. Nuclei were counterstained using Mayer's hematoxylin staining for 1 min, followed by washing with tap water. Sections were dehydrated using an ethanol series (as described above) and mounted using Roti-Histokitt (Carl Roth, Karlsruhe, Germany). Pictures were taken using a brightfield microscope (BX51; Olympus, Japan) with an attached CCD-camera (SPOT RT Slider; Diagnostic Instruments, USA).

For fluorescence co-staining of NKCC2 and SPAK, anti-NKCC2 antibody (from rabbit, diluted 1:250) and anti-SPAK / anti-phospho-SPAK (both from sheep, diluted 1:500) were applied at 4 °C overnight. The next day, sections were rinsed in PBS (3x 5 min) and incubated for 1 h with corresponding fluorescence-labeled

secondary antibodies (Alexa Fluor 488-conjugated anti-rabbit, Alexa Fluor 555-conjugated anti-sheep; both Invitrogen, USA), diluted 1:1,000 each. Finally, sections were washed in PBS (3x 5 min), mounted using Vectashield mounting medium (Vector Labs, USA) and coverslips. Fluorescence pictures were taken using a confocal laser scanning microscope (TCS SP2; Leica Microsystems, Germany).

## **2.5 Protein Biochemistry**

### **2.5.1 Enrichment of Membrane Proteins**

The following protocol was used to enrich proteins that are directly or indirectly bound to the cellular membrane system. All solutions were complemented with protease-inhibitors (Complete Protease Inhibitor; Roche Diagnostics, Mannheim, Germany) and phosphatase-inhibitors (Halt Phosphatase Inhibitor Cocktail; Pierce, USA) and carried out on ice unless otherwise stated. Organs were taken out and weighted after residual adipose tissue was removed. After a brief rinse in PBS, the organs were snap-frozen in liquid nitrogen and stored at  $-80^{\circ}\text{C}$  until processed. The frozen organs were pestled in a cold mortar containing some liquid nitrogen. The ground material was transferred into a 1.5 ml reaction tube by adding 1 ml of sucrose buffer (20 mmol/l Tris-HCl, 2 mmol/l  $\text{MgCl}_2$ , 0.25 mmol/l sucrose, pH 7.5) per 100 mg tissue weight and pipetting the melted solution. The suspension was sonicated for 20 sec and centrifuged for 10 min at  $1,000 \times g$  at  $4^{\circ}\text{C}$  to remove nuclei. The supernatant was spun for 30 min at  $20,000 \times g$  (also  $4^{\circ}\text{C}$ ), enriching cell membrane in the pellet. The supernatant of this step was centrifuged at  $100,000 \times g$  to enrich vesicular membranes in the pellet.  $20,000 \times g$  and  $100,000 \times g$  pellets were collected, the other fractions were discarded. Pellets were dissolved in RIPA buffer (50 mmol/l Tris-HCl, 150 mmol/l NaCl, 0.5%<sub>(w/v)</sub> deoxycholate, 1%<sub>(w/v)</sub> NP40, 0.1%<sub>(w/v)</sub> SDS).

### **2.5.2 Total Protein Preparation**

For the preparation of total protein, organs were taken out and excessive fat removed. The organs were weighted and homogenized on ice in 1 ml/100 mg homogenization buffer (50 mmol/l Tris-HCl, 1 mmol/l EGTA, 1 mmol/l EDTA, 1%<sub>(w/v)</sub> Triton X-100, 1 mmol/l sodium orthovanadate, 50 mmol/l sodium fluoride, 5 mmol/l sodium pyrophosphate, 0.27 mol/l sucrose, 0.1% 2-mercaptoethanol, pH 7.5) complemented with protease-inhibitors (Complete Protease Inhibitor; Roche Diagnostics, Mannheim, Germany) and phosphatase-inhibitors (Halt Phosphatase Inhibitor Cocktail; Pierce, USA) using an Ultra-Turrax (IKA, St. Augustin, Germany). The samples were incubated for 20 min on ice and afterwards centrifuged for 10 min at  $10,000 \times g$  at  $4^{\circ}\text{C}$ . Pellets were discarded, supernatants were frozen in liquid nitrogen and stored at  $-80^{\circ}\text{C}$ .



### **2.5.3 Protein Concentration Estimation**

The concentration of proteins was estimated using either a Bradford (Bio-Rad Protein Assay; Bio-Rad, USA) or a BCA (BCA Protein Assay Kit; Pierce, USA) assay (Bradford, 1976; Smith, et al., 1985). These assays strongly rely on similar properties (e.g. sequence of amino-acid residues, surface charges, etc.) of the protein of interest and a standard of known concentration. As most protein solutions measured were of unknown composition, the cheaply available globular protein BSA (Sigma-Aldrich, USA) was used as a standard, resulting in estimation (not exact determination) of the protein concentration. Both assays were carried out as described in manufacturers' protocols. BSA standards were used for protein preparations. Concentrations of peptide solutions were only compared to each assay other using the BCA assay to estimate coupling efficiency (*vide infra*). This was necessary due to the lack of proper controls, as peptides with a different primary structure can have very different  $\text{Cu}^{2+}$  reduction properties.

### **2.5.4 SDS Polyacrylamide Gel Electrophoresis**

SDS polyacrylamide gel electrophoresis (SDS PAGE) was carried out to separate proteins according to their electrophoretic mobility (mainly influenced by size, struture and charge) in a charge-independent manner (Shapiro, et al., 1967). The detergent SDS denatures proteins and gives them a negative net charge. As a result, the electrophoretic mobility is mostly depending on the size of the protein.

Samples and polyacrylamide gels were prepared as described in 'Molecular cloning: a laboratory manual' (Sambrook, et al., 1989). Before applying to the gel, samples were mixed with sample buffer (final concentrations: 50 mmol/l Tris-HCl, 2%<sub>(w/v)</sub> SDS, 0.01%<sub>(w/v)</sub> bromophenol blue or orange G, 10% glycerol, 100 mmol/l 2-mercaptoethanol, pH 6.8) and denatured for 5 min at 96 °C. The gels were run in a glycine buffer (196 mmol/l glycine, 0.1%<sub>(w/v)</sub> SDS, 50 mmol/l Tris-HCl, pH 8.4) at 45-100 V.

For total protein staining, gels were either stained with Imperial Protein Stain (Pierce, USA) as recommended by manufacturer or with Coomassie blue G250. For the latter method, gels were fixed for 2 h in an aqueous solution containing 50% ethanol and 10% acetic acid. Afterwards, the gels were stained overnight in freshly prepared Coomassie staining solution (770 mg/l Coomassie blue G250, 582 mmol/l ammonium sulfate, 0.92% ortho-phosphoric acid, 23% methanol in ultra-pure water). The next day, the gels were destained *ca.* 10x in distilled water (5 min each).

For specific immunostaining, gels were subjected to Western blotting (described below).

### 2.5.5 Western Blotting

Western blotting is a technique for immunological detection of proteins. After an electrophoresis, the separated proteins are transferred to a membrane and probed with an antibody specific for the protein of interest.

Wet transfer from polyacrylamide gel to Hybond-C nitrocellulose membrane (GE Healthcare, USA) was carried out in permanently cooled transfer buffer (25 mmol/l Tris-HCl, 192 mM Glycine, pH 8.4) at 95 V for 2 h or at 20-30 V

**Table 9: List of primary antibodies.** Target-peptide sequences are listed from amino- to carboxy-terminus. A lower case 'p' indicates phosphorylation of the following amino acid.

Target protein (and -sequence for peptide antibodies)		Source / Supplier	Species
Actin		Sigma-Aldrich, USA	rabbit
Barttin		Santa Cruz Biotechnology, USA	goat
ENaC $\alpha$		AlphaDiagnostics International, USA	rabbit
ERK1/2		Cell Signaling Technologies, USA	rabbit
GAPDH		Abcam, UK	rabbit
KCC4		Abcam, UK	goat
Na <sup>+</sup> /K <sup>+</sup> -ATPase		Abcam, UK	mouse
NCC	CHTKRFEDMIAPFRLNDGFKD	Dario Alessi (Dundee, UK)	sheep
pNCC T55	HPSHLTHSSTFCMRpTFGYNT	Dario Alessi (Dundee, UK)	sheep
pNCC T60	RTFGYNpTIDVVPT	Dario Alessi (Dundee, UK)	sheep
pNCC S91	TLADLHpSFLKQEG	Dario Alessi (Dundee, UK)	sheep
NHE3		Chemicon, USA	rabbit
NKCC2	EYYRNTGSVSGPKVNRPSLQE	self-designed (Eurogentec, Belgium)	rabbit
pNKCC2	YYLQpTFGHNP TMDAVP	S. Bachmann (Berlin, Germany)	rabbit
ROMK (K <sub>ir</sub> 1.1)		Chemicon, USA	rabbit
SORLA		J. Gliemann (Aarhus, Denmark)	goat
SPAK	QSLSVHDSQAQPNAN	Dario Alessi (Dundee, UK)	sheep
pSPAK S373	RRVPGSpSGHLHKT	Dario Alessi (Dundee, UK)	sheep

overnight. To test for efficiency of the transfer and artifacts (e.g. from bubbles), protein on the membrane was reversibly stained with a 0.1%<sub>(w/v)</sub> Ponceau S (Sigma-Aldrich, USA) solution in 5% acetic acid. The membrane was blocked for 2 h with 5%<sub>(w/v)</sub> skimmed milk powder in PBS containing 0.05% Tween-20 (PBST). Antibodies (listed in table 9) were diluted 1:100 to 1:1,000 in 5% skimmed milk/PBST and applied to the membrane overnight at 4 °C on a rocking shaker. The next day, the membrane was washed in PBST (3x 5 min) and a corresponding secondary antibody conjugated to horseradish peroxidase (anti-sheep antibody from Abcam, USA, all others from Sigma-Aldrich, USA), diluted 1:2,000 in 5% skimmed milk/PBST, was added. After 1 to 2 h, the membrane was washed in PBST (3x 10 min) and incubated with luminol (Super Signal West Femto substrate; Pierce, USA). Protein bands were detected using a CCD camera (Fujifilm LAS-1000; Fujifilm, Japan).

### 2.5.6 Peptide Pulldown

Peptides of the cytosolic tail of human SORLA (table 10; obtained from Eurogentec, Belgium) were dissolved in ultra-pure water (1 mg peptide in 200 µl H<sub>2</sub>O), peptide 1 was soaked in 4 µl DMSO prior to dissolving in water). The peptides were coupled to iodoacetyl-activated agarose (SulfoLink Coupling Resin; Pierce, USA) according to the SulfoLink manual (Doc. No. 0527; Pierce, USA). As control for unspecific binding to the resin, one batch of beads was treated in parallel as described, but without adding any peptide. Binding efficiency was estimated by applying a BCA assay (vide supra) on samples of the peptide solution before and after coupling to the sepharose. A signal decrease (and therewith a decrease of peptide in solution) of >90% was considered as efficient coupling. After the coupling, free binding sites were blocked by incubation in 50 mM cysteine.

**Table 10: List of peptides covering the cytosolic tail sequence of human SORLA.** All peptides were synthesized with an amino-terminal CGGG linker. Internal peptides were masked with an amido-group instead of a carboxy-group. Amino acid numbers are quoted as position in unprocessed SORLA (beginning counting with the initial M of the signal peptide).

Peptide	Sequence	Corresponding SORLA Sequence
Peptide 1	<i>NH<sub>2</sub>-CGGG PMITGFSDDVPMVIA-COOH</i>	amino acids 2200 to 2214
Peptide 2	<i>NH<sub>2</sub>-CGGG DDLGEDDEDAPMITG- CONH<sub>2</sub></i>	amino acids 2190 to 2204
Peptide 3	<i>NH<sub>2</sub>-CGGG RLGSAIFSSGDDLGE- CONH<sub>2</sub></i>	amino acids 2180 to 2194
Peptide 4	<i>NH<sub>2</sub>-CGGG TAFANSHYSSRLGSA- CONH<sub>2</sub></i>	amino acids 2170 to 2184
Peptide 5	<i>NH<sub>2</sub>-CGGG TKHRRLQSSFTAFAN-CONH<sub>2</sub></i>	amino acids 2160 to 2174

Animals were sacrificed and kidneys were removed rapidly, rinsed briefly in PBS and homogenized with an Ultra-Turrax (IKA, St. Augustin, Germany) in 1 ml ice-cold RIPA buffer containing 0.2% SDS (0.2%<sub>(w/v)</sub> SDS, 0.1%<sub>(w/v)</sub> sodium deoxy-



cholate, 1%<sub>(w/v)</sub> NP-40, 150 mmol/l NaCl, 50 mmol/l Tris-HCl, 2 mmol/l 2-mercaptoethanol, 5 mmol/l EDTA, pH 7.4) or DOC buffer (10% sodium deoxycholate, 500 mmol/l Tris-Cl, pH 7.4) per 50 mg tissue. After incubating the homogenates for 10 min on ice, they were sonicated. To enrich cytosolic proteins, the lysates were cleared by centrifugation at  $126.200 \times g$  for 30 min at 4 °C. Protein concentrations were estimated by performing a BCA assay (with comparison to a BSA standard).

1 mg of protein was incubated at 4 °C overnight with 50 µl of settled peptide-coupled resin on a rotating wheel. The next day, the column was washed 5x for 5 min with 1 ml of RIPA or DOC buffer each. Bound proteins were eluted by incubating the beads in 20 µl 4x SDS-PAGE sample buffer (200 mmol/l Tris-HCl, 8%<sub>(w/v)</sub> SDS, 0.04%<sub>(w/v)</sub> bromophenol blue or orange G, 40% glycerol, 200 mmol/l 2-mercaptoethanol, pH 6.8) at 95 °C for 5 min. Eluted samples were subjected to SDS polyacrylamide gel electrophoresis as described above. Proteins were stained either with Coomassie blue G250 (Sigma-Aldrich, USA) or with Imperial Stain (Pierce, USA). Interesting bands were cut out and the gel pieces were stored at 4 °C in 1% acetic acid. Mass spectrometry (MS) for protein/peptide identification was carried out either by Gunnar Dittmar (MDC MS core facility), Heike Stephanowitz (Leibniz-Institute for Molecular Pharmacology, FMP Berlin) or Bent Honoré (Aarhus, Denmark). Only identified candidates assessed as 'significantly present' in the corresponding sample with the used MS setup were considered for further analysis.

## 2.6 Special Reagents, Kits and Consumables

**Table 11: List of special chemicals, kits and consumables used.**

Name	Supplier
Acetic anhydride	Sigma Aldrich, USA, cat. No. A6404
Alexa Fluor 488 donkey anti-rabbit IgG (H+L)	Invitrogen, USA, cat. No. A-21206
Alexa Fluor 555 donkey anti-sheep IgG (H+L)	Invitrogen, USA, cat. No. A-21436
Ampicillin, sodium salt	Merck, Darmstadt, Germany, cat. No. 171255
Anti-digoxigenin antibody, HRP-conjugate	Abcam, UK, cat. No. ab6212
anti-sheep antibody, HRP-conjugated	Abcam, UK, cat. No. ab8527
Avidin	Sigma Aldrich, USA, cat. No. A9275
Barium chloride dihydrate	Sigma Aldrich, USA, cat. No. B0750
BCA protein assay kit	Pierce, USA, cat. No. 23225
BigDye Terminator v3.1 cycle sequencing kit	Applied Biosystems, USA, cat. No. 4337456
Bio-Rad Protein Assay dye reagent concentrate	Bio-Rad, USA, cat. No. 500-0006EDU
Biotin	Sigma Aldrich, USA, cat. No. B4501
Biotin-Blocking System	Dako, Denmark, cat. No. X0590
Bovine serum albumin - fraction V (BSA)	Sigma Aldrich, USA, cat. No. 85040C
Bumetanide	Sigma Aldrich, USA, cat. No. B3023
Collagenase, crude type Ia	Sigma Aldrich, USA, cat. No. C2674
Complete protease inhibitor cocktail tablets	Roche Diagnostics, Mannheim, Germany, cat. No. 04693116001
Coomassie Brilliant Blue G 250	Sigma Aldrich, USA, cat. No. 27815
D+ glucose	Sigma Aldrich, USA, cat. No. 49138
DAB substrate kit for peroxidase	Vector Labs, USA, cat. No. SK-4100
dATP, [ $\alpha$ -32P]	Perkin Elmer, USA, cat. No. BLU012H250UC
[deamino-Cys1, D-Arg8]-Vasopressin, acetate salt	Sigma Aldrich, USA, cat. No. V1005
DIG RNA labeling kit (SP6/T7)	Roche Diagnostics, Mannheim, Germany, cat. No. 11175025910
DNase I recombinant, RNase-free	Roche Diagnostics, Mannheim, Germany, cat. No. 4716728
GeneChip mouse genome 430 2.0 array	Affymetrix, USA, cat. No. 900496
GeneChip one-cycle target labeling kit	Affymetrix, USA, cat. No. 900493
GeneChip two-cycle target labeling kit	Affymetrix, USA, cat. No. 900494
Halt phosphatase inhibitor cocktail	Pierce, USA, cat. No. 78420
HEPES	Sigma Aldrich, USA, cat. No. H4034
High Pure PCR product purification kit	Roche Diagnostics, Mannheim, Germany, cat. No. 11732668001
Hybond-C Extra	GE Healthcare, USA, cat. No. RPN203E
Hydrochlorothiazide	Sigma Aldrich, USA, cat. No. H4759
illustra Sephadex G-50 DNA grade F	GE Healthcare, USA, cat. No. 17-0573-01
Imperial protein stain	Pierce, USA, cat. No. 24615
IPTG	Fermentas, Canada, cat. No. R0391
Kodak BioMax MR-1	Perkin Elmer, USA, cat. No. 8222648001EA
MEGAscript T7 Kit	Applied Biosystems, USA, cat. No. AM1333
NucAway spin columns	Applied Biosystems, USA, cat. No. AM10070
O.C.T. <sup>TM</sup> Compound; cryo mounting medium	Sakura, Japan, cat. No. 4583
Ouabain octahydrate	Sigma Aldrich, USA, cat. No. 75640
Perchloric acid 70%	Merck, Darmstadt, Germany, cat. No. 100514
pGEM-T Easy vector system	Promega, USA, cat. No. A1360
Phosphatase, alkaline	Roche Diagnostics, Mannheim, Germany, cat. No. 713023

<b>Name</b>	<b>Supplier</b>
Phusion high-fidelity DNA polymerase	Finnzymes, Finland, cat. No. F-530
Plasmid midi kit	Qiagen, The Netherlands, cat. No. 12143
Plasmid mini kit	Qiagen, The Netherlands, cat. No. 12123
Ponceau S	Sigma Aldrich, USA, cat. No. P3504
Potassium D-gluconate	Sigma Aldrich, USA, cat. No. G4500
Prime-It II random primer labeling kit	Stratagene, USA, cat. No. 300385
qPCR MasterMix Plus	Eurogentec, Belgium, cat. No. RT-QP2X-03-075+
Renaissance blocking reagent	NEN Life Science, USA
RNA 6000 Nano kit	Agilent Technologies, USA, cat. No. 5067-1511
RNeasy mini kit	Qiagen, The Netherlands, cat. No. 74106
Roti-Histokitt	Carl Roth, Karlsruhe, Germany, cat. No. 6638.1
Roti-Histol	Carl Roth, Karlsruhe, Germany, cat. No. 6640.2
Rubidium chloride	Sigma Aldrich, USA, cat. No. R2252
Rubidium-86 radionuclide (86Rb)	Perkin Elmer, USA, cat. No. NEZ072005MC
Skimmed milk powder	different suppliers
Streptavidin, alkaline phosphatase conjugate	Perkin Elmer, USA, cat. No. NEL751001EA
SulfoLink coupling resin	Pierce, USA, cat. No. 20401
SuperFrost Plus object slides	Menzel Gläser, Braunschweig, Germany, cat. No. J1800AMNZ
SuperScript II reverse transcriptase	Invitrogen, USA, cat. No. 18064
SuperSignal West Femto maximum sensitivity substrate	Pierce, USA, cat. No. 34095
T4 DNA ligase	Invitrogen, USA, cat. No. 15224-041
Taq DNA polymerase	Invitrogen, USA, cat. No. 10342-020
Trichloromethane	Carl Roth, Karlsruhe, Germany, cat. No. 3313
TRIzol	Invitrogen, USA, cat. No. 15596-018
VECTASHIELD mounting medium	Vector Labs, USA, cat. No. H-1000
VECTASTAIN Elite ABC kit	Vector Labs, USA, cat. No. PK-6200
X-gal	Invitrogen, USA, cat. No. 15520018

### 3 Results

#### 3.1 Renal expression profile of *Sorla*

Using Northern blot analysis, I initially tested the expression pattern of *Sorla* in human tissue. Figure 5 A shows expression of *SORLA* predominantly in brain, to considerable amounts in leukocytes, liver, kidney, heart, spleen, and thymus, and to lower extent in small intestine, placenta and lung. As a control, I investigated the transcriptional expression pattern of the related VPS10p receptor sortilin (figure 5 B). While also showing highest expression in the brain, *SORTILIN* is also transcribed considerably in heart, kidney and placenta. Weak expression of *SORTILIN* was found in lung, skeletal muscle, colon, small intestine and liver.

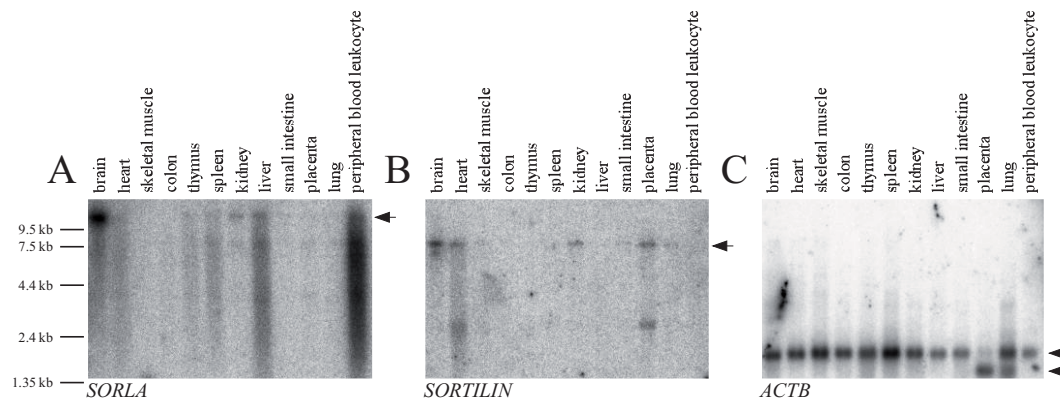


**Figure 5: Northern blot for (A) *SORLA*, (B) *SORTILIN* and (C) *ACTB* (beta-actin).** Highest expression of *SORLA* and *SORTILIN* is seen in the brain. Both genes are also expressed in the kidney. Arrowheads indicate the expected transcript size.

To assess the expression of *Sorla* throughout renal development, quantitative real-time-PCR (TaqMan<sup>®</sup>) experiments were performed on cDNAs obtained from whole kidney (and brain as control) RNA of mouse embryos at day E12.5 (embryonic day 12.5, also referred to as 12.5 dpc, days post coitum), E15.5, E17.5, neonatal mice and adult (12 weeks of age) murine kidneys.

The specificity of the primer/probe pairs used for the TaqMan experiments was confirmed by agarose gel electrophoresis of the amplicons. The single PCR product was excised from the gel, purified and ligated into the pGEM-T Easy vector for DNA-sequencing. Using the nblast algorithm (part of NCBI Blast!), the obtained sequences were compared with the *NCBI nucleotide collection (nr/nt)* and the *NCBI mouse genomic plus transcript (Mouse G+T)* databases, resulting in perfect matches for the regions of interest within the murine forms of the according VPS10p receptor family member transcript sequence (corresponding *Sorla*-sequence shown in figure 6).

end of *Sorla* exon 17  
 5' -ACTTGGCCTCGGGAGCCACAGAGCAGCTTCCTCTCTCGGGGCTGCGGGCGGCTGTGG  
 CCCTGGACTTTGACTA **TGAACGCAACTGCTTGTATTGGTCTGACCTGGCGCTGGACACCA**  
 ← junction exon 17/18      forward primer  
**TCCAGCGTCTCTGCTTGAACGGGAGCACAGGGCAGGAGGTGATCATCAATTCCGGCCTGG**  
 probe      reverse primer  
 AGACCGTGGAGGCTTTGGCCTTCGAACCCCTCAGCCAATTACTTTACTGGGTGGATGCCG  
 ← junction exon 18/19      start of *Sorla* exon 19  
 GCTTTAAAAAGATCGAGGTAGCTAATCCAGATGGTGACTTCCGACTGACAATCGTCA-3'

**Figure 6: Partial sequence of the *Sorla* cDNA covering the template region for realtime PCR.** The forward primer sequence and the reverse complement sequence of the reverse primer are marked in blue. The probe sequence is marked in red. The PCR product, confirmed by sequencing, is shown in bold letters.

Representing the data of three individual experiments, figure 7 A, shows that *Sorla* is expressed throughout kidney development with a distinct increase of expression between E12.5 and E15.5. In the adult, *Sorla* is the Vps10p receptor gene with the strongest renal expression. *Sortilin* is expressed at somewhat lower levels, yet consistent throughout kidney development. None of the three *Sorcs* transcripts is expressed in the adult and the embryonic expression of *Sorcs1* and *Sorcs3* is rather low. It is remarkable, however, that the expression level of *Sorcs2* is comparably high in the developing kidney with a peak around E15.5. Figure 7 B shows the expression pattern in brain. All receptors are highly expressed during CNS development. In the adult mouse, *Sorla* and *Sortilin* show the highest expression of all Vps10p receptors in whole brain.

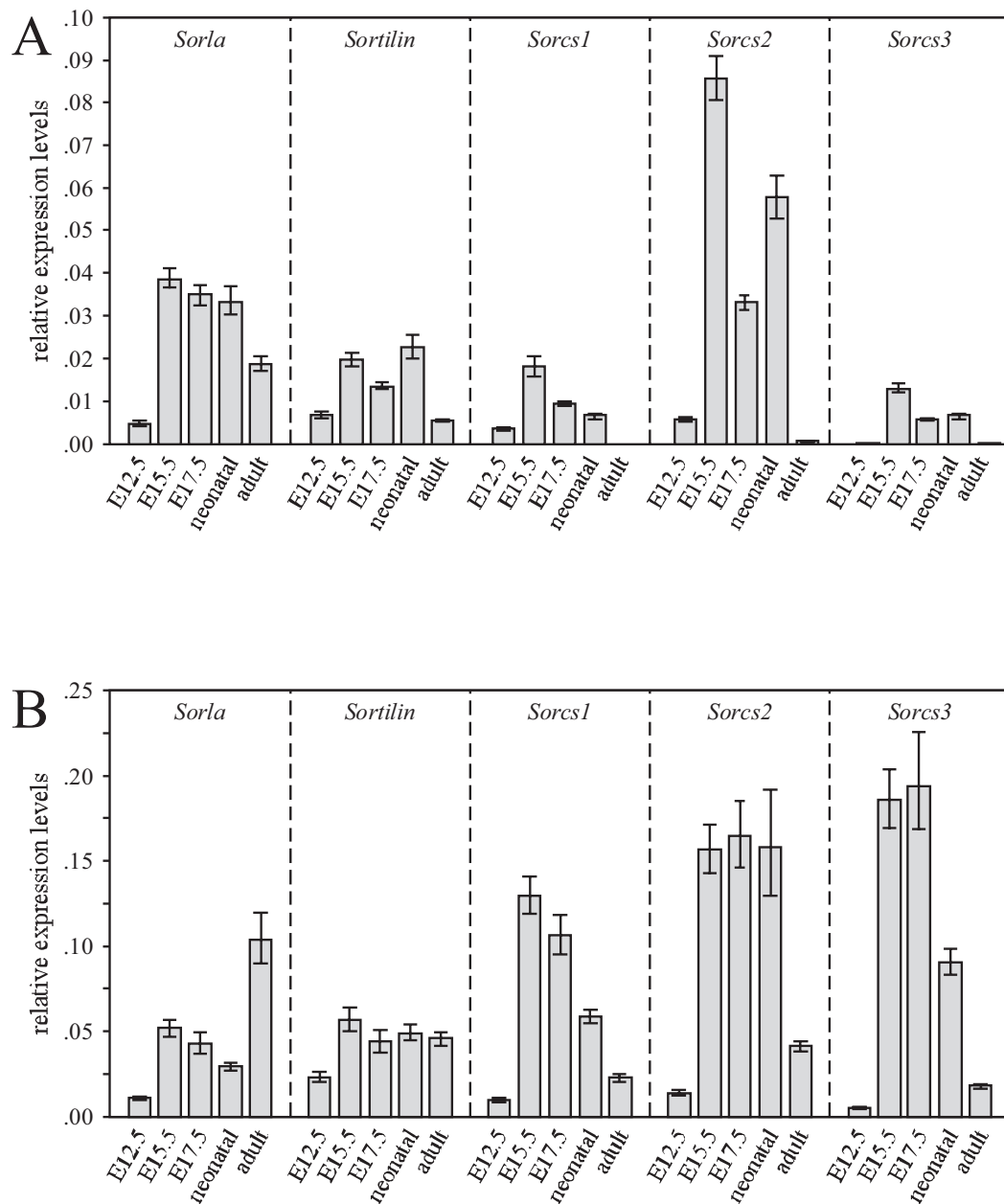


**Figure 7: Transcriptional expression of all members of the VPS10p receptor family in the developing kidney (A) and brain (B) relative to *Gapdh*.** Whereas all members of the VPS10p receptor family are expressed in the brain between embryonic day 12.5 (E12.5) and adulthood, only mRNAs of the *Sorla*- and the *Sortilin*-gene are detectable in the adult kidney. Error bars represent standard error of the mean.

Having established the expression of *Sorla* in the embryonic and adult kidney, my interest turned towards the exact sites of expression of the receptor in this organ.



To localize its expression in the embryonic kidney, in-situ hybridization was carried out on sagittal paraffin-sections of E14.5 mouse embryos. Representative experiments are shown in figure 8. Transcripts of *Sorla* (A) and *Sortilin* (B) are located in tubular structures, resembling collecting ducts of the developing kidney.

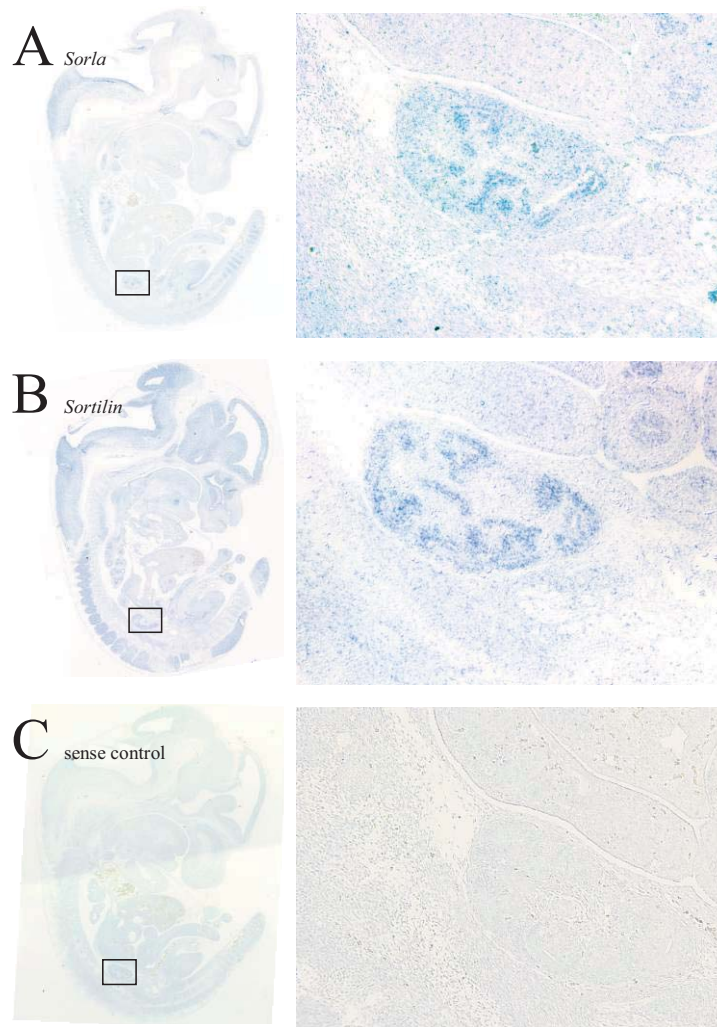


**Figure 8: In-situ hybridization of *Sorla* transcripts (A) and *Sortilin* transcripts (B) in the murine embryonic kidney.** Left site: sagittal paraffin section of an E14.5 embryo indicating the area magnified on the right (magnification: 20x). Right site: area indicated on the left, showing the kidney (200x). C: control with a mixture of sense probes for *Sorla* and *Sortilin*.

The expression of *Sorla* in renal tubules suggested a function in transport processes in distinct nephron segments. To better localize the renal expression of *Sorla* in the adult, I made use of a mouse model with insertion of a  $\beta$ -galactosidase

(lacZ) reporter gene into the murine *Sorla* gene locus (Mitchell, et al., 2001; Rohe, et al., 2008). In this mouse line, expression of lacZ is controlled by the endogenous *Sorla* gene promoter, thus reflecting the expression of the sorting receptor (figure 9 A). To ascertain the exact sites of expression, coronal kidney sections of adult wild type mice were immunostained with an antibody against the extracellular portion of the receptor. Collectively these findings, as exemplified in figure 9, demonstrated expression of *Sorla* in the distal nephron, from the thick ascending limb of Henle's loop through the distal convoluted tubule and connecting tubules to the collecting duct.

### 3.2 Electrolyte homeostasis

Expression of *Sorla* in the collecting duct has been reported before (Riedel, et al., 2002). In addition, I demonstrated that *Sorla* is also expressed in the thick ascending limb of the loop of Henle, in the distal convoluted tubule and in the connecting tubule of the adult kidney.

Each nephron segments fulfills an essential and distinct function in renal physiology. The thick ascending limb of Henle's loop is involved in active reabsorption of approximately 25% of sodium and potassium, while the distal convoluted tubule is responsible for the reabsorption of 5% of the filtered sodium and chloride from tubular fluid. An important task mainly accomplished by the nephron segments expressing *Sorla* is also the maintenance of fluid homeostasis. Mechanisms regulating water homeostasis include the dilution of tubular fluid in the water-impermeable ascending limb of Henle's loop and the activity of the kidney-specific sodium-potassium-chloride cotransporter (NKCC2). As a result, the hypertonic tubular fluid leaving the descending limb is converted into a distinctly hypotonic state. Thus, in contrast to the situation in the proximal tubule, the reabsorption of water and electrolytes is uncoupled in the distal nephron. In addition, water reabsorption in the collecting duct is highly regulated by vasopressin. This hormone triggers water reabsorption. In its absence, the collecting duct is almost water-impermeable.



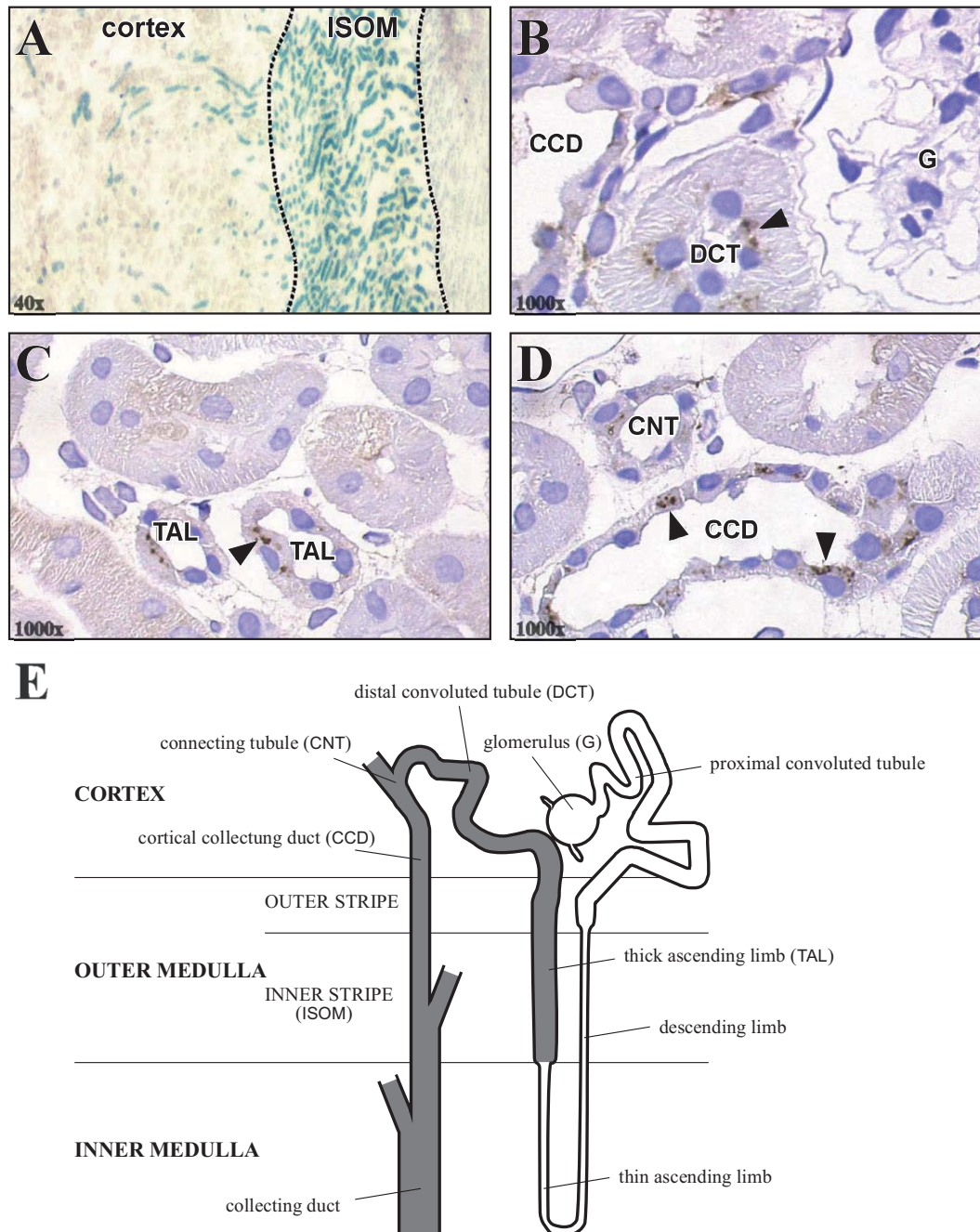


**Figure 9: *Sorla* expression in the adult nephron.** A: Detection of *Sorla*-gene expression in cortex and inner stripe of the outer medulla (ISOM) based on activity of a beta-galactosidase reporter gene inserted into the murine *Sorla* gene locus. B, C, D: Immunohistological staining of SORLA in thick ascending limb (TAL) of Henle's loop, distal convoluted tubule (DCT), connecting tubule (CNT) and cortical collecting duct (CCD) on paraffin sections. Arrowheads mark SORLA-specific staining in perinuclear vesicular structures. E: Schematic drawing of nephric segments based on 'Brenner and Rector's The Kidney' (Brenner, 2007), areas expressing SORLA are marked in grey. Magnifications: 40x for A, 1000x for C-D.

To gain insight into possible functions of SORLA in tubular transport processes, I measured urinary concentrations of sodium ( $\text{Na}^+$ ), chloride ( $\text{Cl}^-$ ), potassium ( $\text{K}^+$ ) and calcium ( $\text{Ca}^{2+}$ ) ions in mice genetically deficient for the receptor. This mouse model has previously been generated in our group (Andersen, et al., 2005). Two receptor-deficient strains harboring the same targeted gene disruption were being bred in our group: the strain SorLA27 was kept on a hybrid 129SvEmcTer  $\times$  C57BL/6N (129Bl/6) background, SorLA18 was kept on a hybrid 129SvEmcTer  $\times$  Balb/c (129Balb/c) background. For the experiments in this study, both strains and corresponding wild type hybrid lines were used. The results shown are representative for both backgrounds unless stated otherwise.

By comparison of *Sorla*<sup>(-/-)</sup> animals with wild type mice of the same genetic background (*Sorla*<sup>(+/+)</sup>), the specific effects of receptor deficiency on renal functions can be studied. In parallel, the animals' ability to concentrate water was stressed by thirsting for 24 hours to check SORLA's influence on any of the abovementioned volume regulation mechanisms.

**Table 12: Urine volume and urinary electrolyte concentrations.** A: Urine of wild type and *Sorla*<sup>(-/-)</sup> animals was collected for 16 hours overnight in metabolic cages with free access to drinking water. B: After a preliminary thirsting period of eight hours, animals were kept in metabolic cages without water and urine was collected for 16 hours overnight. Values are shown  $\pm$  standard error of the mean; *p*-values were calculated using Student's t-test.

	<i>Sorla</i> <sup>(+/+)</sup>	<i>Sorla</i> <sup>(-/-)</sup>	
<b>A: basal conditions</b>			
volume (ml)	1.6 $\pm$ 0.7	1.5 $\pm$ 0.8	
$\text{Na}^+$ (mmol/l)	93 $\pm$ 3.5	102 $\pm$ 4.6	
$\text{Cl}^-$ (mmol/l)	75 $\pm$ 2.6	94 $\pm$ 4.5	<i>p</i> < 0.001
$\text{K}^+$ (mmol/l)	119 $\pm$ 6.7	189 $\pm$ 19	<i>p</i> < 0.001
$\text{Ca}^{2+}$ (mmol/l)	1.2 $\pm$ 0.1	2.1 $\pm$ 0.1	<i>p</i> < 0.001
<b>B: water deprivation</b>			
volume (ml)	0.6 $\pm$ 0.3	0.5 $\pm$ 0.2	
$\text{Na}^+$ (mmol/l)	121 $\pm$ 7.2	174 $\pm$ 16.8	<i>p</i> < 0.01
$\text{Cl}^-$ (mmol/l)	130 $\pm$ 8.1	189 $\pm$ 19.1	<i>p</i> < 0.01
$\text{K}^+$ (mmol/l)	224.7 $\pm$ 28.2	230.7 $\pm$ 19.5	
$\text{Ca}^{2+}$ (mmol/l)	1.4 $\pm$ 0.1	2 $\pm$ 0.1	<i>p</i> < 0.01

Under basal conditions, absence of SORLA resulted in an increase in the secretion of  $\text{K}^+$  by 60% and of  $\text{Ca}^{2+}$  by 75% (table 12 A, figure 10 A). After thirsting, the animals secrete over 40% more  $\text{Na}^+$ ,  $\text{Cl}^-$  and  $\text{Ca}^{2+}$  as the control animals (table 12 B, figure 10 A). This elevated salt loss in *Sorla*<sup>(-/-)</sup> animals is not accompanied by defects in the thirst-induced reduction of urine volume (antidiuresis), as the ani-

mals are able to reduce urine as efficient as their wild type counterparts (figure 10 B).

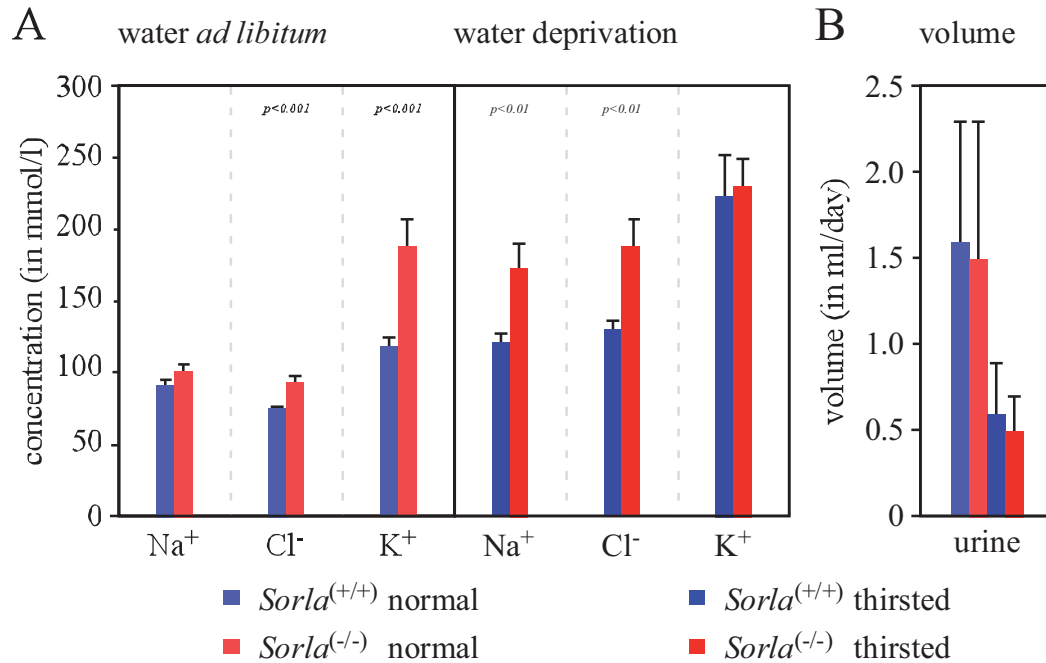


**Figure 10: Excretion of Na<sup>+</sup> Cl<sup>-</sup> and K<sup>+</sup> in wild type and SORLA-deficient mice.** Urinary electrolyte concentrations (A) and urine volume (B) of wild type animals (*Sorla*<sup>(+/+)</sup>) and mice lacking the receptor (*Sorla*<sup>(-/-)</sup>) under basal conditions and after thirsting.

Serum samples were taken under the same conditions, to assess whether the changes in urinary electrolytes are mirrored in the blood of *Sorla*<sup>(-/-)</sup> animals. In addition to the electrolyte measurements, I investigated hormones regulating renal reabsorption processes to discover a potential hormonal mis-regulation.

Three hormones were measured. The first one, renin, is a key component of the renin-angiotensin cascade, converting angiotensinogen to angiotensin I. It is synthesized by the renal juxtaglomerular apparatus. The renin-angiotensin system (RAS) is involved in blood pressure regulation and water balance. One mediator of its action is the adrenal steroid hormone aldosterone, which increases the reabsorption of Na<sup>+</sup> and water and the secretion of K<sup>+</sup> in the distal nephron by activating the basolateral Na<sup>+</sup>/K<sup>+</sup>-ATPase as well as different ion transporters. Another hormone that plays an important role in renal water retention and salt reabsorption is vasopressin. This peptide hormone, also known as antidiuretic hormone, is secreted mainly from the pituitary gland. It increases the water permeability of the collecting duct, e.g. by activating aquaporin-2 (AQP-2), and activates salt reabsorption in the thick ascending limb via NKCC2.

Tables 13 A and 13 B show normal  $\text{Na}^+$  and  $\text{Cl}^-$  levels in blood under normal as well as thirsted conditions. However, it becomes apparent, that SORLA-deficient mice suffer from decreased  $\text{K}^+$  concentrations in serum under normal conditions (hypokalemia).

Water-deprivation leads to induced vasopressin levels in both groups of animals. Animals lacking SORLA show a milder induction of renin upon thirsting as compared to the control animals, implicating a weakened response of the RAS. More strikingly though is the mis-regulation of aldosterone in the receptor-deficient animals. Whereas the amount of aldosterone released to the bloodstream is significantly elevated under basal conditions (table 13 A), it is actually slightly reduced upon thirsting (table 13 B). The situation contrasts with the physiological reaction of the wild type control mice, which increase aldosterone release massively upon thirsting, presumably as a downstream effect of the activated RAS.

**Table 13: Serum electrolyte concentrations.** A: Serum concentrations in wild type and *Sorla*<sup>(-/-)</sup> animals with free access to drinking water. B: Serum concentrations in animals thirsted for 24 hours. Values are shown  $\pm$  standard error of the mean; *p*-values were calculated using Student's *t*-test.

	<i>Sorla</i> <sup>(+/+)</sup>	<i>Sorla</i> <sup>(-/-)</sup>	
<b>A: basal conditions</b>			
$\text{Na}^+$ (mmol/l)	152 $\pm$ 0.3	153 $\pm$ 0.3	
$\text{Cl}^-$ (mmol/l)	110 $\pm$ 0.8	109 $\pm$ 1.2	
$\text{K}^+$ (mmol/l)	6.8 $\pm$ 0.4	5.7 $\pm$ 0.2	<i>p</i> < 0.05
Renin (ng Ang-I/(ml*h))	389 $\pm$ 81	239 $\pm$ 75	
Aldosterone (pmol/l)	347 $\pm$ 65.9	741 $\pm$ 158.1	<i>p</i> < 0.05
Vasopressin (pg/ml)	35.1 $\pm$ 7.5	52.1 $\pm$ 13	
<b>B: water deprivation</b>			
$\text{Na}^+$ (mmol/l)	151 $\pm$ 0.9	154 $\pm$ 0.9	
$\text{Cl}^-$ (mmol/l)	112 $\pm$ 0.7	113 $\pm$ 0.6	
$\text{K}^+$ (mmol/l)	6.5 $\pm$ 0.2	6 $\pm$ 0.2	
Renin (ng Ang-I/(ml*h))	2469 $\pm$ 402	1273 $\pm$ 135	<i>p</i> < 0.05
Aldosterone (pmol/l)	1863 $\pm$ 385.3	578 $\pm$ 141.4	<i>p</i> < 0.05
Vasopressin (pg/ml)	115.3 $\pm$ 1.7	135.7 $\pm$ 14.7	

As indicated above, the renal electrolyte and water homeostasis is intertwined with blood-pressure regulation. In thirsted *Sorla*<sup>(-/-)</sup> mice normally regulated vasopressin, the presumably weakened RAS and the mis-regulated aldosterone are all affecting the blood pressure. Mice lacking SORLA exhibit decreased mean arterial pressure (MAP) during their activity phase and a lower heart rate, as measured by

blood pressure telemetry (table 14 A and 14 B). They are also less active than the wild type animals.

**Table 14: Physiological parameters.** Mean arterial pressure (MAP), heart rate and activity under basal conditions (A) and after water deprivation (B). MAP was measured during the activity phase of the animals from 6 PM to 3 AM. Values are shown  $\pm$  standard error of the mean;  $p$ -values were calculated using Student's t-test.

	<i>Sorla</i> <sup>(+/+)</sup>	<i>Sorla</i> <sup>(-/-)</sup>	
<b>A: basal conditions</b>			
MAP (mmHg)	130.4 $\pm$ 2.5	121.4 $\pm$ 2.5	$p < 0.05$
Heart rate (beats/min)	680.7 $\pm$ 9.2	612.8 $\pm$ 5.0	$p < 0.001$
Activity (counts/min)	11.6 $\pm$ 2.2	5.4 $\pm$ 0.7	$p < 0.05$
<b>B: water deprivation</b>			
MAP (mmHg)	133.7 $\pm$ 1.1	125.1 $\pm$ 1.6	$p < 0.01$
Heart rate (beats/min)	670.7 $\pm$ 9.2	611.0 $\pm$ 5.8	$p < 0.001$
Activity (counts/min)	16.3 $\pm$ 3.4	9.4 $\pm$ 1.4	

### 3.3 Investigating a renal versus an adrenal phenotype in SORLA-deficient mice

The electrolyte measurements revealed a dysfunction in the kidneys of mice lacking SORLA. Especially the urinary  $K^+$ -wasting is mirrored by a systemic hypokalemia. But the complex regulation of renal function and the hormonal misregulation seen in the receptor-deficient animals made it difficult to pinpoint a function of SORLA in this context. Especially the abnormal regulation of aldosterone in SORLA-deficient mice raised the question, whether the observed phenotype is primarily of renal origin or if the phenotypes in the kidney are secondary to defects at the site of aldosterone synthesis – the adrenal glands.

Intriguingly, transcripts of the receptor have been detected in adrenal gland tissue by northern blot analysis (Mörwald, et al., 1997; Yamazaki, et al., 1996). Performing immunohistological staining of SORLA in murine adrenal gland cryosections, I could reveal that SORLA is expressed in the adrenal cortex, but not in the medulla (figure 11 A-C). The receptors strongest expression can be found in the outer layer of the adrenal cortex (zona glomerulosa, figure 11 B), the section where aldosterone is produced. Specificity of the antibody in adrenal tissue was demonstrated by absence of staining on sections from SORLA-deficient animals (figure 11 D-F). No gross morphological abnormalities were detected in adrenal glands of *Sorla*<sup>(-/-)</sup> animals.



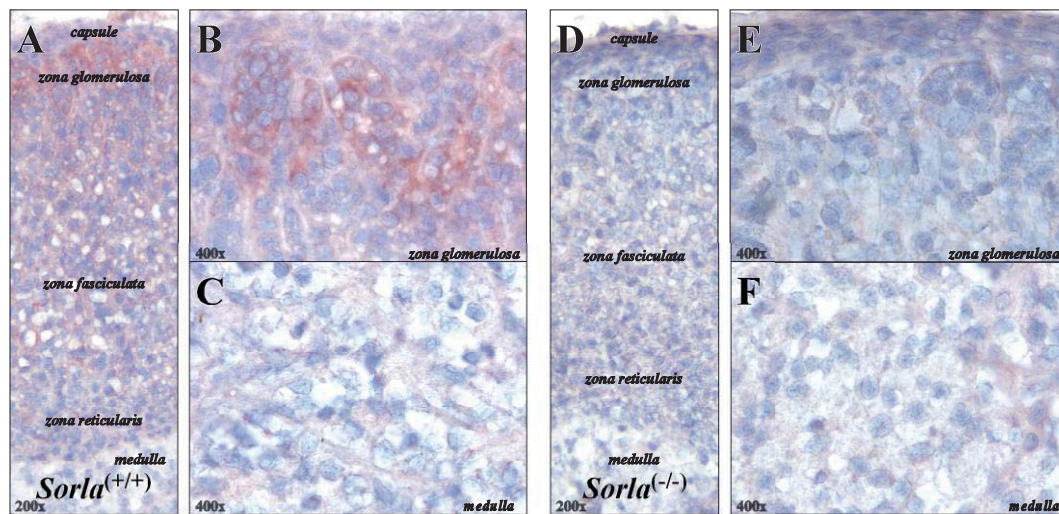


**Figure 11: *Sorla* expression in the adrenal gland.** A-C: Immunohistological staining of SORLA throughout the adrenal cortex – particularly in the zona glomerulosa – on cryosections. No staining was detectable in the adrenal medulla. D-F: Absence of SORLA-specific staining in *Sorla*<sup>(-/-)</sup> mice. Magnifications: 200x for A and D; 400x for B,C,E and F.

To investigate, whether the observed defects result from lack of the receptor in the kidney or in the adrenal gland, the global gene expression patterns of both tissues in receptor-deficient *Sorla*<sup>(-/-)</sup> mice and wild types were compared.

One group of wild type *Sorla*<sup>(+/+)</sup> and receptor-deficient *Sorla*<sup>(-/-)</sup> mice were kept with water ad libitum, the same number of animals was stressed by water-deprivation for 24 hours prior to the experiment to induce the aggravated salt loss phenotype observed before. To reduce experimental variability, three male mice per group were sacrificed between 10 and 11 a.m. at an exact age of 84 days. The kidneys and adrenal glands respectively were taken out and snap-frozen immediately after residual adipose tissue was removed. Total RNA was isolated and used for the synthesis of biotin-labeled cRNA. The cRNA was hybridized to Affymetrix GeneChips (Mouse Genome 430 2.0 Array). This DNA chip collects expression data of over 39.000 transcripts per sample.

Analyses for kidney and adrenal gland were carried out in parallel. For better clarity, the results of the experiments are discussed separately for each tissue.

### 3.3.1 Adrenal glands

DNA microarray expression analysis of adrenal glands was carried out on SorLA18 mice and corresponding hybrid 129Balb/c wild type mice. A two-cycle protocol was used for synthesis of cRNA, due to the amounts of RNA obtained from adrenal glands.

After normalizing the data with a variant of the RMA (robust multichip analysis) algorithm, the validity of the obtained data was tested by carrying out quality assessments tests: Pseudoimages, box-plots of the raw/normalized intensities and RNA degradation plots were comparable for all samples (data not shown). Examination of  $M$  vs.  $A$  plots, which are displaying logarithmic intensity ratios  $M$  versus average logarithmic intensities  $A$  of the red and green channels respectively, unearthed an aberrance: The sample of the first wild type animal supplied with drinking water (*Sorla*<sup>(+/+)</sup> +H<sub>2</sub>O 01) did show an irregularity in the  $M$  vs.  $A$  plot (data not shown). Figure 12 A shows the correlation of the different adrenal gland data sets. Overall, the transcriptional expression is similar. Whereas the data of most chips show a correlation of at least 98%, wild type data set *Sorla*<sup>(+/+)</sup> +H<sub>2</sub>O 01 differs to a significant extent. Unsupervised hierarchical clustering, a method automatically grouping most similar data sets, was able to categorize the data according to genotype (figure 12 B). Again, the first wild type data set did not cluster properly. Because of the clear divergence of this data set from the others, I excluded it from further statistical analyses.

The data sets were subjected to principal component analysis. This statistical method transforms possibly related variables into fewer variables, so called principal components. The first two principal components, A and B, are shown in figure 13. The first component (A) accounts for most of the variability in the adrenal data sets. It clearly separates the data according to the genotype. The second principal component (B) accounts for the second highest variability, distinguishing between normal and thirsted mice. It can be concluded, that the genotype produces a higher divergence between the data sets than thirsting.

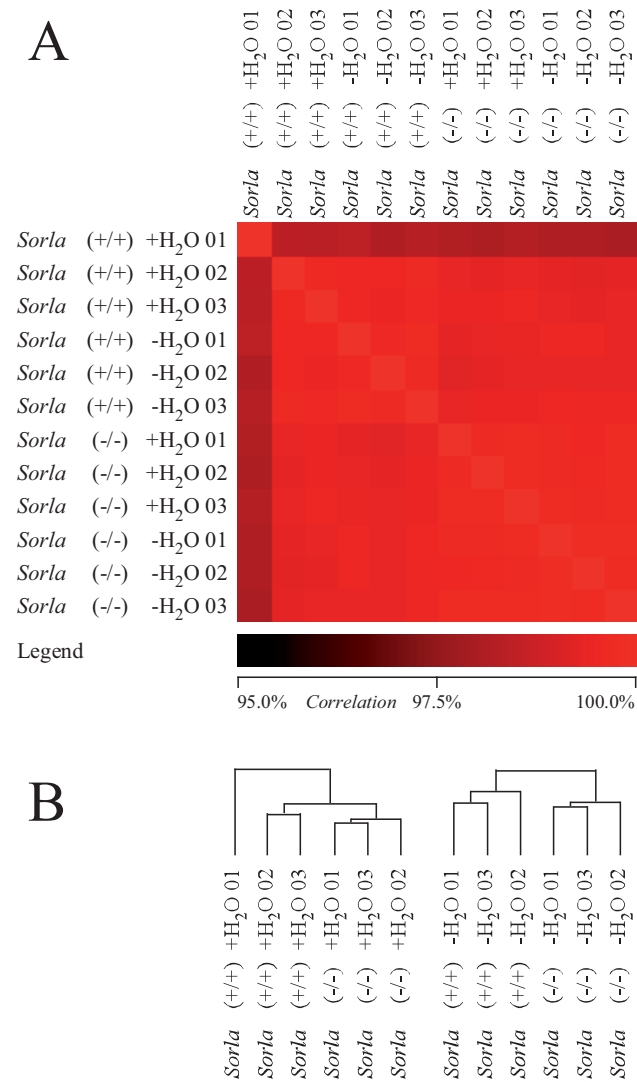


**Figure 12: Correlation plot and unsupervised hierarchical clustering of the adrenal data sets.**

A: Correlation plot showing complete identity of the data sets in bright red and divergence of 5% identity in black; B: Hierarchical trees obtained after performing an unsupervised clustering using the data sets for normal condition (left) and water-deprivation (right).



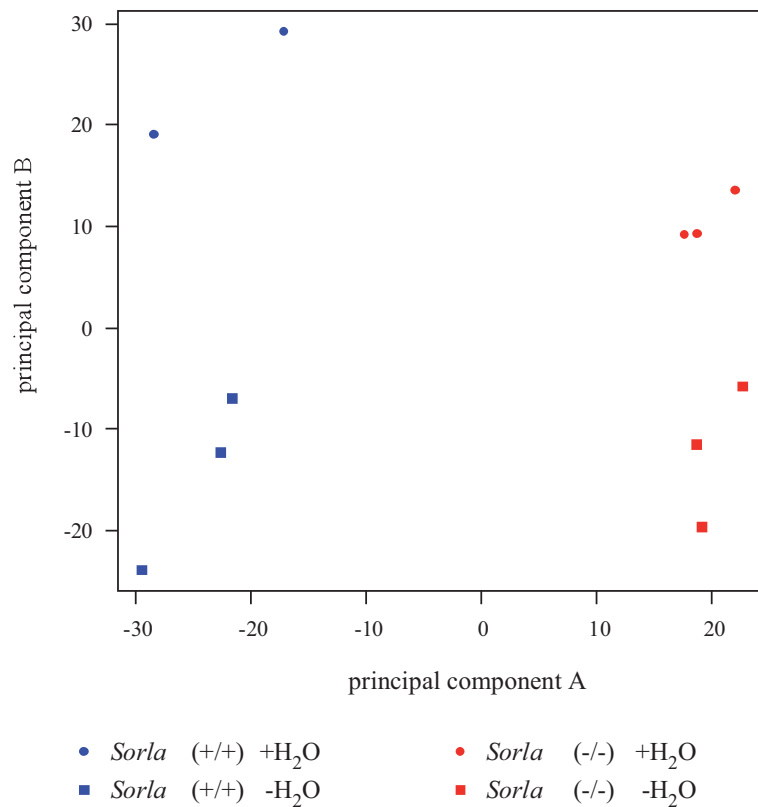


**Figure 13: Principal component plot for adrenal gland Affymetrix data.** Principal component A (abscissa) separates the data set effectively according to genotypes; component B (ordinate) distinguishes between experimental conditions.

To compare the expression levels of individual genes, two values were calculated. The so called fold-change represents the factor by which the average expression in receptor-deficient mice is changed as compared to wild types. To facilitate comprehension and calculation, factors between one and zero (representing downregulation) are shown as negative reciprocals (e.g. -4 instead of 0.25). The second important value is the p-value, representing the likelihood that the observed change occurred by chance. It was calculated using Student's t-test. With data sets this large (>45.000 probe sets) it is likely to observe false positives just by chance. To correct the p-values according to the size of the data sets, the Benjamini-Hochberg correction was used. This very stringent method lowers the t-test p-values.

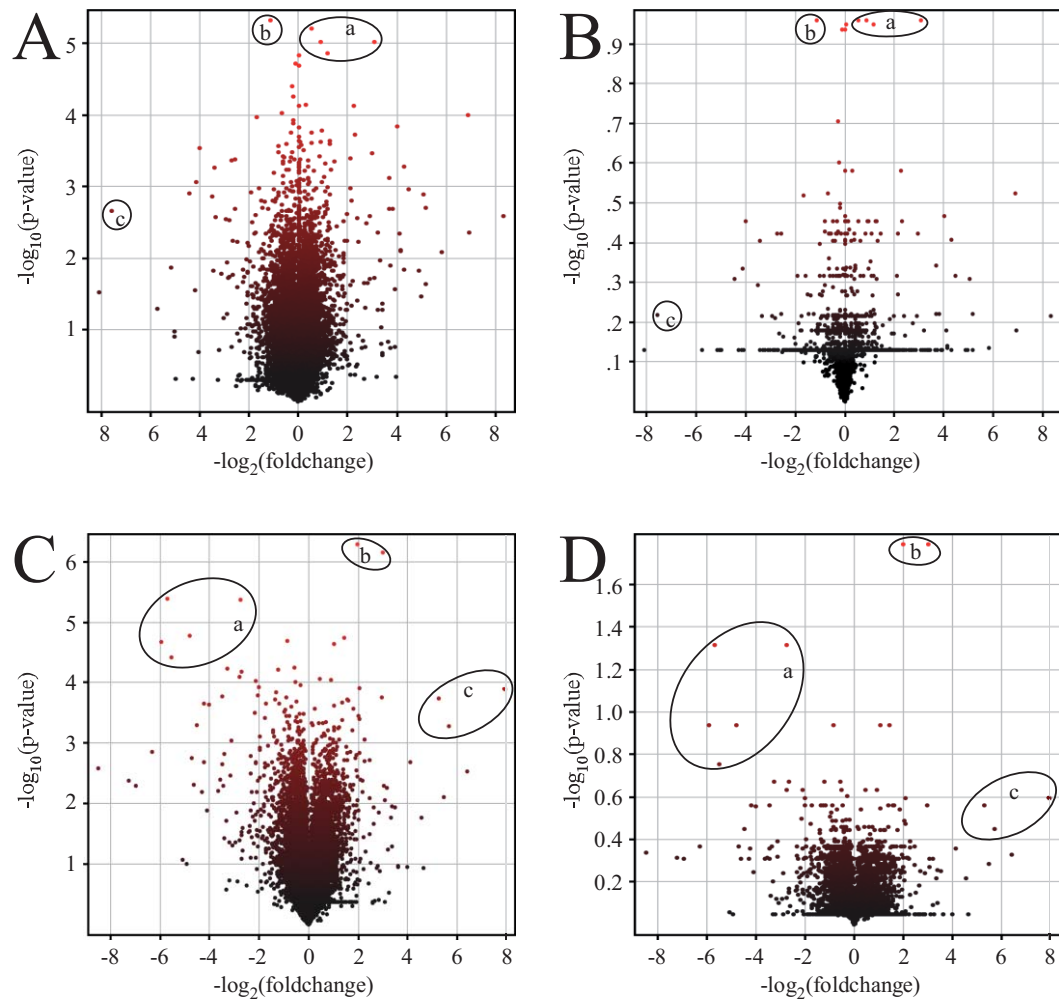


**Figure 14: Volcano plots representing the adrenal Affymetrix data.** Differentially regulated probe sets of normal (A, B) and thirsty (C, D) mice; p-values used for the plots were either uncorrected (A, C) or corrected by the Benjamini-Hochberg method (B, D) to reduce false positives; probe sets underlying a pronounced differential regulation are encircled and listed in table 15.

To look at individual genes strongly affected by the deficiency of SORLA, the negative logarithm of the p-value to the base of ten is plotted against the negative logarithm of the fold-change to the base of two. Dots in the so called volcano plot represent one probe set each (figure 14). Most probe sets, which are neither highly nor significantly regulated, cluster at the lower part of the chart towards the center of the abscissa. However, probe sets with a high fold-change appear towards the outer left and right, significantly regulated probe sets are displayed in the upper part of the plot. Thus, dots appearing in the upper corners represent the most interesting candidate genes.

**Table 15: Highly differential probe sets in the adrenal gland.** List of probe sets marked in figure 14. The p-values listed here are not corrected with the Benjamini-Hochberg algorithm.

		probe set ID	gene symbol	fold-change	p-value
<b>A/B normal</b>	<b>a</b>	1431591_s_at	<i>Isg15</i> <i>LOC100038882</i> <i>LOC100044225</i> <i>LOC677168</i>	1.474	6.19E-06
		1420618_at	<i>Cpeb4</i>	1.863	9.44E-06
		1440624_at	not annotated in NetAffx  (chromosome 4 genomic contig)	8.556	9.70E-06
		1419179_at	<i>Txn14a</i>	2.264	1.36E-05
	<b>b</b>	1445214_at	not annotated in NetAffx  (chromosome 4 genomic contig)	-2.165	4.70E-06
		1424454_at	<i>Tmem87a</i>	-191.133	2.23E-03
	<b>c</b>	1425113_x_at	<i>TranscriptID BI105961</i>	-51.423	4.11E-06
		1438852_x_at	<i>Mcm6</i>	-6.690	4.27E-06
		1419620_at	<i>Pttgl</i>	-27.805	1.71E-05
		1439483_at	<i>AI506816</i>	-61.615	2.14E-05
		1447894_x_at	<i>H2afb3</i>	-45.610	3.90E-05
<b>C/D thirsted</b>	<b>a</b>	1418499_a_at	<i>Kcne3</i>	3.971	5.05E-07
		1452677_at	<i>LOC100044383</i> <i>Pnpt1</i>	7.973	7.15E-07
	<b>b</b>	1457666_s_at	<i>Ifi202b</i>	240.195	1.30E-04
		1421551_s_at		51.633	5.20E-04
		1415824_at	<i>Scd2</i>	38.905	1.83E-04
	<b>c</b>				

To investigate which adrenal functions may be affected by SORLA-deficiency, it is not only important to take single highly differential genes into account but also to consider trends in the overall changes to the transcriptome.

Looking at the non-adjusted p-values, more than 700 genes are significantly changed more than 1.5-fold between the SORLA-deficient and control animals under normal conditions. After thirsting, the number of 1.5-fold changed probe sets increases to more than 1100. With slightly more than 450 probe sets significantly changed more than 1.5-fold while comparing normal and water-deprived animals of the genotype, thirsting as such affects both mice strains to a similar extent. At a transcriptional level, the adrenal glands are affected by the lack of SORLA, with the genotypic effect being more pronounced than the stress effect.

The numbers in table 16 confirm the observation, that more genes are changed due to the lack of SORLA as to the thirsting, a trend already visible in the principal component analysis in figure 13. To get an idea of which functions may be fulfilled by the differentially expressed gene products, all genes with an expression level significantly differing by a factor higher than 1.5 were explored using the web-based database tool DAVID (<http://david.abcc.ncifcrf.gov/>). The data for adrenal glands and kidneys (see chapter 3.3.2) are displayed in figure 15.

**Table 16: Number of probe sets being significantly changed in adrenal glands, sorted by fold change and p-value.** A and B show the number of significant probe sets after Benjamini-Hochberg false discovery rate correction in brackets.

**A** *Sorla*<sup>(-/-)</sup> +H<sub>2</sub>O vs. *Sorla*<sup>(+/+)</sup> +H<sub>2</sub>O

	all	p < 0.05	p < 0.02	p < 0.01	p < 0.005	p < 0.001
<b>all</b>	45101	2275 (0)	1059 (0)	597 (0)	338 (0)	92 (0)
<b>FC &gt; 1.1</b>	14775	1938 (0)	891 (0)	482 (0)	261 (0)	66 (0)
<b>FC &gt; 1.5</b>	2412	729 (0)	406 (0)	238 (0)	142 (0)	38 (0)
<b>FC &gt; 2.0</b>	764	304 (0)	197 (0)	125 (0)	84 (0)	24 (0)
<b>FC &gt; 3.0</b>	248	122 (0)	85 (0)	57 (0)	43 (0)	15 (0)
<i>expected by chance</i>	2255		902	451	225	45

**B** *Sorla*<sup>(-/-)</sup> -H<sub>2</sub>O vs. *Sorla*<sup>(+/+)</sup> -H<sub>2</sub>O

	all	p < 0.05	p < 0.02	p < 0.01	p < 0.005	p < 0.001
<b>All</b>	45101	2856 (4)	1418 (2)	823 (0)	452 (0)	109 (0)
<b>FC &gt; 1.1</b>	13551	2737 (4)	1370 (2)	804 (0)	448 (0)	108 (0)
<b>FC &gt; 1.5</b>	2218	1153 (4)	708 (2)	456 (0)	274 (0)	79 (0)
<b>FC &gt; 2.0</b>	785	483 (4)	342 (2)	241 (0)	156 (0)	57 (0)
<b>FC &gt; 3.0</b>	239	164 (4)	127 (2)	95 (0)	72 (0)	34 (0)
<i>expected by chance</i>	2255		902	451	225	45

A and B: *Welch's t-test, unpaired, unequal variance*  
*asymptotic p-value computation*  
*no multiple testing correction (in brackets: Benjamini-Hochberg correction)*

**C** *Sorla*<sup>(+/+)</sup> +H<sub>2</sub>O vs. *Sorla*<sup>(+/+)</sup> -H<sub>2</sub>O

	all	p < 0.05	p < 0.02	p < 0.01	p < 0.005	p < 0.001
<b>all</b>	45101	1813	741	370	184	33
<b>FC &gt; 1.1</b>	14581	1631	694	350	173	30
<b>FC &gt; 1.5</b>	1922	472	219	113	71	13
<b>FC &gt; 2.0</b>	473	129	65	34	22	5
<b>FC &gt; 3.0</b>	125	32	19	10	6	1
<i>expected by chance</i>	2255		902	451	225	45

**D** *Sorla*<sup>(-/-)</sup> +H<sub>2</sub>O vs. *Sorla*<sup>(-/-)</sup> -H<sub>2</sub>O

	all	p < 0.05	p < 0.02	p < 0.01	p < 0.005	p < 0.001
<b>all</b>	45101	1990	829	406	197	45
<b>FC &gt; 1.1</b>	12038	1787	769	383	191	45
<b>FC &gt; 1.5</b>	1206	457	230	123	73	19
<b>FC &gt; 2.0</b>	257	110	62	36	21	6
<b>FC &gt; 3.0</b>	44	17	4	2	1	0
<i>expected by chance</i>	2255		902	451	225	45

C and D: *Welch's t-test, unpaired, unequal variance*  
*asymptotic p-value computation*  
*no multiple testing correction*

The numbers in table 16 confirm the observation, that more genes are changed due to the lack of SORLA as to the thirsting, a trend already visible in the principal component analysis in figure 13. To get an idea of which functions may be fulfilled by the differentially expressed gene products, all genes with an expression level significantly differing by a factor higher than 1.5 were explored using the web-based database tool DAVID (<http://david.abcc.ncifcrf.gov/>). The data for adrenal glands and kidneys (see chapter 3.3.2) are displayed in figure 15.

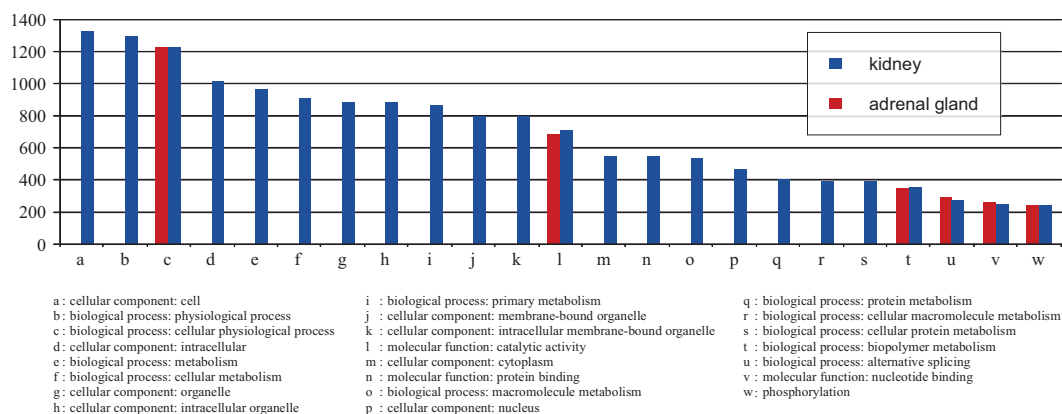


**Figure 15: GO-term categories found for significantly changed probe sets in adrenal gland and kidney.** All probe sets differentially regulated with fold change > 1.5 and p-value < 0.05; each probe set is usually annotated with more than one Gene Ontology (GO) term and hence partially represented in more than one group. Categories *a* through *v* represent GO terms, *w* represents a Swiss-Prot/Protein Information Resource keyword category. It has to be mentioned that each probe set is usually annotated with more than one gene ontology term. Therefore, the probe sets can be represented in more than one bar.

Clustering all probe sets meeting the abovementioned cutoff criteria (fold-change > 1.5;  $p < 0.05$ ; irrespective of the condition) by Gene Ontology (GO) annotation results in quite different distributions in the two organs. In total, much more pathways seem to be affected in the kidney. Interestingly, the total numbers of genes involved in “cellular physiological processes” (figure 15 c), “catalytic activity” (l), “biopolymer metabolism” (t), “alternative splicing” (u), nucleotide binding (v) and “phosphorylation” (w) correlate between the organs.

With my focus on identification of metabolic pathways, I analyzed the rather vaguely GO-terms shown in figure 15 and the corresponding gene lists. While investigating the data using the PANTHER classification System (<http://www.pantherdb.org/>), one specific pathway became apparent: the catecholamine-synthesis pathway. Table 17 shows probe sets corresponding to genes that have been reported to be involved in the catecholamine metabolism. While some of these genes are specific for the nervous system (dopamine acts as a neurotransmitter and -modulator in the central nervous system, norepinephrine act as neuromodulator in the sympathetic nervous system), most genes are also expressed in chromaffin cells of the adrenal medulla.

**Table 17: Probe sets for genes involved in the catecholamine pathway with fol change and p-value in adrenal glands.**

probe set ID	gene symbol	Title	normal		thirsted	
			fold-change	p-value	fold-change	p-value
1418149_at	<i>Chga</i>	chromogranin A	-1.099	6.77E-01	-1.429	2.21E-02
1425409_at	<i>Chrna2</i>	cholinergic receptor, nicotinic, alpha polypeptide 2, neuronal	-1.033	6.99E-01	1.087	2.64E-01
1452010_at	<i>Chrna3</i>	cholinergic receptor, nicotinic, alpha polypeptide 3	-2.398	2.30E-02	-2.758	3.53E-04
1455931_at	<i>Chrna3</i>	cholinergic receptor, nicotinic, alpha polypeptide 3	-1.334	1.92E-01	-1.435	4.74E-02
1440681_at	<i>Chrna7</i>	cholinergic receptor, nicotinic, alpha polypeptide 7	-1.537	1.38E-01	-1.641	2.24E-02
1450299_at	<i>Chrna7</i>	cholinergic receptor, nicotinic, alpha polypeptide 7	-1.117	1.17E-01	1.075	3.38E-01
1425849_at	<i>Chrn4</i>	cholinergic receptor, nicotinic, beta polypeptide 4	-1.148	5.24E-01	1.063	4.59E-01
1457008_at	<i>Chrn4</i>	cholinergic receptor, nicotinic, beta polypeptide 4	-2.065	1.03E-02	-2.101	7.22E-03
1447592_at	<i>Dbh</i>	dopamine beta hydroxylase	-1.480	4.49E-02	-1.717	1.27E-03
1450670_at	<i>Dbh</i>	dopamine beta hydroxylase	-1.414	2.62E-01	-2.026	1.11E-02
1459848_x_at	<i>Dbh</i>	dopamine beta hydroxylase	-1.391	6.70E-02	-1.525	5.83E-03
1426215_at	<i>Ddc</i>	DOPA decarboxylase	-1.456	5.45E-02	-1.695	2.78E-02
1430591_at	<i>Ddc</i>	DOPA decarboxylase	-1.148	1.67E-01	-1.006	8.85E-01
1428667_at	<i>Maoa</i>	monoamine oxidase A	1.025	8.60E-01	-1.081	3.63E-01
1442676_at	<i>Maoa</i>	monoamine oxidase A	1.035	8.01E-01	-1.013	8.33E-01
1434354_at	<i>Maob</i>	monoamine oxidase B	-1.744	4.94E-02	-1.679	1.25E-02
1419127_at	<i>Npy</i>	neuropeptide Y	-1.865	1.40E-02	-2.452	1.30E-03
1421471_at	<i>Npy1r</i>	neuropeptide Y receptor Y1	1.033	9.32E-01	-1.298	6.81E-02
1449804_at	<i>Pnmt</i>	phenylethanolamine-N-methyltransferase	-1.210	2.86E-01	-1.547	1.93E-02
1450606_at	<i>Pnmt</i>	phenylethanolamine-N-methyltransferase	1.040	7.59E-01	-1.905	1.48E-03
1460269_at	<i>Pnmt</i>	Phenylethanolamine-N-methyltransferase	-1.145	2.30E-01	-1.188	5.13E-02
1426595_at	<i>Slc18a1</i>	solute carrier family 18 (vesicular monoamine), chromaffin granule	-1.410	6.67E-02	-1.643	1.67E-02
1446248_at	<i>Slc18a1</i>	solute carrier family 18 (vesicular monoamine), chromaffin granule	-1.405	1.56E-01	-1.585	4.74E-02
1458777_at	<i>Slc18a1</i>	solute carrier family 18 (vesicular monoamine), chromaffin granule	1.072	3.72E-01	-1.038	5.25E-01
1437079_at	<i>Slc18a2</i>	solute carrier family 18 (vesicular monoamine), synaptic vesicle	-1.111	5.63E-01	-1.530	8.45E-03
1420546_at	<i>Th</i>	tyrosine hydroxylase	-1.251	2.41E-01	-1.883	2.64E-02

The adrenal synthesis of catecholamines is depicted in figure 35 (chapter 4.2.2). Starting from the amino acid tyrosine, the enzymes tyrosine hydroxylase (Th) and DOPA decarboxylase (Ddc) synthesize dopamine. The vesicular monoamine transporter (Slc18a1) transports the dopamine into vesicles, where it is converted to norepinephrine by dopamine beta-hydroxylase (Dbh). Due to its hydrophobicity, norepinephrine (as the other catecholamines) passively leaks out of its synthesis and storage vesicles, requiring constant sequestration by Slc18a1. However, cytosolic norepinephrine is substrate to phenylethanolamine N-methyltransferase (Pnmt) which synthesizes epinephrine. As the other catecholamines, epinephrine is also subject to Slc18a1 transport, whereby it is stored in vesicles until released. The degradation of catecholamines is carried out by monoamine oxidase A (Mao a) and catechol-o-methyltransferase (Comt).

In SORLA-deficient mice, the genes of all biosynthetic enzymes are transcriptionally downregulated with a fold-change between -1.2 and -2.0. The differential expression becomes more pronounced with thirsting (cf. table 17 and figure 35 in chapter 4.2.2).

To study whether downregulation has an effect on the catecholamine-synthesis, I measured catecholamine levels in isolated adrenal glands. Mice were sacrificed and adrenal glands quickly taken out. After removal of remaining adipose tissue, the organs were immediately homogenized in 0.2 M perchloric acid and catecholamines were measured via reverse-phase HPLC and subsequent electrochemical detection.



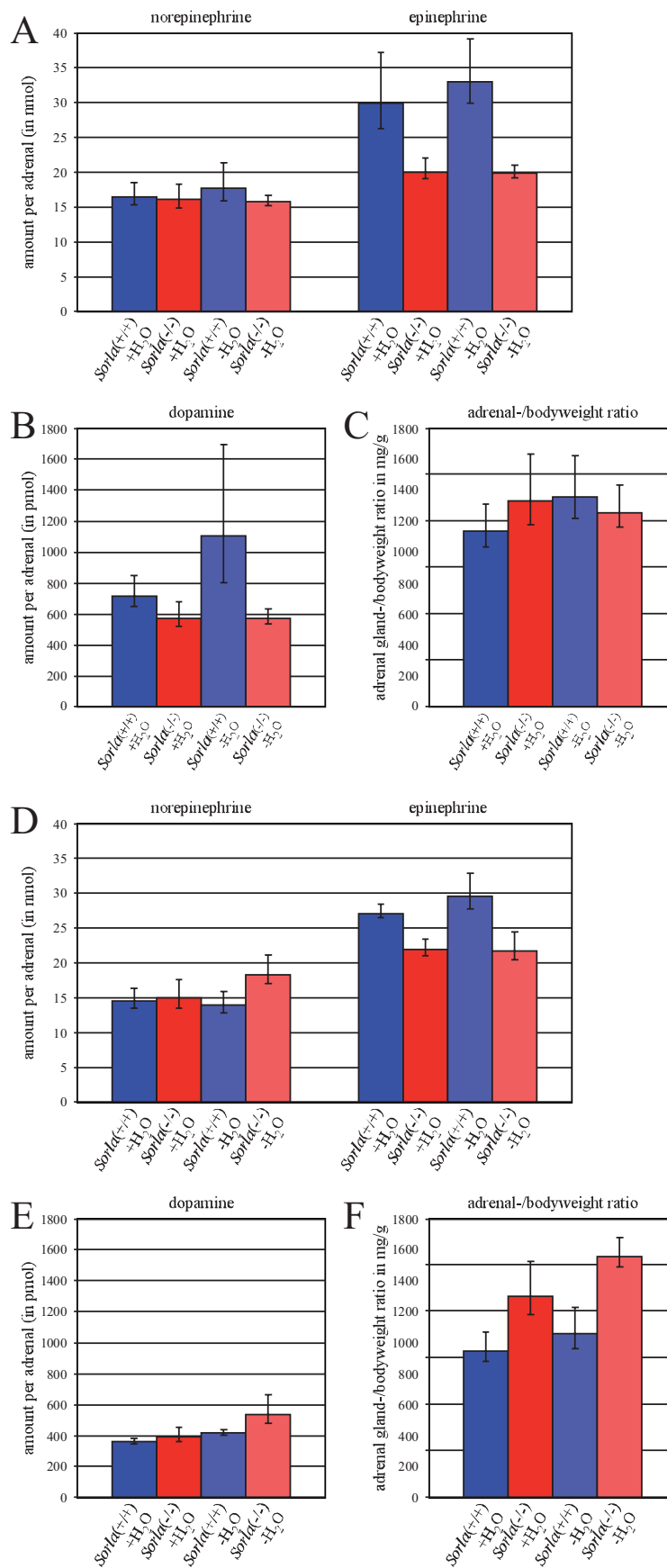


**Figure 16: Amounts of norepinephrine, epinephrine and dopamine in the adrenal glands of wild type and *Sorla*<sup>(-/-)</sup> mice.** A, D: amount of norepinephrine and epinephrine per adrenal gland; A, E: amount of dopamine per adrenal gland. Two different mouse strains were used: SorLA27 and 129B1/6 (A, B and C) and SorLA18 and 129B1b/c (D, E and F). The adrenal weight was significantly higher in SorLA18 animals (as compared to their 129B1b/c controls with comparable body-weight), whereas the SorLA27 animals had comparable adrenal weights as their age- and sex-matched controls, even though their body weight was ~20% lower. Upper error bars show standard deviation, lower error bars show standard error of the mean.

Figure 16 shows reduced levels of the catecholamine epinephrine, the end-product of the down-regulated synthesis pathway. The other catecholamines dopamine and norepinephrine are not significantly changed.

The catecholamine synthesis and degradation pathways share one enzyme each with the serotonin pathway. The final step in the synthesis of serotonin is carried out by DOPA decarboxylase (Ddc). Since one probe set representing the gene for this enzyme is downregulated, the question arises whether this effect extends to (and plays a role in) serotonin-synthesizing organs. This idea could be refuted by measuring serotonin levels in different tissues, as shown in figure 17. No change between SORLA-deficient animals and wild types was obvious.

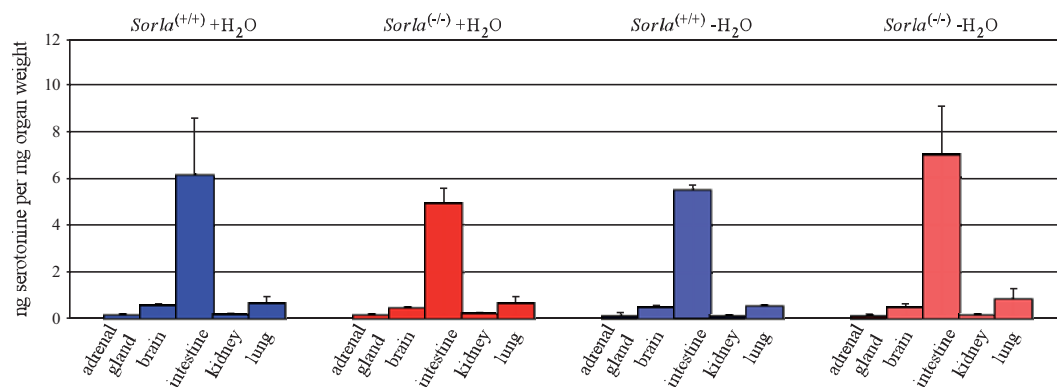


**Figure 17: Amount of serotonin in adrenal gland, brain, intestine kidney and lung of wild type and SORLA-deficient mice under normal conditions and after thirsting.** Amount of serotonin per mg organ weight. Errorbars represent standard deviation.

By comparing the adrenal gene expression pattern of *Sorla*<sup>(-/-)</sup> mice with wild types, I could reveal a mis-regulation of genes of the catecholamine pathway. This observation was supported by lower levels of epinephrine in adrenal glands. Epinephrine could play a role in kidney metabolism, as it activates the basolateral Na<sup>+</sup>/K<sup>+</sup>-exchangers, which are present along the renal nephron. However, the site of adrenal catecholamine synthesis is the medulla, a region in which *Sorla* expression could not be detected (cf. figure 11).

The differential transcriptome in the adrenal glands of mice lacking SORLA does not offer an explanation for mis-regulated aldosterone synthesis or secretion. Nor does it provide any evidence for defects in angiotensin II or K<sup>+</sup>-sensing mechanisms, both required for proper regulation of aldosterone secretion. Therefore, I focused on investigating the renal expression pattern to find an evidence for the primary electrolyte phenotype in the kidney.

### **3.3.2 Kidney**

To develop an idea which renal defects may lead to the observed phenotype in renal ion homeostasis, the kidney was also subjected to comparative gene expression analysis. RNA from whole kidney preparations was used to generate labeled cRNA for hybridization on Affymetrix Mouse Genome 430 2.0 Arrays.

DNA chip expression analysis of kidneys was carried out on SorLA27 mice and corresponding hybrid 129Bl/6 wild type mice. Labeled cRNA was synthesized using a one-cycle protocol.

After normalizing the data with a variant of the RMA algorithm, the obtained data was examined by carrying out quality assessments tests, according to the treatment of the adrenal gland data. Pseudoimages, box-plots of the raw/normalized intensities and RNA degradation plots were comparable for all samples (data not shown). The sample of one SORLA-deficient animal supplied with drinking water (*Sorla*<sup>(-/-)</sup> +H<sub>2</sub>O 01) did show a divergent *M* vs. *A* plot.

Figure 18 shows that transcriptional difference between the genotypes diverges with thirsting. The data set of the untreated SORLA-deficient sample *Sorla*<sup>(-/-)</sup> +H<sub>2</sub>O 01 differs strongly from the others. Together with the irregular *M* vs. *A* plot this was reason to exclude the data set from further statistical analyses. While unsupervised hierarchical clustering is unable to clearly separate two groups under normal conditions, a clear classification is possible in the thirsted subset of animals (figure 18 B).

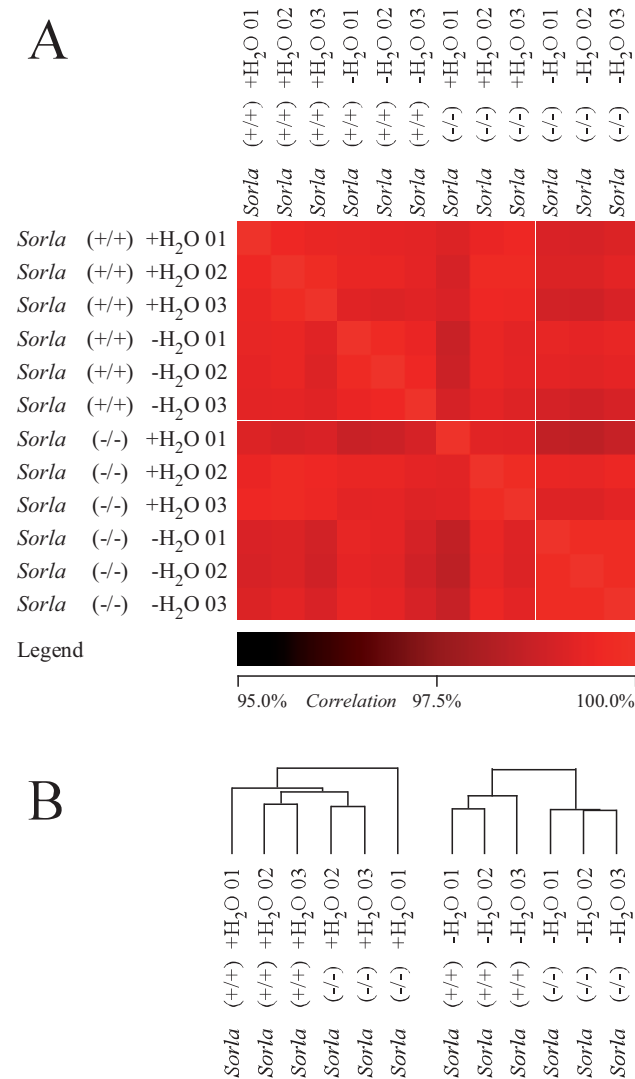


**Figure 18: Correlation plot and unsupervised hierarchical clustering of the adrenal data sets.** A: Correlation plot showing complete identity of the data sets in bright red and divergence of 5% identity in black; B: Hierarchical trees obtained after performing an unsupervised clustering using the data sets for normal condition (left) and water-deprivation (right).

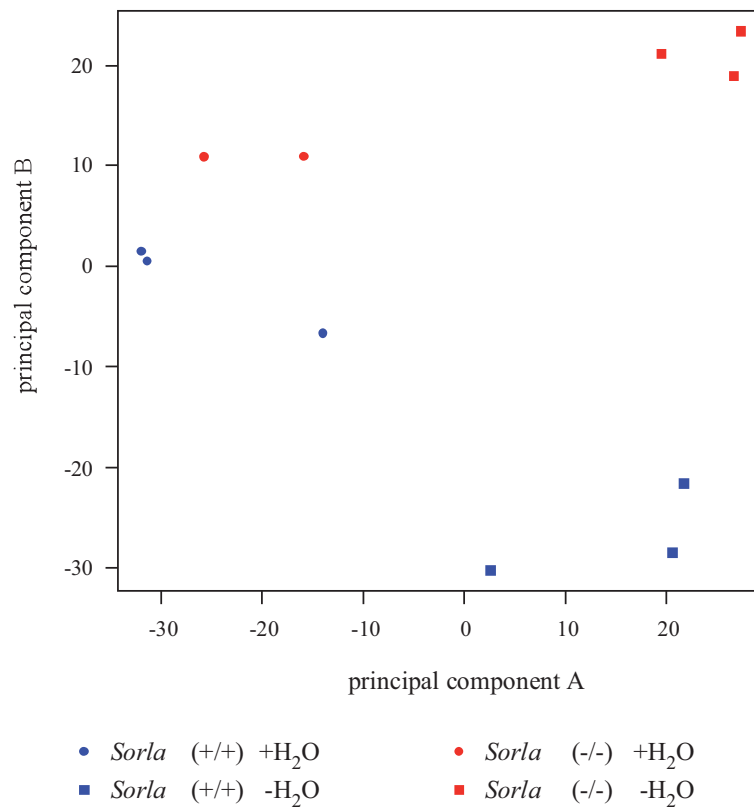


**Figure 19: Principal component plot for kidney Affymetrix data.** Principal component A clearly separates the data sets according to the condition; component B distinguishes the genotypes; the marginal difference between the mice held with water contrasts with the clear difference between thirsted animals.

That the difference between wild types and SORLA-deficient mice markedly increases after thirsting becomes visible in a principal component analysis (figure 19). Principle component B is hardly able to distinguish the unthirsted groups, whereas thirsting clearly increases the distance between the data sets of both genotypes. The antidiuretic stress triggers differential transcriptional responses in wild types and *Sorla*<sup>(-/-)</sup> mice.

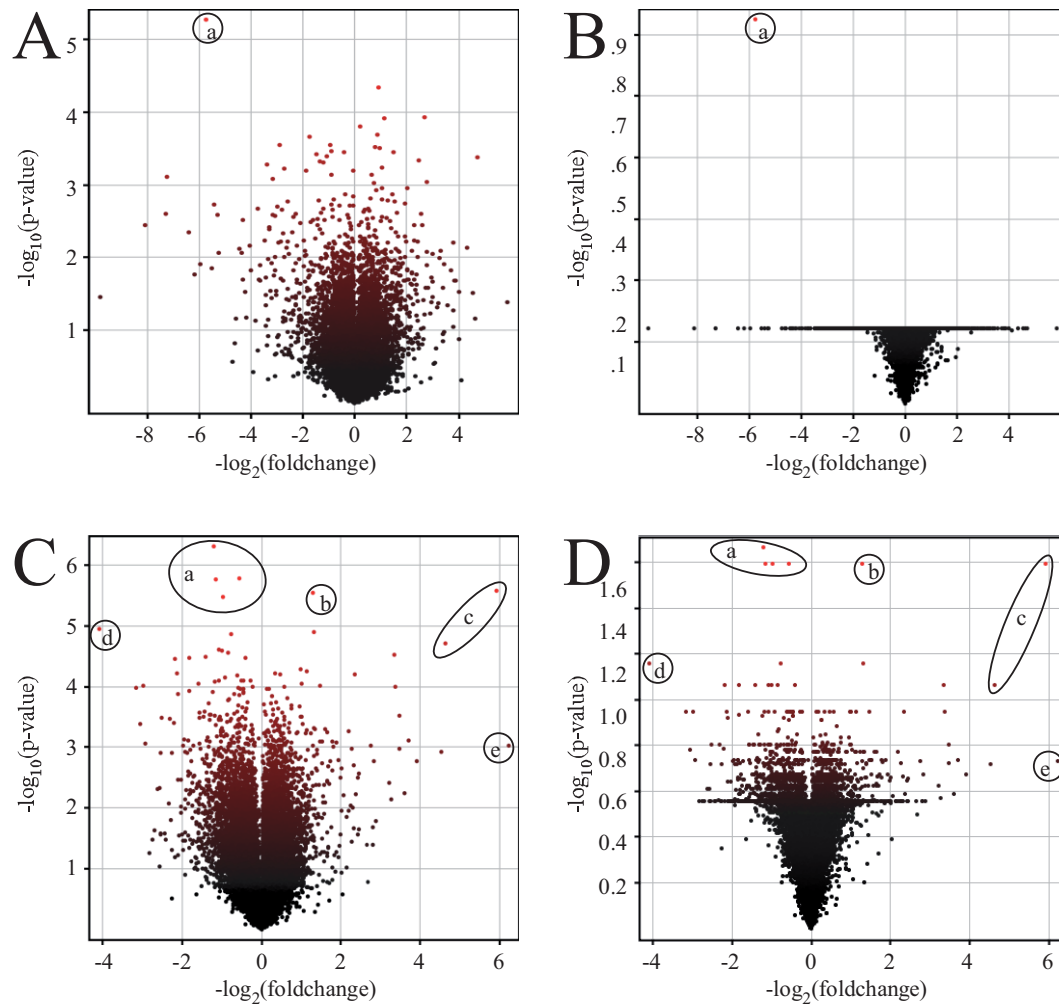


**Figure 20: Volcano plots representing the renal Affymetrix data.** Differentially regulated probe sets of normal (A, B) and thirsty (C, D) mice; p-values used for the plots were either uncorrected (A, C) or corrected by the Benjamini-Hochberg method (B, D) to reduce false positives. Interesting probe sets are encircled and listed in table 18.

Single highly differentially expressed genes become obvious in the volcano plot (figure 20). In the non-thirsted state, very few genes fulfill the significance criteria after applying the Benjamini-Hochberg correction. This situation is completely different in thirsty mice.

**Table 18: Highly differential probe sets in the kidney.** List of probe sets marked in figure 20. The p-values listed here are not adjusted with the Benjamini-Hochberg correction.

		probe set ID	gene symbol	fold-change	p-value
<b>A/B</b>	<b>a</b>	1447396_at	not annotated in NetAffx	-7.346	5.25E-06
			(chromosome 18 genomic contig)		
<b>C/D</b>	<b>a</b>	1457678_at	male epididymis cDNA	-2.303	4.78E-07
			RIKEN clone 9230105B05		
		1437923_at	male hippocampus cDNA	-2.199	1.70E-06
			RIKEN clone C630001M21		
		1441404_at	not annotated in NetAffx	-1.963	3.39E-06
			(chromosome 11 genomic contig)		
		1417547_at	<i>Sart3</i>	-1.476	1.67E-06
	<b>b</b>	1443696_s_at	<i>Habp2</i>	2.457	2.87E-06
	<b>c</b>	1417462_at	<i>Cap1</i>	60.825	2.66E-06
		1417461_at		24.790	1.91E-05
	<b>d</b>	1422603_at	<i>Rnase4</i>	-17.098	1.10E-05
	<b>e</b>	1421144_at	<i>Rpgrip1</i>	74.821	9.50E-04

**Table 19: Number of probe sets being significantly changed in kidneys, sorted by fold change and p-value.** A and B show the number of significant probe sets after Benjamini-Hochberg false discovery rate correction in brackets.

**A** *Sorla*<sup>(-/-)</sup> +H<sub>2</sub>O vs. *Sorla*<sup>(+/+)</sup> +H<sub>2</sub>O

	all	p < 0.05	p < 0.02	p < 0.01	p < 0.005	p < 0.001
<b>all</b>	45101	1156 (0)	445 (0)	228 (0)	109 (0)	31 (0)
<b>FC &gt; 1.1</b>	11788	972 (0)	381 (0)	203 (0)	97 (0)	29 (0)
<b>FC &gt; 1.5</b>	869	310 (0)	161 (0)	95 (0)	58 (0)	16 (0)
<b>FC &gt; 2.0</b>	246	131 (0)	79 (0)	54 (0)	33 (0)	10 (0)
<b>FC &gt; 3.0</b>	70	50 (0)	32 (0)	21 (0)	13 (0)	4 (0)
<i>expected by chance</i>	2255		902	451	225	45

**B** *Sorla*<sup>(-/-)</sup> -H<sub>2</sub>O vs. *Sorla*<sup>(+/+)</sup> -H<sub>2</sub>O

	all	p < 0.05	p < 0.02	p < 0.01	p < 0.005	p < 0.001
<b>all</b>	45101	7453 (6)	2851 (0)	1566 (0)	910 (0)	237 (0)
<b>FC &gt; 1.1</b>	20644	4861 (6)	2444 (0)	1459 (0)	872 (0)	227 (0)
<b>FC &gt; 1.5</b>	2773	1547 (5)	969 (0)	650 (0)	428 (0)	132 (0)
<b>FC &gt; 2.0</b>	721	542 (4)	382 (0)	289 (0)	203 (0)	81 (0)
<b>FC &gt; 3.0</b>	170	138 (1)	103 (0)	91 (0)	72 (0)	33 (0)
<i>expected by chance</i>	2255		902	451	225	45

A and B: *Welch's t-test, unpaired, unequal variance*  
*asymptotic p-value computation*  
*no multiple testing correction (in brackets: Benjamini-Hochberg correction)*

**C** *Sorla*<sup>(+/+)</sup> +H<sub>2</sub>O vs. *Sorla*<sup>(+/+)</sup> -H<sub>2</sub>O

	all	p < 0.05	p < 0.02	p < 0.01	p < 0.005	p < 0.001
<b>all</b>	45101	3720	1823	1019	562	150
<b>FC &gt; 1.1</b>	15735	3412	1744	984	546	147
<b>FC &gt; 1.5</b>	2118	1048	632	399	243	82
<b>FC &gt; 2.0</b>	405	227	144	94	58	15
<b>FC &gt; 3.0</b>	77	42	35	19	13	4
<i>expected by chance</i>	2255		902	451	225	45

**D** *Sorla*<sup>(-/-)</sup> +H<sub>2</sub>O vs. *Sorla*<sup>(-/-)</sup> -H<sub>2</sub>O

	all	p < 0.05	p < 0.02	p < 0.01	p < 0.005	p < 0.001
<b>all</b>	45101	7217	2669	1344	672	134
<b>FC &gt; 1.1</b>	20887	5328	2302	1190	593	109
<b>FC &gt; 1.5</b>	2941	1299	756	443	248	50
<b>FC &gt; 2.0</b>	625	353	226	163	106	17
<b>FC &gt; 3.0</b>	89	57	42	36	23	6
<i>expected by chance</i>	2255		902	451	225	45

B and C: *Welch's t-test, unpaired, unequal variance*  
*asymptotic p-value computation*  
*no multiple testing correction*



In contrast to the adrenal gland, the kidney seems to be less effected by the targeted disruption of the *Sorla* gene (table 19). Under basal conditions, 1156 probe sets differ significantly ( $p < 0.05$ ) between the two genotypes (cf. 2275 probe sets in adrenal glands, table 16 A, chapter 3.3.1). This situation changes dramatically during water-deprivation. In total, more than 7400 probe sets are significantly changed in the kidney, of these more than 1500 with a fold-change higher than 1.5 (table 19 B). The numbers in table 19 C and D also demonstrate, that thirsting exacerbates the renal transcriptional differences between wild types and *Sorla*<sup>(-/-)</sup> animals, an effect not seen in adrenal glands.

Whereas the lack of the receptor alone has a rather mild effect, the combination of SORLA-deficiency with thirsting leads to a differential activation of a broad variety of genes in the murine kidney. The functional range of affected genes was already shown in figure 15 (chapter 3.3.1). In contrast to the adrenal gland data, the kidney data did not reveal groups of genes involved in specific pathways.

### 3.3.3 Confirmation of Affymetrix results via TaqMan analysis

The transcriptional changes in the catecholamine pathway in the adrenal gland could already indirectly be validated by measuring the metabolites. In order to validate the other results obtained from the DNA chip data, the transcriptional expression level of some probe sets was determined via quantitative real-time PCR (TaqMan).

TaqMan primers and probes were selected for genes highly differentially expressed in Affymetrix-Assays under at least one condition (normal/thirsted) in at least three different tissues. Tissues analyzed were: adrenal gland, kidney, brain stem (not shown) and primary hippocampal neurons (not shown). For Affymetrix-Analysis, kidney tissue was taken from SorLA27 and 129Bl/6 animals, all other tissues were taken from SorLA18 and 129Balb/c animals.

Most of the differential regulation seen in the gene chip data could be reproduced in TaqMan assays (table 20, brain stem and primary neurons not shown). The selected assays turned out to be not suitable for validation of the kidney Affymetrix data. This can be explained by the different genetic and transcriptional background of the animals used for the DNA chips and the real-time PCR (129Bl/6 and 129Balb/c respectively). Noteworthy is the gene *Ifi202b*, which is expressed in 129Balb/c mice but whose transcription is not detectable by microarray or TaqMan assays in all analyzed SorLA18 tissues. In contrast to that, it does not seem to be expressed in the tissue of SorLA27 or 129Bl/6 animals at significant levels (table 20, left), therefore resembling an artifact in the hybrid 129Balb/c mice used.

**Table 20: Fold-changes and p-values of selected transcript in adrenal gland (A) and kidney (B), determined by Affymetrix and TaqMan analyses.** An “X” in the “no BG” column indicates expression levels above background noise (antilogarithmic expression level >100). Due to a very low expression of Ifi202b in the kidney, not every TaqMan reaction provided a C<sub>T</sub>-value, rendering the calculation of a valid p-value impossible.

A

ADRENAL GLANDS											
Gene	probe	normal conditions		water-deprivation		TaqMan probe	normal conditions		water-deprivation		
		p-value	regulation	p-value	regulation		p-value	regulation	p-value	regulation	
Atm	1421205_at	5.365E-03	-4.033 X	9.847E-04	-3.546 X	Atm	2.382E-01	-1.568	8.739E-01	1.047	
	1428830_at	9.047E-02	-1.110 X	2.316E-01	1.157 X						
Ifi202b	1421551_s_at	3.279E-03	-17.894 X	3.808E-04	-14.064 X	Ifi202b	2.964E-03	-3363.700	2.032E-03	-2776.721	
	1457666_s_at	1.424E-03	-60.624 X	9.336E-06	-43.304 X						
Mfap1	1419370_a_at	7.210E-06	18.071 X	1.185E-03	14.986 X	Mfap1A	3.772E-05	48.559	4.669E-04	37.639	
	1449444_a_at	9.915E-02	1.670 X	2.587E-02	1.512 X	Mfap1A/B	8.756E-02	1.731	3.040E-02	2.335	
microfibrillar-associated protein 1	1449445_x_at	3.635E-04	8.338 X	1.162E-02	6.129 X						
Ptgi	1419620_at	6.690E-04	3.401 X	1.101E-03	3.131 X	Ptgi	2.059E-04	14.197	1.590E-03	14.115	
	1424105_a_at	1.902E-03	8.495 X	9.673E-03	6.892 X						
Sord	1438390_s_at	3.773E-04	5.054 X	3.890E-05	5.751 X						
Sord	1426584_a_at	1.558E-04	6.351 X	3.826E-02	4.253 X	Sord	4.071E-01	-1.490	6.329E-01	1.253	
	1438183_x_at	1.722E-03	2.016 X	2.433E-02	2.584 X						

B

KIDNEY											
Gene	probe	normal conditions		water-deprivation		TaqMan probe	normal conditions		water-deprivation		
		p-value	regulation	p-value	regulation		p-value	regulation	p-value	regulation	
Atm	1421205_at	9.087E-03	-2.394 X	3.515E-03	-1.640 X	Atm	3.039E-01	-1.911	4.822E-01	1.550	
	1428830_at	3.324E-01	1.054 X	6.107E-01	-1.042 X						
Ifi202b	1421551_s_at	4.060E-01	1.088	5.294E-01	-1.023	Ifi202b	*	-18.464	*	-15.641	
	1457666_s_at	1.053E-01	1.088	4.159E-01	-1.065						
Mfap1	1419370_a_at	5.589E-01	-1.084 X	4.859E-01	-1.047 X	Mfap1A	9.186E-03	-1.583	6.046E-01	-1.056	
	1449444_a_at	3.503E-01	-1.141 X	3.393E-01	1.070 X	Mfap1A/B	6.545E-01	-1.098	2.203E-01	1.320	
microfibrillar-associated protein 1	1449445_x_at	2.972E-01	-1.088 X	1.623E-01	1.086 X						
Ptgi	1419620_at	3.574E-01	-1.096 X	1.029E-01	1.181	Ptgi	8.484E-01	-1.055	1.390E-01	2.048	
	1424105_a_at	4.422E-02	-1.470 X	2.550E-02	1.583 X						
Sord	1438390_s_at	2.237E-02	-1.223 X	5.549E-04	1.592 X	Sord	4.276E-02	-1.530	5.297E-01	-1.231	
	1426584_a_at	5.781E-01	-1.056 X	5.908E-02	-1.084 X						
sorbitol dehydrogenase	1438183_x_at	4.377E-01	-1.150 X	4.089E-01	-1.057 X						

\* due to very low expression levels. Ifi202b-transcripts could not be detected in all samples, making the calculation of a p-value impossible

\* due to very low expression levels, Ifi202b-transcripts could not be detected in all samples, making the calculation of a p-value impossible

Due to the high variability between individual Affymetrix analyses, a validation of such an experiment is usually done by real-time PCR using the same samples that have been used for the microarrays. I could confirm the validity of the chip data by using independent samples. Even though the microarrays were processed in parallel and all steps in the process (such as isolation of RNA and synthesis of cDNA and cRNA) were carefully monitored, the kidney microarray data could not be confirmed by real-time PCR. The divergence of their data resulted most likely from the different hybrid background of the mice used. Due to identical setup and positive examination of all parameters during the Affymetrix analyses, I consider the kidney data as valid.

The analysis of renal gene expression in mice deficient for SORLA shows a differential transcription that strongly aggravates with thirsting, suggesting a role of the receptor in this organ. Still, the data did not reveal any specific transcriptionally mis-regulated pathways. To identify renal mechanisms which may cause the observed electrolyte phenotype in the *Sorla*<sup>(-/-)</sup> mice, I challenged the kidney with specific pharmacological interventions.

### 3.4 Pharmacological Experiments

Mice lacking SORLA display a distinct salt loss – indicating defects in renal ion handling in these animals. Renal mechanisms in sodium transport involve the activation of the sodium-chloride-cotransporter NCC, responsible for regulated Na<sup>+</sup>/Cl<sup>-</sup> transport in the distal convoluted tubule, or the activation of sodium-potassium-chloride-cotransporter NKCC2, the major salt-reabsorption pathway in the thick ascending limb of Henle's loop. Both transporters can be blocked by pharmacological intervention. The supposed mis-regulation of aldosterone levels observed in *Sorla*<sup>(-/-)</sup> mice could be a balancing mechanism as well, as aldosterone increases the reabsorption of sodium. Its effects can be suppressed by pharmacologically blocking the aldosterone-receptor.

By blocking the abovementioned pathways, I intended to separate counterbalancing mechanisms from negative effects that may be produced by the lack of SORLA, and therefore stress the renal system in favor of a more pronounced and less cryptic phenotype.

#### 3.4.1 Blockage of NCC activity with thiazide

Thiazide diuretics (e.g. hydrochlorothiazide) block the thiazide-sensitive sodium-chloride-cotransporter NCC, the major regulated uptake pathway for Na<sup>+</sup> and Cl<sup>-</sup> in the distal convoluted tubule. This intervention results in elevated salt excretion combined with a higher urine volume.

SORLA-deficient mice and wild type control animals were injected with hydrochlorothiazide and urine was collected in metabolic cages. After five hours, the

injections were repeated and urine collected for another five hours. Control urine was collected for five hours prior to the experiment under the same conditions without injection of thiazide.

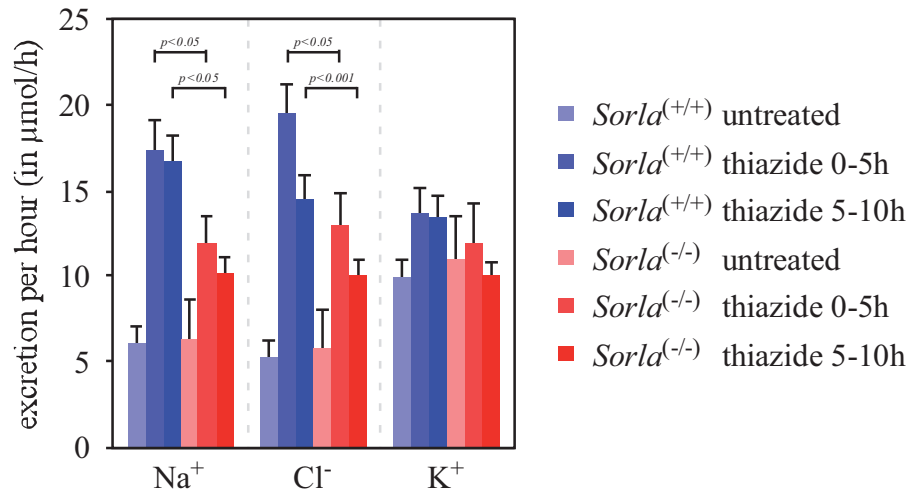


**Figure 21: Secreted hourly amount of Na<sup>+</sup>, Cl<sup>-</sup> and K<sup>+</sup> (in μmol per hour) before and after administration sodium-hydrochlorothiazide.** The blue bars represent wild type mice (*Sorla*<sup>(+/+)</sup>), the red bars show data from SORLA-deficient animals (*Sorla*<sup>(-/-)</sup>). Urine samples were collected for 5 hours each. After collecting control urine samples (untreated), the animals were injected with sodium-hydrochlorothiazide and urine was collected for five hours (thiazide 0-5h). Injections and collection were repeated subsequently (thiazide 5-10h). Error bars represent standard deviation, n ≥ 16 for each bar.

As anticipated, Na<sup>+</sup> and Cl<sup>-</sup> excretion increases after thiazide administration. In SORLA-deficient mice, this effect is less pronounced (figure 21). The fact that thiazide-induced loss of these ions is lower in the receptor-deficient mice suggests a lower basal activity of the thiazide-sensitive NCC in these animals.

Even though thiazide is blocking NCC, a receptor only transporting Na<sup>+</sup> and Cl<sup>-</sup>, some K<sup>+</sup> loss appears. This effect seems to be lower in the knockout mice, though it is not statistically significant.

There are three explanations for elevated K<sup>+</sup> excretion upon thiazide treatment. First, due to reduced NCC activity, a higher Na<sup>+</sup> delivery to the downstream collecting duct occurs. There, increased activity of Na<sup>+</sup>/K<sup>+</sup>-exchangers compensates this loss at the expense of potassium ions. Second, the nephric flow-rate is increased under diuresis. This effectively decreases the tubular concentration of K<sup>+</sup>. As a result, more K<sup>+</sup> enters the lumen via passive channels such as ROMK.

The last explanation for thiazide-induced potassium-wasting is that the diuresis leads to a systemic decrease in the volume of blood serum (hypovolemia), which results in activation of the renin-angiotensin-aldosterone-system. Aldosterone in turn activates the Na<sup>+</sup>/K<sup>+</sup>-exchangers, consequently leading in further loss of K<sup>+</sup>.

This would be in line with the mis-regulated release of aldosterone in *Sorla*<sup>(-/-)</sup> mice.

### 3.4.2 Blockage of aldosterone-induced action with eplerenone

Aldosterone increases the reabsorption of Na<sup>+</sup> and water and the secretion of K<sup>+</sup> in the aldosterone-sensitive distal nephron, which includes the late distal convoluted tubule (DCT2), connecting tubule (CNT), and cortical collecting duct (CD). This happens mainly by activating the basolateral Na<sup>+</sup>/K<sup>+</sup>-ATPase and by translocating the Na<sup>+</sup> channel ENaC to the apical surface. To prevent a critical depletion, the kidney could counterbalance this mechanism by induction of more proximal electrolyte transport processes, such as NKCC2 in the thick ascending limb.

To separate any effects caused by the elevated basal level of aldosterone from the phenotype, *Sorla*<sup>(-/-)</sup> mice and wild type animals were treated with the aldosterone antagonist eplerenone. The potassium-sparing diuretic eplerenone specifically blocks the mineralocorticoid receptor, preventing it from binding aldosterone. Blockage of this receptor – and therefore inhibition of aldosterone action – would reverse the reabsorption of Na<sup>+</sup> and the secretion of K<sup>+</sup> and should consequently result in a higher urinary Na<sup>+</sup>/K<sup>+</sup> ratio.

The hydrophobic substance eplerenone is only slightly soluble in water. I tested several ways of administering the drug to mice. No effects were seen after mixing the substance into the dietary mash of the animals (not shown). The low solubility of eplerenone impeded the approaches to dissolve it in the drinking water or to inject it directly. Finally, the mice were force fed with an aqueous eplerenone-suspension by gavage twice a day (200 mg eplerenone per kg body weight per day in two gavages à 200 µl each, control animals received water) for 13 consecutive days (Keidar, et al., 2005). Urine was collected in metabolic cages overnight.

The diuretic eplerenone increased the average urine volume collected per hour by 12% in wild types (1621.31 ± 283.97 ml before treatment, 1810.40 ± 303.13 ml after treatment) and by 10% (1081.14 ± 192.00 ml before treatment, 1191.34 ± 275.23 ml after treatment) in receptor-deficient mice respectively. As exemplarily visualized in figure 22, the mice did not respond as expected. Even though *Sorla*<sup>(-/-)</sup> animals show a higher ratio of excreted urinary Na<sup>+</sup> to K<sup>+</sup> after treatment with eplerenone (0.573 ± 0.065 before treatment, 0.853 ± 0.124 after treatment), *Sorla*<sup>(+/+)</sup> mice did not react with an increase in that quotient (1.156 ± 0.085 before treatment, 1.174 ± 0.203 after treatment).

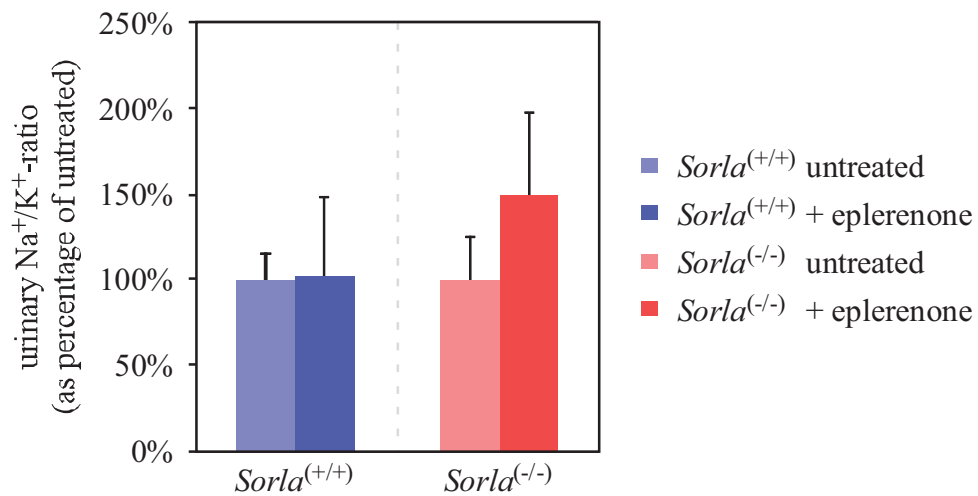


**Figure 22: Ratio of urinary Na<sup>+</sup> and K<sup>+</sup> concentrations before and after administration of eplerenone.** While wildtypes are not reacting to the administration of aldosterone, knockouts are showing a slight increase of the urinary Na<sup>+</sup>/K<sup>+</sup>-ratio.

The eplerenone treatment was not distinctly blocking the action of aldosterone. It is interesting, that the wild type animals reacted differently from the SORLA-deficient mice, eventually responding differently to eplerenone. But most likely, the administration of the drug did not work in the chosen form.

To circumvent problems with the directed application of drugs, a different approach was chosen for testing the activity of NKCC2.

### 3.4.3 Bumetanide-sensitive NKCC2-mediated K<sup>+</sup>-transport in isolated TAL

The diuretic bumetanide acts through blockade of NKCC2, preventing the transporter to conserve Na<sup>+</sup> and K<sup>+</sup> in the thick ascending limb of Henle's loop. Hence it falls into the group of loop-diuretics. As the unsuccessful administration of eplerenone has shown, the readout of systemic pharmacologic intervention in mice *in vivo* can be difficult. To reduce obfuscating interferences by systemic balancing mechanisms and to facilitate the targeted application of the pharmacologic agents, bumetanide-administration was approached from a different *ex vivo* angle.

Bumetanide acts only in the thick ascending limb. This tissue is characterized by a comparably high resistance to collagenase. Hence digestion with this cocktail of degrading enzymatic allows gentle isolation of tubular fragments of this segment from the inner stripe of the outer medulla (ISOM) of the kidney. After the ISOM was excised from the kidney, it was minced and digested with collagenase (depicted in FIGURE 21 A). In this way isolated tubules were separated from contaminating cells (mainly collecting duct cells, also thin ascending limb cells) using their different sedimentation rate. Thick ascending limb tubules were isolated to a purity of more than 85% (exemplified in figure 24).



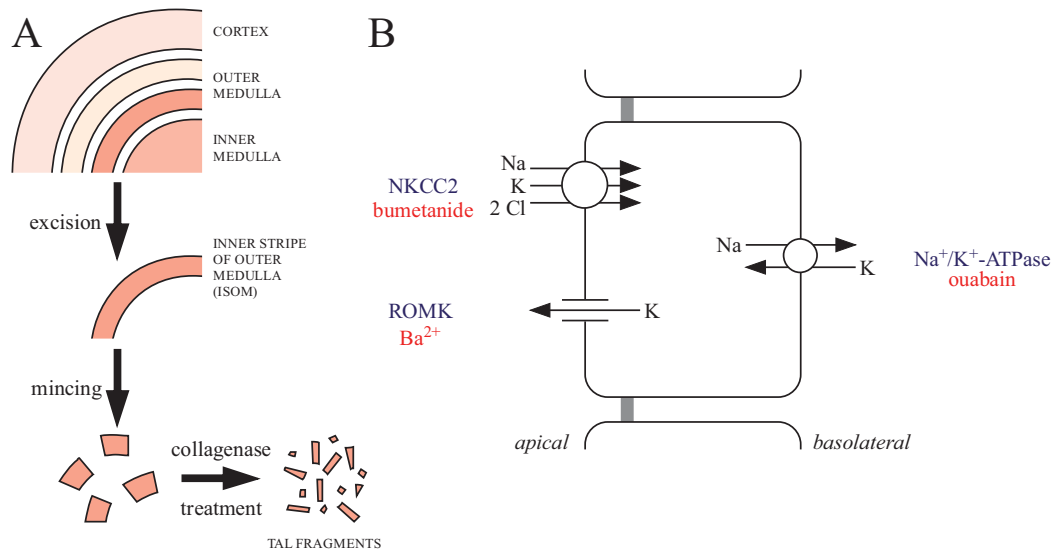


**Figure 23: Isolation of TAL fragments (A) and major  $K^+$  transport mechanisms in TAL (B).** A: Schematic illustration of the TAL isolation process. The inner stripe of the outer medulla (ISOM) is excised from kidney sections, minced and treated with collagenase. The resulting mixture of TAL fragments and contaminating cells is separated by centrifugation. B: Major transcellular pathways accountable for the transmembrane transport of  $K^+$  in TAL cells. Transporting elements are labelled in blue, their inhibitors are in red.

The NKCC2 activity in intact isolated tubules was determined by measuring uptake of radioactive rubidium ( $^{86}\text{Rb}^+$ ), a substitute for potassium. To differentiate between NKCC2 activity and alternative transport mechanism for  $K^+/\text{Rb}^+$ , only bumetanide-sensitive uptake was considered. The  $\text{Na}^+/\text{K}^+$ -ATPase was inhibited by the arrow poison ouabain, potassium channels (ROMK) were blocked by barium ions ( $\text{Ba}^{2+}$ ), as shown in figure 23 B.

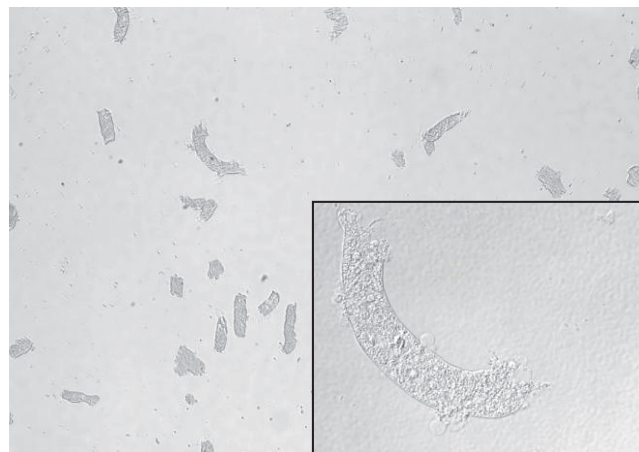


**Figure 24: Isolated thick ascending limb tubules.** TAL tubules were purified from the ISOM to a purity of more than 85% by sequential collagenase treatment and sedimentation (vide figure 23). The inset shows an intact tubule. Magnification: 100x, 400x for the inset.



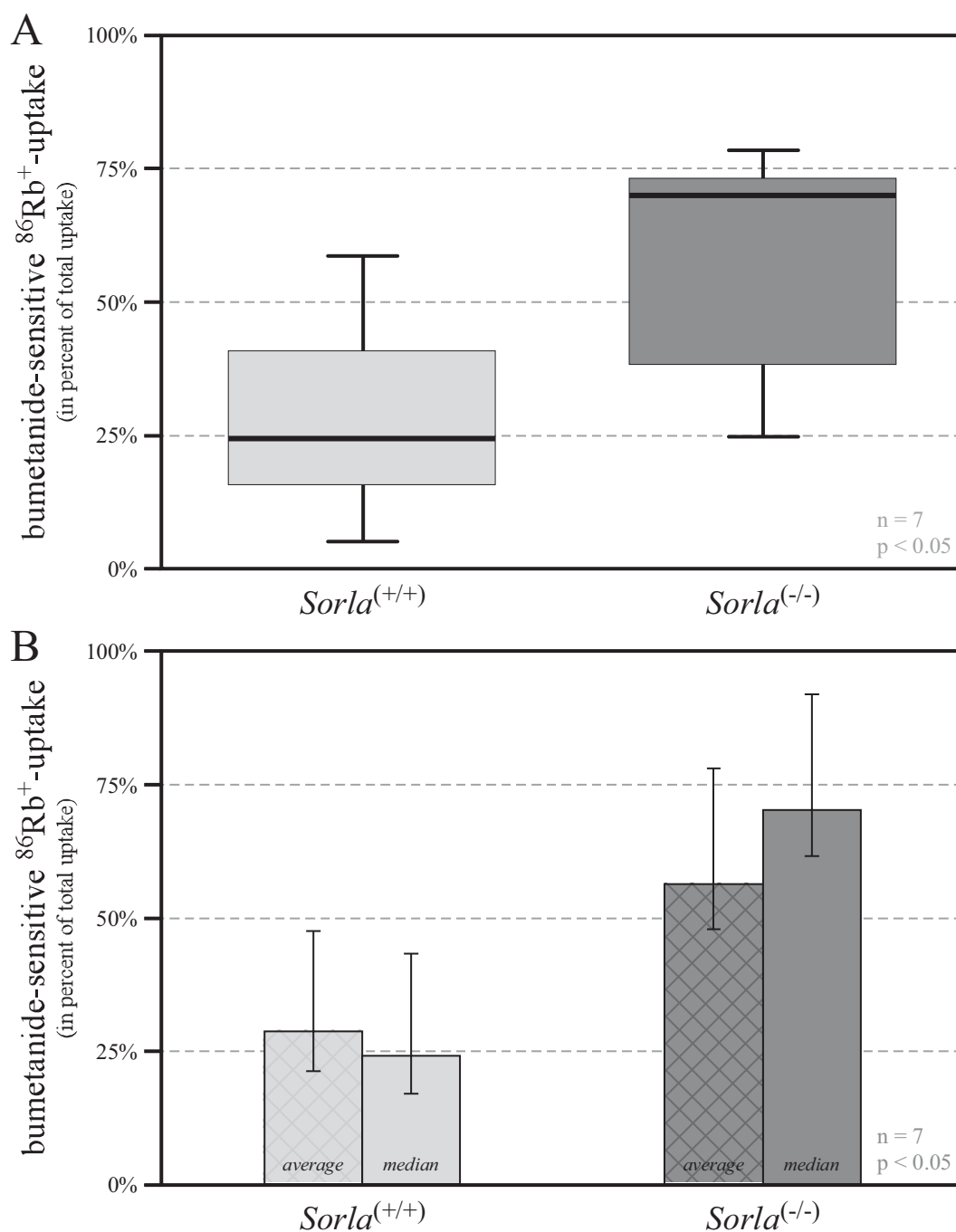


**Figure 25. Bumetanide-sensitive  $^{86}\text{Rb}^+$  uptake in isolated thick ascending limb tubules.** A: box plot. B: bar graph with bars representing the average and the median of each group. Upper error bars in B show standard deviation, lower error bars represent standard error of the mean. The p-value was calculated using Student's t-test for paired samples.

For the uptake assay, each batch of isolated tubules was split into two and treated with and without bumetanide. The difference between  $^{86}\text{Rb}^+$ -uptake with and without bumetanide was considered as bumetanide-sensitive fraction and ex-

pressed as percentage of the uptake without bumetanide (uptake without bumetanide was set to 100%).

Interestingly, SORLA-deficiency led to a higher bumetanide-sensitive  $^{86}\text{Rb}^{+}$ -uptake in isolated thick ascending limb tubules (figure 25), as compared to age- and sex-matched wild type samples.

*Sorla*<sup>(-/-)</sup> mice exhibit a higher NKCC2 activity in isolated TAL tubules. To check whether this is due to changed protein levels of the transporter and if other specific transport processes are also affected in the kidney of these animals, I carried out Western blot analyses of different renal transporters.

### 3.5 Electrolyte transporters in the distal nephron

NKCC2 has been reported to be phosphorylated upon activation (Gimenez and Forbush, 2005). I detected the transporter with an anti-NKCC2 antibody that recognizes all transporter variants, and with an anti-pNKCC2 antibody specific for the variant phosphorylated at two of its three known phosphorylation sites (T100 and T105 in human NKCC2, T96 and T101 in murine NKCC2).

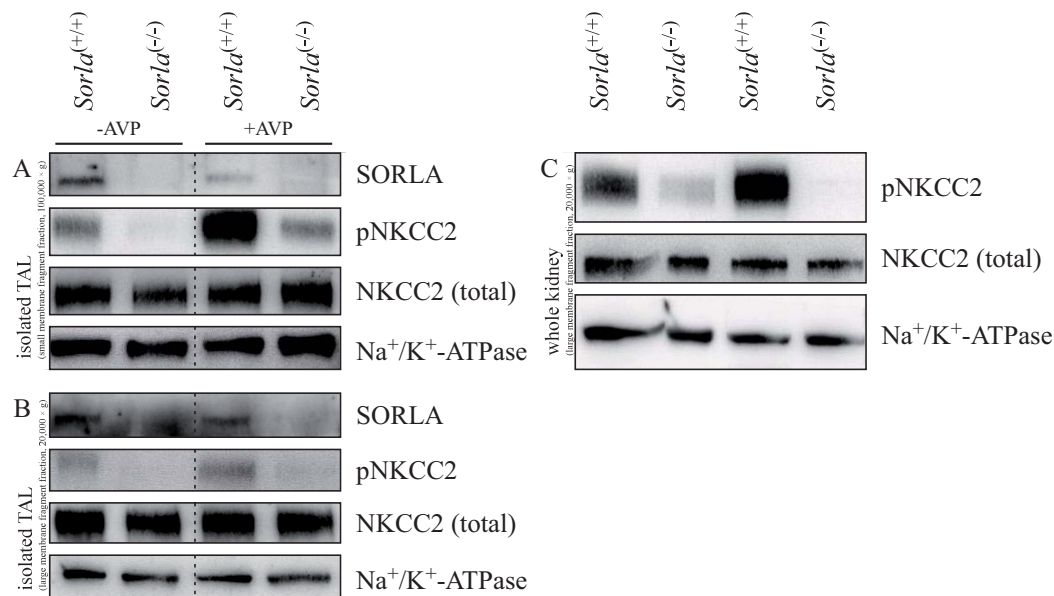


**Figure 26: NKCC2 in the thick ascending limb.** Western blots exemplifying protein levels of total and phosphorylated NKCC2 in isolated thick ascending limb tubules untreated or treated with AVP (A, B) and whole kidney membrane preparations (C) of the same animals. A: SORLA, NKCC2, pNKCC2 and  $\text{Na}^{+}/\text{K}^{+}$ -ATPase in a membrane fraction enriching intracellular vesicles. B: SORLA, NKCC2, pNKCC2 and  $\text{Na}^{+}/\text{K}^{+}$ -ATPase in a membrane fraction enriching cell membrane fragments. C: NKCC2, pNKCC2 and  $\text{Na}^{+}/\text{K}^{+}$ -ATPase in a membrane fraction enriching cell membrane fragments.

In order to test for NKCC2 levels, isolated tubules of the thick ascending limb were purified (one kidney per animal), split into two portions and treated in presence or absence of arginine vasopressin (+/-AVP). Two different membrane preparations of each aliquot of tubules were compared to test for protein levels in intracellular vesicles (smaller vesicular membrane fragments are enriched in the  $100,000 \times g$  fraction, figure 26 A) and at the cell surface (cell membrane fragments are enriched in the  $20,000 \times g$  fraction, figure 26 B). The trans-membrane  $\text{Na}^+/\text{K}^+$ -ATPase was used as a loading control as its expression level does not change between *Sorla*<sup>(+/+)</sup> and *Sorla*<sup>(-/-)</sup> animals (demonstrated in figure 27).

In all *Sorla*<sup>(-/-)</sup> fractions, NKCC2 phosphorylation is markedly reduced, whereas the total protein levels are unchanged, a trend also visible in whole kidney membrane preparations from the same animals (figure 26 C).

Because *Sorla* is expressed in all distal nephron segments, the chances are that NKCC2 is not the only electrolyte transporter affected in SORLA-deficient mice. Expression levels of other proteins involved in electrolyte transport processes in nephron areas that express *Sorla* were analyzed. In particular I was interested in: barttin, the accessory  $\beta$ -subunit of the renal chloride channels  $\text{ClC-Ka}$  and  $\text{ClC-Kb}$ ; the epithelial sodium channel  $\text{ENaC}$ ; the potassium chloride cotransporter KCC4; the sodium hydrogen exchanger NHE3; and the renal outer medulla potassium channel ROMK.

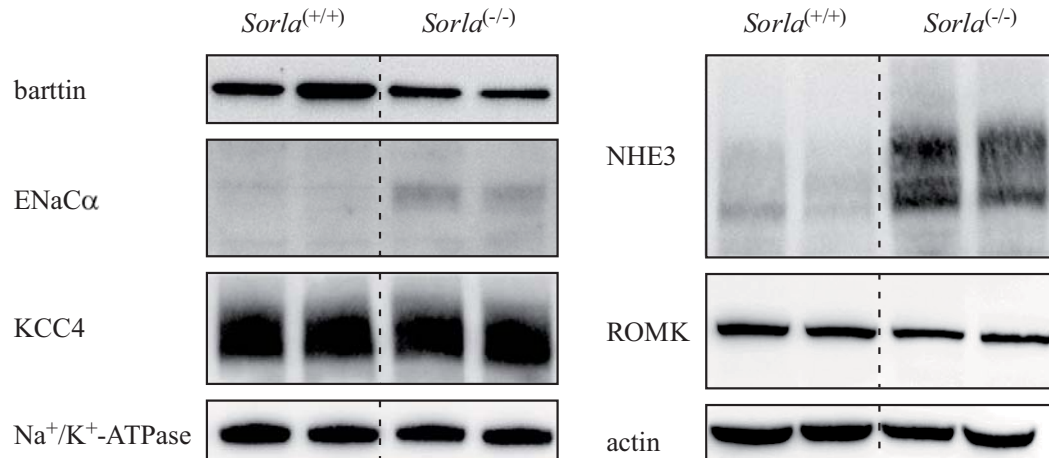


**Figure 27: Western blots of barttin, the  $\alpha$ -subunit of ENaC, KCC4,  $\text{Na}^+/\text{K}^+$ -ATPase, NHE3 and ROMK in wild types and mice lacking SORLA.** Western Blots shown here were carried out on whole kidney lysates. SORLA-deficient animals show increased expression of ENaC $\alpha$ , and NHE3 and slightly reduced expression of ROMK.

As nephron segments other than TAL cannot be isolated specifically, proteins from those segments were quantified in whole kidney lysates. Western blot analysis shows comparable protein levels of barttin, KCC4 and  $\text{Na}^+/\text{K}^+$ -ATPase; ROMK levels are slightly decreased (figure 27). In contrast, expression of the

alpha subunit of ENaC and of NHE3 are more pronounced in mice lacking SORLA.

As SORLA-deficiency in mice led to differential excretion of  $\text{Na}^+$  and  $\text{Cl}^-$  in response to treatment with thiazide, the expression of NCC was also investigated via Western blot. As NKCC2, NCC has been reported to be phosphorylated upon activation. For this reason, phospho-specific antibodies (pNCC T55, T60 and S91) as well as a phospho-unspecific NCC (total) antibody were used. The NCC Western blots were carried out in collaboration with the laboratory of Dario R. Alessi in Dundee, Scotland. As expected from the pharmacological experiment, figure 28 shows differential NCC expression in total kidney lysates of mice lacking SORLA. Interestingly, total NCC protein levels are elevated and the transporter is hyperphosphorylated as compared to control animals. This effect, which is independent of thirsting, is in contrast with the observation that thiazide has a milder effect on SORLA-deficient mice. If NCC is hyperphosphorylated and thus more active, e.g. as counterbalancing response to a defect elsewhere, blocking the transporters (higher) activity should have a larger impact in *Sorla*<sup>(-/-)</sup> mice.

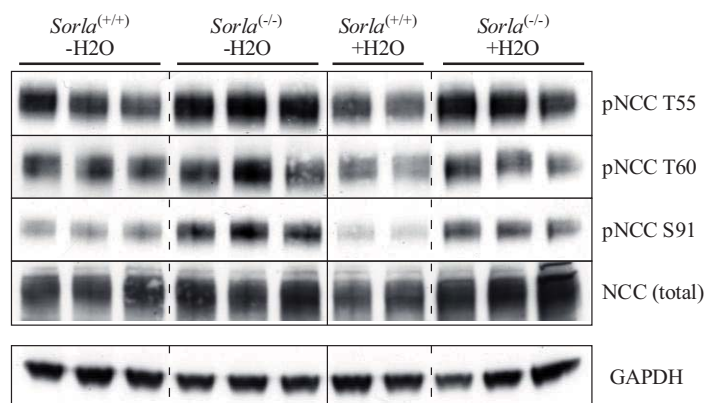


**Figure 28: Western blots of NCC in wild types and in mice lacking SORLA.** Mice were thirsted for 24h (-H<sub>2</sub>O) or treated normally (+H<sub>2</sub>O). NCC and GAPDH western were performed on whole kidney lysates. Westerns shown here were carried out by the group of Dario Alessi.

In conclusion, I demonstrated that the electrolyte homeostasis phenotype in SORLA-deficient mice coincides with an abnormal expression and phosphorylation of several electrolyte transporters, first and foremost NCC and NKCC2.

### 3.6 Signaling in distal renal ion-homeostasis

The lower effectiveness of thiazide and the increased bumetanide-sensitive  $^{86}\text{Rb}^+$ -flux as well as the different phosphorylation patterns of the transporters NCC and NKCC2 in the tissue of SORLA-deficient mice points towards a defective regulation of distal electrolyte reabsorption.

NCC and NKCC2 are members of the same gene family. The *Slc12a* family consists of the sodium-chloride-cotransporter NCC, the two sodium-potassium-chloride cotransporters NKCC1 and NKCC2 as well as the four potassium-chloride cotransporters KCC1-4. A group of kinases have recently been identified as key-players regulating these pathways (Gamba, 2005). These include members of the WNK (with no lysine) kinase family and SPAK (STE20-related, proline-alanine-rich kinase). They have been reported to be involved in the phosphorylation of members of the *Slc12a* family of chloride-cation cotransporters.

To test for defects in regulatory kinases, I investigated the phosphorylation pattern the abovementioned signaling proteins. In cooperation with the lab of Dario R. Alessi, I analyzed the kinases WNK1, 3 and 4 and SPAK by immunoprecipitation and Western blot analysis using phospho-specific antibodies. Unfortunately, the antibodies against the WNK proteins were unable to precipitate enough material to detect the kinases in any of the two labs (not shown). However, the immunoprecipitation of SPAK (figure 29) revealed a stronger phosphorylation of the kinase in *Sorla*<sup>(-/-)</sup> mice, in line with the hyperphosphorylation of NCC.

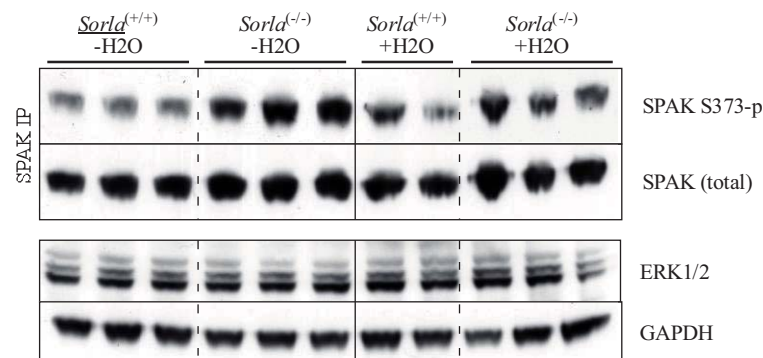


**Figure 29: Western blots of immunoprecipitated SPAK in wild types and in mice lacking SORLA.** Mice were thirsted for 24h (-H<sub>2</sub>O) or treated normally (+H<sub>2</sub>O). NCC, ERK1/2 and GAPDH western were performed on whole kidney lysates, SPAK was immunoprecipitated from the same lysates. Westerns shown here were carried out by the group of Dario Alessi.

SPAK has been reported to phosphorylate both NCC and NKCC2 (Moriguchi, et al., 2005). The lower phosphorylation of NKCC2 in SORLA-deficient mice contradicts the observed hyperphosphorylation of NCC and SPAK, suggesting mechanisms for both transporters that are independent from each other. The expression patterns of NCC and NKCC2 are confined to separate segments of the nephron. NKCC2 is exclusively expressed in the TAL, NCC is only expressed in the more distal DCT.

Immunohistological staining of kidney sections shows a significant difference between *Sorla*<sup>(-/-)</sup> and wild type mice in the TAL (figure 30). While SPAK is localized in vesicles close to the apical membrane of the TAL cells in wild types, where it partially localizes with NKCC2, it mis-localizes in SORLA-deficient

animals. White arrow heads in figure 30 mark SPAK expression in areas distant to the apical cell membrane and SPAK's target NKCC2.

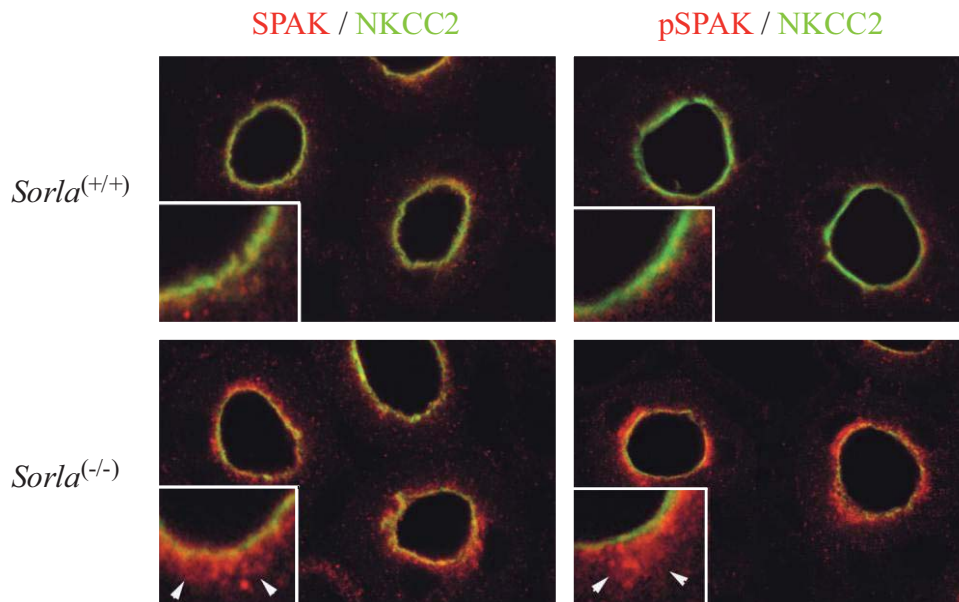


**Figure 30: Localization of SPAK and NKCC2 in the thick ascending limb.** Immunohistological detection of total SPAK (red, left panel) or its phosphorylated form (pSPAK) (red, right panel) and NKCC2 (green) in kidneys of the indicated genotypes. Co-localization of both proteins is indicated by yellow color. The insets represent magnifications of apical cell regions. Arrow heads highlight the different vesicular localization of SPAK/pSPAK in the sub-apical space in TAL cells of *Sorla*<sup>(-/-)</sup> mice. Magnifications: 1000x, 4000x for insets.

The mis-localization of SPAK in TAL cells may be a reason for the massively reduced phosphorylation of NKCC2 in mice lacking SORLA. Since this was observed only in TAL sections and not in the DCT, a different mechanism may be involved in the localization of SPAK to NCC, resulting in an efficient phosphorylation of the latter.

### 3.7 Identification of interaction partners

SORLA has been reported to influence the localization of the transmembrane-protein APP in the brain by binding to adaptor proteins (Schmidt, et al., 2007). A similar function could be possible for SPAK. But as the kinase is a cytosolic protein, a putative interaction with SORLA, direct or indirect, is likely to occur with the cytosolic domain of the receptor.

To discover physiological interactions of the cytosolic portion of SORLA in a renal context, I followed two parallel approaches: yeast two-hybrid screening and peptide pull-down.



### 3.7.1 Yeast Two-Hybrid

The first approach to identify interaction partners was a yeast two-hybrid analysis using the intracellular domain of SORLA. This screening method's concept is based on the property of some transcription factors in yeast, which require two functional subunits: A DNA-interacting domain binds to the specific upstream activating sequence of the DNA and thereby positions a second activating domain, which starts the transcription. In the two-hybrid system, the two subunits are physically separated as each is fused to a different recombinant protein. Both proteins are unable to start transcription on their own. If the protein fused to the DNA-interacting domain (bait) interacts with the fusion-proteins containing the activation domain (prey), both domains come into close vicinity and start transcription.

In a yeast two-hybrid system, separate yeast clones contain bait and prey vectors. Transcription starts only after mating two clones with interacting bait/prey proteins. The separation of the prey proteins in distinct yeast clones is a great advantage of this system. Each clone harbors the cDNA coding for the prey protein, allowing easy identification by DNA-sequencing.

A cDNA encoding the cytosolic portion (amino acids 2163-2214) of the human SORLA was cloned into the bait vector pBTM117c, fusing it to the DNA-binding LexA repressor. In parallel, the cDNA was cloned into the prey vector pACT4-1b, fusing the cytosolic SORLA domain with the activation domain of the transcription activator GAL4 (Ralser, et al., 2006). The automated screening was carried out in collaboration with the group of Prof. Dr. Erich Wanker (Max-Delbrück-Centrum Berlin-Buch) using a custom cDNA library, also based on the pACT4-1b (Erich Wanker, not published).

Transcriptional activation was detected by reporter genes, which were turned on upon positive bait-prey interactions. All yeast strains used require medium supplemented with histidine and uracil (SD2) to grow normally. The reporter genes *HIS3* and *URA3* allow growth on SD4 minimal medium (without amino acids), the *lacZ* gene allows detection via  $\beta$ -galactosidase activity.

The fusion protein of the SORLA cytosolic domain and LexA turned out to be autoactivating in a preliminary test. The yeast clone was able to grow on the nutrient-deficient medium SD4 and induces blue staining in medium containing X-gal (figure 31). SorCS3 constructs cloned in parallel into the same vector backbone were not autoactivating. Hence the SORLA screening could not be carried out as planned.



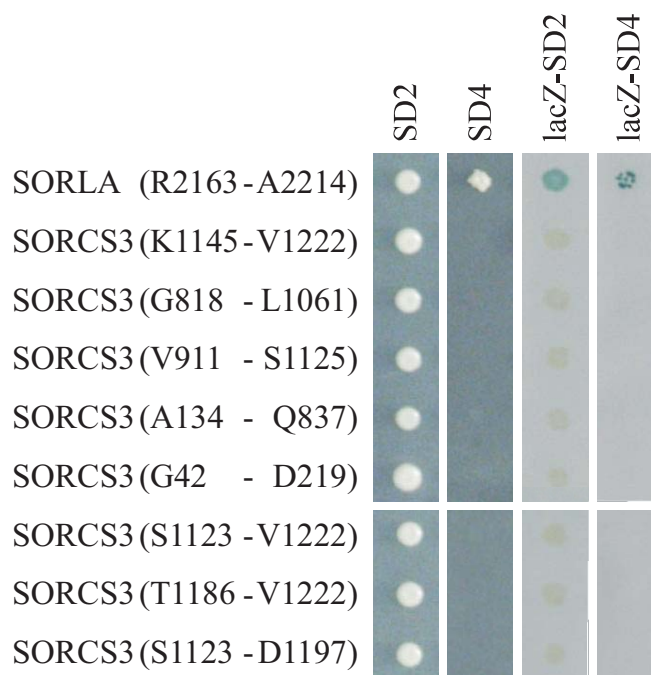


**Figure 31: Auto-activation test of the bait constructs for SORLA and SORCS3.** pBTM117c bait constructs encoding the protein segment specified in brackets were grown on SD2 and SD4 media without and with IPTG and X-gal (lacZ-SD2 and lacZ-SD4). Growth on SD4 medium or blue staining indicate auto-activation.

### 3.7.2 Peptide pull-down

An alternative strategy for screening interaction partners of SORLA was pursued by performing a pull-down with peptides of the receptors cytosolic domain.

In contrast to the yeast two-hybrid approach, this method does not require a cDNA library of interaction partners. Instead, the immobilized peptides interact with endogenous proteins from tissue lysates. Binding proteins are enriched by washing away unspecific interaction partners. Conditions and therefore stringency can be adjusted by changing the buffers used for binding and washing.

This way, it is more difficult to identify individual binding partners, since putative interaction partners are not individually present within the screen (as yeast clones are in a yeast two-hybrid screen), but as a mixture that has to be separated first. I approached this problem by gradient gel electrophoresis. Putative interacting proteins were identified by mass spectrometry.

In this approach, five peptides covering the human cytosolic domain in an overlapping manner (figure 33 B) were coupled to sepharose beads and incubated with whole kidney lysate. After washing, the bound proteins were separated by SDS polyacrylamide gel electrophoresis and stained with Coomassie Blue. Prominent

bands were cut out and sent to Bent Honoré (University of Aarhus, Denmark) for mass spectrometry.

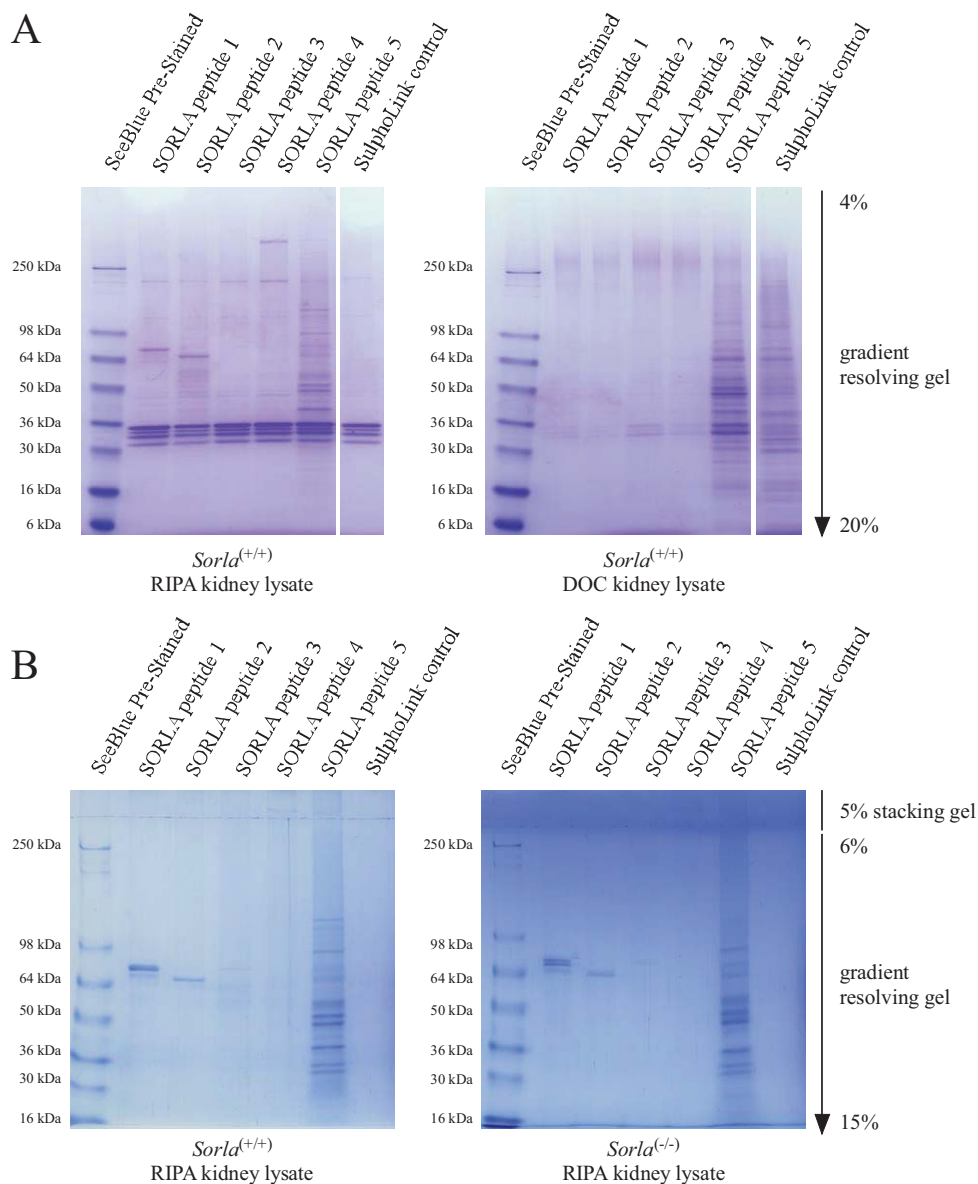


**Figure 32: SORLA peptide pull-down optimization whole kidney lysate.** A: Exemplary Coomassie-stained polyacrylamide gels showing pull-downs using immobilized peptides covering the intracellular tail of SORLA. Pull-downs were performed using RIPA (left site) or DOC (right site) buffer for kidney lysis and washing of the immobilized peptides. B: Comparison of pull-down experiments with wild-type (*Sorla*<sup>(+/+)</sup>) and SORLA-deficient (*Sorla*<sup>(-/-)</sup>) kidneys using RIPA buffer.

RIPA buffer and DOC buffer were tested for whole kidney protein preparations and washing of the immobilized peptides (figure 32 A). RIPA buffer was chosen for the following experiments, as more distinct protein bands could be reproducibly

bly isolated from the eluates. No differences in the band pattern were seen in experiments performed with lysates from wild-type or *Sorla* gene-disrupted kidneys (figure 32 B).

The most prominent bands appeared in the lanes of peptide 1 and 2. They were identified as two heat shock proteins: heat shock 70 kDa protein 9 (alternative name: mortalin, figure 33 A 1) and heat shock 70 kDa protein 8 (figure 33 A 2). It is not uncommon for short, synthesized peptides to bind heat shock proteins, as this class of proteins is binding to un- or misfolded peptides *in vivo*, fulfilling a chaperone-like role.

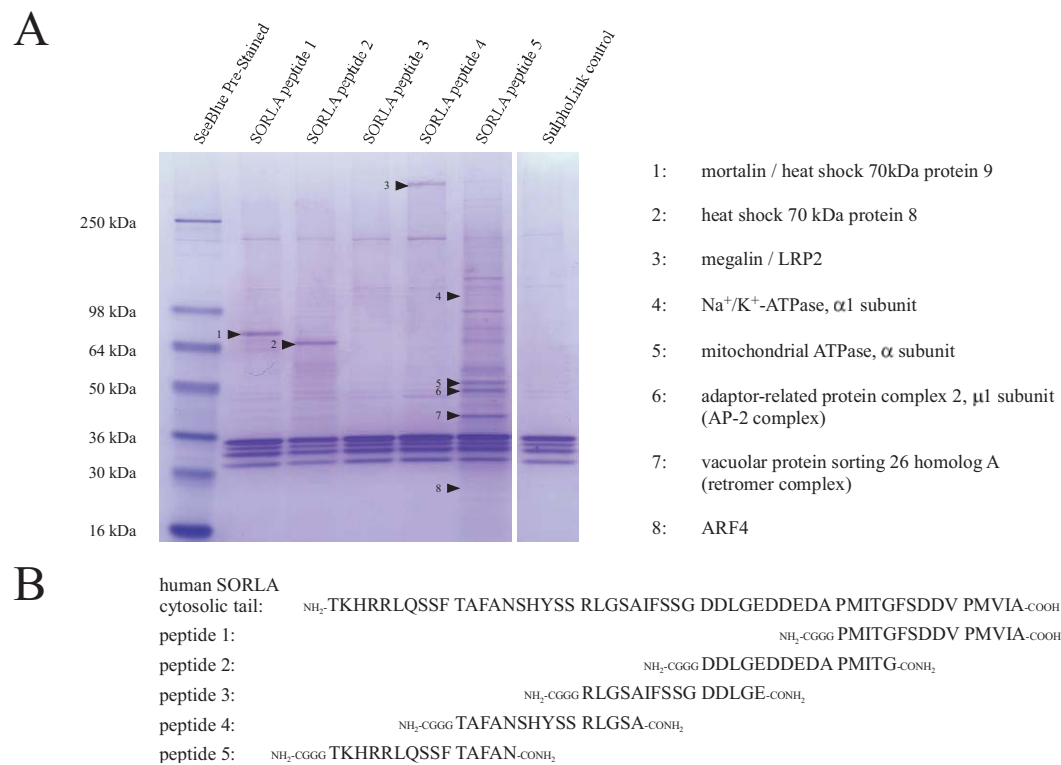


**Figure 33: Pull-down of interaction partners from whole kidney lysate.** A: Representative Coomassie-stained polyacrylamide gradient gel showing the pull-down using immobilized peptides covering the intracellular tail of SORLA. Arrows are marking interaction partners identified by mass spectrometry in several independent screens. B: Amino-acid sequence of the intracellular portion of human SORLA and peptides used for the pull-down.

The transmembrane-receptor megalin was pulled out with peptide 4 (figure 33 A 3). The endocytotic receptor, which is capable of binding various ligands, is highly abundant in the kidney, but its expression in the proximal tubule does not overlap with the distal expression of *Sorla*. This lead to the conclusion, that the observed interaction in whole-kidney lysate does not reflect a physiological situation.

Peptide 5, covering the sequence closest to the transmembrane domain of SORLA, bound most different proteins, as seen in figure 33 A. Identified proteins are the  $\mu 1$  subunit of the adaptor-related protein complex 2 (AP-2), the vacuolar protein sorting 26 homolog A (VPS26A), a subunit of the retromer complex, and the ADP-ribosylation factor 4 (ARF4). These proteins are involved in vesicular trafficking. The alpha subunits of  $\text{Na}^+/\text{K}^+$ -ATPase and mitochondrial ATPase were also pulled down from whole kidney lysate, proteins playing a role in facilitated solute transport.

An interaction of SORLA with the abovementioned proteins implicates the receptor with intracellular trafficking processes. Especially interactions with retromer and the AP-2 complex fit the role of the receptor suggested in neuronal transport processes.

## 4 Discussion

In my thesis, I analyzed the function of the VPS10p receptor SORLA in the kidney. The expression of *Sorla* has been characterized by quantitative realtime-PCR in the developing and adult kidney in mice. Using immunohistochemistry, the expression of the receptor was confined to the thick ascending limb (TAL), the distal convoluted tubule (DCT), the connecting tubule (CNT) and the collecting duct (CD) of the adult murine nephron. Extrarenal expression of SORLA was shown in the adrenal gland cortex, particularly in the zona glomerulosa.

In a mouse model lacking SORLA, a defect in renal solute reabsorption was shown. This phenotype includes defects in handling of electrolytes, especially  $\text{Na}^+$ ,  $\text{Cl}^-$ ,  $\text{K}^+$ , and  $\text{Ca}^{2+}$ . The salt loss phenotype is accompanied by mis-regulated aldosterone-secretion and decreased mean arterial pressure (MAP) and heart rate.

While investigating the cause of the renal phenotype, the comparison of the renal and adrenal transcriptomes of wild type animals and mice lacking SORLA revealed an adrenal defect in the catecholamine synthesis pathway, resulting in lower levels of epinephrine in the adrenal gland.

A more detailed investigation of the kidney uncovered that the electrolyte transporters NKCC2, NCC and NHE3 (and ROMK) are differentially expressed or abnormally phosphorylated.

A signalling kinase regulating the activity of NKCC2 and NCC, SPAK, is abnormally distributed in the TAL epithelium of mice lacking SORLA, suggesting a role of the VPS10p receptor in cellular trafficking of the enzyme. This hypothesis was further substantiated by the identification of putative SORLA-interacting proteins involved in trafficking using peptide pull-down assays.

### 4.1 SORLA in the murine kidney

Expression of the *Sorla* gene locus in adult human (Mörwald, et al., 1997) and murine (Hermans-Borgmeyer, et al., 1998) kidney was first described together with the discovery of the VPS10p-domain containing receptor itself. A more precise study reported expression of the receptor in E14 embryos and adults (Riedel, et al., 2002). I confirmed the embryonic expression by detecting *Sorla* transcripts at the onset of kidney development at E12.5 and stable expression in the kidneys of E14.5 embryos (figures 7 and 8, chapter 3.1).

Concerning the adult kidney, Riedel et al. previously confined the expression of SORLA to the collecting duct epithelium (Riedel, et al., 2002). My findings contrast with this published observation. The expression of the receptor is stretching from thick ascending limb (TAL) of Henle's loop through distal convoluted tubule

(DCT) and connecting tubule (CNT) to the collecting duct system (CD). Epithelial cells in these nephron segments express SORLA mainly in intracellular vesicular structures along their apical side and in perinuclear regions (figure 9, chapter 3.1). This localization of SORLA is in line with earlier studies, which described SORLA expression in brain and cell culture (Jacobsen, et al., 2002; Motoi, et al., 1999). SORLA-positive subcellular compartments in the kidney resemble most likely early endosomal vesicles and TGN, as the receptor is capable of shuttling between these structures (Jacobsen, et al., 2002; Nielsen, et al., 2007; Schmidt, et al., 2007; Seaman, 2004). This route is depicted in figure 2, chapter 1.1.6.1.

Expression of the SORLA-expressing nephron segments allows drawing conclusions concerning the physiological processes the receptor may be involved in.

In contrast to the quantitative (but mostly uncontrolled and passive) transport mechanisms for water and electrolytes in the proximal tubule, the SORLA-expressing segments from TAL to CD are essential for active and highly regulated reabsorption of essential electrolytes and water. The most proximal expression of SORLA can be found in the TAL of Henle's loop. Overall, the function of the loop of Henle can be described as uncoupling of water and salt reabsorption. While isoosmotic transport processes are dominant in the proximal tubule, the thin descending limb reabsorbs around 10% of the water filtered at the glomerulus. The high water permeability of this nephron segment combined with the inability to reabsorb  $\text{Na}^+$  results in concentrated tubular fluid entering the following segment. This creates a favorable gradient for  $\text{Na}^+$  reabsorption in the thin ascending limb, whose epithelium permits this gradient to drive passive paracellular reabsorption. As the tubular fluid enters the virtually water impermeable TAL, active ion transport mechanisms become dominant. 25% of the filtered  $\text{Na}^+$  are reabsorbed in this segment, making the net salt reabsorption of Henle's loop larger than the water reabsorption. As a result, hypo-osmotic tubular fluid (as compared to plasma) is leaving the loop.

The main luminal entry step for  $\text{Na}^+$  and  $\text{Cl}^-$  in TAL is via the kidney specific apical form of the  $\text{Na}^+/\text{K}^+/\text{Cl}^-$ -symporter NKCC2 (Haas and Forbush, 1998; Molony, et al., 1987). The cotransporter requires equal amounts of  $\text{K}^+$  and  $\text{Na}^+$  to be transported, even though there is far less  $\text{K}^+$  available in the lumen than  $\text{Na}^+$ . To prevent tubular depletion of  $\text{K}^+$  long before much  $\text{Na}^+$  is reabsorbed, the luminal membrane has a large number of  $\text{K}^+$ -channels (ROMK) (Xu, et al., 1997), allowing much of the intracellular potassium to leak back into the tubular fluid (see also figure 23 B, chapter 3.4.3). Thus under normal conditions, the limited amount of potassium does not restrict sodium and chloride transport through the cotransporter. A permanent activity of the basolateral  $\text{Na}^+/\text{K}^+$ -ATPase is creating an increasing  $\text{Na}^+$ -gradient towards the interstitium to facilitate the required transport. In addition to the transcellular reabsorption of sodium via NKCC2, a considerable portion of total reabsorption in the thick ascending limb occurs by paracellular diffusion. A high paracellular conductance for sodium and a positive luminal po-

tential in this segment form a significant driving force for cations, also maintained by  $\text{Na}^+/\text{K}^+$ -ATPase activity.

The next tubular segment, the DCT, is responsible for the reabsorption of 5% of the filtered  $\text{Na}^+$  and  $\text{Cl}^-$  from tubular fluid leaving the loop of Henle in an already hypo-osmotic state, while – similar to the TAL – this segment remains impermeable for water. Accordingly, the DCT also acts as a diluting segment. The major entry step for active reabsorption of  $\text{Na}^+$  by this segment is via the sodium-chloride symporter (NCC). Besides sodium and chloride reabsorption, epithelial cells in the distal convoluted tubule have apical  $\text{Ca}^{2+}$ -channels that are regulated by parathyroid hormone, rendering this segment the major site for the control of  $\text{Ca}^{2+}$  homeostasis.

In the CD, several different cell types act in concert to maintain electrolyte balance. Reabsorption of  $\text{Na}^+$  and water is accomplished by the aldosterone-sensitive principal cells that make up approximately 70% of the epithelium. The luminal entry of  $\text{Na}^+$  into these cells functions via epithelial  $\text{Na}^+$  channels. Reabsorption of  $\text{Cl}^-$  occurs partially via paracellular routes but is also actively carried out by another class of cells, the type B intercalated cells.

The reabsorption and the permeability of most of the CD system can vary between very low or very high. In the absence of hormonal stimuli, the hypo-osmotic tubular fluid entering this system remains hypo-osmotic. When it reaches the medullary portion of the CD, an enormous osmotic gradient induces medullary reabsorption to some extent, even though there is vanishingly low cortical water reabsorption without hormonal stimulation. However, because of the high tubular volume at this point – due to no reabsorption in earlier collecting duct portions – most of the water entering the medullary collecting duct flows through to the ureter.

#### 4.1.1 *Sorla*<sup>(-/-)</sup> animals are wasting $\text{Na}^+$ and $\text{K}^+$ respectively

Judging from its distal expression pattern, SORLA may influence the regulated electrolyte and water reabsorption. To test this hypothesis, I investigated the renal salt and water handling in a SORLA-deficient mouse model, previously generated by targeted disruption of the *Sorla*-gene (Andersen, et al., 2005).

Reabsorption in DCT, CNT and CD is crucial for fine-tuning electrolyte levels in the blood. Compared to plasma, tubular fluid leaves the loop of Henle in a hypo-osmotic state, making active processes compulsory for further reabsorption of electrolytes. Many of these processes are governed by the interplay of two hormonal regulators. One important player in the distal nephron is the peptide hormone vasopressin, which controls the adjustment of blood pressure (Brenner, 2007). Vasopressin-induced action includes the activation of apical water channels (aquaporins) in the CD, allowing reabsorption of water. Additionally it activates



NKCC2 in the TAL segment, therewith enhancing the hypo-osmolarity of the tubular fluid entering the CD to facilitate passive uptake of water. However, vasopressin levels are not significantly altered by SORLA-deficiency (table 13, chapter 3.2). This goes in line with the ability of *Sorla*<sup>(-/-)</sup> mice to concentrate urine normally (figure 10 B, chapter 3.2).

The second important hormone regulating the function of the distal tubule is aldosterone. It promotes both kaliuretic as well as NaCl-retaining function (Mene-ton, et al., 2004), which is already reflected by how the hormone's release is triggered: Aldosterone is released upon low NaCl levels (mediated by angiotensin II) as well as high K<sup>+</sup>-levels in serum (detected directly by aldosterone secreting cells in the adrenal cortex).

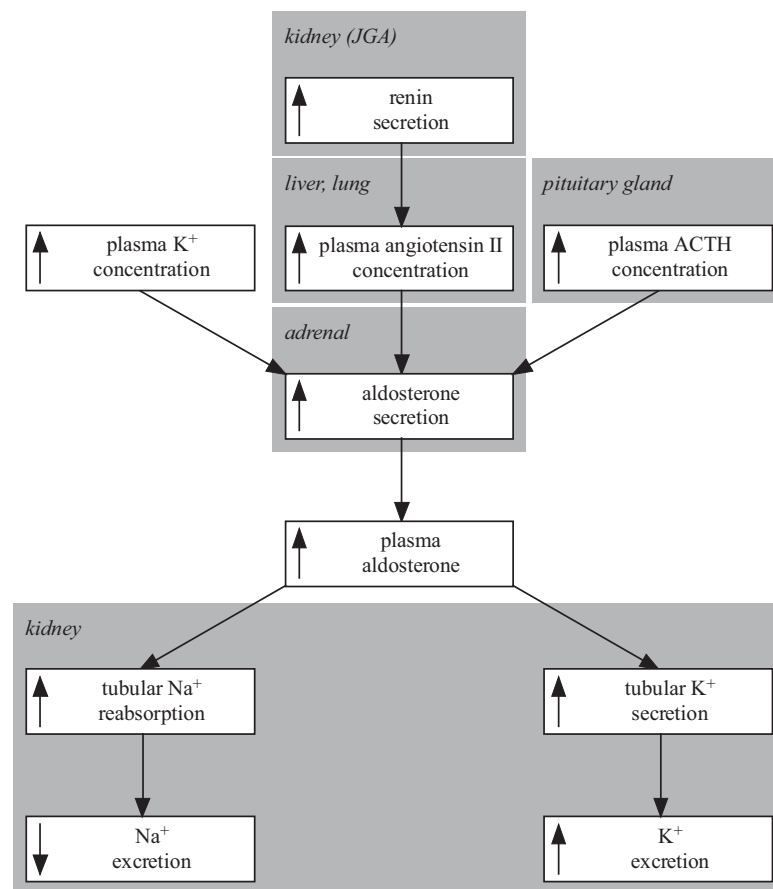


**Figure 34: Induction of aldosterone and its effects.** The release of the mineralcorticoid hormone is triggered by three main stimuli. Renin secreted in the renal juxtaglomerular apparatus (JGA) induces angiotensin I release in the liver, which in turn triggers angiotensin II release (predominantly in lung). High levels of plasma angiotensin II, K<sup>+</sup> or the adrenocorticotrophic hormone (ACTH, produced in the anterior pituitary gland) induce aldosterone secretion in the adrenal cortex. Circulating aldosterone promotes reabsorption of Na<sup>+</sup> and secretion of K<sup>+</sup> in distal nephrons of the kidney. Except for the pituitary gland, *Sorla* is expressed in all organs mentioned above (cf. chapter 1.1.6).



Judging from the urinary  $\text{Na}^+$  and  $\text{K}^+$  levels, it becomes obvious that *Sorla*<sup>(-/-)</sup> mice are able to retain  $\text{Na}^+$  but at the same time are wasting  $\text{K}^+$  under normal conditions. However, after thirsting, the mice excrete more  $\text{Na}^+$  and less  $\text{K}^+$  than wild type controls. Explaining this observation with differential aldosterone-induced mechanisms would imply higher aldosterone-action under basal conditions and a lower action in the thirsted state. This was confirmed after measuring serum levels of the mineralcorticoid: The receptor-deficient mice have significantly higher basal aldosterone levels but fail to increase those levels upon thirsting, a physiological response shown by the wild type controls (table 13, chapter 3.2), providing a physiological explanation for the altered  $\text{Na}^+/\text{K}^+$  levels.

High aldosterone does also explain elevated expression levels of  $\alpha\text{ENaC}$  and NHE3 (figure 27, chapter 3.5), as both proteins are reported to be induced by the hormone (Alvarez de la Rosa, et al., 2002; Drumm, et al., 2006).

## 4.2 SORLA and aldosterone

One explanation for the inability of the gene-targeted mice to increase the release of aldosterone is the basal loss of  $\text{K}^+$  (accompanied by hypokalemia), that the animals suffer from (table 13, chapter 3.2). Even higher aldosterone levels would lead to critical loss of  $\text{K}^+$ , eventually inducing a lethal hypokalemic state. But the mice show high blood levels of aldosterone – eliciting increased  $\text{K}^+$ -secretion – under basal conditions in the first place, long before any safeguard mechanism would be necessary in wild type animals.

The mineralcorticoid aldosterone is synthesized in and secreted from cells of the outer layer of the adrenal cortex (zona glomerulosa) in response to increased  $\text{K}^+$  levels or upon activation by the renin-angiotensin system (Bravo, 1977; Vecsei, et al., 1978).

### 4.2.1 SORLA is expressed in the adrenal gland

An expression of *Sorla* in adrenal glands of rabbit (Yamazaki, et al., 1996) and chicken (Mörwald, et al., 1997) has been shown by Northern Blot analysis. Here, expression of SORLA was confined to the cortex of murine adrenal glands by immunohistology (figure 11, chapter 3.3). The pronounced expression of the receptor in this most superficial cortical layer (figure 11 A and B) suggests a role of the receptor in aldosterone release.

To get an idea of whether the renal phenotype seen in *Sorla*<sup>(-/-)</sup> mice is a result of SORLA-deficiency in the kidney or is rather caused by a defect in the adrenal gland, I performed comparative transcriptome analysis in both tissues of wild type and receptor-deficient mice.

#### 4.2.2 SORLA-deficiency influences adrenal gland function

Alongside with the potential involvement of the receptor in the release of aldosterone in the zona glomerulosa (as discussed above), gene expression analyses in wild type and *Sorla*<sup>(-/-)</sup> mice suggests that receptor-deficiency may interfere with more processes: More than 700 probesets were differentially regulated between animals with and without SORLA in this screen, dividing the resulting expression data clearly into two groups according to the genotype (figure 13, chapter 3.1).

One striking finding that caught one's eye was an alteration in transcripts for enzymes involved in the synthesis of the catecholamine epinephrine (also referred to as adrenaline). All genes involved in its synthesis pathway are expressed at lower levels in mice lacking *Sorla* (summarized in figure 35). The consequence of this transcriptional down-regulation could be measured directly in form of lower epinephrine levels in adrenal glands of these mice (figure 16, chapter 3.3.1).

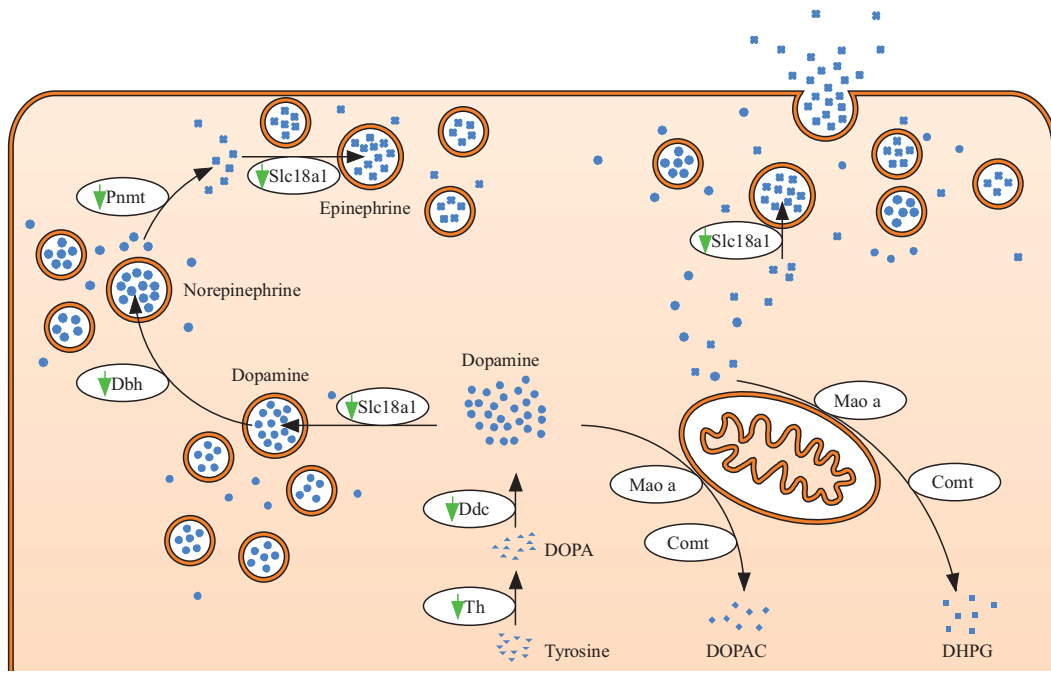


**Figure 35: Adrenal catecholamine synthesis pathway.** The synthesis of catecholamines – starting at the amino acid tyrosine – is characterized by several enzymatic steps (arrows labelled with white ellipses), that are taking place both in the cytosol as well as in vesicular structures; enzymes down-regulated in *Sorla*<sup>(-/-)</sup> animals are marked by green arrows. See also table 17, chapter 3.3.1.

In short-term stress situations, the “fight-or-flight” hormone’s function sets in. One of its various actions is to prepare the body for sustained muscle activity. Intermittent exercise (e.g. during sprints) can greatly increase the extracellular  $K^+$  concentration, due to the excessive release of this electrolyte upon muscle cell depolarisation. Epinephrine counteracts by activating plasma-membrane  $Na^+/K^+$ -

ATPases, a function without which the suddenly high levels of  $K^+$  could become dangerous for sensitive tissues such as the heart. Plasma-membrane  $Na^+/K^+$ -ATPases are also the driving force for most active reabsorption processes along the renal nephron, suggesting an influence of epinephrine release on kidney function.

The catecholamine epinephrine is released from chromaffin cells of the adrenal medulla. These cells closely resemble postganglionic neurons and are innervated by preganglionic fibers of the autonomous sympathetic nervous system. The sympathetic nervous system is coordinated by superior centers such as the hypothalamus, which itself is tightly linked with the central nervous system. SORLA is not only expressed in the central nervous system (Motoi, et al., 1999), it has been detected in cell bodies and proximal axons of sympathetic neurons as well (Posse De Chaves, et al., 2000). However, SORLA expression was not detectable in the adrenal medulla by immunohistological stainings (figure 11 C, chapter 3.3). This observation makes a direct influence of SORLA on epinephrine release in chromaffin cells very unlikely, but does not rule out an upstream effect on the sympathetic nervous system.

### 4.3 Effect of *Sorla*-deficiency on the renal transcriptome

Gene expression analysis in kidney of gene-disrupted and wild type mice revealed that absence of the receptor has only modest effects on the renal transcriptome under basal conditions. Slightly more than 300 genes are significantly changed by a factor higher than 1.5. However, stressing the organ by depriving the animals of water increases the total number of differentially expressed genes massively. More than 1,500 genes are differentially regulated in the thirsted state.

This effect illustrates the importance of SORLA for renal stress function. Under normal conditions, absence of SORLA results in salt loss. Yet, the organism can cope with the receptor deficiency. The salt loss phenotype of the *Sorla*<sup>(-/-)</sup> mice does not suggest a more severe phenotype after thirsting, as the animals lose large quantities of salt under basal conditions already. However, looking at the transcriptional data, the underlying primary phenotype seems to deteriorate with thirsting, as SORLA-deficient kidneys require activation of regulative processes at a transcriptional level – a process unnecessary under basal conditions.

Transcriptional gene expression analysis in kidney tissues did not reveal any obviously affected pathways. Regulatory effects on solute transport activity independent of gene transcription might be an explanation for this phenomenon. Therefore, my focus shifted towards specific reabsorptive processes that could explain the urine electrolyte phenotype.

#### 4.4 Electrolyte transporters in the kidney

Based on the salt loss phenotype in receptor-deficient animals, possible defects in cotransporters NCC and NKCC2 were considered. Together with the ubiquitous basolateral  $\text{Na}^+/\text{K}^+/\text{Cl}^-$ -cotransporter NKCC1, the transporters NCC and NKCC2 form the sodium driven branch of the electroneutral cation/ $\text{Cl}^-$ -cotransporter family (Slc12a family) (Gamba, 2005; Gimenez, 2006). Activity of the latter two transporters can only be found on the apical epithelium of the renal nephron (figure 36) where both contribute significantly to tubular salt reabsorption (Molony, et al., 1987; Obermüller, et al., 1995).

##### 4.4.1 Pharmacological intervention

To stress the reabsorptive processes depending on these transporters, their functions were blocked either with an NCC-specific thiazide diuretic or the NKCC2-specific drug bumetanide.

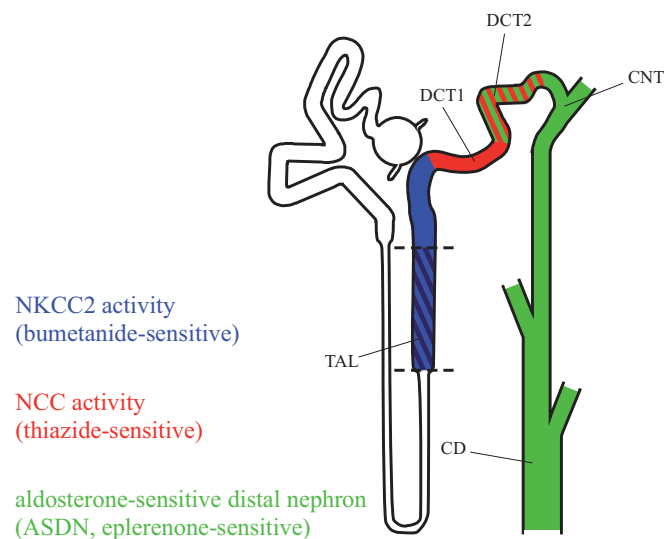


**Figure 36: Nephron segments targeted by pharmacological intervention.** NCC activity (in red) was inhibited by treatment with thiazide. NKCC2 activity (in blue) was targeted with bumetanide in TAL tubules isolated from the inner stripe of the outer medulla (ISOM), as marked by dashed lines. Eplerenone was administered to inhibit aldosterone-mediated processes in the aldosterone-sensitive distal nephron (ASDN). TAL: thick ascending limb of Henle's loop; DCT1/2: first and second segment of the distal convoluted tubule; CNT: connecting tubule; CD: collecting duct system. Cf. FIGURE 9 in chapter 3.1.

Compared to wild types, NCC-specific uptake of  $\text{Na}^+$  and  $\text{Cl}^-$  seems to be decreased in *Sorla*<sup>(-/-)</sup> mice (figure 21, chapter 3.4.1). The animals lose less salt upon thiazide-treatment. This observation contradicts with the findings that NCC is hyperphosphorylated in these animals (figure 28 in chapter 3.5, see also next chapter), as phosphorylation of the transporter was suggested to be required for its full activation (Moriguchi, et al., 2005).

To explain the effects of thiazide treatment, secondary physiological events – passive effects as well as active balancing mechanisms – have to be taken into consideration. An inactivity of NCC results in a substantial decrease of salt reabsorption in the DCT. Subsequently, tubular segments following the DCT have to handle tubular fluid with a higher osmolality as compared to the normal situation. This impairs normal water reabsorption in the CD, which could lead to the release of the antidiuretic hormone vasopressin. A subsequent increase of NKCC2 activity in TAL (see 4.1.1), would attenuate the salt loss. As vasopressin levels could not be measured, the results obtained allow only the limited conclusion whether mice lacking SORLA handle thiazide-induced stress differently to wild types.

To circumvent compensatory mechanisms in the process of blocking NKCC2 activity with bumetanide, I took advantage of the TALs resistance to collagenase and isolated tubules of this segment. In this context, fewer factors are blurring the effects of the pharmacological treatment.

NKCC2 activity, measured as bumetanide-sensitive  $^{86}\text{Rb}^+$ -uptake appears to be higher in isolated tubules of mice lacking SORLA (figure 25, chapter 3.4.3). This contrasts with the hypophosphorylation of the cotransporter in these animals (figure 26 in chapter 3.5, see next chapter). As for NCC, NKCC2 has been reported to be phosphorylated upon activation (Gimenez and Forbush, 2003), thus a decreased phosphorylation suggests a lower NKCC2 activity in *Sorla*<sup>(-/-)</sup> mice.

Since only TAL fragments were treated, no other tubular segments could interfere with the measurements. But even in isolated TAL, uptake of  $\text{K}^+/\text{Rb}^+$  may occur via different routes (depicted in figure 23, chapter 3.4.3).  $\text{Na}^+/\text{K}^+$ -ATPases (total expression not changed, figures 26 and 27, chapter 3.5), physiologically building up a driving  $\text{Na}^+$  gradient across the basolateral membrane, were inhibited by the arrow poison ouabain. The  $\text{K}^+$  channel ROMK was blocked with  $\text{Ba}^{2+}$  ions. Protein levels of the channel were slightly reduced in whole kidney lysates of *Sorla*<sup>(-/-)</sup> mice (figure 27, chapter 3.5). Assuming an incomplete blockage of the channels, this difference on protein level could be mirrored by a slightly different residual outward flux rate of  $\text{Rb}^+$ , resulting in an accumulation of  $\text{Rb}^+$  inside the cells.

The third pharmacological approach, the blockage of the mineralcorticoid receptor with the antagonist eplerenone, and therewith impeding aldosterone action, failed due to technical difficulties in properly administering this poorly soluble drug to animals.

Taken together, the pharmacological intervention in the kidney did show differential NCC and NKCC2 specific salt uptake in *Sorla* gene-targeted mice, but it did not clearly answer the question, which pathways may primarily be affected by SORLA deficiency.

#### 4.4.2 Evidence for a misregulation of NCC: *Sorla*<sup>(-/-)</sup> mice suffer from calciuria

Another evidence for mis-regulated NCC activity is the increased urinary excretion of calcium (calciuria), which was observed in *Sorla* gene-targeted animals.

Around 60% of the urinary  $\text{Ca}^{2+}$  are reabsorbed in the proximal tubule. Most of the remaining portion is taken up in the distal nephron, where it mainly undergoes transcellular transport via luminal calcium channels and basolateral  $\text{Ca}^{2+}$ -ATPases and Na/Ca-antiporters. In the DCT, the Na/Ca-antiport activity leads to a negative correlation of  $\text{Ca}^{2+}$  uptake with the uptake of  $\text{Na}^+$ . Consequently, thiazide diuretics, blocking the  $\text{Na}^+/\text{Cl}^-$ -cotransporter NCC in DCT, boost the reabsorption of  $\text{Ca}^{2+}$  in that segment (Costanzo, 1985; Suki, 1979).

Activity of NCC is regulated by phosphorylation via the WNK-SPAK pathway (Pacheco-Alvarez, et al., 2006; Reinhard, et al., 2005; Richardson, et al., 2008), comparable to the related NKCCs (vide infra). The calciuria observed in *Sorla*<sup>(-/-)</sup> mice (table 12, chapter 3.2) points towards a hyperactivity of the thiazide-sensitive cotransporter. In line with this observation, NCC is hyperphosphorylated in these animals (figure 28, chapter 3.5).

Aldosterone has been reported to increase phosphorylation of the cotransporter (Chiga, et al., 2008). This does not fit with the data from thirsted mice (cf. table 13 in chapter 3.2, and figure 28 in chapter 3.5): aldosterone levels are lower in thirsted *Sorla*<sup>(-/-)</sup> mice as compared to equally treated wild types. Further investigation is required to test, whether this hyper-phosphorylation of NCC is determined by mechanisms overruling the aldosterone signalling, or if SORLA is required for its proper regulation.

#### 4.4.3 Evidence for a misregulation of NKCC2: The renal *Sorla*<sup>(-/-)</sup> phenotype shares elements with the Bartter syndrome

The uncoupling of reabsorptive processes for salt and water in the thin descending and thick ascending limb renders Henle's loop a critical player in the regulated salt uptake in the distal nephron.

$\text{Na}^+$  transport in the TAL is a multi-component system (figure 37). The basolateral  $\text{Na}^+/\text{K}^+$ -ATPase transports  $\text{Na}^+$  from TAL-cells into the interstitium, creating a  $\text{Na}^+$ -gradient across the epithelium. This gradient is used by the  $\text{Na}^+/\text{K}^+/\text{Cl}^-$ -cotransporter NKCC2 to drive not only  $\text{Na}^+$  but also  $\text{K}^+$  and  $\text{Cl}^-$  transport into the cells. Accordingly,  $\text{K}^+$  is transported into the TAL cells from the basolateral side ( $\text{Na}^+/\text{K}^+$ -ATPase) and the apical side (NKCC2). To balance intracellular concentrations of this electrolyte, it is recycled by the  $\text{K}^+$ -channel ROMK, mainly into the tubular lumen. Following the electrochemical gradient created by the  $\text{Na}^+/\text{K}^+$ -ATPase,  $\text{Cl}^-$  exits towards the interstitium mainly via the  $\text{Cl}^-$ -channels  $\text{ClCNKB}$



and, to a lesser degree, CLCNKA. Both  $\text{Cl}^-$ -channels require the subunit Barttin for proper function.

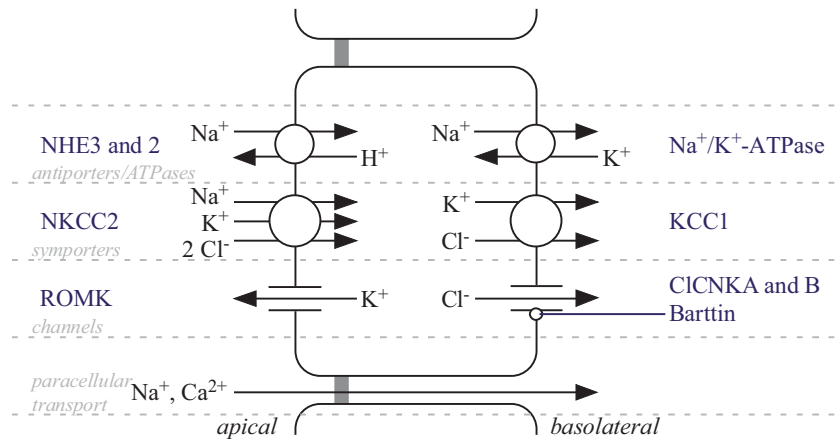


**Figure 37:  $\text{Na}^+$ -transporting components in TAL.** Arrows mark the physiological transport direction of the indicated ions; transporting components are labeled in blue. This cartoon does not show stoichiometric transport ratios.

In humans, mutations in the genes encoding NKCC2, ROMK, CLCNKB or Barttin cause Bartter-syndrome type I, II, III or IV, respectively (Birkenhager, et al., 2001; Scheinman, et al., 1999). Patients suffering from autosomal-recessive Bartter-syndromes exhibit disturbances in renal salt and volume handling. Lower than normal reabsorption of  $\text{Na}^+$  in the TAL results in hyperreninemic hyperaldosteronism (high blood levels of renin and aldosterone), accompanied by polyuria, enhanced excretion of  $\text{K}^+$  (hyperkaliuria) and  $\text{Ca}^{2+}$  (hypercalciuria), as well as low  $\text{K}^+$  levels in blood (hypokalemia). In some patients, a low blood pressure can be observed, even though renin and aldosterone are high.

Taken together, the observations made in *Sorla*<sup>(-/-)</sup> mice resemble some of the defects seen in Bartter syndrome: Under basal conditions, the animals suffer from hypercalciuria, hyperkaliuria with hypokalemia and high aldosterone (tables 12 and 13, figure 10, in chapter 3.2). The MAP of mice lacking SORLA is reduced during their activity phase (table 14, chapter 3.2). As SORLA is expressed in TAL these findings hint towards a possible function for the receptor in salt reabsorption processes in this nephron segment.

Even though NKCC2 levels are normal in *Sorla*<sup>(-/-)</sup> mice, the animals fail to phosphorylate the transporter at Thr 96 and Thr 101 (figure 26, chapter 3.5). Together with a third threonine (Thr 114 in mice), these phospho-acceptor residues comprise a regulatory domain for the activation of the cotransporter. Initially identified in *Squalus acanthias* NKCC1, the three sites are highly conserved in the sodium-driven branch of cation-coupled cotransporter protein family and their phosphorylation has been reported to mediate activation of NKCC1/2 upon stimu-

lation (Darman and Forbush, 2002; Gimenez and Forbush, 2003). In the case of NKCC2 however, Giménez and Forbush could show in *Xenopus laevis* oocytes, that the transporter still retains 50% of its activity in the absence of phosphorylation at these sites (Gimenez and Forbush, 2005).

#### 4.4.4 *Sorla*<sup>(-/-)</sup> mice are hypotonic

A clinical symptom of hypokalemia is high blood pressure (Krishna, et al., 1989). However, mice deficient for SORLA show a reduced mean arterial pressure (MAP) during their activity phase as well as a reduced heart rate (table 14, chapter 3.2).

In general, changes in Na<sup>+</sup> levels and blood pressure have greater effects on the aldosterone secretion than do equivalent changes in K<sup>+</sup> balance. In SORLA-deficient mice, however, it is unlikely that the high aldosterone levels are consequence of the low blood pressure because blood pressure-driven aldosterone activation is mediated by the renin-angiotensin-system (RAS), requiring high renin levels. In fact, the low levels of circulating renin in *Sorla*<sup>(-/-)</sup> mice suggest a low activation of the RAS (table 13, chapter 3.2).

Renin is released from granular cells of the juxtaglomerular apparatus, which lies between the macula densa (MD) and the renal corpuscle of a nephron. Renin release is triggered by several stimuli, including decreased blood pressure, sympathetic nervous activity and decreases in tubular sodium chloride levels. SORLA is expressed in the MD (not shown), together with NKCC2 (Lapointe, et al., 1990; Lorenz, et al., 1991).

Concerning juxtaglomerular renin secretion, MD cells act as sensing elements for tubular NaCl concentrations (Skøtt and Briggs, 1987). In contrast to TAL, MD cells do not possess basolateral Na<sup>+</sup>/K<sup>+</sup>-ATPase activity. It was proposed that Na<sup>+</sup>-extrusion in these cells is regulated via an ouabain-sensitive apical form of H<sup>+</sup>/K<sup>+</sup>-ATPase (Peti-Peterdi and Bell, 1999). Because of the low effectivity of this Na<sup>+</sup>-efflux system and the absence of other alternatives, the intracellular Na<sup>+</sup> concentration should reflect the luminal NaCl delivery to MD cells.

NKCC2 activity is responsible for 80 % of the NaCl-influx into MD cells, thus being an important element in the NaCl-sensing mechanism. Absence of SORLA, which leads to a nearly complete lack of phosphorylation of NKCC2, has no or little impact on this mechanism in the MD, as renin-release is downregulated upon increased NaCl levels in urine: Renin levels are only partly down-regulated under basal conditions, under which Na<sup>+</sup>-levels are only slightly increased, and massively down after thirsting, when receptor-deficient mice waste Na<sup>+</sup> (viz. tables 12 and 13, chapter 3.2).



An inactivity of NKCC2 in *Sorla*-deficient mice would lead to low intracellular levels of NaCl and subsequent release of renin. In mice lacking SORLA, levels of circulating renin are lower as in control animals, providing evidence for an increased activity of NKCC2 in this tissue.

#### 4.4.5 SORLA influences SPAK activity

Mechanisms responsible for the activating phosphorylation of NKCC2 are still not fully understood. Using a yeast two-hybrid approach, the kinases SPAK and OSR1 were recently identified as interaction partners of NKCC1's NH<sub>2</sub>-terminus through a RFQV-motif (Piechotta, et al., 2002), which is also conserved in NKCC2. The NH<sub>2</sub>-terminus NCC harbours a RFTI motif, which could act as a SPAK/OSR1 consensus sequence, and it has been demonstrated, that both NKCC2 and NCC can be phosphorylated by SPAK (Moriguchi, et al., 2005). NKCC2 activation by SPAK is governed by kinases of the WNK family (Ponce-Coria, et al., 2008; Richardson and Alessi, 2008).

In whole kidney lysates of mice lacking SORLA, SPAK is hyperphosphorylated (figure 29, chapter 3.6). Surprisingly, increased activity of SPAK does not translate into an increased phosphorylation rate of its downstream target NKCC2. Rather NKCC2 is not phosphorylated at all. Mislocalization of SPAK in the TAL of SORLA-deficient mice may provide an explanation for the apparant paradox, as for successful phosphorylation, the kinase needs to interact with its target.

The antibody used in this study only detects murine NKCC2 residues T96 and T101 if both are phosphorylated (Gimenez and Forbush, 2005). No statements can be made concerning phosphorylation at T114, and other modulating phosphorylation sites in NKCC2 cannot be ruled out either (Darman and Forbush, 2002). Under these circumstances, NKCC2 can be assumed to bear residual activity. This partial reduction of NKCC2-activity in *Sorla* gene disrupted mice could explain the observation of some – but not all – hallmarks of the human Bartter syndrome.

Interestingly, some aspects of the observed phenotype differ from the human Bartter syndrome: The hypokalemic state is milder after thirsting; the animals are not hyperkaliuric (as compared to control animals under the same conditions). The animals also do not suffer from hyperreninemia. While deprived from water, the mice actually react with a milder increase of blood renin-levels as wild type controls. These observations are indicating a role of SORLA in other mechanisms as well.

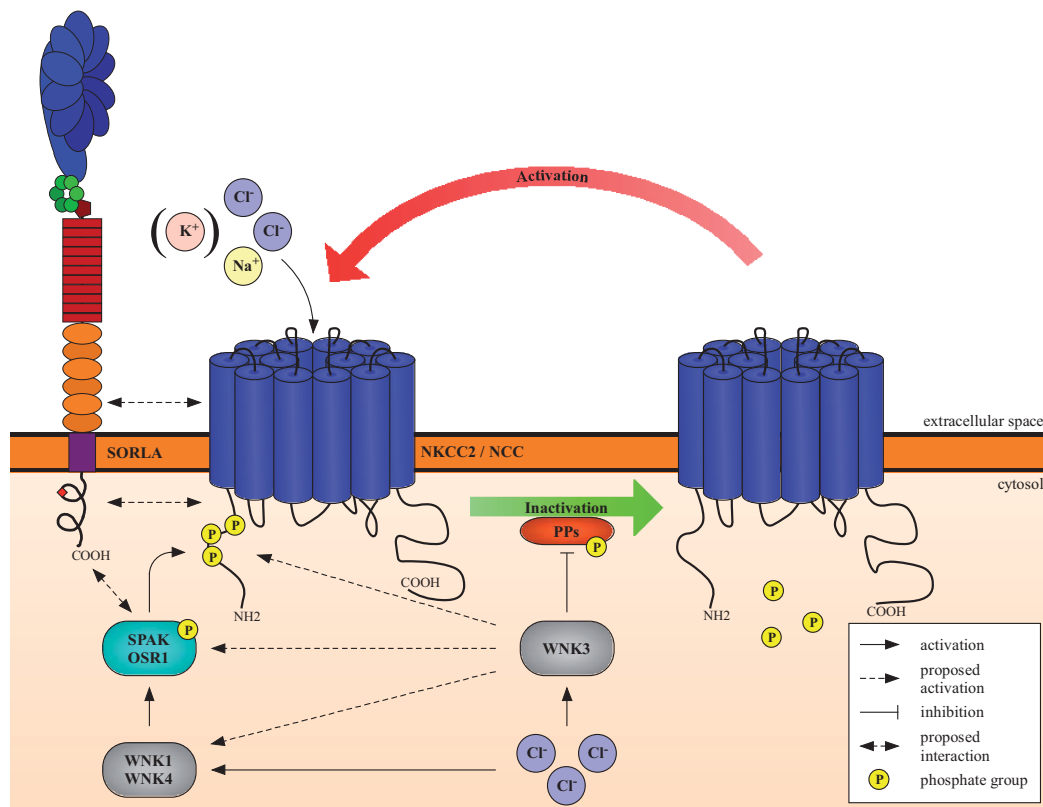


**Figure 38: Mechanisms responsible for the activation of NKCC2 and NCC.** NKCC2 and NCC are both activated upon WNK signalling via phosphorylation by SPAK/OSR1. SPAK/OSR1 can phosphorylate the cotransporters at three conserved threonines in its N-terminal region. While NCC is hyperphosphorylated in *Sorla*<sup>-/-</sup> mice, phosphorylation of NKCC2 in the same animals is dramatically decreased. The abnormal localization of SPAK in TAL, suggests a role of SORLA in establishing proper localization of the kinase towards NKCC2-containing vesicles. On the contrary, lack of SORLA in DCT does not negatively influence phosphorylation of NCC. Due to the high homology of the three transporters, some of the depicted interactions were published for NKCC1 but are proposed for NKCC2 and NCC as well (Gimenez, 2006).

#### 4.5 Conclusion: *Sorla*-deficiency has an impact on regulated salt homeostasis

In this work, I provided evidence for an involvement of SORLA in regulated salt reabsorption pathways. As a result, Na<sup>+</sup> and K<sup>+</sup> homeostasis is disturbed in mice deficient for the *Sorla* gene. This finding can be explained with mis-regulation of aldosterone release in the adrenal glands of these animals. SORLA is expressed in the zona glomerulosa, the site of aldosterone synthesis. Future work has to determine at which point the receptor is involved in the synthesis or release of aldosterone. The approach presented in this work – comparative analysis of adrenal

transcriptomes of mice with and deficient for *Sorla* – did not reveal the molecular mechanisms how the receptor influences aldosterone release.

A complicating fact is that not only adrenal glands influence kidney function by the release of hormones such as aldosterone. Kidneys do also affect adrenal gland function, for example by activating the renin-angiotensin-aldosterone system. A possible concept to separate the action of SORLA in both organs could be a bilateral adrenalectomy in wild type and receptor-deficient mice. Kidney functions of animals treated in such a way could be investigated without being influenced by differential adrenal functions. However, this concept is unidirectional: While adult mice can survive several weeks without adrenal glands (Hoffman-Goetz, et al., 2004) a bilateral nephrectomy would be lethal. Mice with a tissue-specific disruption of the *Sorla* gene in the distal nephron, e.g. using the CLCNKB promoter (Kobayashi, et al., 2002), could enable investigation of adrenal gland function depending on presence or absence of the receptor in the kidney.

The adrenal hormone aldosterone governs two functions in kidney: Secretion of  $K^+$  and retention of NaCl (Halperin, et al., 2006). In some situations however, the kidney only needs to fulfill one of these two tasks. A recently discovered group of kinases does play an important role in deciding which way to go: the WNK kinases (Gamba, 2005; Kahle, et al., 2003; Subramanya, et al., 2006). Members of this protein family have been shown to regulate downstream targets through the proline-alanine-rich STE20-related kinase SPAK (Vitari, et al., 2005).

SPAK is hyperphosphorylated in *Sorla*<sup>(-/-)</sup> mice. Recently, this kinase has been reported to be responsible for mediating phosphorylation in order to activate members of the sodium-driven branch of the chloride-coupled cotransporters (coded by the Slc12a gene family) (Moriguchi, et al., 2005; Ponce-Coria, et al., 2008). Two members of this family, the bumetanide-sensitive apical  $Na^+/K^+/Cl^-$ -cotransporter NKCC2 and the thiazide-sensitive  $Na^+/Cl^-$ -cotransporter NCC are expressed within the same nephron segments as SORLA. And indeed, both NKCC2 and NCC are mis-phosphorylated in mice lacking SORLA. Additionally, both transporters show altered activity in these animals, finally resulting in urinary salt wasting and hypokalemia.

This work presents evidence that SORLA is involved in the WNK-SPAK-Slc12a pathway, regulating  $Na^+$  and  $K^+$  homeostasis. Future research needs to address at which point SORLA influences this signaling cascade.

A cue is given by the proposed function of the receptor. Due to its homology to the yeast sorting receptor VPS10p, its intracellular localization and trafficking motifs within its cytosolic domain, the receptor could be involved in transporting cargo proteins (such as NKCC2 or NCC) to its proper location. SORLA fulfils a similar function in the CNS, where it reroutes the amyloid precursor APP and affects plaque-formation in Alzheimer's disease (Andersen, et al., 2006; Schmidt, et

al., 2007). This idea is strengthened by the identification of putative interaction partners (ARF4, AP2 and the retromer complex, see figure 33, chapter 3.7.2), which are involved in intracellular transport (Chang, et al., 1993; Collins, 2008; Deretic, 2006). Due to its features, it could also act as a scaffold, bringing kinases in close vicinity to its target, as suggested by the mis-localization of SPAK in TAL cells lacking SORLA.

The different phosphorylation state of NKCC2 and NCC can be explained by SORLA being involved in bringing together SPAK and NKCC2, while SPAK and NCC meet in a SORLA-independent manner (figure 38). However, without directly measuring the phosphorylation state and activity of both transporters from wild type and *Sorla*<sup>(-/-)</sup> mice, it is difficult to prove that statement. Activity measurements under defined conditions could be achieved by microperfusion experiments either in intact kidneys or in isolated tubule segments, as described for rats (Bank, et al., 1974).

The discovered extra-renal phenotype of mice lacking SORLA – the receptor's influence on the catecholamine metabolism – could also have an implication for kidney function: Catecholamines influence renin release through  $\beta$ -adrenergic receptors. This defect could be the reason for the hypotension in the activity phase of *Sorla*<sup>(-/-)</sup> mice. Additionally, epinephrine has a modulating effect on Na<sup>+</sup>/K<sup>+</sup>-ATPases, which are the driving force of active electrolyte reabsorption along the nephron (Brenner, 2007; Churchill, 1988). An influence of the adrenal lack of SORLA on kidney function can clearly be hypothesized in this context. However, future studies have to substantiate the receptor's role in the adrenal and its systemic impact.

## Bibliography

- Alberts, B. M.; Bray, D.; Lewis, J.; Raff, M.; Roberts, K. and Watson, J. D. (1995): *Molekularbiologie der Zelle*, 3rd. ed., VCH, Weinheim, Germany, ISBN: 3527300554.
- Alvarez de la Rosa, D.; Li, H. and Canessa, C. M. (2002): Effects of aldosterone on biosynthesis, traffic, and functional expression of epithelial sodium channels in A6 cells, *J Gen Physiol* (vol. 119), No. 5, pp. 427-42. URL: [http://www.ncbi.nlm.nih.gov/entrez/query.fcgi?cmd=Retrieve&db=PubMed&dopt=Citation&list\\_uids=11981022](http://www.ncbi.nlm.nih.gov/entrez/query.fcgi?cmd=Retrieve&db=PubMed&dopt=Citation&list_uids=11981022)
- Andersen, O. M.; Reiche, J.; Schmidt, V.; Gotthardt, M.; Spoelgen, R.; Behlke, J.; von Arnim, C. A.; Breiderhoff, T.; Jansen, P.; Wu, X.; Bales, K. R.; Cappai, R.; Masters, C. L.; Gliemann, J.; Mufson, E. J.; Hyman, B. T.; Paul, S. M.; Nykjaer, A. and Willnow, T. E. (2005): Neuronal sorting protein-related receptor sorLA/LR11 regulates processing of the amyloid precursor protein, *Proc Natl Acad Sci U S A* (vol. 102), No. 38, pp. 13461-6. URL: [http://www.ncbi.nlm.nih.gov/entrez/query.fcgi?cmd=Retrieve&db=PubMed&dopt=Citation&list\\_uids=16174740](http://www.ncbi.nlm.nih.gov/entrez/query.fcgi?cmd=Retrieve&db=PubMed&dopt=Citation&list_uids=16174740)
- Andersen, O. M.; Schmidt, V.; Spoelgen, R.; Gliemann, J.; Behlke, J.; Galatis, D.; McKinstry, W. J.; Parker, M. W.; Masters, C. L.; Hyman, B. T.; Cappai, R. and Willnow, T. E. (2006): Molecular dissection of the interaction between amyloid precursor protein and its neuronal trafficking receptor SorLA/LR11, *Biochemistry* (vol. 45), No. 8, pp. 2618-28. URL: [http://www.ncbi.nlm.nih.gov/entrez/query.fcgi?cmd=Retrieve&db=PubMed&dopt=Citation&list\\_uids=16489755](http://www.ncbi.nlm.nih.gov/entrez/query.fcgi?cmd=Retrieve&db=PubMed&dopt=Citation&list_uids=16489755)
- Arnett, M. G.; Ryals, J. M. and Wright, D. E. (2007): Pro-NGF, sortilin, and p75NTR: potential mediators of injury-induced apoptosis in the mouse dorsal root ganglion, *Brain Res* (vol. 1183), pp. 32-42. URL: [http://www.ncbi.nlm.nih.gov/entrez/query.fcgi?cmd=Retrieve&db=PubMed&dopt=Citation&list\\_uids=17964555](http://www.ncbi.nlm.nih.gov/entrez/query.fcgi?cmd=Retrieve&db=PubMed&dopt=Citation&list_uids=17964555)
- Bank, N.; Aynedjian, H. S. and Weinstein, S. W. (1974): A microperfusion study of phosphate reabsorption by the rat proximal renal tubule. Effect of parathyroid hormone, *J Clin Invest* (vol. 54), No. 5, pp. 1040-8. URL: <http://www.pubmedcentral.nih.gov/articlerender.fcgi?artid=301651>
- Ben-Ari, Y. (2001): Developing networks play a similar melody, *Trends Neurosci* (vol. 24), No. 6, pp. 353-60. URL: [http://www.ncbi.nlm.nih.gov/entrez/query.fcgi?cmd=Retrieve&db=PubMed&dopt=Citation&list\\_uids=11356508](http://www.ncbi.nlm.nih.gov/entrez/query.fcgi?cmd=Retrieve&db=PubMed&dopt=Citation&list_uids=11356508)
- Benjamini, Y. and Hochberg, Y. (1995): Controlling the False Discovery Rate: A Practical and Powerful Approach to Multiple Testing, *Journal of the Royal Statistical Society. Series B (Methodological)* (vol. 57), No. 1, pp. 289-300. URL: [http://www.math.tau.ac.il/~ybenja/MyPapers/benjamini\\_hochberg1995.pdf](http://www.math.tau.ac.il/~ybenja/MyPapers/benjamini_hochberg1995.pdf)
- Birkenhager, R.; Otto, E.; Schurmann, M. J.; Vollmer, M.; Ruf, E. M.; Maier-Lutz, I.; Beekmann, F.; Fekete, A.; Omran, H.; Feldmann, D.; Milford, D. V.; Jeck, N.; Konrad, M.; Landau, D.; Knoers, N. V.; Antignac, C.; Sudbrak, R.; Kispert, A. and Hildebrandt, F. (2001): Mu-

- tation of BSND causes Bartter syndrome with sensorineural deafness and kidney failure, *Nat Genet* (vol. 29), No. 3, pp. 310-4. URL:  
[http://www.ncbi.nlm.nih.gov/entrez/query.fcgi?cmd=Retrieve&db=PubMed&dopt=Citation&list\\_uids=11687798](http://www.ncbi.nlm.nih.gov/entrez/query.fcgi?cmd=Retrieve&db=PubMed&dopt=Citation&list_uids=11687798)
- Bolstad, B. M.; Irizarry, R. A.; Astrand, M. and Speed, T. P. (2003): A comparison of normalization methods for high density oligonucleotide array data based on variance and bias, *Bioinformatics* (vol. 19), No. 2, pp. 185-93. URL:  
[http://www.ncbi.nlm.nih.gov/entrez/query.fcgi?cmd=Retrieve&db=PubMed&dopt=Citation&list\\_uids=12538238](http://www.ncbi.nlm.nih.gov/entrez/query.fcgi?cmd=Retrieve&db=PubMed&dopt=Citation&list_uids=12538238)
- Bonifacino, J. S. and Rojas, R. (2006): Retrograde transport from endosomes to the trans-Golgi network, *Nat Rev Mol Cell Biol* (vol. 7), No. 8, pp. 568-79. URL:  
[http://www.ncbi.nlm.nih.gov/entrez/query.fcgi?cmd=Retrieve&db=PubMed&dopt=Citation&list\\_uids=16936697](http://www.ncbi.nlm.nih.gov/entrez/query.fcgi?cmd=Retrieve&db=PubMed&dopt=Citation&list_uids=16936697)
- Bonifacino, J. S. and Traub, L. M. (2003): Signals for sorting of transmembrane proteins to endosomes and lysosomes, *Annu Rev Biochem* (vol. 72), pp. 395-447. URL:  
[http://www.ncbi.nlm.nih.gov/entrez/query.fcgi?cmd=Retrieve&db=PubMed&dopt=Citation&list\\_uids=12651740](http://www.ncbi.nlm.nih.gov/entrez/query.fcgi?cmd=Retrieve&db=PubMed&dopt=Citation&list_uids=12651740)
- Boutillier, J.; Ceni, C.; Pagdala, P. C.; Forgie, A.; Neet, K. E. and Barker, P. A. (2008): Proneurotrophins require endocytosis and intracellular proteolysis to induce TrkA activation, *J Biol Chem* (vol. 283), No. 19, pp. 12709-16. URL:  
[http://www.ncbi.nlm.nih.gov/entrez/query.fcgi?cmd=Retrieve&db=PubMed&dopt=Citation&list\\_uids=18299325](http://www.ncbi.nlm.nih.gov/entrez/query.fcgi?cmd=Retrieve&db=PubMed&dopt=Citation&list_uids=18299325)
- Bradford, M. M. (1976): A rapid and sensitive method for the quantitation of microgram quantities of protein utilizing the principle of protein-dye binding, *Anal Biochem* (vol. 72), pp. 248-54. URL:  
[http://www.ncbi.nlm.nih.gov/entrez/query.fcgi?cmd=Retrieve&db=PubMed&dopt=Citation&list\\_uids=942051](http://www.ncbi.nlm.nih.gov/entrez/query.fcgi?cmd=Retrieve&db=PubMed&dopt=Citation&list_uids=942051)
- Bravo, E. L. (1977): Regulation of aldosterone secretion: current concepts and newer aspects, *Adv Nephrol Necker Hosp* (vol. 7), pp. 105-20. URL:  
[http://www.ncbi.nlm.nih.gov/entrez/query.fcgi?cmd=Retrieve&db=PubMed&dopt=Citation&list\\_uids=208405](http://www.ncbi.nlm.nih.gov/entrez/query.fcgi?cmd=Retrieve&db=PubMed&dopt=Citation&list_uids=208405)
- Brenner, B. M. (2007): Brenner and Rector's *The Kidney*: 2-Volume Set, 8. ed., Elsevier Saunders, Philadelphia, ISBN: 978-1-4160-3105-5.
- Bronfman, F. C.; Tcherpakov, M.; Jovin, T. M. and Fainzilber, M. (2003): Ligand-induced internalization of the p75 neurotrophin receptor: a slow route to the signaling endosome, *J Neurosci* (vol. 23), No. 8, pp. 3209-20. URL:  
[http://www.ncbi.nlm.nih.gov/entrez/query.fcgi?cmd=Retrieve&db=PubMed&dopt=Citation&list\\_uids=12716928](http://www.ncbi.nlm.nih.gov/entrez/query.fcgi?cmd=Retrieve&db=PubMed&dopt=Citation&list_uids=12716928)
- Bujo, H. and Saito, Y. (2000): Markedly induced expression of LR11 in atherosclerosis, *J Atheroscler Thromb* (vol. 7), No. 1, pp. 21-5. URL:  
[http://www.ncbi.nlm.nih.gov/entrez/query.fcgi?cmd=Retrieve&db=PubMed&dopt=Citation&list\\_uids=11425040](http://www.ncbi.nlm.nih.gov/entrez/query.fcgi?cmd=Retrieve&db=PubMed&dopt=Citation&list_uids=11425040)



- Carter, B. D. and Lewin, G. R. (1997): Neurotrophins live or let die: does p75NTR decide?, *Neuron* (vol. 18), No. 2, pp. 187-90. URL:  
[http://www.ncbi.nlm.nih.gov/entrez/query.fcgi?cmd=Retrieve&db=PubMed&dopt=Citation&list\\_uids=9052790](http://www.ncbi.nlm.nih.gov/entrez/query.fcgi?cmd=Retrieve&db=PubMed&dopt=Citation&list_uids=9052790)
- Cereghino, J. L.; Marcusson, E. G. and Emr, S. D. (1995): The cytoplasmic tail domain of the vacuolar protein sorting receptor Vps10p and a subset of VPS gene products regulate receptor stability, function, and localization, *Mol Biol Cell* (vol. 6), No. 9, pp. 1089-102. URL:  
[http://www.ncbi.nlm.nih.gov/entrez/query.fcgi?cmd=Retrieve&db=PubMed&dopt=Citation&list\\_uids=8534908](http://www.ncbi.nlm.nih.gov/entrez/query.fcgi?cmd=Retrieve&db=PubMed&dopt=Citation&list_uids=8534908)
- Chang, M. P.; Mallet, W. G.; Mostov, K. E. and Brodsky, F. M. (1993): Adaptor self-aggregation, adaptor-receptor recognition and binding of alpha-adaptin subunits to the plasma membrane contribute to recruitment of adaptor (AP2) components of clathrin-coated pits, *EMBO J* (vol. 12), No. 5, pp. 2169-80. URL:  
[http://www.ncbi.nlm.nih.gov/entrez/query.fcgi?cmd=Retrieve&db=PubMed&dopt=Citation&list\\_uids=8491205](http://www.ncbi.nlm.nih.gov/entrez/query.fcgi?cmd=Retrieve&db=PubMed&dopt=Citation&list_uids=8491205)
- Chao, M. V. (2003): Neurotrophins and their receptors: a convergence point for many signalling pathways, *Nat Rev Neurosci* (vol. 4), No. 4, pp. 299-309. URL:  
[http://www.ncbi.nlm.nih.gov/entrez/query.fcgi?cmd=Retrieve&db=PubMed&dopt=Citation&list\\_uids=12671646](http://www.ncbi.nlm.nih.gov/entrez/query.fcgi?cmd=Retrieve&db=PubMed&dopt=Citation&list_uids=12671646)
- Chen, W. J.; Goldstein, J. L. and Brown, M. S. (1990): NPXY, a sequence often found in cytoplasmic tails, is required for coated pit-mediated internalization of the low density lipoprotein receptor, *J Biol Chem* (vol. 265), No. 6, pp. 3116-23. URL:  
[http://www.ncbi.nlm.nih.gov/entrez/query.fcgi?cmd=Retrieve&db=PubMed&dopt=Citation&list\\_uids=1968060](http://www.ncbi.nlm.nih.gov/entrez/query.fcgi?cmd=Retrieve&db=PubMed&dopt=Citation&list_uids=1968060)
- Chen, Zhe-Yu; Ieraci, Alessandro; Teng, Henry; Dall, Henning; Meng, Chui-Xiang; Herrera, Daniel G.; Nykjaer, Anders; Hempstead, Barbara L. and Lee, Francis S. (2005): Sortilin Controls Intracellular Sorting of Brain-Derived Neurotrophic Factor to the Regulated Secretory Pathway, *J. Neurosci.* (vol. 25), No. 26, pp. 6156-6166. URL:  
<http://www.jneurosci.org/cgi/content/abstract/25/26/6156>
- Chiga, M.; Rai, T.; Yang, S. S.; Ohta, A.; Takizawa, T.; Sasaki, S. and Uchida, S. (2008): Dietary salt regulates the phosphorylation of OSR1/SPAK kinases and the sodium chloride co-transporter through aldosterone, *Kidney Int* (vol. 74), No. 11, pp. 1403-9. URL:  
[http://www.ncbi.nlm.nih.gov/entrez/query.fcgi?cmd=Retrieve&db=PubMed&dopt=Citation&list\\_uids=18800028](http://www.ncbi.nlm.nih.gov/entrez/query.fcgi?cmd=Retrieve&db=PubMed&dopt=Citation&list_uids=18800028)
- Churchill, P. C. (1988): Cellular mechanisms of renin release, *Clin Exp Hypertens A* (vol. 10), No. 6, pp. 1189-202. URL:  
[http://www.ncbi.nlm.nih.gov/entrez/query.fcgi?cmd=Retrieve&db=PubMed&dopt=Citation&list\\_uids=2852076](http://www.ncbi.nlm.nih.gov/entrez/query.fcgi?cmd=Retrieve&db=PubMed&dopt=Citation&list_uids=2852076)
- Clee, S. M.; Yandell, B. S.; Schueler, K. M.; Rabaglia, M. E.; Richards, O. C.; Raines, S. M.; Kabara, E. A.; Klass, D. M.; Mui, E. T.; Stapleton, D. S.; Gray-Keller, M. P.; Young, M. B.; Stoehr, J. P.; Lan, H.; Boronenkov, I.; Raess, P. W.; Flowers, M. T. and Attie, A. D. (2006): Positional cloning of Sorcs1, a type 2 diabetes quantitative trait locus, *Nat Genet* (vol. 38), No. 6, pp. 688-93. URL:



[http://www.ncbi.nlm.nih.gov/entrez/query.fcgi?cmd=Retrieve&db=PubMed&dopt=Citation&list\\_uids=16682971](http://www.ncbi.nlm.nih.gov/entrez/query.fcgi?cmd=Retrieve&db=PubMed&dopt=Citation&list_uids=16682971)

Cohen, G. B.; Ren, R. and Baltimore, D. (1995): Modular binding domains in signal transduction proteins, *Cell* (vol. 80), No. 2, pp. 237-48. URL:  
[http://www.ncbi.nlm.nih.gov/entrez/query.fcgi?cmd=Retrieve&db=PubMed&dopt=Citation&list\\_uids=7834743](http://www.ncbi.nlm.nih.gov/entrez/query.fcgi?cmd=Retrieve&db=PubMed&dopt=Citation&list_uids=7834743)

Collins, B. M. (2008): The structure and function of the retromer protein complex, *Traffic* (vol. 9), No. 11, pp. 1811-22. URL:  
[http://www.ncbi.nlm.nih.gov/entrez/query.fcgi?cmd=Retrieve&db=PubMed&dopt=Citation&list\\_uids=18541005](http://www.ncbi.nlm.nih.gov/entrez/query.fcgi?cmd=Retrieve&db=PubMed&dopt=Citation&list_uids=18541005)

Cooper, A. A. and Stevens, T. H. (1996): Vps10p cycles between the late-Golgi and prevacuolar compartments in its function as the sorting receptor for multiple yeast vacuolar hydrolases, *J Cell Biol* (vol. 133), No. 3, pp. 529-41. URL:  
[http://www.ncbi.nlm.nih.gov/entrez/query.fcgi?cmd=Retrieve&db=PubMed&dopt=Citation&list\\_uids=8636229](http://www.ncbi.nlm.nih.gov/entrez/query.fcgi?cmd=Retrieve&db=PubMed&dopt=Citation&list_uids=8636229)

Costanzo, L. S. (1985): Localization of diuretic action in microperfused rat distal tubules: Ca and Na transport, *Am J Physiol* (vol. 248), No. 4 Pt 2, pp. F527-35. URL:  
[http://www.ncbi.nlm.nih.gov/entrez/query.fcgi?cmd=Retrieve&db=PubMed&dopt=Citation&list\\_uids=3985160](http://www.ncbi.nlm.nih.gov/entrez/query.fcgi?cmd=Retrieve&db=PubMed&dopt=Citation&list_uids=3985160)

Darman, R. B. and Forbush, B. (2002): A regulatory locus of phosphorylation in the N terminus of the Na-K-Cl cotransporter, NKCC1, *J Biol Chem* (vol. 277), No. 40, pp. 37542-50. URL:  
[http://www.ncbi.nlm.nih.gov/entrez/query.fcgi?cmd=Retrieve&db=PubMed&dopt=Citation&list\\_uids=12145304](http://www.ncbi.nlm.nih.gov/entrez/query.fcgi?cmd=Retrieve&db=PubMed&dopt=Citation&list_uids=12145304)

Deretic, D. (2006): A role for rhodopsin in a signal transduction cascade that regulates membrane trafficking and photoreceptor polarity, *Vision Res* (vol. 46), No. 27, pp. 4427-33. URL:  
[http://www.ncbi.nlm.nih.gov/entrez/query.fcgi?cmd=Retrieve&db=PubMed&dopt=Citation&list\\_uids=17010408](http://www.ncbi.nlm.nih.gov/entrez/query.fcgi?cmd=Retrieve&db=PubMed&dopt=Citation&list_uids=17010408)

Dodson, S. E.; Gearing, M.; Lippa, C. F.; Montine, T. J.; Levey, A. I. and Lah, J. J. (2006): LR11/SorLA expression is reduced in sporadic Alzheimer disease but not in familial Alzheimer disease, *J Neuropathol Exp Neurol* (vol. 65), No. 9, pp. 866-72. URL:  
[http://www.ncbi.nlm.nih.gov/entrez/query.fcgi?cmd=Retrieve&db=PubMed&dopt=Citation&list\\_uids=16957580](http://www.ncbi.nlm.nih.gov/entrez/query.fcgi?cmd=Retrieve&db=PubMed&dopt=Citation&list_uids=16957580)

Drumm, K.; Kress, T. R.; Gassner, B.; Krug, A. W. and Gekle, M. (2006): Aldosterone stimulates activity and surface expression of NHE3 in human primary proximal tubule epithelial cells (RPTEC), *Cell Physiol Biochem* (vol. 17), No. 1-2, pp. 21-8. URL:  
[http://www.ncbi.nlm.nih.gov/entrez/query.fcgi?cmd=Retrieve&db=PubMed&dopt=Citation&list\\_uids=16543718](http://www.ncbi.nlm.nih.gov/entrez/query.fcgi?cmd=Retrieve&db=PubMed&dopt=Citation&list_uids=16543718)

Dufau, M. L. (1998): The luteinizing hormone receptor, *Annu Rev Physiol* (vol. 60), pp. 461-96. URL:  
[http://www.ncbi.nlm.nih.gov/entrez/query.fcgi?cmd=Retrieve&db=PubMed&dopt=Citation&list\\_uids=9558473](http://www.ncbi.nlm.nih.gov/entrez/query.fcgi?cmd=Retrieve&db=PubMed&dopt=Citation&list_uids=9558473)

- Fahnestock, M.; Michalski, B.; Xu, B. and Coughlin, M. D. (2001): The precursor pro-nerve growth factor is the predominant form of nerve growth factor in brain and is increased in Alzheimer's disease, *Mol Cell Neurosci* (vol. 18), No. 2, pp. 210-20. URL: [http://www.ncbi.nlm.nih.gov/entrez/query.fcgi?cmd=Retrieve&db=PubMed&dopt=Citation&list\\_uids=11520181](http://www.ncbi.nlm.nih.gov/entrez/query.fcgi?cmd=Retrieve&db=PubMed&dopt=Citation&list_uids=11520181)
- Gallagher, S. R. and Desjardins, P. R. (2006): Quantitation of DNA and RNA with absorption and fluorescence spectroscopy, *Curr Protoc Mol Biol* (vol. Appendix 3), p. Appendix 3D. URL: [http://www.ncbi.nlm.nih.gov/entrez/query.fcgi?cmd=Retrieve&db=PubMed&dopt=Citation&list\\_uids=18265369](http://www.ncbi.nlm.nih.gov/entrez/query.fcgi?cmd=Retrieve&db=PubMed&dopt=Citation&list_uids=18265369)
- Gamba, G. (2005): Molecular physiology and pathophysiology of electroneutral cation-chloride cotransporters, *Physiol Rev* (vol. 85), No. 2, pp. 423-93. URL: [http://www.ncbi.nlm.nih.gov/entrez/query.fcgi?cmd=Retrieve&db=PubMed&dopt=Citation&list\\_uids=15788703](http://www.ncbi.nlm.nih.gov/entrez/query.fcgi?cmd=Retrieve&db=PubMed&dopt=Citation&list_uids=15788703)
- Gamba, G. (2005): Role of WNK kinases in regulating tubular salt and potassium transport and in the development of hypertension, *Am J Physiol Renal Physiol* (vol. 288), No. 2, pp. F245-52. URL: [http://www.ncbi.nlm.nih.gov/entrez/query.fcgi?cmd=Retrieve&db=PubMed&dopt=Citation&list\\_uids=15637347](http://www.ncbi.nlm.nih.gov/entrez/query.fcgi?cmd=Retrieve&db=PubMed&dopt=Citation&list_uids=15637347)
- Gargano, N.; Levi, A. and Alema, S. (1997): Modulation of nerve growth factor internalization by direct interaction between p75 and TrkA receptors, *J Neurosci Res* (vol. 50), No. 1, pp. 1-12. URL: [http://www.ncbi.nlm.nih.gov/entrez/query.fcgi?cmd=Retrieve&db=PubMed&dopt=Citation&list\\_uids=9379485](http://www.ncbi.nlm.nih.gov/entrez/query.fcgi?cmd=Retrieve&db=PubMed&dopt=Citation&list_uids=9379485)
- Gimenez, I. (2006): Molecular mechanisms and regulation of furosemide-sensitive Na-K-Cl cotransporters, *Curr Opin Nephrol Hypertens* (vol. 15), No. 5, pp. 517-23. URL: [http://www.ncbi.nlm.nih.gov/entrez/query.fcgi?cmd=Retrieve&db=PubMed&dopt=Citation&list\\_uids=16914965](http://www.ncbi.nlm.nih.gov/entrez/query.fcgi?cmd=Retrieve&db=PubMed&dopt=Citation&list_uids=16914965)
- Gimenez, I. and Forbush, B. (2003): Short-term stimulation of the renal Na-K-Cl cotransporter (NKCC2) by vasopressin involves phosphorylation and membrane translocation of the protein, *J Biol Chem* (vol. 278), No. 29, pp. 26946-51. URL: [http://www.ncbi.nlm.nih.gov/entrez/query.fcgi?cmd=Retrieve&db=PubMed&dopt=Citation&list\\_uids=12732642](http://www.ncbi.nlm.nih.gov/entrez/query.fcgi?cmd=Retrieve&db=PubMed&dopt=Citation&list_uids=12732642)
- Gimenez, I. and Forbush, B. (2005): Regulatory phosphorylation sites in the NH2 terminus of the renal Na-K-Cl cotransporter (NKCC2), *Am J Physiol Renal Physiol* (vol. 289), No. 6, pp. F1341-5. URL: [http://www.ncbi.nlm.nih.gov/entrez/query.fcgi?cmd=Retrieve&db=PubMed&dopt=Citation&list\\_uids=16077079](http://www.ncbi.nlm.nih.gov/entrez/query.fcgi?cmd=Retrieve&db=PubMed&dopt=Citation&list_uids=16077079)
- Gimenez, I.; Isenring, P. and Forbush, B. (2002): Spatially distributed alternative splice variants of the renal Na-K-Cl cotransporter exhibit dramatically different affinities for the transported ions, *J Biol Chem* (vol. 277), No. 11, pp. 8767-70. URL: [http://www.ncbi.nlm.nih.gov/entrez/query.fcgi?cmd=Retrieve&db=PubMed&dopt=Citation&list\\_uids=11815599](http://www.ncbi.nlm.nih.gov/entrez/query.fcgi?cmd=Retrieve&db=PubMed&dopt=Citation&list_uids=11815599)

- Goldstein, B. G.; Chao, H. H.; Yang, Y.; Yermolina, Y. A.; Tobias, J. W. and Katz, J. P. (2007): Overexpression of Kruppel-like factor 5 in esophageal epithelia in vivo leads to increased proliferation in basal but not suprabasal cells, *Am J Physiol Gastrointest Liver Physiol* (vol. 292), No. 6, pp. G1784-92. URL: [http://www.ncbi.nlm.nih.gov/entrez/query.fcgi?cmd=Retrieve&db=PubMed&dopt=Citation&list\\_uids=17395897](http://www.ncbi.nlm.nih.gov/entrez/query.fcgi?cmd=Retrieve&db=PubMed&dopt=Citation&list_uids=17395897)
- Goodarzi, M. O.; Lehman, D. M.; Taylor, K. D.; Guo, X.; Cui, J.; Quinones, M. J.; Clee, S. M.; Yandell, B. S.; Blangero, J.; Hsueh, W. A.; Attie, A. D.; Stern, M. P. and Rotter, J. I. (2007): SORCS1: a novel human type 2 diabetes susceptibility gene suggested by the mouse, *Diabetes* (vol. 56), No. 7, pp. 1922-9. URL: [http://www.ncbi.nlm.nih.gov/entrez/query.fcgi?cmd=Retrieve&db=PubMed&dopt=Citation&list\\_uids=17426289](http://www.ncbi.nlm.nih.gov/entrez/query.fcgi?cmd=Retrieve&db=PubMed&dopt=Citation&list_uids=17426289)
- Gross, V.; Tank, J.; Obst, M.; Plehm, R.; Blumer, K. J.; Diedrich, A.; Jordan, J. and Luft, F. C. (2005): Autonomic nervous system and blood pressure regulation in RGS2-deficient mice, *Am J Physiol Regul Integr Comp Physiol* (vol. 288), No. 5, pp. R1134-42. URL: [http://www.ncbi.nlm.nih.gov/entrez/query.fcgi?cmd=Retrieve&db=PubMed&dopt=Citation&list\\_uids=15661972](http://www.ncbi.nlm.nih.gov/entrez/query.fcgi?cmd=Retrieve&db=PubMed&dopt=Citation&list_uids=15661972)
- Grupe, A.; Li, Y.; Rowland, C.; Nowotny, P.; Hinrichs, A. L.; Smemo, S.; Kauwe, J. S.; Maxwell, T. J.; Cherny, S.; Doil, L.; Tacey, K.; van Luchene, R.; Myers, A.; Wavrant-De Vrieze, F.; Kaleem, M.; Hollingworth, P.; Jehu, L.; Foy, C.; Archer, N.; Hamilton, G.; Holmans, P.; Morris, C. M.; Catanese, J.; Sninsky, J.; White, T. J.; Powell, J.; Hardy, J.; O'Donovan, M.; Lovestone, S.; Jones, L.; Morris, J. C.; Thal, L.; Owen, M.; Williams, J. and Goate, A. (2006): A scan of chromosome 10 identifies a novel locus showing strong association with late-onset Alzheimer disease, *Am J Hum Genet* (vol. 78), No. 1, pp. 78-88. URL: [http://www.ncbi.nlm.nih.gov/entrez/query.fcgi?cmd=Retrieve&db=PubMed&dopt=Citation&list\\_uids=16385451](http://www.ncbi.nlm.nih.gov/entrez/query.fcgi?cmd=Retrieve&db=PubMed&dopt=Citation&list_uids=16385451)
- Haas, M. and Forbush, B., 3rd (1998): The Na-K-Cl cotransporters, *J Bioenerg Biomembr* (vol. 30), No. 2, pp. 161-72. URL: [http://www.ncbi.nlm.nih.gov/entrez/query.fcgi?cmd=Retrieve&db=PubMed&dopt=Citation&list\\_uids=9672238](http://www.ncbi.nlm.nih.gov/entrez/query.fcgi?cmd=Retrieve&db=PubMed&dopt=Citation&list_uids=9672238)
- Hallböök, F. (1999): Evolution of the vertebrate neurotrophin and Trk receptor gene families, *Curr Opin Neurobiol* (vol. 9), No. 5, pp. 616-21. URL: [http://www.ncbi.nlm.nih.gov/entrez/query.fcgi?cmd=Retrieve&db=PubMed&dopt=Citation&list\\_uids=10508739](http://www.ncbi.nlm.nih.gov/entrez/query.fcgi?cmd=Retrieve&db=PubMed&dopt=Citation&list_uids=10508739)
- Halperin, M. L.; Cheema-Dhadli, S.; Lin, S. H. and Kamel, K. S. (2006): Control of potassium excretion: a Paleolithic perspective, *Curr Opin Nephrol Hypertens* (vol. 15), No. 4, pp. 430-6. URL: [http://www.ncbi.nlm.nih.gov/entrez/query.fcgi?cmd=Retrieve&db=PubMed&dopt=Citation&list\\_uids=16775458](http://www.ncbi.nlm.nih.gov/entrez/query.fcgi?cmd=Retrieve&db=PubMed&dopt=Citation&list_uids=16775458)
- Hampe, W.; Rezgaoui, M.; Hermans-Borgmeyer, I. and Schaller, H. C. (2001): The genes for the human VPS10 domain-containing receptors are large and contain many small exons, *Hum Genet* (vol. 108), No. 6, pp. 529-36. URL: [http://www.ncbi.nlm.nih.gov/entrez/query.fcgi?cmd=Retrieve&db=PubMed&dopt=Citation&list\\_uids=11499680](http://www.ncbi.nlm.nih.gov/entrez/query.fcgi?cmd=Retrieve&db=PubMed&dopt=Citation&list_uids=11499680)

- Hampe, W.; Riedel, I. B.; Lintzel, J.; Bader, C. O.; Franke, I. and Schaller, H. C. (2000): Ectodomain shedding, translocation and synthesis of SorLA are stimulated by its ligand head activator, *J Cell Sci* (vol. 113 Pt 24), pp. 4475-85. URL: [http://www.ncbi.nlm.nih.gov/entrez/query.fcgi?cmd=Retrieve&db=PubMed&dopt=Citation&list\\_uids=11082041](http://www.ncbi.nlm.nih.gov/entrez/query.fcgi?cmd=Retrieve&db=PubMed&dopt=Citation&list_uids=11082041)
- Hampe, W.; Urny, J.; Franke, I.; Hoffmeister-Ullerich, S. A.; Herrmann, D.; Petersen, C. M.; Lohmann, J. and Schaller, H. C. (1999): A head-activator binding protein is present in hydra in a soluble and a membrane-anchored form, *Development* (vol. 126), No. 18, pp. 4077-86. URL: [http://www.ncbi.nlm.nih.gov/entrez/query.fcgi?cmd=Retrieve&db=PubMed&dopt=Citation&list\\_uids=10457016](http://www.ncbi.nlm.nih.gov/entrez/query.fcgi?cmd=Retrieve&db=PubMed&dopt=Citation&list_uids=10457016)
- Harrington, A. W.; Leiner, B.; Blechschmitt, C.; Arevalo, J. C.; Lee, R.; Morl, K.; Meyer, M.; Hempstead, B. L.; Yoon, S. O. and Giehl, K. M. (2004): Secreted proNGF is a pathological death-inducing ligand after adult CNS injury, *Proc Natl Acad Sci U S A* (vol. 101), No. 16, pp. 6226-30. URL: [http://www.ncbi.nlm.nih.gov/entrez/query.fcgi?cmd=Retrieve&db=PubMed&dopt=Citation&list\\_uids=15026568](http://www.ncbi.nlm.nih.gov/entrez/query.fcgi?cmd=Retrieve&db=PubMed&dopt=Citation&list_uids=15026568)
- Hassan, A. J.; Zeng, J.; Ni, X. and Morales, C. R. (2004): The trafficking of prosaposin (SGP-1) and GM(2)AP to the lysosomes of TM4 sertoli cells is mediated by sortilin and monomeric adaptor proteins, *Mol Reprod Dev* (vol. 68), No. 4, pp. 476-83. URL: [http://www.ncbi.nlm.nih.gov/entrez/query.fcgi?cmd=Retrieve&db=PubMed&dopt=Citation&list\\_uids=15236333](http://www.ncbi.nlm.nih.gov/entrez/query.fcgi?cmd=Retrieve&db=PubMed&dopt=Citation&list_uids=15236333)
- Hauser, F.; Nothacker, H. P. and Grimmelikhuijzen, C. J. (1997): Molecular cloning, genomic organization, and developmental regulation of a novel receptor from *Drosophila melanogaster* structurally related to members of the thyroid-stimulating hormone, follicle-stimulating hormone, luteinizing hormone/choriogonadotropin receptor family from mammals, *J Biol Chem* (vol. 272), No. 2, pp. 1002-10. URL: [http://www.ncbi.nlm.nih.gov/entrez/query.fcgi?cmd=Retrieve&db=PubMed&dopt=Citation&list\\_uids=8995395](http://www.ncbi.nlm.nih.gov/entrez/query.fcgi?cmd=Retrieve&db=PubMed&dopt=Citation&list_uids=8995395)
- Hermans-Borgmeyer, I.; Hampe, W.; Schinke, B.; Methner, A.; Nykjaer, A.; Susens, U.; Fenger, U.; Herbarth, B. and Schaller, H. C. (1998): Unique expression pattern of a novel mosaic receptor in the developing cerebral cortex, *Mech Dev* (vol. 70), No. 1-2, pp. 65-76. URL: [http://www.ncbi.nlm.nih.gov/entrez/query.fcgi?cmd=Retrieve&db=PubMed&dopt=Citation&list\\_uids=9510025](http://www.ncbi.nlm.nih.gov/entrez/query.fcgi?cmd=Retrieve&db=PubMed&dopt=Citation&list_uids=9510025)
- Hermans-Borgmeyer, I.; Hermey, G.; Nykjaer, A. and Schaller, C. (1999): Expression of the 100-kDa neurotensin receptor sortilin during mouse embryonal development, *Brain Res Mol Brain Res* (vol. 65), No. 2, pp. 216-9. URL: [http://www.ncbi.nlm.nih.gov/entrez/query.fcgi?cmd=Retrieve&db=PubMed&dopt=Citation&list\\_uids=10064893](http://www.ncbi.nlm.nih.gov/entrez/query.fcgi?cmd=Retrieve&db=PubMed&dopt=Citation&list_uids=10064893)
- Hermey, G.; Keat, S. J.; Madsen, P.; Jacobsen, C.; Petersen, C. M. and Gliemann, J. (2003): Characterization of sorCS1, an alternatively spliced receptor with completely different cytoplasmic domains that mediate different trafficking in cells, *J Biol Chem* (vol. 278), No. 9, pp. 7390-6. URL: [http://www.ncbi.nlm.nih.gov/entrez/query.fcgi?cmd=Retrieve&db=PubMed&dopt=Citation&list\\_uids=12482870](http://www.ncbi.nlm.nih.gov/entrez/query.fcgi?cmd=Retrieve&db=PubMed&dopt=Citation&list_uids=12482870)

- Hermey, G.; Plath, N.; Hubner, C. A.; Kuhl, D.; Schaller, H. C. and Hermans-Borgmeyer, I. (2004): The three sorCS genes are differentially expressed and regulated by synaptic activity, *J Neurochem* (vol. 88), No. 6, pp. 1470-6. URL: [http://www.ncbi.nlm.nih.gov/entrez/query.fcgi?cmd=Retrieve&db=PubMed&dopt=Citation&list\\_uids=15009648](http://www.ncbi.nlm.nih.gov/entrez/query.fcgi?cmd=Retrieve&db=PubMed&dopt=Citation&list_uids=15009648)
- Hermey, G.; Riedel, I. B.; Hampe, W.; Schaller, H. C. and Hermans-Borgmeyer, I. (1999): Identification and characterization of SorCS, a third member of a novel receptor family, *Biochem Biophys Res Commun* (vol. 266), No. 2, pp. 347-51. URL: [http://www.ncbi.nlm.nih.gov/entrez/query.fcgi?cmd=Retrieve&db=PubMed&dopt=Citation&list\\_uids=10600506](http://www.ncbi.nlm.nih.gov/entrez/query.fcgi?cmd=Retrieve&db=PubMed&dopt=Citation&list_uids=10600506)
- Hermey, G.; Riedel, I. B.; Rezgaoui, M.; Westergaard, U. B.; Schaller, C. and Hermans-Borgmeyer, I. (2001): SorCS1, a member of the novel sorting receptor family, is localized in somata and dendrites of neurons throughout the murine brain, *Neurosci Lett* (vol. 313), No. 1-2, pp. 83-7. URL: [http://www.ncbi.nlm.nih.gov/entrez/query.fcgi?cmd=Retrieve&db=PubMed&dopt=Citation&list\\_uids=11684345](http://www.ncbi.nlm.nih.gov/entrez/query.fcgi?cmd=Retrieve&db=PubMed&dopt=Citation&list_uids=11684345)
- Hermey, G. and Schaller, H. C. (2000): Alternative splicing of murine SorCS leads to two forms of the receptor that differ completely in their cytoplasmic tails, *Biochim Biophys Acta* (vol. 1491), No. 1-3, pp. 350-4. URL: [http://www.ncbi.nlm.nih.gov/entrez/query.fcgi?cmd=Retrieve&db=PubMed&dopt=Citation&list\\_uids=10760602](http://www.ncbi.nlm.nih.gov/entrez/query.fcgi?cmd=Retrieve&db=PubMed&dopt=Citation&list_uids=10760602)
- Hermey, G.; Schaller, H. C. and Hermans-Borgmeyer, I. (2001): Transient expression of SorCS in developing telencephalic and mesencephalic structures of the mouse, *Neuroreport* (vol. 12), No. 1, pp. 29-32. URL: [http://www.ncbi.nlm.nih.gov/entrez/query.fcgi?cmd=Retrieve&db=PubMed&dopt=Citation&list\\_uids=11201086](http://www.ncbi.nlm.nih.gov/entrez/query.fcgi?cmd=Retrieve&db=PubMed&dopt=Citation&list_uids=11201086)
- Hermey, G.; Sjogaard, S. S.; Petersen, C. M.; Nykjaer, A. and Gliemann, J. (2006): Tumour necrosis factor alpha-converting enzyme mediates ectodomain shedding of Vps10p-domain receptor family members, *Biochem J* (vol. 395), No. 2, pp. 285-93. URL: [http://www.ncbi.nlm.nih.gov/entrez/query.fcgi?cmd=Retrieve&db=PubMed&dopt=Citation&list\\_uids=16393139](http://www.ncbi.nlm.nih.gov/entrez/query.fcgi?cmd=Retrieve&db=PubMed&dopt=Citation&list_uids=16393139)
- Hoffman-Goetz, L.; Quadrilatero, J.; Boudreau, J. and Guan, J. (2004): Adrenalectomy in mice does not prevent loss of intestinal lymphocytes after exercise, *J Appl Physiol* (vol. 96), No. 6, pp. 2073-81. URL: [http://www.ncbi.nlm.nih.gov/entrez/query.fcgi?cmd=Retrieve&db=PubMed&dopt=Citation&list\\_uids=15133013](http://www.ncbi.nlm.nih.gov/entrez/query.fcgi?cmd=Retrieve&db=PubMed&dopt=Citation&list_uids=15133013)
- Holman, G. D. and Sandoval, I. V. (2001): Moving the insulin-regulated glucose transporter GLUT4 into and out of storage, *Trends Cell Biol* (vol. 11), No. 4, pp. 173-9. URL: [http://www.ncbi.nlm.nih.gov/entrez/query.fcgi?cmd=Retrieve&db=PubMed&dopt=Citation&list\\_uids=11306298](http://www.ncbi.nlm.nih.gov/entrez/query.fcgi?cmd=Retrieve&db=PubMed&dopt=Citation&list_uids=11306298)
- Hou, J. C.; Suzuki, N.; Pessin, J. E. and Watson, R. T. (2006): A specific dileucine motif is required for the GGA-dependent entry of newly synthesized insulin-responsive aminopeptidase into the insulin-responsive compartment, *J Biol Chem* (vol. 281), No. 44, pp. 33457-66. URL:

- [http://www.ncbi.nlm.nih.gov/entrez/query.fcgi?cmd=Retrieve&db=PubMed&dopt=Citation&list\\_uids=16945927](http://www.ncbi.nlm.nih.gov/entrez/query.fcgi?cmd=Retrieve&db=PubMed&dopt=Citation&list_uids=16945927)
- Irizarry, R. A.; Hobbs, B.; Collin, F.; Beazer-Barclay, Y. D.; Antonellis, K. J.; Scherf, U. and Speed, T. P. (2003): Exploration, normalization, and summaries of high density oligonucleotide array probe level data, *Biostatistics* (vol. 4), No. 2, pp. 249-64. URL: [http://www.ncbi.nlm.nih.gov/entrez/query.fcgi?cmd=Retrieve&db=PubMed&dopt=Citation&list\\_uids=12925520](http://www.ncbi.nlm.nih.gov/entrez/query.fcgi?cmd=Retrieve&db=PubMed&dopt=Citation&list_uids=12925520)
- Jacobsen, L.; Madsen, P.; Jacobsen, C.; Nielsen, M. S.; Gliemann, J. and Petersen, C. M. (2001): Activation and functional characterization of the mosaic receptor SorLA/LR11, *J Biol Chem* (vol. 276), No. 25, pp. 22788-96. URL: [http://www.ncbi.nlm.nih.gov/entrez/query.fcgi?cmd=Retrieve&db=PubMed&dopt=Citation&list\\_uids=11294867](http://www.ncbi.nlm.nih.gov/entrez/query.fcgi?cmd=Retrieve&db=PubMed&dopt=Citation&list_uids=11294867)
- Jacobsen, L.; Madsen, P.; Moestrup, S. K.; Lund, A. H.; Tommerup, N.; Nykjaer, A.; Sottrup-Jensen, L.; Gliemann, J. and Petersen, C. M. (1996): Molecular characterization of a novel human hybrid-type receptor that binds the alpha2-macroglobulin receptor-associated protein, *J Biol Chem* (vol. 271), No. 49, pp. 31379-83. URL: [http://www.ncbi.nlm.nih.gov/entrez/query.fcgi?cmd=Retrieve&db=PubMed&dopt=Citation&list\\_uids=8940146](http://www.ncbi.nlm.nih.gov/entrez/query.fcgi?cmd=Retrieve&db=PubMed&dopt=Citation&list_uids=8940146)
- Jacobsen, L.; Madsen, P.; Nielsen, M. S.; Geraerts, W. P.; Gliemann, J.; Smit, A. B. and Petersen, C. M. (2002): The sorLA cytoplasmic domain interacts with GGA1 and -2 and defines minimum requirements for GGA binding, *FEBS Lett* (vol. 511), No. 1-3, pp. 155-8. URL: [http://www.ncbi.nlm.nih.gov/entrez/query.fcgi?cmd=Retrieve&db=PubMed&dopt=Citation&list\\_uids=11821067](http://www.ncbi.nlm.nih.gov/entrez/query.fcgi?cmd=Retrieve&db=PubMed&dopt=Citation&list_uids=11821067)
- Jansen, P.; Giehl, K.; Nyengaard, J. R.; Teng, K.; Liubinski, O.; Sjoegaard, S. S.; Breiderhoff, T.; Gotthardt, M.; Lin, F.; Eilers, A.; Petersen, C. M.; Lewin, G. R.; Hempstead, B. L.; Willnow, T. E. and Nykjaer, A. (2007): Roles for the pro-neurotrophin receptor sortilin in neuronal development, aging and brain injury, *Nat Neurosci* (vol. 10), No. 11, pp. 1449-57. URL: [http://www.ncbi.nlm.nih.gov/entrez/query.fcgi?cmd=Retrieve&db=PubMed&dopt=Citation&list\\_uids=17934455](http://www.ncbi.nlm.nih.gov/entrez/query.fcgi?cmd=Retrieve&db=PubMed&dopt=Citation&list_uids=17934455)
- Jiang, M.; Bujo, H.; Ohwaki, K.; Unoki, H.; Yamazaki, H.; Kanaki, T.; Shibasaki, M.; Azuma, K.; Harigaya, K.; Schneider, W. J. and Saito, Y. (2008): Ang II-stimulated migration of vascular smooth muscle cells is dependent on LR11 in mice, *J Clin Invest* (vol. 118), No. 8, pp. 2733-46. URL: [http://www.ncbi.nlm.nih.gov/entrez/query.fcgi?cmd=Retrieve&db=PubMed&dopt=Citation&list\\_uids=18618022](http://www.ncbi.nlm.nih.gov/entrez/query.fcgi?cmd=Retrieve&db=PubMed&dopt=Citation&list_uids=18618022)
- Jiang, X.; Dreano, M.; Buckler, D. R.; Cheng, S.; Ythier, A.; Wu, H.; Hendrickson, W. A. and el Tayar, N. (1995): Structural predictions for the ligand-binding region of glycoprotein hormone receptors and the nature of hormone-receptor interactions, *Structure* (vol. 3), No. 12, pp. 1341-53. URL: [http://www.ncbi.nlm.nih.gov/entrez/query.fcgi?cmd=Retrieve&db=PubMed&dopt=Citation&list\\_uids=8747461](http://www.ncbi.nlm.nih.gov/entrez/query.fcgi?cmd=Retrieve&db=PubMed&dopt=Citation&list_uids=8747461)
- Kahle, K. T.; Wilson, F. H.; Leng, Q.; Lalioti, M. D.; O'Connell, A. D.; Dong, K.; Rapson, A. K.; MacGregor, G. G.; Giebisch, G.; Hebert, S. C. and Lifton, R. P. (2003): WNK4 regulates



- the balance between renal NaCl reabsorption and K<sup>+</sup> secretion, *Nat Genet* (vol. 35), No. 4, pp. 372-6. URL:  
[http://www.ncbi.nlm.nih.gov/entrez/query.fcgi?cmd=Retrieve&db=PubMed&dopt=Citation&list\\_uids=14608358](http://www.ncbi.nlm.nih.gov/entrez/query.fcgi?cmd=Retrieve&db=PubMed&dopt=Citation&list_uids=14608358)
- Kajava, A. V.; Vassart, G. and Wodak, S. J. (1995): Modeling of the three-dimensional structure of proteins with the typical leucine-rich repeats, *Structure* (vol. 3), No. 9, pp. 867-77. URL:  
[http://www.ncbi.nlm.nih.gov/entrez/query.fcgi?cmd=Retrieve&db=PubMed&dopt=Citation&list\\_uids=8535781](http://www.ncbi.nlm.nih.gov/entrez/query.fcgi?cmd=Retrieve&db=PubMed&dopt=Citation&list_uids=8535781)
- Keidar, S.; Gamliel-Lazarovich, A.; Kaplan, M.; Pavlotzky, E.; Hamoud, S.; Hayek, T.; Karry, R. and Abassi, Z. (2005): Mineralocorticoid receptor blocker increases angiotensin-converting enzyme 2 activity in congestive heart failure patients, *Circ Res* (vol. 97), No. 9, pp. 946-53. URL:  
[http://www.ncbi.nlm.nih.gov/entrez/query.fcgi?cmd=Retrieve&db=PubMed&dopt=Citation&list\\_uids=16179584](http://www.ncbi.nlm.nih.gov/entrez/query.fcgi?cmd=Retrieve&db=PubMed&dopt=Citation&list_uids=16179584)
- Kikeri, D.; Azar, S.; Sun, A.; Zeidel, M. L. and Hebert, S. C. (1990): Na<sup>(+)</sup>-H<sup>+</sup> antiporter and Na<sup>(+)</sup>-(HCO<sub>3</sub><sup>-</sup>)<sub>n</sub> symporter regulate intracellular pH in mouse medullary thick limbs of Henle, *Am J Physiol* (vol. 258), No. 3 Pt 2, pp. F445-56. URL:  
[http://www.ncbi.nlm.nih.gov/entrez/query.fcgi?cmd=Retrieve&db=PubMed&dopt=Citation&list\\_uids=2156445](http://www.ncbi.nlm.nih.gov/entrez/query.fcgi?cmd=Retrieve&db=PubMed&dopt=Citation&list_uids=2156445)
- Kikuno, R.; Nagase, T.; Ishikawa, K.; Hirosawa, M.; Miyajima, N.; Tanaka, A.; Kotani, H.; Nomura, N. and Ohara, O. (1999): Prediction of the coding sequences of unidentified human genes. XIV. The complete sequences of 100 new cDNA clones from brain which code for large proteins in vitro, *DNA Res* (vol. 6), No. 3, pp. 197-205. URL:  
[http://www.ncbi.nlm.nih.gov/entrez/query.fcgi?cmd=Retrieve&db=PubMed&dopt=Citation&list\\_uids=10470851](http://www.ncbi.nlm.nih.gov/entrez/query.fcgi?cmd=Retrieve&db=PubMed&dopt=Citation&list_uids=10470851)
- King, G. D. and Scott Turner, R. (2004): Adaptor protein interactions: modulators of amyloid precursor protein metabolism and Alzheimer's disease risk?, *Exp Neurol* (vol. 185), No. 2, pp. 208-19. URL:  
[http://www.ncbi.nlm.nih.gov/entrez/query.fcgi?cmd=Retrieve&db=PubMed&dopt=Citation&list\\_uids=14736502](http://www.ncbi.nlm.nih.gov/entrez/query.fcgi?cmd=Retrieve&db=PubMed&dopt=Citation&list_uids=14736502)
- Kobayashi, K.; Uchida, S.; Okamura, H. O.; Marumo, F. and Sasaki, S. (2002): Human CLC-KB gene promoter drives the EGFP expression in the specific distal nephron segments and inner ear, *J Am Soc Nephrol* (vol. 13), No. 8, pp. 1992-8. URL:  
[http://www.ncbi.nlm.nih.gov/entrez/query.fcgi?cmd=Retrieve&db=PubMed&dopt=Citation&list\\_uids=12138129](http://www.ncbi.nlm.nih.gov/entrez/query.fcgi?cmd=Retrieve&db=PubMed&dopt=Citation&list_uids=12138129)
- Kobe, B. and Deisenhofer, J. (1995): A structural basis of the interactions between leucine-rich repeats and protein ligands, *Nature* (vol. 374), No. 6518, pp. 183-6. URL:  
[http://www.ncbi.nlm.nih.gov/entrez/query.fcgi?cmd=Retrieve&db=PubMed&dopt=Citation&list\\_uids=7877692](http://www.ncbi.nlm.nih.gov/entrez/query.fcgi?cmd=Retrieve&db=PubMed&dopt=Citation&list_uids=7877692)
- Kornfeld, S. (1992): Structure and function of the mannose 6-phosphate/insulinlike growth factor II receptors, *Annu Rev Biochem* (vol. 61), pp. 307-30. URL:  
[http://www.ncbi.nlm.nih.gov/entrez/query.fcgi?cmd=Retrieve&db=PubMed&dopt=Citation&list\\_uids=1323236](http://www.ncbi.nlm.nih.gov/entrez/query.fcgi?cmd=Retrieve&db=PubMed&dopt=Citation&list_uids=1323236)



- Krishna, G. G.; Miller, E. and Kapoor, S. (1989): Increased blood pressure during potassium depletion in normotensive men, *N Engl J Med* (vol. 320), No. 18, pp. 1177-82. URL: [http://www.ncbi.nlm.nih.gov/entrez/query.fcgi?cmd=Retrieve&db=PubMed&dopt=Citation&list\\_uids=2624617](http://www.ncbi.nlm.nih.gov/entrez/query.fcgi?cmd=Retrieve&db=PubMed&dopt=Citation&list_uids=2624617)
- Lapointe, J. Y.; Bell, P. D. and Cardinal, J. (1990): Direct evidence for apical Na<sup>+</sup>:2Cl<sup>-</sup>:K<sup>+</sup> co-transport in macula densa cells, *Am J Physiol* (vol. 258), No. 5 Pt 2, pp. F1466-9. URL: [http://www.ncbi.nlm.nih.gov/entrez/query.fcgi?cmd=Retrieve&db=PubMed&dopt=Citation&list\\_uids=2337159](http://www.ncbi.nlm.nih.gov/entrez/query.fcgi?cmd=Retrieve&db=PubMed&dopt=Citation&list_uids=2337159)
- Lee, R.; Kermani, P.; Teng, K. K. and Hempstead, B. L. (2001): Regulation of cell survival by secreted proneurotrophins, *Science* (vol. 294), No. 5548, pp. 1945-8. URL: [http://www.ncbi.nlm.nih.gov/entrez/query.fcgi?cmd=Retrieve&db=PubMed&dopt=Citation&list\\_uids=11729324](http://www.ncbi.nlm.nih.gov/entrez/query.fcgi?cmd=Retrieve&db=PubMed&dopt=Citation&list_uids=11729324)
- Lefrancois, S.; Zeng, J.; Hassan, A. J.; Canuel, M. and Morales, C. R. (2003): The lysosomal trafficking of sphingolipid activator proteins (SAPs) is mediated by sortilin, *Embo J* (vol. 22), No. 24, pp. 6430-7. URL: [http://www.ncbi.nlm.nih.gov/entrez/query.fcgi?cmd=Retrieve&db=PubMed&dopt=Citation&list\\_uids=14657016](http://www.ncbi.nlm.nih.gov/entrez/query.fcgi?cmd=Retrieve&db=PubMed&dopt=Citation&list_uids=14657016)
- Lewin, G. R. and Barde, Y. A. (1996): Physiology of the neurotrophins, *Annu Rev Neurosci* (vol. 19), pp. 289-317. URL: [http://www.ncbi.nlm.nih.gov/entrez/query.fcgi?cmd=Retrieve&db=PubMed&dopt=Citation&list\\_uids=8833445](http://www.ncbi.nlm.nih.gov/entrez/query.fcgi?cmd=Retrieve&db=PubMed&dopt=Citation&list_uids=8833445)
- Li, L. V. and Kandror, K. V. (2005): Golgi-localized, gamma-ear-containing, Arf-binding protein adaptors mediate insulin-responsive trafficking of glucose transporter 4 in 3T3-L1 adipocytes, *Mol Endocrinol* (vol. 19), No. 8, pp. 2145-53. URL: [http://www.ncbi.nlm.nih.gov/entrez/query.fcgi?cmd=Retrieve&db=PubMed&dopt=Citation&list\\_uids=15774496](http://www.ncbi.nlm.nih.gov/entrez/query.fcgi?cmd=Retrieve&db=PubMed&dopt=Citation&list_uids=15774496)
- Lorenz, J. N.; Weihprecht, H.; Schnermann, J.; Skott, O. and Briggs, J. P. (1991): Renin release from isolated juxtaglomerular apparatus depends on macula densa chloride transport, *Am J Physiol* (vol. 260), No. 4 Pt 2, pp. F486-93. URL: [http://www.ncbi.nlm.nih.gov/entrez/query.fcgi?cmd=Retrieve&db=PubMed&dopt=Citation&list\\_uids=2012204](http://www.ncbi.nlm.nih.gov/entrez/query.fcgi?cmd=Retrieve&db=PubMed&dopt=Citation&list_uids=2012204)
- Marcusson, E. G.; Horazdovsky, B. F.; Cereghino, J. L.; Gharakhanian, E. and Emr, S. D. (1994): The sorting receptor for yeast vacuolar carboxypeptidase Y is encoded by the VPS10 gene, *Cell* (vol. 77), No. 4, pp. 579-86. URL: [http://www.ncbi.nlm.nih.gov/entrez/query.fcgi?cmd=Retrieve&db=PubMed&dopt=Citation&list\\_uids=8187177](http://www.ncbi.nlm.nih.gov/entrez/query.fcgi?cmd=Retrieve&db=PubMed&dopt=Citation&list_uids=8187177)
- Mari, M.; Bujny, M. V.; Zeuschner, D.; Geerts, W. J.; Griffith, J.; Petersen, C. M.; Cullen, P. J.; Klumperman, J. and Geuze, H. J. (2008): SNX1 defines an early endosomal recycling exit for sortilin and mannose 6-phosphate receptors, *Traffic* (vol. 9), No. 3, pp. 380-93. URL: [http://www.ncbi.nlm.nih.gov/entrez/query.fcgi?cmd=Retrieve&db=PubMed&dopt=Citation&list\\_uids=18088323](http://www.ncbi.nlm.nih.gov/entrez/query.fcgi?cmd=Retrieve&db=PubMed&dopt=Citation&list_uids=18088323)

- Matsuo, M.; Ebinuma, H.; Fukamachi, I.; Jiang, M.; Bujo, H. and Saito, Y. (2009): Development of an immunoassay for the quantification of soluble LR11, a circulating marker of atherosclerosis, *Clin Chem* (vol. 55), No. 10, pp. 1801-8. URL: [http://www.ncbi.nlm.nih.gov/entrez/query.fcgi?cmd=Retrieve&db=PubMed&dopt=Citation&list\\_uids=19661140](http://www.ncbi.nlm.nih.gov/entrez/query.fcgi?cmd=Retrieve&db=PubMed&dopt=Citation&list_uids=19661140)
- Mazella, J.; Zsuger, N.; Navarro, V.; Chabry, J.; Kaghad, M.; Caput, D.; Ferrara, P.; Vita, N.; Gully, D.; Maffrand, J. P. and Vincent, J. P. (1998): The 100-kDa neurotensin receptor is gp95/sortilin, a non-G-protein-coupled receptor, *J Biol Chem* (vol. 273), No. 41, pp. 26273-6. URL: [http://www.ncbi.nlm.nih.gov/entrez/query.fcgi?cmd=Retrieve&db=PubMed&dopt=Citation&list\\_uids=9756851](http://www.ncbi.nlm.nih.gov/entrez/query.fcgi?cmd=Retrieve&db=PubMed&dopt=Citation&list_uids=9756851)
- Meneton, P.; Loffing, J. and Warnock, D. G. (2004): Sodium and potassium handling by the aldosterone-sensitive distal nephron: the pivotal role of the distal and connecting tubule, *Am J Physiol Renal Physiol* (vol. 287), No. 4, pp. F593-601. URL: [http://www.ncbi.nlm.nih.gov/entrez/query.fcgi?cmd=Retrieve&db=PubMed&dopt=Citation&list\\_uids=15345493](http://www.ncbi.nlm.nih.gov/entrez/query.fcgi?cmd=Retrieve&db=PubMed&dopt=Citation&list_uids=15345493)
- Mitchell, K. J.; Pinson, K. I.; Kelly, O. G.; Brennan, J.; Zupicich, J.; Scherz, P.; Leighton, P. A.; Goodrich, L. V.; Lu, X.; Avery, B. J.; Tate, P.; Dill, K.; Pangilinan, E.; Wakenight, P.; Tessier-Lavigne, M. and Skarnes, W. C. (2001): Functional analysis of secreted and transmembrane proteins critical to mouse development, *Nat Genet* (vol. 28), No. 3, pp. 241-9. URL: [http://www.ncbi.nlm.nih.gov/entrez/query.fcgi?cmd=Retrieve&db=PubMed&dopt=Citation&list\\_uids=11431694](http://www.ncbi.nlm.nih.gov/entrez/query.fcgi?cmd=Retrieve&db=PubMed&dopt=Citation&list_uids=11431694)
- Mohapel, P.; Frielingsdorf, H.; Haggblad, J.; Zachrisson, O. and Brundin, P. (2005): Platelet-derived growth factor (PDGF-BB) and brain-derived neurotrophic factor (BDNF) induce striatal neurogenesis in adult rats with 6-hydroxydopamine lesions, *Neuroscience* (vol. 132), No. 3, pp. 767-76. URL: [http://www.ncbi.nlm.nih.gov/entrez/query.fcgi?cmd=Retrieve&db=PubMed&dopt=Citation&list\\_uids=15837137](http://www.ncbi.nlm.nih.gov/entrez/query.fcgi?cmd=Retrieve&db=PubMed&dopt=Citation&list_uids=15837137)
- Molony, D. A.; Reeves, W. B.; Hebert, S. C. and Andreoli, T. E. (1987): ADH increases apical Na<sup>+</sup>, K<sup>+</sup>, 2Cl<sup>-</sup> entry in mouse medullary thick ascending limbs of Henle, *Am J Physiol* (vol. 252), No. 1 Pt 2, pp. F177-87. URL: [http://www.ncbi.nlm.nih.gov/entrez/query.fcgi?cmd=Retrieve&db=PubMed&dopt=Citation&list\\_uids=3812700](http://www.ncbi.nlm.nih.gov/entrez/query.fcgi?cmd=Retrieve&db=PubMed&dopt=Citation&list_uids=3812700)
- Moriguchi, T.; Urushiyama, S.; Hisamoto, N.; Iemura, S.; Uchida, S.; Natsume, T.; Matsumoto, K. and Shibuya, H. (2005): WNK1 regulates phosphorylation of cation-chloride-coupled co-transporters via the STE20-related kinases, SPAK and OSR1, *J Biol Chem* (vol. 280), No. 52, pp. 42685-93. URL: [http://www.ncbi.nlm.nih.gov/entrez/query.fcgi?cmd=Retrieve&db=PubMed&dopt=Citation&list\\_uids=16263722](http://www.ncbi.nlm.nih.gov/entrez/query.fcgi?cmd=Retrieve&db=PubMed&dopt=Citation&list_uids=16263722)
- Morinville, A.; Martin, S.; Lavalley, M.; Vincent, J. P.; Beaudet, A. and Mazella, J. (2004): Internalization and trafficking of neurotensin via NTS3 receptors in HT29 cells, *Int J Biochem Cell Biol* (vol. 36), No. 11, pp. 2153-68. URL: [http://www.ncbi.nlm.nih.gov/entrez/query.fcgi?cmd=Retrieve&db=PubMed&dopt=Citation&list\\_uids=15313463](http://www.ncbi.nlm.nih.gov/entrez/query.fcgi?cmd=Retrieve&db=PubMed&dopt=Citation&list_uids=15313463)

- Morris, N. J.; Ross, S. A.; Lane, W. S.; Moestrup, S. K.; Petersen, C. M.; Keller, S. R. and Lienhard, G. E. (1998): Sortilin is the major 110-kDa protein in GLUT4 vesicles from adipocytes, *J Biol Chem* (vol. 273), No. 6, pp. 3582-7. URL:  
[http://www.ncbi.nlm.nih.gov/entrez/query.fcgi?cmd=Retrieve&db=PubMed&dopt=Citation&list\\_uids=9452485](http://www.ncbi.nlm.nih.gov/entrez/query.fcgi?cmd=Retrieve&db=PubMed&dopt=Citation&list_uids=9452485)
- Mörwald, S.; Yamazaki, H.; Bujo, H.; Kusunoki, J.; Kanaki, T.; Seimiya, K.; Morisaki, N.; Nimpf, J.; Schneider, W. J. and Saito, Y. (1997): A novel mosaic protein containing LDL receptor elements is highly conserved in humans and chickens, *Arterioscler Thromb Vasc Biol* (vol. 17), No. 5, pp. 996-1002. URL:  
[http://www.ncbi.nlm.nih.gov/entrez/query.fcgi?cmd=Retrieve&db=PubMed&dopt=Citation&list\\_uids=9157966](http://www.ncbi.nlm.nih.gov/entrez/query.fcgi?cmd=Retrieve&db=PubMed&dopt=Citation&list_uids=9157966)
- Motoi, Y.; Aizawa, T.; Haga, S.; Nakamura, S.; Namba, Y. and Ikeda, K. (1999): Neuronal localization of a novel mosaic apolipoprotein E receptor, LR11, in rat and human brain, *Brain Res* (vol. 833), No. 2, pp. 209-15. URL:  
[http://www.ncbi.nlm.nih.gov/entrez/query.fcgi?cmd=Retrieve&db=PubMed&dopt=Citation&list\\_uids=10375696](http://www.ncbi.nlm.nih.gov/entrez/query.fcgi?cmd=Retrieve&db=PubMed&dopt=Citation&list_uids=10375696)
- Muhammad, A.; Flores, I.; Zhang, H.; Yu, R.; Staniszewski, A.; Planel, E.; Herman, M.; Ho, L.; Kreber, R.; Honig, L. S.; Ganetzky, B.; Duff, K.; Arancio, O. and Small, S. A. (2008): Retromer deficiency observed in Alzheimer's disease causes hippocampal dysfunction, neurodegeneration, and Abeta accumulation, *Proc Natl Acad Sci U S A* (vol. 105), No. 20, pp. 7327-32. URL:  
[http://www.ncbi.nlm.nih.gov/entrez/query.fcgi?cmd=Retrieve&db=PubMed&dopt=Citation&list\\_uids=18480253](http://www.ncbi.nlm.nih.gov/entrez/query.fcgi?cmd=Retrieve&db=PubMed&dopt=Citation&list_uids=18480253)
- Munck Petersen, C.; Nielsen, M. S.; Jacobsen, C.; Tauris, J.; Jacobsen, L.; Gliemann, J.; Moestrup, S. K. and Madsen, P. (1999): Propeptide cleavage conditions sortilin/neurotensin receptor-3 for ligand binding, *Embo J* (vol. 18), No. 3, pp. 595-604. URL:  
[http://www.ncbi.nlm.nih.gov/entrez/query.fcgi?cmd=Retrieve&db=PubMed&dopt=Citation&list\\_uids=9927419](http://www.ncbi.nlm.nih.gov/entrez/query.fcgi?cmd=Retrieve&db=PubMed&dopt=Citation&list_uids=9927419)
- Nagase, T.; Kikuno, R.; Ishikawa, K. I.; Hirosawa, M. and Ohara, O. (2000): Prediction of the coding sequences of unidentified human genes. XVI. The complete sequences of 150 new cDNA clones from brain which code for large proteins in vitro, *DNA Res* (vol. 7), No. 1, pp. 65-73. URL:  
[http://www.ncbi.nlm.nih.gov/entrez/query.fcgi?cmd=Retrieve&db=PubMed&dopt=Citation&list\\_uids=10718198](http://www.ncbi.nlm.nih.gov/entrez/query.fcgi?cmd=Retrieve&db=PubMed&dopt=Citation&list_uids=10718198)
- Nakamura, K.; Namekata, K.; Harada, C. and Harada, T. (2007): Intracellular sortilin expression pattern regulates proNGF-induced naturally occurring cell death during development, *Cell Death Differ* (vol. 14), No. 8, pp. 1552-4. URL:  
[http://www.ncbi.nlm.nih.gov/entrez/query.fcgi?cmd=Retrieve&db=PubMed&dopt=Citation&list\\_uids=17541425](http://www.ncbi.nlm.nih.gov/entrez/query.fcgi?cmd=Retrieve&db=PubMed&dopt=Citation&list_uids=17541425)
- Navarro, V.; Martin, S.; Sarret, P.; Nielsen, M. S.; Petersen, C. M.; Vincent, J. and Mazella, J. (2001): Pharmacological properties of the mouse neurotensin receptor 3. Maintenance of cell surface receptor during internalization of neurotensin, *FEBS Lett* (vol. 495), No. 1-2, pp. 100-5. URL:  
[http://www.ncbi.nlm.nih.gov/entrez/query.fcgi?cmd=Retrieve&db=PubMed&dopt=Citation&list\\_uids=11322955](http://www.ncbi.nlm.nih.gov/entrez/query.fcgi?cmd=Retrieve&db=PubMed&dopt=Citation&list_uids=11322955)

- Ni, X. and Morales, C. R. (2006): The lysosomal trafficking of acid sphingomyelinase is mediated by sortilin and mannose 6-phosphate receptor, *Traffic* (vol. 7), No. 7, pp. 889-902. URL: [http://www.ncbi.nlm.nih.gov/entrez/query.fcgi?cmd=Retrieve&db=PubMed&dopt=Citation&list\\_uids=16787399](http://www.ncbi.nlm.nih.gov/entrez/query.fcgi?cmd=Retrieve&db=PubMed&dopt=Citation&list_uids=16787399)
- Nielsen, M. S.; Gustafsen, C.; Madsen, P.; Nyengaard, J. R.; Hermey, G.; Bakke, O.; Mari, M.; Schu, P.; Pohlmann, R.; Dennes, A. and Petersen, C. M. (2007): Sorting by the cytoplasmic domain of the amyloid precursor protein binding receptor SorLA, *Mol Cell Biol* (vol. 27), No. 19, pp. 6842-51. URL: [http://www.ncbi.nlm.nih.gov/entrez/query.fcgi?cmd=Retrieve&db=PubMed&dopt=Citation&list\\_uids=17646382](http://www.ncbi.nlm.nih.gov/entrez/query.fcgi?cmd=Retrieve&db=PubMed&dopt=Citation&list_uids=17646382)
- Nielsen, M. S.; Jacobsen, C.; Olivecrona, G.; Gliemann, J. and Petersen, C. M. (1999): Sortilin/neurotensin receptor-3 binds and mediates degradation of lipoprotein lipase, *J Biol Chem* (vol. 274), No. 13, pp. 8832-6. URL: [http://www.ncbi.nlm.nih.gov/entrez/query.fcgi?cmd=Retrieve&db=PubMed&dopt=Citation&list\\_uids=10085125](http://www.ncbi.nlm.nih.gov/entrez/query.fcgi?cmd=Retrieve&db=PubMed&dopt=Citation&list_uids=10085125)
- Nielsen, M. S.; Keat, S. J.; Hamati, J. W.; Madsen, P.; Gutzmann, J. J.; Engelsberg, A.; Pedersen, K. M.; Gustafsen, C.; Nykjaer, A.; Gliemann, J.; Hermans-Borgmeyer, I.; Kuhl, D.; Petersen, C. M. and Hermey, G. (2008): Different motifs regulate trafficking of SorCS1 isoforms, *Traffic* (vol. 9), No. 6, pp. 980-94. URL: [http://www.ncbi.nlm.nih.gov/entrez/query.fcgi?cmd=Retrieve&db=PubMed&dopt=Citation&list\\_uids=18315530](http://www.ncbi.nlm.nih.gov/entrez/query.fcgi?cmd=Retrieve&db=PubMed&dopt=Citation&list_uids=18315530)
- Nielsen, M. S.; Madsen, P.; Christensen, E. I.; Nykjaer, A.; Gliemann, J.; Kasper, D.; Pohlmann, R. and Petersen, C. M. (2001): The sortilin cytoplasmic tail conveys Golgi-endosome transport and binds the VHS domain of the GGA2 sorting protein, *Embo J* (vol. 20), No. 9, pp. 2180-90. URL: [http://www.ncbi.nlm.nih.gov/entrez/query.fcgi?cmd=Retrieve&db=PubMed&dopt=Citation&list\\_uids=11331584](http://www.ncbi.nlm.nih.gov/entrez/query.fcgi?cmd=Retrieve&db=PubMed&dopt=Citation&list_uids=11331584)
- Nixon, R. A. and Cataldo, A. M. (2006): Lysosomal system pathways: genes to neurodegeneration in Alzheimer's disease, *J Alzheimers Dis* (vol. 9), No. 3 Suppl, pp. 277-89. URL: [http://www.ncbi.nlm.nih.gov/entrez/query.fcgi?cmd=Retrieve&db=PubMed&dopt=Citation&list\\_uids=16914867](http://www.ncbi.nlm.nih.gov/entrez/query.fcgi?cmd=Retrieve&db=PubMed&dopt=Citation&list_uids=16914867)
- Nothwehr, S. F.; Ha, S. A. and Bruinsma, P. (2000): Sorting of yeast membrane proteins into an endosome-to-Golgi pathway involves direct interaction of their cytosolic domains with Vps35p, *J Cell Biol* (vol. 151), No. 2, pp. 297-310. URL: [http://www.ncbi.nlm.nih.gov/entrez/query.fcgi?cmd=Retrieve&db=PubMed&dopt=Citation&list\\_uids=11038177](http://www.ncbi.nlm.nih.gov/entrez/query.fcgi?cmd=Retrieve&db=PubMed&dopt=Citation&list_uids=11038177)
- Nykjaer, A.; Lee, R.; Teng, K. K.; Jansen, P.; Madsen, P.; Nielsen, M. S.; Jacobsen, C.; Klieman, M.; Schwarz, E.; Willnow, T. E.; Hempstead, B. L. and Petersen, C. M. (2004): Sortilin is essential for proNGF-induced neuronal cell death, *Nature* (vol. 427), No. 6977, pp. 843-8. URL: [http://www.ncbi.nlm.nih.gov/entrez/query.fcgi?cmd=Retrieve&db=PubMed&dopt=Citation&list\\_uids=14985763](http://www.ncbi.nlm.nih.gov/entrez/query.fcgi?cmd=Retrieve&db=PubMed&dopt=Citation&list_uids=14985763)
- Nykjaer, A. and Willnow, T. E. (2002): The low-density lipoprotein receptor gene family: a cellular Swiss army knife?, *Trends Cell Biol* (vol. 12), No. 6, pp. 273-80. URL:

- [http://www.ncbi.nlm.nih.gov/entrez/query.fcgi?cmd=Retrieve&db=PubMed&dopt=Citation&list\\_uids=12074887](http://www.ncbi.nlm.nih.gov/entrez/query.fcgi?cmd=Retrieve&db=PubMed&dopt=Citation&list_uids=12074887)
- Obermüller, N.; Bernstein, P.; Velazquez, H.; Reilly, R.; Moser, D.; Ellison, D. H. and Bachmann, S. (1995): Expression of the thiazide-sensitive Na-Cl cotransporter in rat and human kidney, *Am J Physiol* (vol. 269), No. 6 Pt 2, pp. F900-10. URL: [http://www.ncbi.nlm.nih.gov/entrez/query.fcgi?cmd=Retrieve&db=PubMed&dopt=Citation&list\\_uids=8594886](http://www.ncbi.nlm.nih.gov/entrez/query.fcgi?cmd=Retrieve&db=PubMed&dopt=Citation&list_uids=8594886)
- Offe, K.; Dodson, S. E.; Shoemaker, J. T.; Fritz, J. J.; Gearing, M.; Levey, A. I. and Lah, J. J. (2006): The lipoprotein receptor LR11 regulates amyloid beta production and amyloid precursor protein traffic in endosomal compartments, *J Neurosci* (vol. 26), No. 5, pp. 1596-603. URL: [http://www.ncbi.nlm.nih.gov/entrez/query.fcgi?cmd=Retrieve&db=PubMed&dopt=Citation&list\\_uids=16452683](http://www.ncbi.nlm.nih.gov/entrez/query.fcgi?cmd=Retrieve&db=PubMed&dopt=Citation&list_uids=16452683)
- Pacheco-Alvarez, D.; Cristobal, P. S.; Meade, P.; Moreno, E.; Vazquez, N.; Munoz, E.; Diaz, A.; Juarez, M. E.; Gimenez, I. and Gamba, G. (2006): The Na<sup>+</sup>:Cl<sup>-</sup> cotransporter is activated and phosphorylated at the amino-terminal domain upon intracellular chloride depletion, *J Biol Chem* (vol. 281), No. 39, pp. 28755-63. URL: [http://www.ncbi.nlm.nih.gov/entrez/query.fcgi?cmd=Retrieve&db=PubMed&dopt=Citation&list\\_uids=16887815](http://www.ncbi.nlm.nih.gov/entrez/query.fcgi?cmd=Retrieve&db=PubMed&dopt=Citation&list_uids=16887815)
- Paiardini, A. and Caputo, V. (2008): Insights into the interaction of sortilin with proneurotrophins: a computational approach, *Neuropeptides* (vol. 42), No. 2, pp. 205-14. URL: [http://www.ncbi.nlm.nih.gov/entrez/query.fcgi?cmd=Retrieve&db=PubMed&dopt=Citation&list\\_uids=18191449](http://www.ncbi.nlm.nih.gov/entrez/query.fcgi?cmd=Retrieve&db=PubMed&dopt=Citation&list_uids=18191449)
- Pawson, T. (1995): Protein modules and signalling networks, *Nature* (vol. 373), No. 6515, pp. 573-80. URL: [http://www.ncbi.nlm.nih.gov/entrez/query.fcgi?cmd=Retrieve&db=PubMed&dopt=Citation&list\\_uids=7531822](http://www.ncbi.nlm.nih.gov/entrez/query.fcgi?cmd=Retrieve&db=PubMed&dopt=Citation&list_uids=7531822)
- Pawson, T. and Scott, J. D. (1997): Signaling through scaffold, anchoring, and adaptor proteins, *Science* (vol. 278), No. 5346, pp. 2075-80. URL: [http://www.ncbi.nlm.nih.gov/entrez/query.fcgi?cmd=Retrieve&db=PubMed&dopt=Citation&list\\_uids=9405336](http://www.ncbi.nlm.nih.gov/entrez/query.fcgi?cmd=Retrieve&db=PubMed&dopt=Citation&list_uids=9405336)
- Pessin, J. E.; Thurmond, D. C.; Elmendorf, J. S.; Coker, K. J. and Okada, S. (1999): Molecular basis of insulin-stimulated GLUT4 vesicle trafficking. Location! Location! Location!, *J Biol Chem* (vol. 274), No. 5, pp. 2593-6. URL: [http://www.ncbi.nlm.nih.gov/entrez/query.fcgi?cmd=Retrieve&db=PubMed&dopt=Citation&list\\_uids=9915783](http://www.ncbi.nlm.nih.gov/entrez/query.fcgi?cmd=Retrieve&db=PubMed&dopt=Citation&list_uids=9915783)
- Petersen, C. M.; Nielsen, M. S.; Nykjaer, A.; Jacobsen, L.; Tommerup, N.; Rasmussen, H. H.; Roigaard, H.; Gliemann, J.; Madsen, P. and Moestrup, S. K. (1997): Molecular identification of a novel candidate sorting receptor purified from human brain by receptor-associated protein affinity chromatography, *J Biol Chem* (vol. 272), No. 6, pp. 3599-605. URL: [http://www.ncbi.nlm.nih.gov/entrez/query.fcgi?cmd=Retrieve&db=PubMed&dopt=Citation&list\\_uids=9013611](http://www.ncbi.nlm.nih.gov/entrez/query.fcgi?cmd=Retrieve&db=PubMed&dopt=Citation&list_uids=9013611)

- Petersen, C. Munck; Nielsen, M. S.; Jacobsen, C.; Tauris, J.; Jacobsen, L.; Gliemann, J.; Moestrup, S. K. and Madsen, P. (1999): Propeptide cleavage conditions sortilin/neurotensin receptor-3 for ligand binding, *EMBO J.* (vol. 18), No. 3, pp. 595-604. URL: <http://embojournal.npgjournals.com/cgi/content/abstract/18/3/595>
- Peti-Peterdi, J. and Bell, P. D. (1999): Cytosolic [Ca<sup>2+</sup>] signaling pathway in macula densa cells, *Am J Physiol* (vol. 277), No. 3 Pt 2, pp. F472-6. URL: [http://www.ncbi.nlm.nih.gov/entrez/query.fcgi?cmd=Retrieve&db=PubMed&dopt=Citation&list\\_uids=10484531](http://www.ncbi.nlm.nih.gov/entrez/query.fcgi?cmd=Retrieve&db=PubMed&dopt=Citation&list_uids=10484531)
- Piechotta, K.; Lu, J. and Delpire, E. (2002): Cation chloride cotransporters interact with the stress-related kinases Ste20-related proline-alanine-rich kinase (SPAK) and oxidative stress response 1 (OSR1), *J Biol Chem* (vol. 277), No. 52, pp. 50812-9. URL: [http://www.ncbi.nlm.nih.gov/entrez/query.fcgi?cmd=Retrieve&db=PubMed&dopt=Citation&list\\_uids=12386165](http://www.ncbi.nlm.nih.gov/entrez/query.fcgi?cmd=Retrieve&db=PubMed&dopt=Citation&list_uids=12386165)
- Ponce-Coria, J.; San-Cristobal, P.; Kahle, K. T.; Vazquez, N.; Pacheco-Alvarez, D.; de Los Heros, P.; Juarez, P.; Munoz, E.; Michel, G.; Bobadilla, N. A.; Gimenez, I.; Lifton, R. P.; Hebert, S. C. and Gamba, G. (2008): Regulation of NKCC2 by a chloride-sensing mechanism involving the WNK3 and SPAK kinases, *Proc Natl Acad Sci U S A* (vol. 105), No. 24, pp. 8458-63. URL: [http://www.ncbi.nlm.nih.gov/entrez/query.fcgi?cmd=Retrieve&db=PubMed&dopt=Citation&list\\_uids=18550832](http://www.ncbi.nlm.nih.gov/entrez/query.fcgi?cmd=Retrieve&db=PubMed&dopt=Citation&list_uids=18550832)
- Posse De Chaves, E. I.; Vance, D. E.; Campenot, R. B.; Kiss, R. S. and Vance, J. E. (2000): Uptake of lipoproteins for axonal growth of sympathetic neurons, *J Biol Chem* (vol. 275), No. 26, pp. 19883-90. URL: [http://www.ncbi.nlm.nih.gov/entrez/query.fcgi?cmd=Retrieve&db=PubMed&dopt=Citation&list\\_uids=10867025](http://www.ncbi.nlm.nih.gov/entrez/query.fcgi?cmd=Retrieve&db=PubMed&dopt=Citation&list_uids=10867025)
- Quistgaard, E. M.; Madsen, P.; Groftehauge, M. K.; Nissen, P.; Petersen, C. M. and Thirup, S. S. (2009): Ligands bind to Sortilin in the tunnel of a ten-bladed beta-propeller domain, *Nat Struct Mol Biol* (vol. 16), No. 1, pp. 96-8. URL: [http://www.ncbi.nlm.nih.gov/entrez/query.fcgi?cmd=Retrieve&db=PubMed&dopt=Citation&list\\_uids=19122660](http://www.ncbi.nlm.nih.gov/entrez/query.fcgi?cmd=Retrieve&db=PubMed&dopt=Citation&list_uids=19122660)
- Ralser, M.; Heeren, G.; Breitenbach, M.; Lehrach, H. and Krobitsch, S. (2006): Triose phosphate isomerase deficiency is caused by altered dimerization--not catalytic inactivity--of the mutant enzymes, *PLoS One* (vol. 1), p. e30. URL: [http://www.ncbi.nlm.nih.gov/entrez/query.fcgi?cmd=Retrieve&db=PubMed&dopt=Citation&list\\_uids=17183658](http://www.ncbi.nlm.nih.gov/entrez/query.fcgi?cmd=Retrieve&db=PubMed&dopt=Citation&list_uids=17183658)
- Reichardt, L. F. (2006): Neurotrophin-regulated signalling pathways, *Philos Trans R Soc Lond B Biol Sci* (vol. 361), No. 1473, pp. 1545-64. URL: [http://www.ncbi.nlm.nih.gov/entrez/query.fcgi?cmd=Retrieve&db=PubMed&dopt=Citation&list\\_uids=16939974](http://www.ncbi.nlm.nih.gov/entrez/query.fcgi?cmd=Retrieve&db=PubMed&dopt=Citation&list_uids=16939974)
- Reinhard, C.; Hebert, S. S. and De Strooper, B. (2005): The amyloid-beta precursor protein: integrating structure with biological function, *EMBO J* (vol. 24), No. 23, pp. 3996-4006. URL: [http://www.ncbi.nlm.nih.gov/entrez/query.fcgi?cmd=Retrieve&db=PubMed&dopt=Citation&list\\_uids=16252002](http://www.ncbi.nlm.nih.gov/entrez/query.fcgi?cmd=Retrieve&db=PubMed&dopt=Citation&list_uids=16252002)



- Rezgaoui, M.; Hermey, G.; Riedel, I. B.; Hampe, W.; Schaller, H. C. and Hermans-Borgmeyer, I. (2001): Identification of SorCS2, a novel member of the VPS10 domain containing receptor family, prominently expressed in the developing mouse brain, *Mech Dev* (vol. 100), No. 2, pp. 335-8. URL:  
[http://www.ncbi.nlm.nih.gov/entrez/query.fcgi?cmd=Retrieve&db=PubMed&dopt=Citation&list\\_uids=11165493](http://www.ncbi.nlm.nih.gov/entrez/query.fcgi?cmd=Retrieve&db=PubMed&dopt=Citation&list_uids=11165493)
- Richardson, C. and Alessi, D. R. (2008): The regulation of salt transport and blood pressure by the WNK-SPAK/OSR1 signalling pathway, *J Cell Sci* (vol. 121), No. Pt 20, pp. 3293-304. URL:  
[http://www.ncbi.nlm.nih.gov/entrez/query.fcgi?cmd=Retrieve&db=PubMed&dopt=Citation&list\\_uids=18843116](http://www.ncbi.nlm.nih.gov/entrez/query.fcgi?cmd=Retrieve&db=PubMed&dopt=Citation&list_uids=18843116)
- Richardson, C.; Rafiqi, F. H.; Karlsson, H. K.; Moleleki, N.; Vandewalle, A.; Campbell, D. G.; Morrice, N. A. and Alessi, D. R. (2008): Activation of the thiazide-sensitive Na<sup>+</sup>-Cl<sup>-</sup> co-transporter by the WNK-regulated kinases SPAK and OSR1, *J Cell Sci* (vol. 121), No. Pt 5, pp. 675-84. URL:  
[http://www.ncbi.nlm.nih.gov/entrez/query.fcgi?cmd=Retrieve&db=PubMed&dopt=Citation&list\\_uids=18270262](http://www.ncbi.nlm.nih.gov/entrez/query.fcgi?cmd=Retrieve&db=PubMed&dopt=Citation&list_uids=18270262)
- Riedel, I. B.; Hermans-Borgmeyer, I. and Hubner, C. A. (2002): SorLA, a member of the LDL receptor family, is expressed in the collecting duct of the murine kidney, *Histochem Cell Biol* (vol. 118), No. 3, pp. 183-91. URL:  
[http://www.ncbi.nlm.nih.gov/entrez/query.fcgi?cmd=Retrieve&db=PubMed&dopt=Citation&list\\_uids=12271354](http://www.ncbi.nlm.nih.gov/entrez/query.fcgi?cmd=Retrieve&db=PubMed&dopt=Citation&list_uids=12271354)
- Rogaeva, E.; Meng, Y.; Lee, J. H.; Gu, Y.; Kawarai, T.; Zou, F.; Katayama, T.; Baldwin, C. T.; Cheng, R.; Hasegawa, H.; Chen, F.; Shibata, N.; Lunetta, K. L.; Pardossi-Piquard, R.; Bohm, C.; Wakutani, Y.; Cupples, L. A.; Cuenco, K. T.; Green, R. C.; Pinessi, L.; Rainero, I.; Sorbi, S.; Bruni, A.; Duara, R.; Friedland, R. P.; Inzelberg, R.; Hampe, W.; Bujo, H.; Song, Y. Q.; Andersen, O. M.; Willnow, T. E.; Graff-Radford, N.; Petersen, R. C.; Dickson, D.; Der, S. D.; Fraser, P. E.; Schmitt-Ulms, G.; Younkin, S.; Mayeux, R.; Farrer, L. A. and St George-Hyslop, P. (2007): The neuronal sortilin-related receptor SORL1 is genetically associated with Alzheimer disease, *Nat Genet* (vol. 39), No. 2, pp. 168-77. URL:  
[http://www.ncbi.nlm.nih.gov/entrez/query.fcgi?cmd=Retrieve&db=PubMed&dopt=Citation&list\\_uids=17220890](http://www.ncbi.nlm.nih.gov/entrez/query.fcgi?cmd=Retrieve&db=PubMed&dopt=Citation&list_uids=17220890)
- Rohe, M.; Carlo, A. S.; Breyhan, H.; Sporbert, A.; Militz, D.; Schmidt, V.; Wozny, C.; Harmeier, A.; Erdmann, B.; Bales, K. R.; Wolf, S.; Kempermann, G.; Paul, S. M.; Schmitz, D.; Bayer, T. A.; Willnow, T. E. and Andersen, O. M. (2008): Sortilin-related receptor with A-type repeats (SORLA) affects the amyloid precursor protein-dependent stimulation of ERK signaling and adult neurogenesis, *J Biol Chem* (vol. 283), No. 21, pp. 14826-34. URL:  
[http://www.ncbi.nlm.nih.gov/entrez/query.fcgi?cmd=Retrieve&db=PubMed&dopt=Citation&list\\_uids=18362153](http://www.ncbi.nlm.nih.gov/entrez/query.fcgi?cmd=Retrieve&db=PubMed&dopt=Citation&list_uids=18362153)
- Sambrook, Joseph; Fritsch, E. F. and Maniatis, Tom (1989): *Molecular cloning : a laboratory manual*, 2nd. ed., Cold Spring Harbor Laboratory, Cold Spring Harbor, N.Y., ISBN: 0879693096.



- Sanger, F.; Nicklen, S. and Coulson, A. R. (1977): DNA sequencing with chain-terminating inhibitors, *Proc Natl Acad Sci U S A* (vol. 74), No. 12, pp. 5463-7. URL: [http://www.ncbi.nlm.nih.gov/entrez/query.fcgi?cmd=Retrieve&db=PubMed&dopt=Citation&list\\_uids=271968](http://www.ncbi.nlm.nih.gov/entrez/query.fcgi?cmd=Retrieve&db=PubMed&dopt=Citation&list_uids=271968)
- Sarret, P.; Krzykowski, P.; Segal, L.; Nielsen, M. S.; Petersen, C. M.; Mazella, J.; Stroh, T. and Beaudet, A. (2003): Distribution of NTS3 receptor/sortilin mRNA and protein in the rat central nervous system, *J Comp Neurol* (vol. 461), No. 4, pp. 483-505. URL: [http://www.ncbi.nlm.nih.gov/entrez/query.fcgi?cmd=Retrieve&db=PubMed&dopt=Citation&list\\_uids=12746864](http://www.ncbi.nlm.nih.gov/entrez/query.fcgi?cmd=Retrieve&db=PubMed&dopt=Citation&list_uids=12746864)
- Schaller, H. C.; Hermans-Borgmeyer, I. and Hoffmeister, S. A. (1996): Neuronal control of development in hydra, *Int J Dev Biol* (vol. 40), No. 1, pp. 339-44. URL: [http://www.ncbi.nlm.nih.gov/entrez/query.fcgi?cmd=Retrieve&db=PubMed&dopt=Citation&list\\_uids=8735946](http://www.ncbi.nlm.nih.gov/entrez/query.fcgi?cmd=Retrieve&db=PubMed&dopt=Citation&list_uids=8735946)
- Scheinman, S. J.; Guay-Woodford, L. M.; Thakker, R. V. and Warnock, D. G. (1999): Genetic disorders of renal electrolyte transport, *N Engl J Med* (vol. 340), No. 15, pp. 1177-87. URL: [http://www.ncbi.nlm.nih.gov/entrez/query.fcgi?cmd=Retrieve&db=PubMed&dopt=Citation&list\\_uids=10202170](http://www.ncbi.nlm.nih.gov/entrez/query.fcgi?cmd=Retrieve&db=PubMed&dopt=Citation&list_uids=10202170)
- Scherzer, C. R.; Offe, K.; Gearing, M.; Rees, H. D.; Fang, G.; Heilman, C. J.; Schaller, C.; Bujo, H.; Levey, A. I. and Lah, J. J. (2004): Loss of apolipoprotein E receptor LR11 in Alzheimer disease, *Arch Neurol* (vol. 61), No. 8, pp. 1200-5. URL: [http://www.ncbi.nlm.nih.gov/entrez/query.fcgi?cmd=Retrieve&db=PubMed&dopt=Citation&list\\_uids=15313836](http://www.ncbi.nlm.nih.gov/entrez/query.fcgi?cmd=Retrieve&db=PubMed&dopt=Citation&list_uids=15313836)
- Schmidt, V.; Sporbert, A.; Rohe, M.; Reimer, T.; Rehm, A.; Andersen, O. M. and Willnow, T. E. (2007): SorLA/LR11 regulates processing of amyloid precursor protein via interaction with adaptors GGA and PACS-1, *J Biol Chem* (vol. 282), No. 45, pp. 32956-64. URL: [http://www.ncbi.nlm.nih.gov/entrez/query.fcgi?cmd=Retrieve&db=PubMed&dopt=Citation&list\\_uids=17855360](http://www.ncbi.nlm.nih.gov/entrez/query.fcgi?cmd=Retrieve&db=PubMed&dopt=Citation&list_uids=17855360)
- Seaman, M. N. (2004): Cargo-selective endosomal sorting for retrieval to the Golgi requires retromer, *J Cell Biol* (vol. 165), No. 1, pp. 111-22. URL: [http://www.ncbi.nlm.nih.gov/entrez/query.fcgi?cmd=Retrieve&db=PubMed&dopt=Citation&list\\_uids=15078902](http://www.ncbi.nlm.nih.gov/entrez/query.fcgi?cmd=Retrieve&db=PubMed&dopt=Citation&list_uids=15078902)
- Seaman, M. N. (2005): Recycle your receptors with retromer, *Trends Cell Biol* (vol. 15), No. 2, pp. 68-75. URL: [http://www.ncbi.nlm.nih.gov/entrez/query.fcgi?cmd=Retrieve&db=PubMed&dopt=Citation&list\\_uids=15695093](http://www.ncbi.nlm.nih.gov/entrez/query.fcgi?cmd=Retrieve&db=PubMed&dopt=Citation&list_uids=15695093)
- Seaman, M. N. (2007): Identification of a novel conserved sorting motif required for retromer-mediated endosome-to-TGN retrieval, *J Cell Sci* (vol. 120), No. Pt 14, pp. 2378-89. URL: [http://www.ncbi.nlm.nih.gov/entrez/query.fcgi?cmd=Retrieve&db=PubMed&dopt=Citation&list\\_uids=17606993](http://www.ncbi.nlm.nih.gov/entrez/query.fcgi?cmd=Retrieve&db=PubMed&dopt=Citation&list_uids=17606993)
- Selfors, L. M.; Schutzman, J. L.; Borland, C. Z. and Stern, M. J. (1998): soc-2 encodes a leucine-rich repeat protein implicated in fibroblast growth factor receptor signaling, *Proc Natl Acad Sci U S A* (vol. 95), No. 12, pp. 6903-8. URL:

[http://www.ncbi.nlm.nih.gov/entrez/query.fcgi?cmd=Retrieve&db=PubMed&dopt=Citation&list\\_uids=9618511](http://www.ncbi.nlm.nih.gov/entrez/query.fcgi?cmd=Retrieve&db=PubMed&dopt=Citation&list_uids=9618511)

Shapiro, A. L.; Vinuela, E. and Maizel, J. V., Jr. (1967): Molecular weight estimation of polypeptide chains by electrophoresis in SDS-polyacrylamide gels, *Biochem Biophys Res Commun* (vol. 28), No. 5, pp. 815-20. URL: [http://www.ncbi.nlm.nih.gov/entrez/query.fcgi?cmd=Retrieve&db=PubMed&dopt=Citation&list\\_uids=4861258](http://www.ncbi.nlm.nih.gov/entrez/query.fcgi?cmd=Retrieve&db=PubMed&dopt=Citation&list_uids=4861258)

Shi, J. and Kandror, K. V. (2005): Sortilin is essential and sufficient for the formation of Glut4 storage vesicles in 3T3-L1 adipocytes, *Dev Cell* (vol. 9), No. 1, pp. 99-108. URL: [http://www.ncbi.nlm.nih.gov/entrez/query.fcgi?cmd=Retrieve&db=PubMed&dopt=Citation&list\\_uids=15992544](http://www.ncbi.nlm.nih.gov/entrez/query.fcgi?cmd=Retrieve&db=PubMed&dopt=Citation&list_uids=15992544)

Shi, J. and Kandror, K. V. (2007): The luminal Vps10p domain of sortilin plays the predominant role in targeting to insulin-responsive Glut4-containing vesicles, *J Biol Chem* (vol. 282), No. 12, pp. 9008-16. URL: [http://www.ncbi.nlm.nih.gov/entrez/query.fcgi?cmd=Retrieve&db=PubMed&dopt=Citation&list\\_uids=17220298](http://www.ncbi.nlm.nih.gov/entrez/query.fcgi?cmd=Retrieve&db=PubMed&dopt=Citation&list_uids=17220298)

Skøtt, O. and Briggs, J. P. (1987): Direct demonstration of macula densa-mediated renin secretion, *Science* (vol. 237), No. 4822, pp. 1618-20. URL: [http://www.ncbi.nlm.nih.gov/entrez/query.fcgi?cmd=Retrieve&db=PubMed&dopt=Citation&list\\_uids=3306925](http://www.ncbi.nlm.nih.gov/entrez/query.fcgi?cmd=Retrieve&db=PubMed&dopt=Citation&list_uids=3306925)

Small, S. A. (2008): Retromer sorting: a pathogenic pathway in late-onset Alzheimer disease, *Arch Neurol* (vol. 65), No. 3, pp. 323-8. URL: [http://www.ncbi.nlm.nih.gov/entrez/query.fcgi?cmd=Retrieve&db=PubMed&dopt=Citation&list\\_uids=18332244](http://www.ncbi.nlm.nih.gov/entrez/query.fcgi?cmd=Retrieve&db=PubMed&dopt=Citation&list_uids=18332244)

Small, S. A.; Kent, K.; Pierce, A.; Leung, C.; Kang, M. S.; Okada, H.; Honig, L.; Vonsattel, J. P. and Kim, T. W. (2005): Model-guided microarray implicates the retromer complex in Alzheimer's disease, *Ann Neurol* (vol. 58), No. 6, pp. 909-19. URL: [http://www.ncbi.nlm.nih.gov/entrez/query.fcgi?cmd=Retrieve&db=PubMed&dopt=Citation&list\\_uids=16315276](http://www.ncbi.nlm.nih.gov/entrez/query.fcgi?cmd=Retrieve&db=PubMed&dopt=Citation&list_uids=16315276)

Smith, P. K.; Krohn, R. I.; Hermanson, G. T.; Mallia, A. K.; Gartner, F. H.; Provenzano, M. D.; Fujimoto, E. K.; Goeke, N. M.; Olson, B. J. and Klenk, D. C. (1985): Measurement of protein using bicinchoninic acid, *Anal Biochem* (vol. 150), No. 1, pp. 76-85. URL: [http://www.ncbi.nlm.nih.gov/entrez/query.fcgi?cmd=Retrieve&db=PubMed&dopt=Citation&list\\_uids=3843705](http://www.ncbi.nlm.nih.gov/entrez/query.fcgi?cmd=Retrieve&db=PubMed&dopt=Citation&list_uids=3843705)

Stoica, G.; Lungu, G.; Kim, H. T. and Wong, P. K. (2008): Up-regulation of pro-nerve growth factor, neurotrophin receptor p75, and sortilin is associated with retrovirus-induced spongiform encephalomyelopathy, *Brain Res* (vol. 1208), pp. 204-16. URL: [http://www.ncbi.nlm.nih.gov/entrez/query.fcgi?cmd=Retrieve&db=PubMed&dopt=Citation&list\\_uids=18395188](http://www.ncbi.nlm.nih.gov/entrez/query.fcgi?cmd=Retrieve&db=PubMed&dopt=Citation&list_uids=18395188)

Subramanya, A. R.; Yang, C. L.; McCormick, J. A. and Ellison, D. H. (2006): WNK kinases regulate sodium chloride and potassium transport by the aldosterone-sensitive distal nephron, *Kidney Int* (vol. 70), No. 4, pp. 630-4. URL:

- [http://www.ncbi.nlm.nih.gov/entrez/query.fcgi?cmd=Retrieve&db=PubMed&dopt=Citation&list\\_uids=16820787](http://www.ncbi.nlm.nih.gov/entrez/query.fcgi?cmd=Retrieve&db=PubMed&dopt=Citation&list_uids=16820787)
- Suki, W. N. (1979): Calcium transport in the nephron, *Am J Physiol* (vol. 237), No. 1, pp. F1-6. URL: [http://www.ncbi.nlm.nih.gov/entrez/query.fcgi?cmd=Retrieve&db=PubMed&dopt=Citation&list\\_uids=380361](http://www.ncbi.nlm.nih.gov/entrez/query.fcgi?cmd=Retrieve&db=PubMed&dopt=Citation&list_uids=380361)
- Taglialatela, M.; Drewe, J. A. and Brown, A. M. (1993): Barium blockade of a clonal potassium channel and its regulation by a critical pore residue, *Mol Pharmacol* (vol. 44), No. 1, pp. 180-90. URL: [http://www.ncbi.nlm.nih.gov/entrez/query.fcgi?cmd=Retrieve&db=PubMed&dopt=Citation&list\\_uids=8341271](http://www.ncbi.nlm.nih.gov/entrez/query.fcgi?cmd=Retrieve&db=PubMed&dopt=Citation&list_uids=8341271)
- Takatsu, H.; Katoh, Y.; Shiba, Y. and Nakayama, K. (2001): Golgi-localizing, gamma-adaptin ear homology domain, ADP-ribosylation factor-binding (GGA) proteins interact with acidic dileucine sequences within the cytoplasmic domains of sorting receptors through their Vps27p/Hrs/STAM (VHS) domains, *J Biol Chem* (vol. 276), No. 30, pp. 28541-5. URL: [http://www.ncbi.nlm.nih.gov/entrez/query.fcgi?cmd=Retrieve&db=PubMed&dopt=Citation&list\\_uids=11390366](http://www.ncbi.nlm.nih.gov/entrez/query.fcgi?cmd=Retrieve&db=PubMed&dopt=Citation&list_uids=11390366)
- Teng, H. K.; Teng, K. K.; Lee, R.; Wright, S.; Tevar, S.; Almeida, R. D.; Kermani, P.; Torkin, R.; Chen, Z. Y.; Lee, F. S.; Kraemer, R. T.; Nykjaer, A. and Hempstead, B. L. (2005): ProBDNF induces neuronal apoptosis via activation of a receptor complex of p75NTR and sortilin, *J Neurosci* (vol. 25), No. 22, pp. 5455-63. URL: [http://www.ncbi.nlm.nih.gov/entrez/query.fcgi?cmd=Retrieve&db=PubMed&dopt=Citation&list\\_uids=15930396](http://www.ncbi.nlm.nih.gov/entrez/query.fcgi?cmd=Retrieve&db=PubMed&dopt=Citation&list_uids=15930396)
- Tooze, S. A. (2001): Cell biology. GGAs tie up the loose ends, *Science* (vol. 292), No. 5522, pp. 1663-5. URL: [http://www.ncbi.nlm.nih.gov/entrez/query.fcgi?cmd=Retrieve&db=PubMed&dopt=Citation&list\\_uids=11387461](http://www.ncbi.nlm.nih.gov/entrez/query.fcgi?cmd=Retrieve&db=PubMed&dopt=Citation&list_uids=11387461)
- Vecsei, P.; Hackenthal, E. and Ganten, D. (1978): The renin-angiotensin-aldosterone system. Past, present and future, *Klin Wochenschr* (vol. 56 Suppl 1), pp. 5-21. URL: [http://www.ncbi.nlm.nih.gov/entrez/query.fcgi?cmd=Retrieve&db=PubMed&dopt=Citation&list\\_uids=366278](http://www.ncbi.nlm.nih.gov/entrez/query.fcgi?cmd=Retrieve&db=PubMed&dopt=Citation&list_uids=366278)
- Vida, T. A.; Huyer, G. and Emr, S. D. (1993): Yeast vacuolar proenzymes are sorted in the late Golgi complex and transported to the vacuole via a prevacuolar endosome-like compartment, *J Cell Biol* (vol. 121), No. 6, pp. 1245-56. URL: [http://www.ncbi.nlm.nih.gov/entrez/query.fcgi?cmd=Retrieve&db=PubMed&dopt=Citation&list\\_uids=8509446](http://www.ncbi.nlm.nih.gov/entrez/query.fcgi?cmd=Retrieve&db=PubMed&dopt=Citation&list_uids=8509446)
- Vitari, A. C.; Deak, M.; Morrice, N. A. and Alessi, D. R. (2005): The WNK1 and WNK4 protein kinases that are mutated in Gordon's hypertension syndrome phosphorylate and activate SPAK and OSR1 protein kinases, *Biochem J* (vol. 391), No. Pt 1, pp. 17-24. URL: [http://www.ncbi.nlm.nih.gov/entrez/query.fcgi?cmd=Retrieve&db=PubMed&dopt=Citation&list\\_uids=16083423](http://www.ncbi.nlm.nih.gov/entrez/query.fcgi?cmd=Retrieve&db=PubMed&dopt=Citation&list_uids=16083423)
- Volosin, M.; Trotter, C.; Cragolini, A.; Kenchappa, R. S.; Light, M.; Hempstead, B. L.; Carter, B. D. and Friedman, W. J. (2008): Induction of proneurotrophins and activation of p75NTR-

- mediated apoptosis via neurotrophin receptor-interacting factor in hippocampal neurons after seizures, *J Neurosci* (vol. 28), No. 39, pp. 9870-9. URL:  
[http://www.ncbi.nlm.nih.gov/entrez/query.fcgi?cmd=Retrieve&db=PubMed&dopt=Citation&list\\_uids=18815271](http://www.ncbi.nlm.nih.gov/entrez/query.fcgi?cmd=Retrieve&db=PubMed&dopt=Citation&list_uids=18815271)
- Wan, L.; Molloy, S. S.; Thomas, L.; Liu, G.; Xiang, Y.; Rybak, S. L. and Thomas, G. (1998): PACS-1 defines a novel gene family of cytosolic sorting proteins required for trans-Golgi network localization, *Cell* (vol. 94), No. 2, pp. 205-16. URL:  
[http://www.ncbi.nlm.nih.gov/entrez/query.fcgi?cmd=Retrieve&db=PubMed&dopt=Citation&list\\_uids=9695949](http://www.ncbi.nlm.nih.gov/entrez/query.fcgi?cmd=Retrieve&db=PubMed&dopt=Citation&list_uids=9695949)
- Wanker, E. E.; Rovira, C.; Scherzinger, E.; Hasenbank, R.; Walter, S.; Tait, D.; Colicelli, J. and Lehrach, H. (1997): HIP-1: a huntingtin interacting protein isolated by the yeast two-hybrid system, *Hum Mol Genet* (vol. 6), No. 3, pp. 487-95. URL:  
[http://www.ncbi.nlm.nih.gov/entrez/query.fcgi?cmd=Retrieve&db=PubMed&dopt=Citation&list\\_uids=9147654](http://www.ncbi.nlm.nih.gov/entrez/query.fcgi?cmd=Retrieve&db=PubMed&dopt=Citation&list_uids=9147654)
- Welch, B. L. (1947): The generalization of 'Student's' problem when several different population variances are involved, *Biometrika* (vol. 34), No. 1-2, pp. 28-35. URL:  
<http://biomet.oxfordjournals.org>
- Westergaard, U. B.; Kirkegaard, K.; Sorensen, E. S.; Jacobsen, C.; Nielsen, M. S.; Petersen, C. M. and Madsen, P. (2005): SorCS3 does not require propeptide cleavage to bind nerve growth factor, *FEBS Lett* (vol. 579), No. 5, pp. 1172-6. URL:  
[http://www.ncbi.nlm.nih.gov/entrez/query.fcgi?cmd=Retrieve&db=PubMed&dopt=Citation&list\\_uids=15710408](http://www.ncbi.nlm.nih.gov/entrez/query.fcgi?cmd=Retrieve&db=PubMed&dopt=Citation&list_uids=15710408)
- Westergaard, U. B.; Sorensen, E. S.; Hermey, G.; Nielsen, M. S.; Nykjaer, A.; Kirkegaard, K.; Jacobsen, C.; Gliemann, J.; Madsen, P. and Petersen, C. M. (2004): Functional organization of the sortilin Vps10p-domain, *J Biol Chem*. URL:  
[http://www.ncbi.nlm.nih.gov/entrez/query.fcgi?cmd=Retrieve&db=PubMed&dopt=Citation&list\\_uids=15364913](http://www.ncbi.nlm.nih.gov/entrez/query.fcgi?cmd=Retrieve&db=PubMed&dopt=Citation&list_uids=15364913)
- Willnow, T. E.; Petersen, C. M. and Nykjaer, A. (2008): VPS10P-domain receptors - regulators of neuronal viability and function, *Nat Rev Neurosci* (vol. 9), No. 12, pp. 899-909. URL:  
[http://www.ncbi.nlm.nih.gov/entrez/query.fcgi?cmd=Retrieve&db=PubMed&dopt=Citation&list\\_uids=19002190](http://www.ncbi.nlm.nih.gov/entrez/query.fcgi?cmd=Retrieve&db=PubMed&dopt=Citation&list_uids=19002190)
- Wu, Z. and Irizarry, R. A. (2004): Preprocessing of oligonucleotide array data, *Nat Biotechnol* (vol. 22), No. 6, pp. 656-8; author reply 658. URL:  
[http://www.ncbi.nlm.nih.gov/entrez/query.fcgi?cmd=Retrieve&db=PubMed&dopt=Citation&list\\_uids=15175677](http://www.ncbi.nlm.nih.gov/entrez/query.fcgi?cmd=Retrieve&db=PubMed&dopt=Citation&list_uids=15175677)
- Xu, J. Z.; Hall, A. E.; Peterson, L. N.; Bienkowski, M. J.; Eessalu, T. E. and Hebert, S. C. (1997): Localization of the ROMK protein on apical membranes of rat kidney nephron segments, *Am J Physiol* (vol. 273), No. 5 Pt 2, pp. F739-48. URL:  
[http://www.ncbi.nlm.nih.gov/entrez/query.fcgi?cmd=Retrieve&db=PubMed&dopt=Citation&list\\_uids=9374837](http://www.ncbi.nlm.nih.gov/entrez/query.fcgi?cmd=Retrieve&db=PubMed&dopt=Citation&list_uids=9374837)
- Yamazaki, H.; Bujo, H.; Kusunoki, J.; Seimiya, K.; Kanaki, T.; Morisaki, N.; Schneider, W. J. and Saito, Y. (1996): Elements of neural adhesion molecules and a yeast vacuolar protein sorting receptor are present in a novel mammalian low density lipoprotein receptor family

member, J Biol Chem (vol. 271), No. 40, pp. 24761-8. URL:  
[http://www.ncbi.nlm.nih.gov/entrez/query.fcgi?cmd=Retrieve&db=PubMed&dopt=Citation&list\\_uids=8798746](http://www.ncbi.nlm.nih.gov/entrez/query.fcgi?cmd=Retrieve&db=PubMed&dopt=Citation&list_uids=8798746)

Zhu, Y.; Bujo, H.; Yamazaki, H.; Ohwaki, K.; Jiang, M.; Hirayama, S.; Kanaki, T.; Shibasaki, M.; Takahashi, K.; Schneider, W. J. and Saito, Y. (2004): LR11, an LDL receptor gene family member, is a novel regulator of smooth muscle cell migration, Circ Res (vol. 94), No. 6, pp. 752-8. URL:  
[http://www.ncbi.nlm.nih.gov/entrez/query.fcgi?cmd=Retrieve&db=PubMed&dopt=Citation&list\\_uids=14764453](http://www.ncbi.nlm.nih.gov/entrez/query.fcgi?cmd=Retrieve&db=PubMed&dopt=Citation&list_uids=14764453)

Zhu, Y.; Doray, B.; Poussu, A.; Lehto, V. P. and Kornfeld, S. (2001): Binding of GGA2 to the lysosomal enzyme sorting motif of the mannose 6-phosphate receptor, Science (vol. 292), No. 5522, pp. 1716-8. URL:  
[http://www.ncbi.nlm.nih.gov/entrez/query.fcgi?cmd=Retrieve&db=PubMed&dopt=Citation&list\\_uids=11387476](http://www.ncbi.nlm.nih.gov/entrez/query.fcgi?cmd=Retrieve&db=PubMed&dopt=Citation&list_uids=11387476)

## **Appendix**

### **Selbständigkeitserklärung**

Hiermit erkläre ich, dass ich die vorliegende Arbeit mit dem Titel "SORLA in Renal and Adrenal Function" selbstständig und ohne Hilfe Dritter angefertigt habe. Sämtliche Hilfsmittel, Hilfen sowie Literaturquellen sind als solche kenntlich gemacht.

Ausserdem erkläre ich hiermit, dass ich mich nicht anderweitig um einen entsprechenden Doktorgrad beworben habe und keinen Doktorgrad besitze.

Die Promotionsordnung der Mathematisch-Naturwissenschaftlichen Fakultät I der Humboldt-Universität zu Berlin habe ich gelesen und akzeptiert.

Daniel Militz

Berlin, Oktober 2009

## **Danksagung**

Zuallererst muss ich mich aufrichtig bei Prof. Dr. Thomas E. Willnow für die Überlassung des Forschungsthemas und die hervorragende Betreuung meiner Arbeit bedanken.

Ein großes Dankeschön gilt ebenfalls meinen Arbeitskollegen in der AG Willnow, für die angenehme Arbeitsatmosphäre und sämtliche Unterstützung. Dr. Tilman Breiderhoff ist dabei besonders zu erwähnen, da er sich als Ansprechpartner oft Zeit genommen hat um sich in die vielen kleineren und größeren Problemen hineinzuversetzen. Aus dem gleichen Grund danke ich auch Dr. Olav Andersen, der nebenbei einige kritische, oft aber auch sehr humorvolle Anmerkungen parat hatte.

Außerhalb der Arbeitsgruppe gilt Prof. Dr. Wolfgang Uckert von der Humboldt-Universität besonderer Dank für die Betreuung meiner Arbeit. Ebenfalls danke ich Prof. Ignacio Gimenez von der Universidad de Zaragoza, der mir neben der Aktivitätsbestimmung von NKCC2 vor allem physiologische Denkweisen nähergebracht hat.

Von Susann Förster erhielt ich Unterstützung bei der statistischen Auswertung von Microarray-Daten, insbesondere beim Begreifen der statistischen Methoden. Ihr bin ich auch für darüber hinaus gehenden extensiven fachlichen (und nicht-fachlichen) Austausch dankbar.

Zu guter Letzt danke ich meiner Familie für Ihre Unterstützung während meines Studiums und meiner Zeit als Doktorand. Ohne sie wäre mein Weg nicht der gleiche gewesen.



## **Lebenslauf**

**Der Lebenslauf wird nicht im Internet veröffentlicht.**

## Publikationen

Petersen, H. H.; Hilpert, J.; Militz, D.; Zandler, V.; Jacobsen, C.; Roebroek, A. J. and Willnow, T. E. (2003): Functional interaction of megalin with the megalinbinding protein (MegBP), a novel tetratrico peptide repeat-containing adaptor molecule, J Cell Sci (vol. 116), No. Pt 3, pp. 453-61.  
[http://www.ncbi.nlm.nih.gov/entrez/query.fcgi?cmd=Retrieve&db=PubMed&dopt=Citation&list\\_uids=12508107](http://www.ncbi.nlm.nih.gov/entrez/query.fcgi?cmd=Retrieve&db=PubMed&dopt=Citation&list_uids=12508107)

Rohe, M.; Carlo, A. S.; Breyhan, H.; Sporbert, A.; Militz, D.; Schmidt, V.; Wozny, C.; Harmeier, A.; Erdmann, B.; Bales, K. R.; Wolf, S.; Kempermann, G.; Paul, S. M.; Schmitz, D.; Bayer, T. A.; Willnow, T. E. and Andersen, O. M. (2008): Sortilin-related receptor with A-type repeats (SORLA) affects the amyloid precursor protein-dependent stimulation of ERK signaling and adult neurogenesis, J Biol Chem (vol. 283), No. 21, pp. 14826-34.  
[http://www.ncbi.nlm.nih.gov/entrez/query.fcgi?cmd=Retrieve&db=PubMed&dopt=Citation&list\\_uids=18362153](http://www.ncbi.nlm.nih.gov/entrez/query.fcgi?cmd=Retrieve&db=PubMed&dopt=Citation&list_uids=18362153)